

SHAPE EFFECT OF SHALLOW FOOTINGS ON SEISMIC BEARING CAPACITY FOR  
FOUNDATIONS LOCATED NEAR SLOPES

by

Mehmet Çelebi

B.S., Civil Engineering, Istanbul University, 2007

Submitted to the Institute for Graduate Studies in  
Science and Engineering in partial fulfillment of  
the requirements for the degree of  
Master of Science

Graduate Program in Civil Engineering

Boğaziçi University

2019

*To my wife,*

## ACKNOWLEDGEMENTS

I am very excited to present such a subject which is not discussed in the current literature up until now.

I would like to express the deepest appreciation to my thesis supervisor Assoc. Prof. Özer Çiniciođlu for his valuable help, convincingly conveyed a spirit of adventure in regard to the solution of this study and scholarship and an engineering judgement guiding me throughout the whole duration of the thesis. Without his guidance and persistent support, this dissertation would have not been possible.

I would like to thank also the members of my Master's thesis examination committee: Asst. Prof. Zeynep Yıldırım and Asst. Prof. Adlen Altunbaş for their efficient comments and supportive attitude towards me and in valuable advice.

Special thanks to Ahmet Talha Gezgin for his endless support and great patience all times. I am also thankful to Geogrup family members for their polite assistance and good wishes.

And finally, I would like to thank my wife Hacer Çelebi for her endless love, moral support and great patience at all times. I am also very thankful to my mother Emel Çelebi and my brother Orhan Çelebi since they have given me their support throughout the thesis, as always they do during my educational life.

## **ABSTRACT**

### **EFFECT OF THE SHAPE OF SHALLOW FOOTINGS ON SEISMIC BEARING CAPACITY FOR FOUNDATIONS LOCATED NEAR SLOPES**

In this study, the factors that are effective on the collapsing behaviour such as the soil strength which is forceful on calculating the bearing capacity under dynamic loads, the slope height and angle, the foundation geometry and the distance of the foundation to the slope were taken into consideration and studied from variety of recent studies. As a result of these studies, relations and design charts have been presented in order to calculate the seismic bearing capacity. The main aspect of all existing studies is that the problem has been investigated for the plane deformation conditions. In consequence of the adoption of the plane deformation, the presented and created charts are valid only for the continuous footings. The aim of this study is to investigate the effect of the shape effect of foundation which has not been studied in previous studies on the seismic bearing capacity of the shallow foundations constructed on or near the slopes. The approach used in this study will consider the undrained behavior during the earthquake by staying on the safe side. In accordance with the purpose of this thesis, finite elements methods will be created to determine seismic bearing capacity and parametric study will be done. The factors which will be investigated in the parametric study are the shape and size of foundation, the distance to the slope, undrained strength of soil, slope height, slope angle and earthquake acceleration. The effect of the earthquake on seismic bearing capacity will be described by using the pseudo-static method. The inertia effect of soil and the structural loads will be defined in the models. Design tables will be prepared by using the obtained results, and various failure systems such as the foundation sliding, bearing capacity failure, base failure and foundation failure will be discussed.

## ÖZET

### ŞEV YAKININDA BULUNAN TEMELLERİN DEPREMLİ TAŞIMA GÜCÜNE TEMEL ŞEKLİNİN ETKİSİ

Şev üzerinde veya yakınında bulunan temeller için dinamik yükler altında taşıma kapasitesinin hesaplanmasında etkili olan temel zemini mukavemet özellikleri, şev yüksekliği ve eğimi, temel geometrisi ve temelin şeve olan mesafesi gibi göçme davranışını etkileyen faktörler çeşitli yakın zaman çalışmalarından göze alınmış ve incelenmiştir. Bu çalışmaların sonucunda tasarıma yönelik depremlı taşıma gücünün hesaplanabilmesi için bağlantılar ve tasarım abakları sunulmuştur. Tüm mevcut çalışmaların ortak yönü problemin düzlem şekil değiştirme şartları için incelenmiş olmasıdır. Düzlem şekil değiştirme kabulünün sonucunda ise sunulan ve oluşturulan abaklar sadece mütemadi temeller için geçerlidir. Bu çalışmanın amacı daha önceki çalışmalarda incelenmemiş olan temel şekil etkisinin şevler üzerine veya yakınına inşa edilen yüzeysel temellerin depremlı taşıma güçleri üzerine etkisinin incelenmesidir. Çalışmada kullanılan yaklaşım, güvenli tarafta kalarak deprem sırasında drenajsız davranışı göz önüne alacaktır. Bu amaçla üç boyutlu sonlu elemanlar modelleri oluşturulacak ve parametrik çalışma yapılacaktır. Parametrik çalışmada incelenecek etkiler temel şekli, boyutu, şeve uzaklığı, zeminin drenajsız mukavemeti, şev yüksekliği, şev açısı ve deprem ivmesidir. Depremin taşıma gücü üzerinde etkisi eşdeğer-dinamik yöntemle tanımlanacaktır. Hem zeminin, hem de yapısal yüklerin eylemsizliği modellerde tanımlanacaktır. Elde edilen sonuçlar kullanılarak tasarım abakları hazırlanacak, ortaya çıkabilecek temel kayması, taşıma gücü göçmesi, şev göçmesi, toptan göçme gibi farklı göçme sistemleri tartışılacaktır.

## TABLE OF CONTENTS

|  |      |
|--|------|
| ACKNOWLEDGEMENTS.....  | iv   |
| ABSTRACT.....  | v    |
| ÖZET .....   | vi   |
| LIST OF FIGURES .....  | ix   |
| LIST OF TABLES.....  | xxi  |
| LIST OF SYMBOLS .....  | xxii |
| LIST OF ACRONYMS/ABBREVIATIONS.....  | xxiv |
| 1. INTRODUCTION .....  | 1    |
| 2. LITERATURE REVIEW .....   | 3    |
| 2.1 Static Bearing Capacity of Shallow Foundation Around Cohesive Slopes ..... | 4    |
| 2.2 Seismic Bearing Capacity of Foundations Around Cohesive Slopes .....       | 22   |
| 2.3 Shape Effect of Shallow Foundation On Seismic Bearing Capacity .....       | 45   |
| 3. METHODOLOGY .....   | 81   |
| 3.1 FEM in Geotechnical Engineering and Plaxis 3D .....                        | 81   |
| 3.2 Definition and Assumptions of the Problem.....                             | 82   |
| 3.3 Suggested Solution Method .....  | 84   |
| 3.4 Model Geometry .....   | 85   |
| 3.5 Data Input in Plaxis 3D .....  | 86   |
| 3.5.1 General Settings .....   | 86   |
| 3.5.2 Numerical Model .....  | 89   |
| 3.5.3 Boundary Conditions .....  | 90   |
| 3.5.4 Loads.....   | 91   |
| 3.5.5 Material Properties .....  | 92   |
| 3.5.6 Finite Element Mesh Generation .....                                     | 94   |
| 3.6 Design Steps.....  | 94   |
| 3.7 Evaluation of Plaxis 3D Outputs.....                                       | 98   |
| 4. RESULTS AND DISCUSSIONS.....  | 100  |
| 4.1 Determination of Influential Parameters .....                              | 100  |
| 4.1.1 Influence of Horizontal Seismic Acceleration Coefficient.....            | 101  |

|   |     |
|---|-----|
| 4.1.2 Influence of Slope Angle .....  | 101 |
| 4.1.3 Influence of Slope Height .....   | 103 |
| 4.1.4 Influence of Slope Soil Strength .....  | 103 |
| 4.2 Examination of Failure Mechanisms .....   | 104 |
| 4.3 Design Charts .....   | 106 |
| 5. CONCLUSIONS .....  | 124 |
| REFERENCES .....  | 126 |
| APPENDIX A: LIST OF RESULTS OF FINITE ELEMENTS MODELS CREATED<br>FOR STATIC CONDITION ..... | 131 |
| APPENDIX B: LIST OF RESULTS OF FINITE ELEMENTS MODELS CREATED<br>FOR SEISMIC CONDITION..... | 135 |

## LIST OF FIGURES

|              |  |    |
|--------------|--|----|
| Figure 2.1.  | Plastic zones near the strip foundation on the face of a slope (Meyerhof, 1957) .....                                      | 5  |
| Figure 2.2.  | Factors of bearing capacity for the shallow foundation on a purely cohesive and granular slope (Meyerhof, 1957) .....      | 6  |
| Figure 2.3.  | Slip surfaces and plastic zones around the rough strip foundation on top of the slope (Meyerhof,1957) .....                | 7  |
| Figure 2.4.  | Factors of strip foundation's bearing capacity on a purely cohesive incline (Meyerhof, 1957) .....                         | 8  |
| Figure 2.5.  | Footings on or adjacent to a slope (Bowles,1997) .....   | 9  |
| Figure 2.6.  | Failure surfaces and stress trajectories in the plastic zone beneath the footing (Bowles, 1997).....                       | 10 |
| Figure 2.7.  | Bearing capacity factors ( $N'_c$ and $N'_q$ ) for footings on or adjacent to a slope (Bowles, 1997).....                  | 11 |
| Figure 2.8.  | Failure mechanism adopted for the upper bound solution (Kusakabe <i>et al.</i> , 1981) .....                               | 11 |
| Figure 2.9.  | No.1 design chart presented to calculate the dimensionless factor ( $\mu$ ) (Kusakabe <i>et al.</i> , 1981).....           | 12 |
| Figure 2.10. | No.2 and No.3 design charts presented to calculate the dimensionless factor ( $\mu$ ) Kusakabe <i>et al.</i> , 1981) ..... | 13 |

|              |  |    |
|--------------|--|----|
| Figure 2.11. | Schematic representation of the problem<br>(Georgiadis,2010).....  | 15 |
| Figure 2.12. | Modes of failure (a) and (b) failure of bearing capacity and (c) overall<br>failure of incline (Georgiadis, 2010).....   | 15 |
| Figure 2.13. | Variation of failure mode and $N_c$ with $H/B$ for $\lambda= 0$ and $\beta= 45^\circ$<br>(Georgiadis, 2010).....   | 16 |
| Figure 2.14. | Variety of $N_c$ with $\lambda$ for $c_u/\gamma B= 0.5$ (Georgiadis, 2010).....  | 17 |
| Figure 2.15. | Variety of $N_c$ with $\lambda$ for $c_u/\gamma B= 1$ (Georgiadis, 2010).....  | 17 |
| Figure 2.16. | Variety of $N_c$ with $\lambda$ for $c_u/\gamma B= 1.5$ (Georgiadis, 2010).....  | 18 |
| Figure 2.17. | Variety of $N_c$ with $\lambda$ for $c_u/\gamma B= 2, 2.5,$ and $5$ (Georgiadis, 2010).....  | 18 |
| Figure 2.18. | Variation of $\lambda_o$ with $\beta$ (Georgiadis, 2010).....  | 19 |
| Figure 2.19. | The applied forces and the mechanism of failure used in the examination<br>(Castelli and Motta, 2010).....   | 20 |
| Figure 2.20. | Variation of ground factors ( $N_c^*/N_c$ ) in a static condition with the<br>distance of foundation from the edge of the incline (Castelli and<br>Motta, 2010).....   | 21 |
| Figure 2.21. | Both sides mechanism of failure used in the study (Kumar and Rao,<br>2003).....  | 23 |
| Figure 2.22. | Single side mechanism of failure used in the study (Kumar and Rao,<br>2003).....   | 23 |
| Figure 2.23. | Change of $N_q$ with $\alpha h$ for various amounts of $\Phi$ and $\beta$ : (a) $\Phi= 10^\circ$ ;<br>(b) $\Phi= 20^\circ$ ; (c) $\Phi= 30^\circ$ ; (d) $\Phi= 40^\circ$ ; (e) $\Phi= 50^\circ$ (Kumar and Rao,<br>2003) ..... | 24 |

|              |  |    |
|--------------|--|----|
| Figure 2.24. | Change of $N_c$ with $ah$ for various amounts of $\Phi$ and $\beta$ : (a) $\Phi= 0^\circ$ ; (b) $\Phi= 10^\circ$ ; (c) $\Phi= 20^\circ$ ; (d) $\Phi= 30^\circ$ ; (e) $\Phi= 40^\circ$ ; (f) $\Phi= 50^\circ$ (Kumar and Rao, 2003) ..... | 25 |
| Figure 2.25. | Change of $N_\gamma$ with $ah$ for various amounts of $\Phi$ and $\beta$ : (a) $\Phi= 10^\circ$ ; (b) $\Phi= 20^\circ$ ; (c) $\Phi= 30^\circ$ ; (d) $\Phi= 40^\circ$ ; (e) $\Phi= 50^\circ$ (Kumar and Rao, 2003).....                   | 26 |
| Figure 2.26. | Graphical representation of the problem (Shiau <i>et al.</i> , 2006).....  | 27 |
| Figure 2.27. | Effect of $\tan\theta$ on $p/\gamma B$ for various $\Phi$ (Shiau <i>et al.</i> , 2006).....  | 28 |
| Figure 2.28. | Comparison of upper bound velocity diagrams for the effect of inertia forces (Shiau <i>et al.</i> , 2006).....   | 29 |
| Figure 2.29. | Effect of $q/\gamma B$ on $p/\gamma B$ for various $\beta$ (Shiau <i>et al.</i> , 2006).....   | 30 |
| Figure 2.30. | Effect of soil inertia $k_h$ on $p/\gamma B$ (Shiau <i>et al.</i> , 2006).....   | 30 |
| Figure 2.31. | Mechanism of failure used in the analysis (Yamamoto, 2010).....  | 32 |
| Figure 2.32. | Mechanisms of failure for various amounts of $\Phi$ , $\beta$ , $\alpha$ , and $K_h$ (Yamamoto, 2010).....   | 34 |
| Figure 2.33. | Charts of design for $N_{ce}$ ( $\Phi= 30^\circ, 40^\circ, D/B= 0, a= 0.0$ ) (Yamamoto, 2010).....   | 34 |
| Figure 2.34. | Charts of design for $N_{ce}$ ( $\Phi= 30^\circ, 40^\circ, D/B= 1, a= 0.0$ ) (Yamamoto, 2010).....   | 35 |
| Figure 2.35. | Charts of design for $N_{ce}$ ( $\Phi= 30^\circ, 40^\circ, D/B= 0, a= 0.5$ ) (Yamamoto, 2010).....   | 35 |
| Figure 2.36. | Charts of design for $N_{\gamma e}$ ( $\Phi= 30^\circ, 40^\circ, D/B= 0, a= 0.0$ ) (Yamamoto, 2010).....   | 35 |

|              |  |    |
|--------------|--|----|
| Figure 2.37. | Charts of design for $N_{\gamma e}$ ( $\Phi= 30^\circ, 40^\circ, D/B= 1, a= 0.0$ ) (Yamamoto, 2010).....   | 36 |
| Figure 2.38. | Charts of design for $N_{\gamma e}$ ( $\Phi= 30^\circ, 40^\circ, D/B= 0, a= 0.5$ ) (Yamamoto, 2010).....   | 36 |
| Figure 2.39. | $N_c^*/N_c$ rates as a function of the normalized $d/B$ distance of incline (Castelli and Motta, 2010).....  | 37 |
| Figure 2.40. | Model geometry and a typical FELA mesh.....  | 39 |
| Figure 2.41. | Comparison of the results of the present study with those presented by previous researchers (A. Keshavarz <i>et al.</i> , 2019).....                             | 40 |
| Figure 2.42. | Comparison of the variation in $N_c$ against $L/B$ for $\beta = 30^\circ$ ; $H/B=1, 2, 4$ ; and $c_{u0}/(\gamma B)=2.5$ (A. Keshavarz <i>et al.</i> , 2019)..... | 41 |
| Figure 2.43. | Variation of the $q_u/(\gamma B)$ with $L/B$ (A. Keshavarz <i>et al.</i> , 2019).....  | 41 |
| Figure 2.44. | The effect of $k_h$ on $q_u/(\gamma B)$ ( $H/B=3, c_{u0}/(\gamma B)=3.5$ , and $\beta=35^\circ$ ) (A. Keshavarz <i>et al.</i> , 2019).....                       | 42 |
| Figure 2.45. | Variation of $k_h q_u/c_{u0}$ against $k_h$ for the level ground (A. Keshavarz <i>et al.</i> , 2019).....  | 42 |
| Figure 2.46. | Typical foundation failure pattern for $c_{u0}/(\gamma B)= 4, k_B/c_{u0}=0, k_h =0.1, \beta=45^\circ, (H/B = 4)$ (A. Keshavarz <i>et al.</i> , 2019).....        | 43 |
| Figure 2.47. | The effect of $c_{u0} / (\gamma B)$ on the failure mode ( $k_B/c_{u0}=0, k_h =0, \beta=45^\circ, H/B = 1$ ) (A. Keshavarz <i>et al.</i> , 2019).....             | 44 |
| Figure 2.48. | The effect of $k_h$ on the failure mode $c_{u0} / (\gamma B) =4, (k_B/c_{u0}=0, L/B = 0, \beta=45^\circ, H/B =4)$ (A. Keshavarz <i>et al.</i> , 2019).....       | 44 |

|              |  |    |
|--------------|--|----|
| Figure 2.49. | Design charts for average values of lower and upper bounds of normalized bearing capacity of a rough strip footing located on slope with $\beta = 10^0$ (A. Keshavarz <i>et al.</i> , 2019).....                       | 45 |
| Figure 2.50. | Lower bound analysis of finite element coarse mesh (H. Yang <i>et al.</i> , 2003).....   | 46 |
| Figure 2.51. | Lower bound analysis of finite element fine mesh (H. Yang <i>et al.</i> , 2003)...   | 46 |
| Figure 2.52. | Comparison of 3-dimensional lower and bound bearing capacity $N_c$ for strip foundations on a weightless and purely adhesive soil (H. Yang <i>et al.</i> , 2003). .....  | 47 |
| Figure 2.53. | Various solutions for 3-dimensional bearing capacity for shallow foundations (H. Yang <i>et al.</i> , 2003).....   | 48 |
| Figure 2.54. | Shape and depth factors usually utilized for clays (Salgado <i>et al.</i> , 2004)...   | 50 |
| Figure 2.55. | Ratio of net bearing capacity factor to undrained shear strength, $q_{bL}^{net}/s_u$ , for foundations in clay (L = lower, U= upper bound) (Salgado <i>et al.</i> , 2004). .....                                       | 51 |
| Figure 2.56. | Constants of regression in the shape factor equation (Salgado <i>et al.</i> , 2004). .....   | 52 |
| Figure 2.57. | Shape factor for foundations of various shapes as a function of relative depth as calculated by limit analysis plotted together with best-fit lines with the form of Equation 2.25 (Salgado <i>et al.</i> , 2004)..... | 52 |
| Figure 2.58. | Finite element mesh (Zhu and Michalowski, 2005).....   | 53 |
| Figure 2.59. | The analogy of results: (a) factor $N_c$ and (b) factor $N_\gamma$ (Zhu and Michalowski, 2005).....  | 56 |

|              |   |    |
|--------------|---|----|
| Figure 2.60. | Factor $s_\gamma$ (finite element method) as a function of aspect ratio $L/B$ and internal friction angle $\varphi$ (Zhu and Michalowski, 2005).....                          | 57 |
| Figure 2.61. | Movement in the region of squared foundation: (a) 3-D distribution of vertical displacement intensity and (b) horizontal movement at surface (Zhu and Michalowski, 2005)..... | 57 |
| Figure 2.62. | Model test programme (Pathak <i>et al.</i> , 2008).....   | 58 |
| Figure 2.63. | Typical penetration response of a footing on strong over weak soils (Yu <i>et al.</i> , 2011).....  | 61 |
| Figure 2.64. | Typical finite element mesh (Yu <i>et al.</i> , 2011).....  | 62 |
| Figure 2.65. | Factors of bearing capacity for surface rough squared foundations on smooth soils (Yu <i>et al.</i> , 2011).....  | 63 |
| Figure 2.66. | $N_c$ for surface square foundations on two-layer weightless soils (small strain analyses) (Yu <i>et al.</i> , 2011).....   | 64 |
| Figure 2.67. | The meshing of the computational model (quarter symmetry) (Li <i>et al.</i> , 2009).....  | 65 |
| Figure 2.68. | Bearing capacity for rectangular foundations of different forms (Li <i>et al.</i> , 2009).....  | 66 |
| Figure 2.69. | Plan representation of the foundation's impact scope (Li <i>et al.</i> , 2009).....   | 67 |
| Figure 2.70. | Problem notation and potential failure mechanism (Shiau <i>et al.</i> , 2011).....  | 68 |
| Figure 2.71. | Bearing capacity of upper and lower bound for weightless slopes (smooth base, $\beta=90^\circ$ ) (Shiau <i>et al.</i> , 2011).....  | 69 |
| Figure 2.72. | The analogy of transformed forms and swiftness profiles for smooth and rough foundations ( $\beta=90^\circ$ , $L/B=0$ ) (Shiau <i>et al.</i> , 2011).....                     | 70 |

|              |   |    |
|--------------|---|----|
| Figure 2.73. | Upper Bound Results for Rough and Smooth Foundations ( $\beta=90^\circ$ )<br>(Shiau <i>et al.</i> , 2011).....  | 70 |
| Figure 2.74. | Averaged upper and lower bounds for different angles of inclination<br>(Shiau <i>et al.</i> , 2011).....  | 71 |
| Figure 2.75. | Averaged upper and lower bounds for different angles of inclination<br>(Shiau <i>et al.</i> , 2011).....  | 71 |
| Figure 2.76. | Velocity contours for different angles of inclination ( $c_u/\gamma B=5$ , $L/B=0$ ,<br>flat bottom) (Shiau <i>et al.</i> , 2011).....  | 72 |
| Figure 2.77. | Velocity contours for different angles of inclination ( $c_u/\gamma B=1$ , $L/B=0$ ,<br>flat bottom) (Shiau <i>et al.</i> , 2011).....  | 72 |
| Figure 2.78. | Impact of $L/B$ on the bearing capacity (smooth base ) (Shiau <i>et al.</i> , 2011)..   | 73 |
| Figure 2.79. | Velocity contours for different $L/B$ (smooth base, $\beta =90^\circ$ , $c_u/\gamma B=5$ )<br>(Shiau <i>et al.</i> , 2011).....   | 74 |
| Figure 2.80. | Effect of $H/B$ (flat bottom, $L/B=0$ ) (Shiau <i>et al.</i> , 2011).....   | 75 |
| Figure 2.81. | FE meshes: (a) half of a square footing; (b) half of a circular footing<br>(Islam <i>et al.</i> , 2017).....  | 76 |
| Figure 2.82. | Shape factor $s_c$ as a function of $\phi$ and $D/B$ : (a) comparison with previous<br>studies ( $D/B =0$ ); (b) square footing ; (c) circular footing (Islam <i>et al.</i> ,<br>2017).....                                     | 76 |
| Figure 2.83. | The failure mechanism is shown in plan view ( a and b ) and elevational<br>view ( c and d): (a) circular foundation: (b) square foundation: (c)<br>circular foundation: (d) square foundation (Islam <i>et al.</i> , 2017)..... | 77 |

|              |   |    |
|--------------|---|----|
| Figure 2.84. | Shape factor $s_y$ as a function of $\phi$ and D/B: (a) Comparison with previous studies (D/B=0); (b) Square footing; (c) circular footing. (Islam <i>et al.</i> , 2017)..... | 79 |
| Figure 2.85. | Continued (Islam <i>et al.</i> , 2017).....   | 79 |
| Figure 3.1.  | Graphical representation of the problem.....  | 83 |
| Figure 3.2.  | Three dimensional model of created finite elements model .....  | 86 |
| Figure 3.3.  | 'Project' tab sheet of 'General Settings' window .....  | 87 |
| Figure 3.4.  | 'Dimensions' tab sheet of 'General settings' window.....  | 88 |
| Figure 3.5.  | Distribution of nodes (.) and stress points ( x ) in a 15-node wedge element.....   | 89 |
| Figure 3.6.  | Schematic representation of created finite elements model.....  | 90 |
| Figure 3.7.  | Finite element mesh generation .....  | 94 |
| Figure 3.8.  | Typical view of "Calculation Module" window.....  | 95 |
| Figure 3.9.  | Typical view of 'Initial Phase' window.....   | 95 |
| Figure 3.10. | Activation of inertia force applying on soil clusters .....   | 96 |
| Figure 3.11. | The load stage ( $\Sigma$ -Mstage) found by Calculations module of Plaxis 3D for the final limit state .....  | 97 |
| Figure 3.12. | Failure mechanism obtained for the finite element model named as C_45_4_0_16_25_0.1_D and enlarged view of the failure mechanism .....  | 98 |
| Figure 3.13. | Shear surfaces obtained for the finite element model named as C_45_4_0_16_25_0.1_D .....  | 99 |

|              |  |     |
|--------------|--|-----|
| Figure 4.1.  | Variation of $N_{cse}$ with $k_h$ for $\lambda=0$ ( $\beta=15^\circ$ , $c_u/\gamma B = 2.5$ ) .....  | 101 |
| Figure 4.2.  | Variation of $N_{cse}$ with $\beta$ for $\lambda=0$ ( $k_h=0$ , $c_u/\gamma B = 2.5$ ).....  | 102 |
| Figure 4.3.  | Variation of $N_{cse}$ with $\beta$ for $\lambda=0$ ( $k_h=0.1$ , $c_u/\gamma B = 2.5$ ).....  | 102 |
| Figure 4.4.  | Variation of $N_{cse}$ with $\beta$ for $\lambda=0$ ( $k_h=0.2$ , $c_u/\gamma B = 2.5$ ).....  | 102 |
| Figure 4.5.  | Variation of $N_{cse}$ with $\beta$ for $\lambda=0$ ( $k_h=0.3$ , $c_u/\gamma B = 2.5$ ).....  | 103 |
| Figure 4.6.  | Variation of $N_{cse}$ with $c_u/\gamma B$ for all $k_h$ values ( $\beta=30^\circ$ , $L/B=1$ , $\lambda=0$ ). .....  | 104 |
| Figure 4.7.  | Base failure due to self-weight of cohesive slope ( $\beta=45^\circ$ , $H/B=4.0$ m,<br>and $c_u/\gamma B = 0.625$ ) .....  | 105 |
| Figure 4.8.  | Base failure due to self-weight of cohesive slope ( $\beta=45^\circ$ , $H/B=4.0$ m,<br>$c_u/\gamma B = 0.625$ and $k_h=0.2$ ).....   | 105 |
| Figure 4.9.  | Typical “Foundation failure” approaches for $\lambda=0$ condition (a) $\beta=45^\circ$ ,<br>$H/B=1.0$ m, $c_u/\gamma B = 1.25$ and $k_h=0.2$ ); (b) $\beta=45^\circ$ , $H/B=2.0$ m,<br>$c_u/\gamma B = 0.625$ and $k_h=0.1$ )..... | 106 |
| Figure 4.10. | Variation of bearing capacity factor with horizontal seismic acceleration<br>coefficient for $\beta=15^\circ$ .....  | 107 |
| Figure 4.11. | Variation of bearing capacity factor with horizontal seismic acceleration<br>coefficient for $\beta=15^\circ$ .....  | 107 |
| Figure 4.12. | Variation of bearing capacity factor with horizontal seismic acceleration<br>coefficient for $\beta=15^\circ$ .....  | 108 |
| Figure 4.13. | Variation of bearing capacity factor with horizontal seismic acceleration<br>coefficient for $\beta=15^\circ$ .....  | 108 |

|              |  |     |
|--------------|--|-----|
| Figure 4.14. | Variation of bearing capacity factor with horizontal seismic acceleration coefficient for $\beta=15^\circ$ ..... | 109 |
| Figure 4.15. | Variation of bearing capacity factor with horizontal seismic acceleration coefficient for $\beta=15^\circ$ ..... | 109 |
| Figure 4.16. | Variation of bearing capacity factor with horizontal seismic acceleration coefficient for $\beta=15^\circ$ ..... | 110 |
| Figure 4.17. | Variation of bearing capacity factor with horizontal seismic acceleration coefficient for $\beta=15^\circ$ ..... | 110 |
| Figure 4.18. | Variation of bearing capacity factor with horizontal seismic acceleration coefficient for $\beta=15^\circ$ ..... | 111 |
| Figure 4.19. | Variation of bearing capacity factor with horizontal seismic acceleration coefficient for $\beta=15^\circ$ ..... | 111 |
| Figure 4.20. | Variation of bearing capacity factor with horizontal seismic acceleration coefficient for $\beta=15^\circ$ ..... | 112 |
| Figure 4.21. | Variation of bearing capacity factor with horizontal seismic acceleration coefficient for $\beta=30^\circ$ ..... | 112 |
| Figure 4.22. | Variation of bearing capacity factor with horizontal seismic acceleration coefficient for $\beta=30^\circ$ ..... | 113 |
| Figure 4.23. | Variation of bearing capacity factor with horizontal seismic acceleration coefficient for $\beta=30^\circ$ ..... | 113 |
| Figure 4.24. | Variation of bearing capacity factor with horizontal seismic acceleration coefficient for $\beta=30^\circ$ ..... | 114 |

|              |  |     |
|--------------|--|-----|
| Figure 4.25. | Variation of bearing capacity factor with horizontal seismic acceleration coefficient for $\beta=30^\circ$ ..... | 114 |
| Figure 4.26. | Variation of bearing capacity factor with horizontal seismic acceleration coefficient for $\beta=30^\circ$ ..... | 115 |
| Figure 4.27. | Variation of bearing capacity factor with horizontal seismic acceleration coefficient for $\beta=30^\circ$ ..... | 115 |
| Figure 4.28. | Variation of bearing capacity factor with horizontal seismic acceleration coefficient for $\beta=30^\circ$ ..... | 116 |
| Figure 4.29. | Variation of bearing capacity factor with horizontal seismic acceleration coefficient for $\beta=30^\circ$ ..... | 116 |
| Figure 4.30. | Variation of bearing capacity factor with horizontal seismic acceleration coefficient for $\beta=30^\circ$ ..... | 117 |
| Figure 4.31. | Variation of bearing capacity factor with horizontal seismic acceleration coefficient for $\beta=30^\circ$ ..... | 117 |
| Figure 4.32. | Variation of bearing capacity factor with horizontal seismic acceleration coefficient for $\beta=45^\circ$ ..... | 118 |
| Figure 4.33. | Variation of bearing capacity factor with horizontal seismic acceleration coefficient for $\beta=45^\circ$ ..... | 118 |
| Figure 4.34. | Variation of bearing capacity factor with horizontal seismic acceleration coefficient for $\beta=45^\circ$ ..... | 119 |
| Figure 4.35. | Variation of bearing capacity factor with horizontal seismic acceleration coefficient for $\beta=45^\circ$ ..... | 119 |

|              |  |     |
|--------------|--|-----|
| Figure 4.36. | Variation of bearing capacity factor with horizontal seismic acceleration coefficient for $\beta=45^\circ$ ..... | 120 |
| Figure 4.37. | Variation of bearing capacity factor with horizontal seismic acceleration coefficient for $\beta=45^\circ$ ..... | 120 |
| Figure 4.38. | Variation of bearing capacity factor with horizontal seismic acceleration coefficient for $\beta=45^\circ$ ..... | 121 |
| Figure 4.39. | Variation of bearing capacity factor with horizontal seismic acceleration coefficient for $\beta=45^\circ$ ..... | 121 |
| Figure 4.40. | Variation of bearing capacity factor with horizontal seismic acceleration coefficient for $\beta=45^\circ$ ..... | 122 |
| Figure 4.41. | Variation of bearing capacity factor with horizontal seismic acceleration coefficient for $\beta=45^\circ$ ..... | 122 |
| Figure 4.42. | Variation of bearing capacity factor with horizontal seismic acceleration coefficient For $\beta=45^\circ$ ..... | 123 |
| Figure 4.43. | Variation of bearing capacity factor with horizontal seismic acceleration coefficient for $\beta=0^\circ$ .....  | 123 |

## LIST OF TABLES

|            |  |    |
|------------|--|----|
| Table 2.1. | Comparison of 3-dimensional upper and lower bound coefficient of bearing capacity $N_c$ for shallow foundations on a weightless and frictional cohesive soil ..... | 48 |
| Table 2.2. | Soil characteristics .....   | 59 |
| Table 2.3. | Ultimate bearing capacity (UBC) for footings .....   | 60 |
| Table 3.1. | Physical and elastic properties of rigid plate element .....   | 90 |
| Table 3.2. | Horizontal seismic acceleration coefficients .....   | 91 |
| Table 3.3. | Properties of the cohesive slope soils employed in present study .....   | 93 |

## LIST OF SYMBOLS

|             |  |
|-------------|--|
| $B$         | Footing width  |
| $c_u$       | Undrained shear strength of cohesive slope soil                                  |
| $d_{eq}$    | Equivalent plate thickness   |
| $D_f$       | Depth of footing   |
| $EA$        | Axial stiffness of the plate element   |
| $EI$        | Flexural stiffness of the plate element  |
| $E_u$       | Undrained elasticity modulus of cohesive soil                                    |
| $g$         | Gravitational acceleration   |
| $q_c$       | Seismic bearing capacity of surficial strip footings near cohesive slopes        |
| $H$         | Slope height   |
| $L$         | Length of foundation   |
| $k_h$       | Horizontal seismic acceleration coefficient                                      |
| $k_x$       | Permeability in horizontal direction (x axis)                                    |
| $k_y$       | Permeability in vertical direction ( y axis)                                     |
| $\alpha_u$  | Undrained dilatancy angle  |
| $\varphi_u$ | Undrained friction angle   |
| $N_{ce}$    | Seismic bearing capacity factor for surficial strip footings on level ground     |
| $N_{cse}$   | Seismic bearing capacity factor of surficial strip footings near cohesive slopes |
| $N_{cs}$    | Static bearing capacity factor for surficial strip footings near cohesive slopes |
| $R_{inter}$ | Interface strength reduction factor  |
| $R^2$       | Correlation coefficient  |
| $u_x$       | Nodal displacement in horizontal direction (x axis)                              |
| $u_y$       | Nodal displacement in vertical direction (y axis)                                |
| $w$         | Weight of the plate element  |

|                    |   |
|--------------------|---|
| $\beta$            | Slope angle                                     |
| $W$                | Weight of slope                                 |
| $\gamma_{sat}$     | Soil unit weight below phreatic level           |
| $\gamma_{unsat}$   | Soil unit weight above phreatic level           |
| $\lambda$          | Normalized footing distance from the slope edge |
| $\nu$              | Poisson ratio of the plate element              |
| $\nu_u$            | Undrained Poisson ratio of soil                 |
| $\Sigma M_{stage}$ | Magnitude of the applied load on ground         |

**LIST OF ACRONYMS/ABBREVIATIONS**

|        |  |
|--------|--|
| WSDOT  | Washington State Department of Transportation                  |
| AASHTO | American Association of State Highway Transportation Officials |
| FEM    | Finite Elements Method   |
| RITSS  | Remeshing and Interpolation Method with Small Strain Model     |
| UU     | Unconsolidated-Undrained                                       |

## 1. INTRODUCTION

Foundation is the lowest and most important part of structure that transfer the loads from structure to ground. Especially, it has become a big deal with high-rise structures touching the sky. Therefore, a well design of foundation must be deeply considered about the bearing capacity of the soil.

Foundations are divided into two main categories as shallow and deep foundations depending on the location of the load bearing layer. If the layer of soil of foundation which is satisfactory for load bearing, structure can be supported by shallow footings. Spread footings and mat foundations also can be regarded as shallow foundations. On the other hand, if the upper strata is not strong to carry itself in weight or more compressible, structure may be supported by deep foundations.

A shallow foundation is preferred when surface soils are enough strong and stiff to carry the applied loads. It has an important type of foundation because of utilization and affordable of it. Shallow foundations are commonly built close to the finished ground surface.

Bearing capacity is net bearing pressure that causes the foundation failure. The assumption of the bearing capacity of a shallow foundations has become a big deal for geotechnical engineering. Slopes can be exposed different loads. Seismic loads may cause serious defects to soil and foundations. Due to seismic events, foundations can tend to a decline at limit bearing pressure and increment in compressibility. Therefore, design of foundations in seismic region needs different precaution compared to the static condition.

Analytical and numerical approaches are possible to assess seismic bearing capacity of shallow footings such as the limit equilibrium method, limit analysis and finite element analysis for the calculation of the seismic bearing capacity coefficients needed for the design of the foundation. Since the pseudo-static approach is more practical and simple, the analyses are based on pseudo-static method.

The main purpose of this study is to present suitable design charts for the determination of undrained seismic bearing capacity factor linked with various shape of shallow foundations. The method used in this study will take account the undrained conditions because undrained circumstances are related to the most significant conditions. In the present study, the finite element method is used to evaluate the seismic bearing capacity of shallow foundations on soil which satisfies Mohr-Coulomb strength criterion, different slope angles and seismic coefficients. More than 1000 analyses were carried out in PLAXIS 3D to investigate the shape effect of shallow footings on undrained seismic bearing capacity. Lastly, the final purpose is to pioneer research studies in the literature for showing the effect of different shapes when seismic bearing capacity problem is regarded for shallow foundations.

## 2. LITERATURE REVIEW

This thesis aims to look at the issue of 'real life' shallow foundation states, in a foundation at nearby positions to human-made slopes consisting of pure cohesive soil. Foundations are modelled to transmit and spread their loading to the underneath soil. Three main design criteria play an essential role to ensure the stability of foundations, respectively ultimate bearing capacity, settlement, and the cost feasibility of foundation. Primarily in this dissertation, the shallow foundation's bearing capacity on cohesive soil will be handled.

When the soil backing of foundation fails in shear, bearing capacity failure happens, which can include different type of failure mechanism, namely; punching, local, and general shear failure (Bowles,1988). In geotechnical engineering, prediction and determination of the final bearing capacity are one of the most fundamental and problematic issues (Poulos *et al.*,2001)

'Literature review' section is composed of three parts, as briefly explained in the 'Introduction' section of the thesis. First of all, the static bearing of various shape footings will be handled using past studies. The main reason for addressing these studies is that the certainties of the advanced numerical model are investigated by comparing numerical model results with those obtained by previous researchers mentioned in Chapter 2.1.

Secondly, we will mention experimental investigations of shallow foundations seismic bearing capacity on cohesive soils around inclinations. According to the results of those studies mentioned in Chapter 2.2 are shed light on investigating the accuracy of developed numerical model results.

Lastly, research studies related to shape effects on the bearing capacity of various footings located on cohesive slopes which have been investigated so far will be examined. There are very few literature that exist related to analytical studies for circular, rectangular, and square foundations on slopes. Therefore, Chapter 2.3 will contribute to the studies and shed light on this matter.

## 2.1. Static Bearing Capacity of Shallow Foundation Around Cohesive Slopes

Shallow foundations which are generally referred to as footings can be divided into two types as per the following;

- (i). Spread footings, which are supported by a single structural member.
- (ii). Strip footings, which are supported by two or more structural members.

On slopes, near the hills or close to proposed excavation are the places where civil engineering structures are generally imposed to be built on. The investigation of bearing capacity of loaded slopes is crucial in this case because they are more susceptible to failure than other types of earth structures.

While in cohesive soil, the bearing capacity of the building may be stabilized, in the case of noncohesive soils, the bearing capacity is entirely determined by foundation failure (Saran *et al.*, 1989).

Nowadays, researchers have presented a variety of techniques to establish the bearing capacity for shallow foundations on a slope, which some of them are as follows:

- (i). Limit equilibrium analysis
- (ii). Slip line analysis
- (iii). Limit analysis
- (iv). Finite element analysis

Meyerhof (1957) is the prominent research study which has been adopted by well-known design manuals such as "Standard Specification of Highway Bridges," Washington State Department of Transportation (WSDOT, 2005), "Geotechnical Design Manual.", and the American Association of State Highway Transportation Officials (AASHTO, 1996). He proposed a methodology combining bearing capacity theory for foundations on level ground with slope stability theory in order to determine the static final bearing capacity of a footing on or near cohesive and granular inclines.

Meyerhof (1957) pointed out that the final bearing capacity of a footing placed on the surface of the incline or close to the edge of the hill can be obtained using by Equation 2.1 and nature of plastic zones evolved in soil under the continuous foundation in both cases are indicated in Figure 2.1.

$$q_c = cN_{cq} + \frac{1}{2}\gamma B N_{\gamma q} \quad (2.1)$$

$N_{cq}$  and  $N_{\gamma q}$  are the bearing capacity factors assigned depending on inclination angle ( $\beta$ ), angle of internal friction ( $\Phi$ ) and the depth of footing to footing width ( $D/B$ ) ratio, and the unit weight of soil; and the footing width indicated by  $\gamma$  and  $B$  respectively.

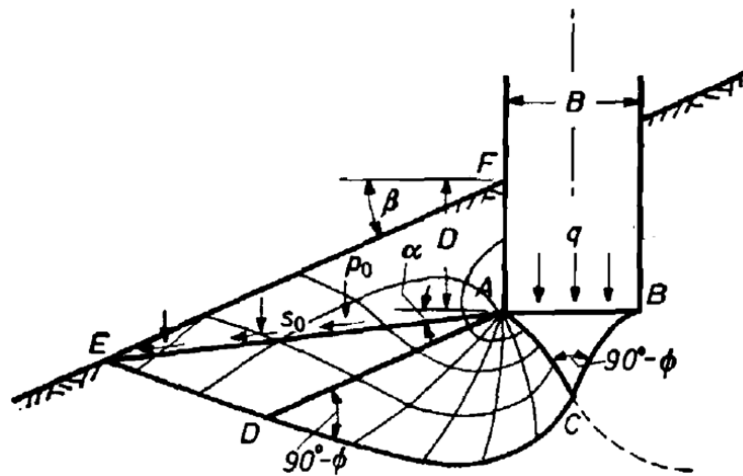


Figure 2.1. Plastic zones near the strip foundation on the face of a slope (Meyerhof, 1957).

Footing's static final bearing capacity on a cohesive incline is calculated by the given formula shown in Equation 2.2.

$$q_u = c_u N_{cq} \quad (2.2)$$

where  $q_u$  is the final bearing capacity of a strip footing;  $c_u$  is the undrained shear strength;  $N_{cq}$  is the factor of bearing capacity determined depending on slope angle ( $\beta$ ); rate of footing depth to footing width ( $D/B$ ) and slope stability number ( $N_s = \gamma H / c_u$ );  $\gamma$  is the soil's unit weight;  $B$  is the width of footing ;  $D$  is the footing depth .

The bearing capacity factor ( $N_{cq}$ ) given in Equation 2.2 is determined by using design charts shown in Figure 2.2.

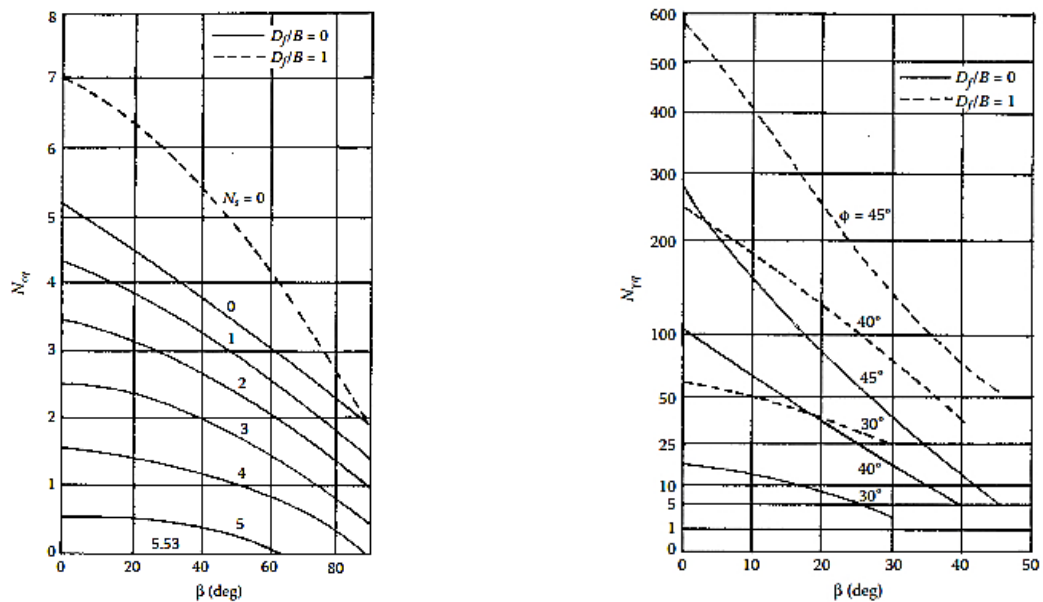


Figure 2.2. Factors of bearing capacity for the shallow foundation on a purely cohesive and granular slope (Meyerhof, 1957).

When the charts are compared, the inclination of the slope angle increases with the decrease of the bearing capacity. Furthermore, the reduction of bearing capacity on cohesive soils is less than granular soils for slope angles ( $\beta < 30^\circ$ ) that figured by author.

The author defined that the plastic zone on the slope side is reasonably smaller compared to the similar foundation on leveled ground, which indicates that the length of the failure surface is decreased and in turn will reduce the resistance of the soil.

Ultimate footing's bearing capacity on cohesive soil located near the top edge of the incline might result in some cases on the overall stability of the slope. When the ultimate bearing capacity is exceeded, Meyerhof (1957) assumed three types of failure mechanisms for this situation. These are foundation failure, toe failure, and base failure, respectively. Foundation failure is defined as where failure surface intersects with slope surface above the slope toe level. Another two failure modes can also be called as 'slope failure.' While the failure surface passes from the edge of the slope, base failure passes under the toe level as footing exceeds its bearing capacity. These failure modes are depicted in Figure 2.3 below.

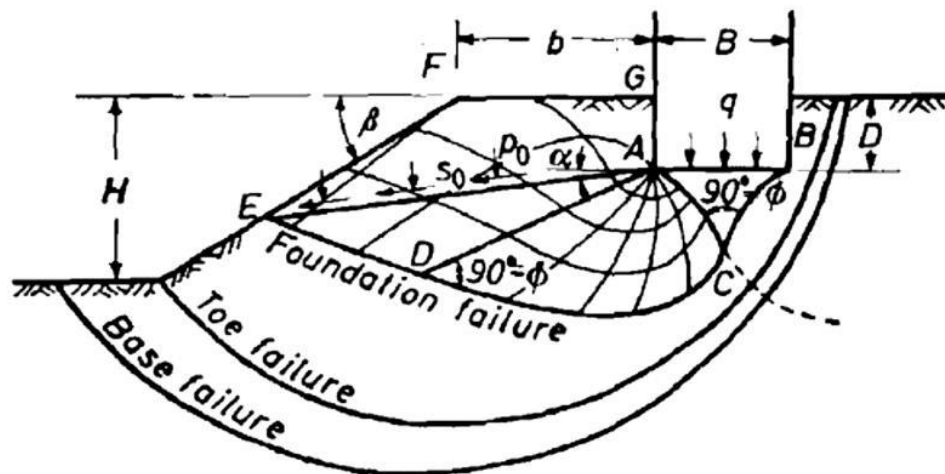


Figure 2.3. Slip surfaces and plastic zones around the rough strip foundation on top of the slope (Meyerhof,1957).

In Equation 2.2, a theoretical connection is presented for the final bearing capacity of shallow rigid foundations located on a slope (Meyerhof, 1957). In this equation, bearing capacity coefficient ( $N_{cq}$ ) given in Equation 2.2 is calculated by using the design chart shown in Figure 2.4. Bearing capacity coefficient ( $N_{cq}$ ) is a function rate of footing depth to width of footing ( $D/B$ ), angle of slope ( $\beta$ ), stability number of slope ( $N_s = \gamma H / c_u$ ) and the ratio of

the distance between the footing and the slope edge to the slope height ( $b/H$ ). As shown in Figure 2.4, the impact of slope stability is remarkable when compared to the effect of slope angle on the footing's bearing capacity in static conditions. The more distance between the footing and slope edge, the higher the bearing capacity coefficient will be. When a footing is more than twice the slope height away from the inclined edge, the static final footing's bearing capacity is not affected by the slope angle.

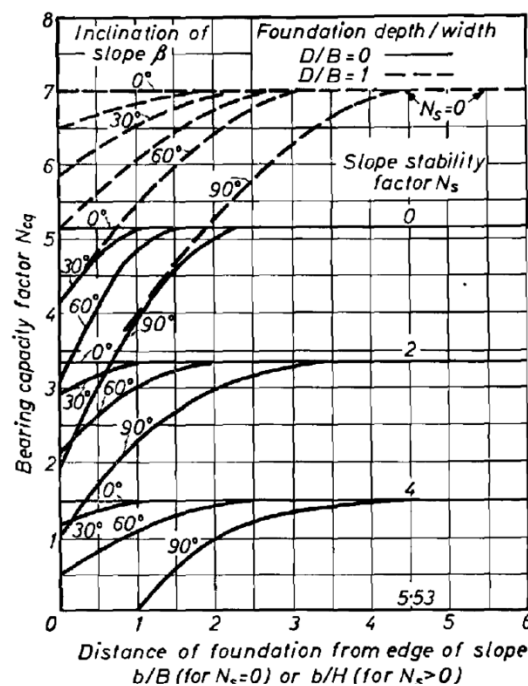


Figure 2.4. Factors of strip foundation's bearing capacity on a purely cohesive incline (Meyerhof, 1957).

Bowles (1997) proposed a model of a compiled computer code to predict the static final bearing capacity of a footing near inclines or excavations and developed the design table in Figure 2.7. Mathematical equations are shown in Figure 2.5 and have been employed after the obtained failure surface. A new bearing capacity coefficient is computed using the approach mentioned below. It should be pointed out that failure surfaces occurred under an equal footing placed on level ground (refer to Figure 2.6) are considered.

- The reduced bearing capacity factor ( $N_c$ ) based on the failure surface  $ade=L_0$  of Figure 2.6 and the failure surface  $adE=L_1$  of Figure 2.5 to derive

$$N'_c = N_c \frac{L_1}{L_0} \quad (2.3)$$

- Calculate a reduced  $N_q$  based on the ratio of area  $ecfg$  ( $A_0$ ) of Figure 2.6 to the equivalent area  $Efg=A_1$  (footings on the slope) or  $Efgh=A_1$  (footings near slope) of Figure 2.5 to derive the equation in below

$$N'_q = N_q \frac{A_1}{A_0} \quad (2.4)$$

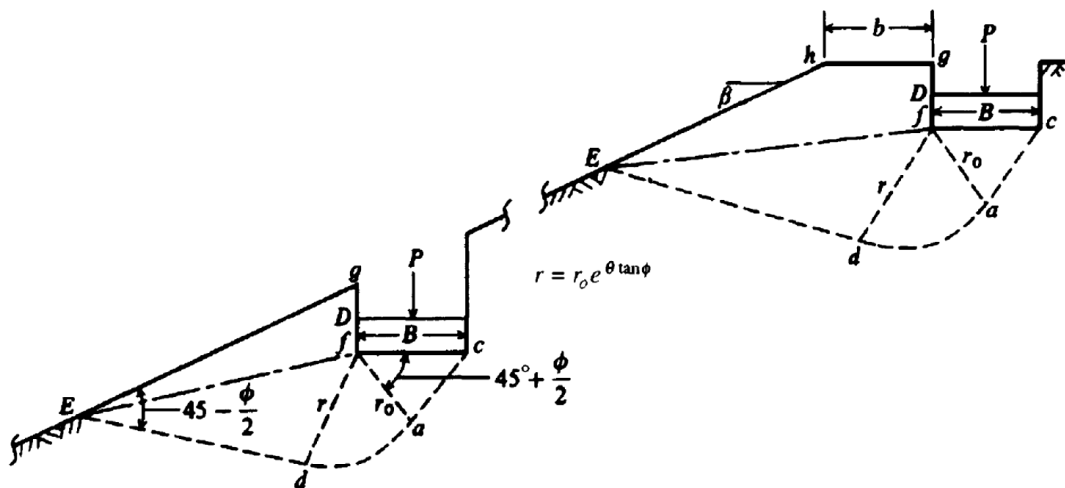


Figure 2.5. Footings on or adjacent to a slope (Bowles, 1997).

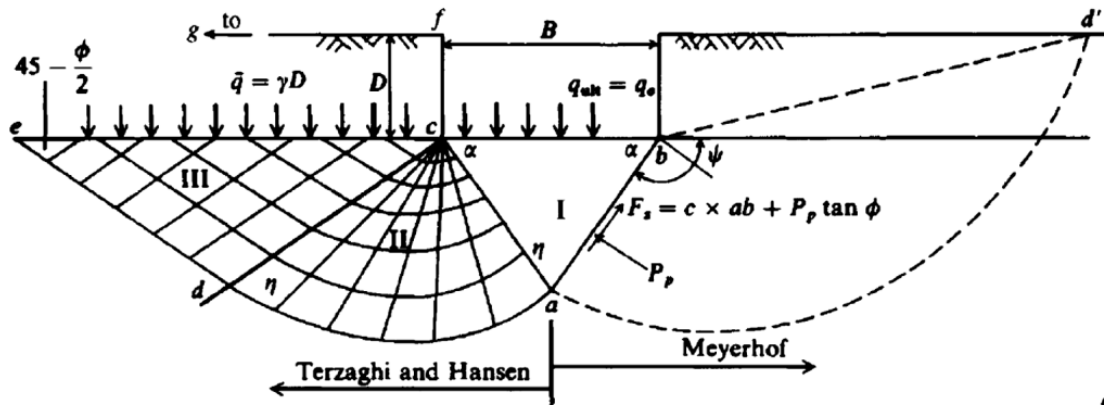


Figure 2.6. Failure surfaces and stress trajectories in the plastic zone beneath the footing (Bowles, 1997).

The design table presented in Figure 2.7. should be integrated with bearing capacity equation given by Hansen in order to calculate the static strip foundations' bearing capacity located near to cohesive inclines. In Figure 2.7., it is seen that ( $N'_c$  and  $N'_q$ ) as bearing capacity coefficients are function of slope angle ( $\beta$ ), rate footing depth to width of footing ( $D/B$ ), ratio of distance between the footing and slope edge to width of footing ( $b/B$ ) and internal friction angle ( $\phi_u=0^\circ$ ). It is noted that the area ratio given in Equation 2.4 equals to unity or the rate of ( $b/B$ ) changes between 1.5 and 2, reducing effect because of the presence of slope on bearing capacity coefficients disappears.

| $\beta \downarrow$ | $\Phi \rightarrow$ | $D/B = 0$ |      |       |       |       | $b/B = 0$ |      |       |       |       | $D/B = 0.75$ |      |       |       |       | $b/B = 0$ |      |       |       |       | $D/B = 1.50$ |      |       |       |       | $b/B = 0$ |      |       |       |       |
|--------------------|--------------------|-----------|------|-------|-------|-------|-----------|------|-------|-------|-------|--------------|------|-------|-------|-------|-----------|------|-------|-------|-------|--------------|------|-------|-------|-------|-----------|------|-------|-------|-------|
|                    |                    | 0         | 10   | 20    | 30    | 40    | 0         | 10   | 20    | 30    | 40    | 0            | 10   | 20    | 30    | 40    | 0         | 10   | 20    | 30    | 40    | 0            | 10   | 20    | 30    | 40    | 0         | 10   | 20    | 30    | 40    |
| $0^\circ$          | $N'_c =$           | 5.14      | 8.35 | 14.83 | 30.14 | 75.31 | 5.14      | 8.35 | 14.83 | 30.14 | 75.31 | 5.14         | 8.25 | 14.83 | 30.14 | 75.31 | 5.14      | 8.35 | 14.83 | 30.14 | 75.31 | 5.14         | 8.35 | 14.83 | 30.14 | 75.31 | 5.14      | 8.35 | 14.83 | 30.14 | 75.31 |
|                    | $N'_q =$           | 1.03      | 2.47 | 6.40  | 18.40 | 64.20 | 1.03      | 2.47 | 6.40  | 18.40 | 64.20 | 1.03         | 2.47 | 6.40  | 18.40 | 64.20 | 1.03      | 2.47 | 6.40  | 18.40 | 64.20 | 1.03         | 2.47 | 6.40  | 18.40 | 64.20 | 1.03      | 2.47 | 6.40  | 18.40 | 64.20 |
| $10^\circ$         | $N'_c =$           | 4.89      | 7.80 | 13.37 | 26.80 | 64.42 | 5.14      | 8.35 | 14.83 | 30.14 | 75.31 | 5.14         | 8.35 | 14.83 | 30.14 | 75.31 | 5.14      | 8.35 | 14.83 | 30.14 | 75.31 | 5.14         | 8.35 | 14.83 | 30.14 | 75.31 | 5.14      | 8.35 | 14.83 | 30.14 | 75.31 |
|                    | $N'_q =$           | 1.03      | 2.47 | 6.40  | 18.40 | 64.20 | 0.92      | 1.95 | 4.43  | 11.16 | 33.94 | 1.03         | 2.47 | 6.40  | 18.40 | 64.20 | 1.03      | 2.47 | 6.40  | 18.40 | 64.20 | 1.03         | 2.47 | 6.40  | 18.40 | 64.20 | 1.03      | 2.47 | 6.40  | 18.40 | 64.20 |
| $20^\circ$         | $N'_c =$           | 4.63      | 7.28 | 12.39 | 23.78 | 55.01 | 5.14      | 8.35 | 14.83 | 30.14 | 66.81 | 5.14         | 8.35 | 14.83 | 30.14 | 75.31 | 5.14      | 8.35 | 14.83 | 30.14 | 75.31 | 5.14         | 8.35 | 14.83 | 30.14 | 75.31 | 5.14      | 8.35 | 14.83 | 30.14 | 75.31 |
|                    | $N'_q =$           | 1.03      | 2.47 | 6.40  | 18.40 | 64.20 | 0.94      | 1.90 | 4.11  | 9.84  | 28.21 | 1.03         | 2.47 | 6.40  | 18.40 | 64.20 | 1.03      | 2.47 | 6.40  | 18.40 | 64.20 | 1.03         | 2.47 | 6.40  | 18.40 | 64.20 | 1.03      | 2.47 | 6.40  | 18.40 | 64.20 |
| $25^\circ$         | $N'_c =$           | 4.51      | 7.02 | 11.82 | 22.38 | 50.80 | 5.14      | 8.35 | 14.83 | 28.76 | 62.18 | 5.14         | 8.35 | 14.83 | 30.14 | 73.57 | 5.14      | 8.35 | 14.83 | 30.14 | 73.57 | 5.14         | 8.35 | 14.83 | 30.14 | 73.57 | 5.14      | 8.35 | 14.83 | 30.14 | 73.57 |
|                    | $N'_q =$           | 1.03      | 2.47 | 6.40  | 18.40 | 64.20 | 0.92      | 1.82 | 3.85  | 9.00  | 25.09 | 1.03         | 2.47 | 6.40  | 18.40 | 64.20 | 1.03      | 2.47 | 6.40  | 18.40 | 64.20 | 1.03         | 2.47 | 6.40  | 18.40 | 64.20 | 1.03      | 2.47 | 6.40  | 18.40 | 64.20 |
| $30^\circ$         | $N'_c =$           | 4.38      | 6.77 | 11.28 | 21.05 | 46.88 | 5.14      | 8.35 | 14.83 | 27.14 | 57.76 | 5.14         | 8.35 | 14.83 | 30.14 | 68.64 | 5.14      | 8.35 | 14.83 | 30.14 | 68.64 | 5.14         | 8.35 | 14.83 | 30.14 | 68.64 | 5.14      | 8.35 | 14.83 | 30.14 | 68.64 |
|                    | $N'_q =$           | 1.03      | 2.47 | 6.40  | 18.40 | 64.20 | 0.88      | 1.71 | 3.54  | 8.08  | 21.91 | 1.03         | 2.47 | 6.40  | 18.40 | 64.20 | 1.03      | 2.47 | 6.40  | 18.40 | 64.20 | 1.03         | 2.47 | 6.40  | 18.40 | 64.20 | 1.03      | 2.47 | 6.40  | 18.40 | 64.20 |
| $60^\circ$         | $N'_c =$           | 3.62      | 5.33 | 8.33  | 14.34 | 28.56 | 4.70      | 6.83 | 10.55 | 17.85 | 34.84 | 5.14         | 8.34 | 12.76 | 21.37 | 41.12 | 5.14      | 8.34 | 12.76 | 21.37 | 41.12 | 5.14         | 8.34 | 12.76 | 21.37 | 41.12 | 5.14      | 8.34 | 12.76 | 21.37 | 41.12 |
|                    | $N'_q =$           | 1.03      | 2.47 | 6.40  | 18.40 | 64.20 | 0.37      | 0.63 | 1.17  | 2.36  | 5.52  | 0.62         | 1.04 | 1.83  | 3.52  | 7.80  | 0.62      | 1.04 | 1.83  | 3.52  | 7.80  | 0.62         | 1.04 | 1.83  | 3.52  | 7.80  | 0.62      | 1.04 | 1.83  | 3.52  | 7.80  |

Figure 2.7. Bearing capacity factors ( $N'_c$  and  $N'_q$ ) for footings on or adjacent to a slope (Bowles, 1997).

Kusakabe *et al.* (1981) suggested an approach to determine the final bearing capacity of a footing located around the slope using an upper bound solution with the mechanism of failure that is shown in Figure 2.8. A failure mechanism which was responsible for this problem is shown in Figure 2.8, where  $\beta$ =slope angle, the  $\alpha B$ =distance incline edge,  $HB$ =height of incline,  $hB$ =failure point depth 'A' on the face of the slope.

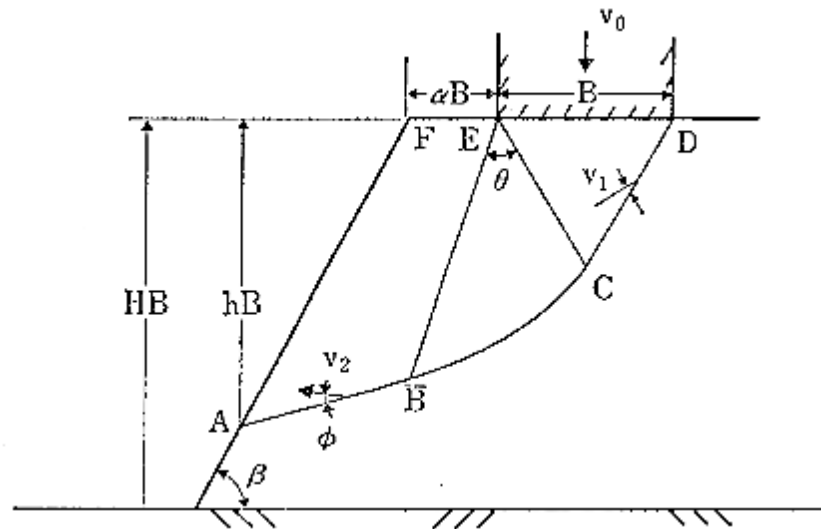


Figure 2.8. Failure mechanism adopted for the upper bound solution (Kusakabe *et al.*,1981).

The author adopted the limit analysis upper bound theorem to reach the static ultimate bearing capacity of a footing located adjacent near slope given by Equation 2.5.

$$q_s = \mu q_L \quad (2.5)$$

Authors compared their results with bearing capacities obtained from those of previous studies and concluded that results were in good agreement with previous findings. Bearing capacity factor  $N_c$  varies with  $c/\gamma B$  parameter. According to the author, this parameter has

a positive impact on bearing capacity factor ( $N_c$ ).  $c/\gamma B$  parameter was defined as 0.5, 1, 2. It was also mentioned experimental tests, in which Kanto loam was used, can be regarded undrained due to the rapid loading capacity of the test devices. During the test period, both mechanical and physical properties were used. Details of the test apparatus can be obtained in detail in the related reference (Kusakabe *et al.*, 1981).

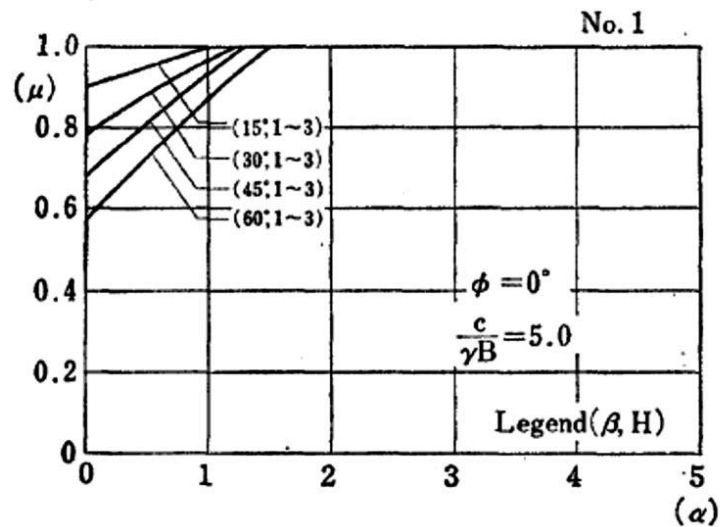
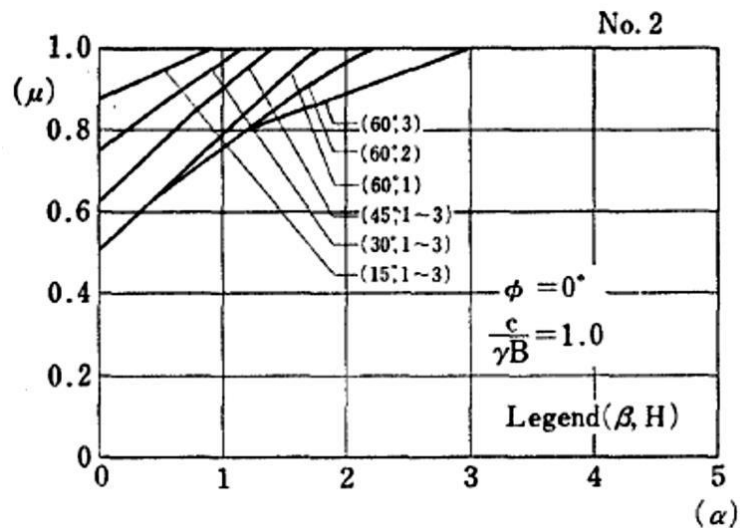


Figure 2.9. No.1 design chart presented to calculate the dimensionless factor ( $\mu$ ) (Kusakabe *et al.*, 1981).



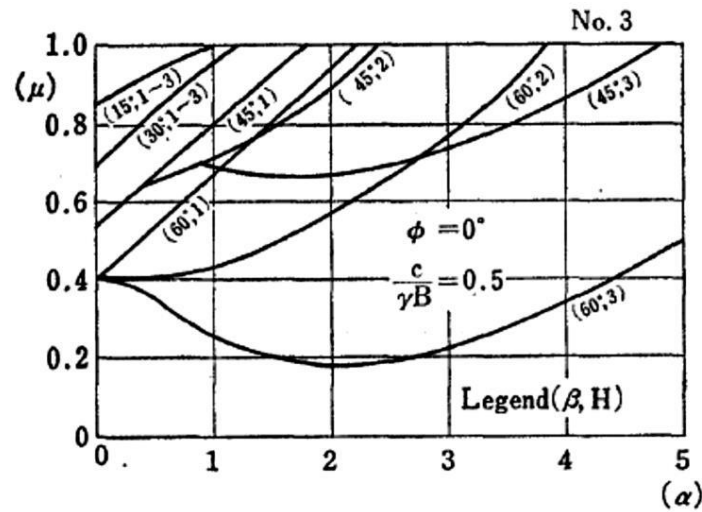


Figure 2.10. No.2 and No.3 design charts presented to calculate the dimensionless factor  $(\mu)$  (Kusakabe *et al.*, 1981).

Unconfined compression strengths of consolidated samples were measured in this study (Kusakabe *et al.*, 1981). The results of obtained from the proposed calculation method are less than the results found during experimental model tests; failure surfaces observed the preliminary tests were in good agreement with expected failure surfaces. It is concluded that computed bearing capacity values using the proposed method are less than that found in the model tests. This is primarily based on the effect of the side friction in the test apparatus. Another reason is the variation in stress states between those assumed in the proposed methodology and those established in test models.

To study the impact of the different parameters on undrained bearing capacity, Georgiadis (2010) presented the finite element analysis of shallow foundations located around undrained soil inclines. The author suggested that undrained bearing capacity of a surficial strip footing near slopes can be computed as the following Equation 2.6.

$$q_u = \frac{V_u}{B} = c_u N_c \quad (2.6)$$

Where  $q_u$  is the near slope ultimate footing static bearing capacity ;  $V_u$  is the final vertical weight;  $B$  is the breadth of the footing;  $c_u$  is the strength of the undrained shear, and  $Nc$  is the factor of undrained bearing capacity.

Various parameters are taken into consideration in this study to determine their impact on bearing capacity. Incline angle, the distance of footing , and earth characteristics are the impacting factors of the undrained bearing capacity. The figures of the investigated study are schematically presented in Figure 2.11. Three widths for footing (respectively 1,2 and 4 m) and three different angles for inclines (15, 30, 45) were examined. In addition, some incline heights ( $H$ ) and normalized distances of footing ( $\lambda$ ) were considered to show influences of all critical parameters on ultimate bearing capacity .Slope soil material was identified by elastic-perfectly plastic Mohr-Coulomb constitutive model. The undrained shear strength was changed while undrained elasticity modulus ( $E_u$ ),saturated unit weight( $\gamma_{sat}$ ), and Poisson's ratio( $\nu_u$ ) were kept constant as 30 MPa, 20 kN/m<sup>3</sup> and 0.49 respectively. Seven different undrained shear strength was considered to indicate the influence of undrained shear strength ( $c_u$ ), respectively 20,40,100,150,200,300 and 1000 kPa. Footing, which has 1.0 m thickness, was modeled using beam element. ‘Rough footing’ assumption was used in all analyses.

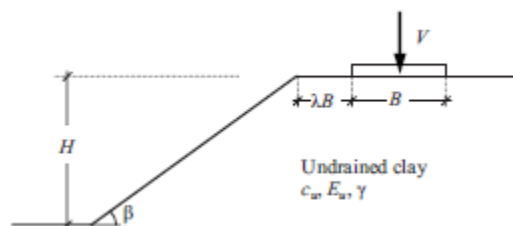


Figure 2.11. Schematic representation of the problem (Georgiadis, 2010).

Various soil characteristics and geometries were regarded. The outcomes of the investigations were correlated with those of the calculation methods presented by other writers. According to the results of previous studies, the author concluded that the results of the suggested approach obtained for specific soil and various shape combinations reflects a sensible conclusion with those given by the previous researchers. For some instances, the

differences between the results of the different calculation methods were also determined. The main reason of detected differences is that these solutions do not consider all affecting parameters. The author identified three different failure mechanisms shown in Figure 2.12 that can occur depending on the combination of soil and geometry of foundations.

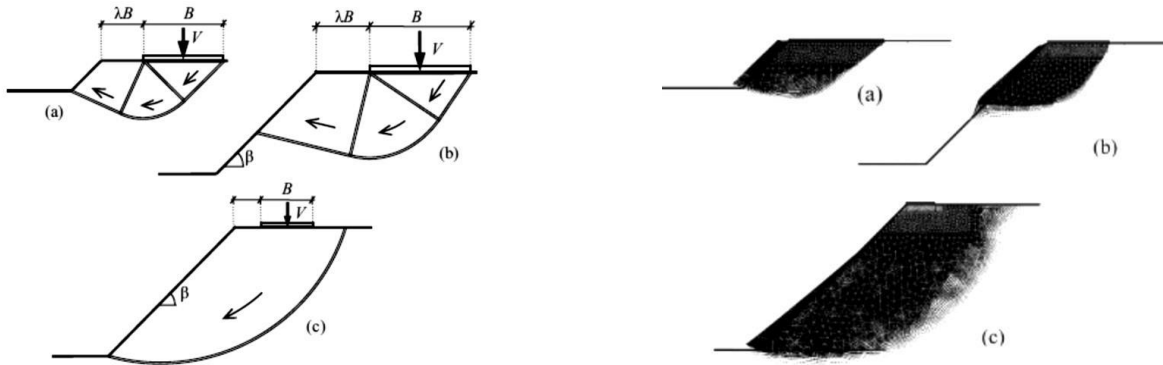


Figure 2.12. Modes of failure (a) and (b) failure of bearing capacity and (c) overall failure of incline (Georgiadis, 2010).

In this study, the FE method was used to examine all essential variables. According to the slope height normalized by the width of footing ( $H/B$ ), the results showed that the failure mechanism could be identified. It is illustrated in the chart presented in Figure 2.13. a sheer decrease of the amount of  $N_c$  from the flat ground amount is perceived in a primary mode. Where the undrained bearing capacity representative falls quickly to 0, it is the second mode and a final mode of constant  $N_c$ . These modes of failures were sequentially outlined above as bearing capacity and overall incline failure mechanisms for the first second and third modes of failure. Moreover, the undrained bearing capacity factor  $N_c$  grows steeply with the rise of  $c_u/\gamma B$ . Additionally, with the rise of  $c_u/\gamma B$ , the second failure mode starts more aggressive.

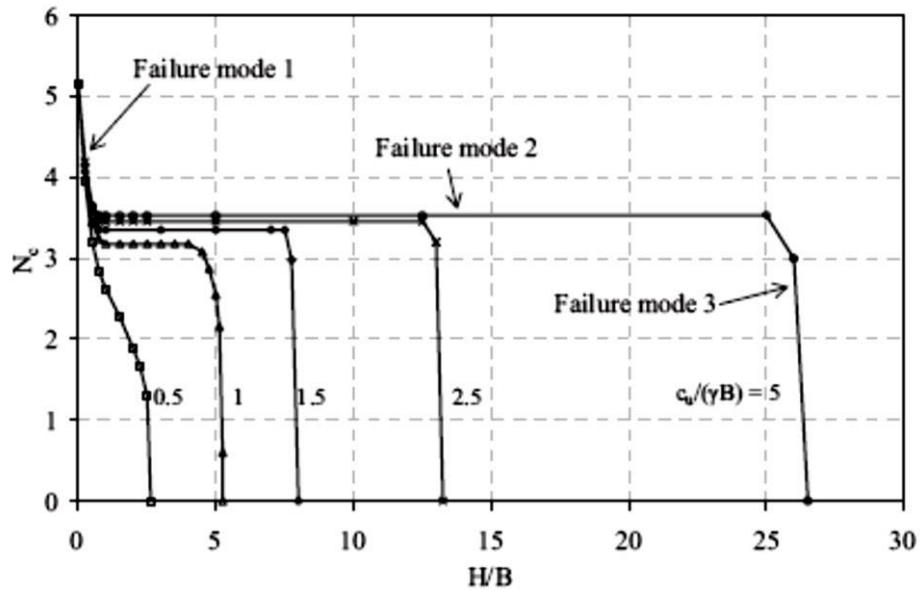


Figure 2.13. Variation of failure mode and  $N_c$  with  $H/B$  for  $\lambda=0$  and  $\beta=45^\circ$  (Georgiadis, 2010).

Any of these diagrams ensure trajectories for angles of incline ( $\beta$ ) of  $0^\circ$ ,  $15^\circ$ ,  $30^\circ$ , and  $45^\circ$  and several rates of  $H/B$ . Figures 2.14, 2.15, 2.16 and 2.17 present a variety of  $N_c$  with  $\lambda$  for rates of  $c_u/\gamma B$ .

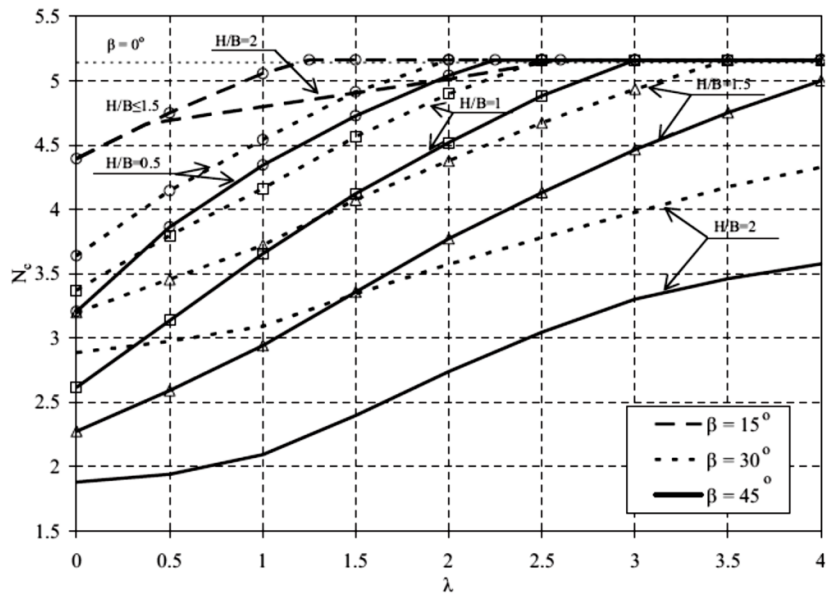


Figure 2.14. Variety of  $N_c$  with  $\lambda$  for  $c_u/\gamma B=0.5$  (Georgiadis, 2010).

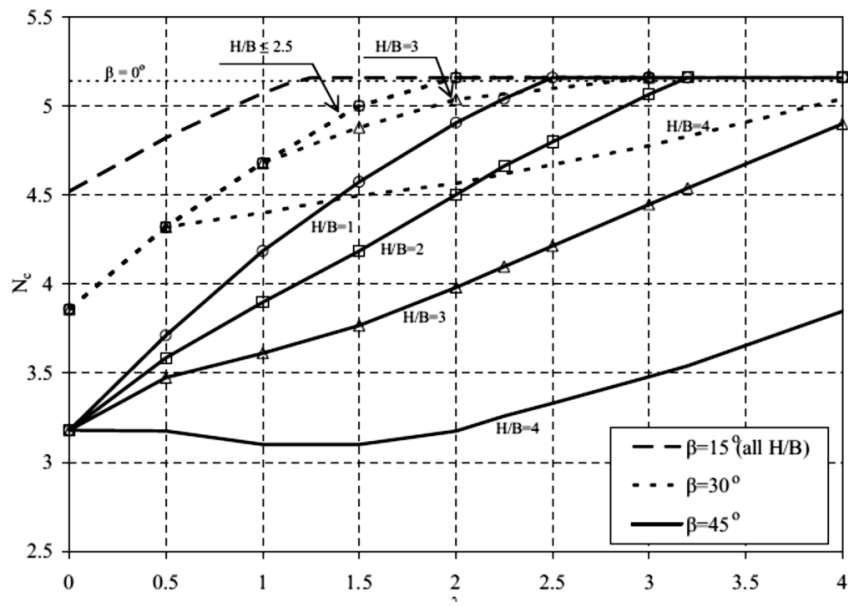


Figure 2.15. Variety of  $N_c$  with  $\lambda$  for  $c_u/\gamma B= 1$  (Georgiadis, 2010).

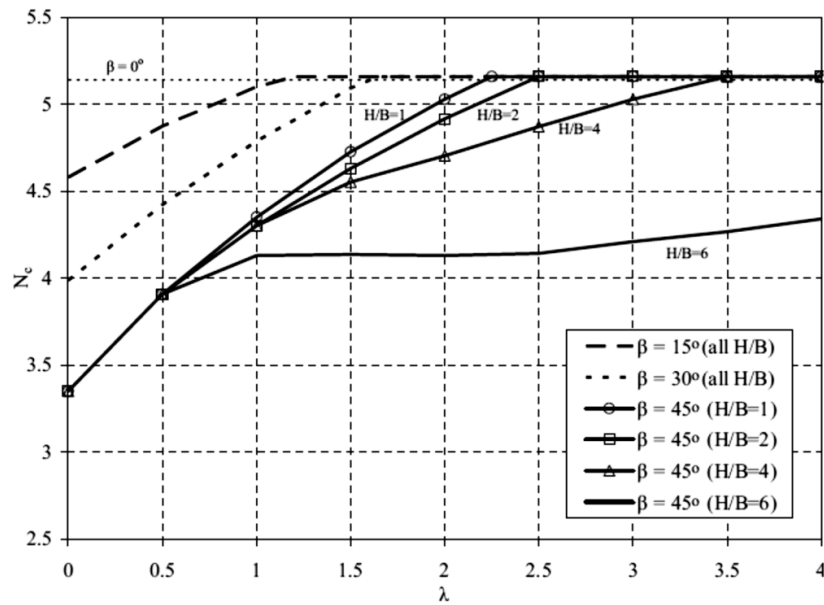


Figure 2.16. Variety of  $N_c$  with  $\lambda$  for  $c_u/\gamma B= 1.5$  (Georgiadis, 2010).

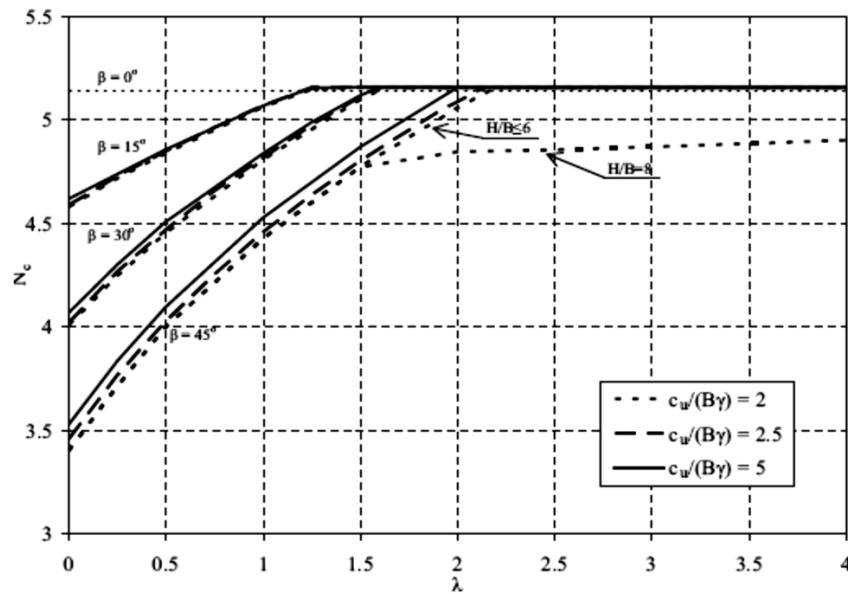


Figure 2.17. Variety of  $N_c$  with  $\lambda$  for  $c_u/\gamma B = 2, 2.5,$  and  $5$  (Georgiadis, 2010).

It can be clearly seen from the chart that factor of undrained bearing capacity ( $N_c$ ) increase with the rise of  $c_u/\gamma B$  ratio. For low amounts of  $c_u/\gamma B$  and high amounts of  $\lambda$  and inclination angle  $\beta$ , it is observed that the factor of undrained bearing capacity ( $N_c$ ) is related to the  $H/B$  rate. Since the second failure mode is regarded for large amounts of  $c_u/\gamma B$ , the factor of undrained bearing capacity is separated from  $H/B$ .

With the rising of the distance of footing from the incline, the factor of undrained bearing capacity ( $N_c$ ) is also growing. If a significant amount of the normalized footing span ( $\lambda_0$ ) is given exceeding the factor of undrained bearing capacity for the flat ground surface, the increment stops. The change of essential values of normalized span ( $\lambda_0$ ) is presented in Figure 2.18 depending on slope angle ( $\beta$ ) and  $c_u/\gamma B$  ratio (shown for values as 2, 2.5, 3.75, 5 and 7.5). The critical value of normalized distance can be computed by using Equation 2.7.

$$\lambda_0 = \left(\frac{5.14}{2}\right)^\beta \quad (2.7)$$

where  $\beta$  is the slope angle (in radian).

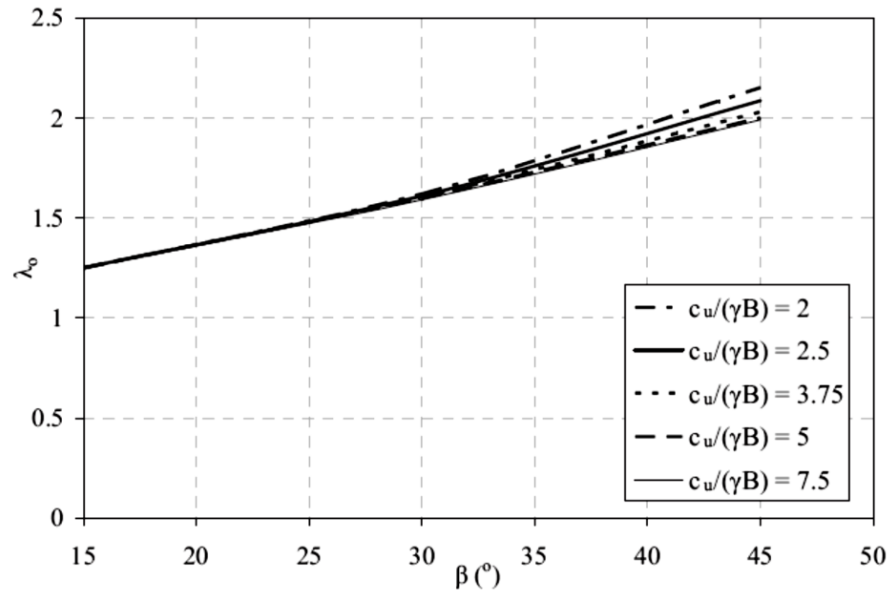


Figure 2.18. Variation of  $\lambda_o$  with  $\beta$  (Georgiadis, 2010).

As observed from the chart, the critical normalized distance has sharply increased with the increase of slope angle. It changes between 1.25 and 2.25 approximately.

For any returned  $c_u/\gamma B$ , angle of inclination  $\beta$ , normalized footing span  $\lambda_o$ , and normalized height of incline  $H/B$ , the author could obtain the determinant of undrained bearing capacity from the outcomes of examinations. As stated in the methodology, by using linear interpolation among amounts received from the plan outlines given in Figure 2.14, the bearing capacity coefficient ( $N_c$ ) can be calculated - Figure 2.17 for all combinations of  $c_u/\gamma B$  ratio and slope angle ( $\beta$ ).

Castelli and Motta (2010) used the limit equilibrium method to develop a model for footing with circular failure surface. The proposed process of review is also related to a solution of an upper bound of the ultimate capacity of the footing. In this sense, circular failure surface occurs distribution from footing edge after it keeps its relative movement until reaching the sloping ground surface. The mechanism of failure and involved energies of foundation regarded as the calculation model are illustrated in Figure 2.19. The limit base pressure can be computed for an arbitrary circular failure surface based on the principle of moment equilibrium ( $\Sigma M_{\text{mobilizing}} = \Sigma M_{\text{resisting}}$ ). In the proposed method, failure mechanism on the surface for minimum base pressure is computed the most sensitive surface among all

possible circular surfaces whose locates and radii are different. Therefore, minimum base pressure can be detected for the critical circular failure surface correlated with the shallow footing's final bearing capacity.

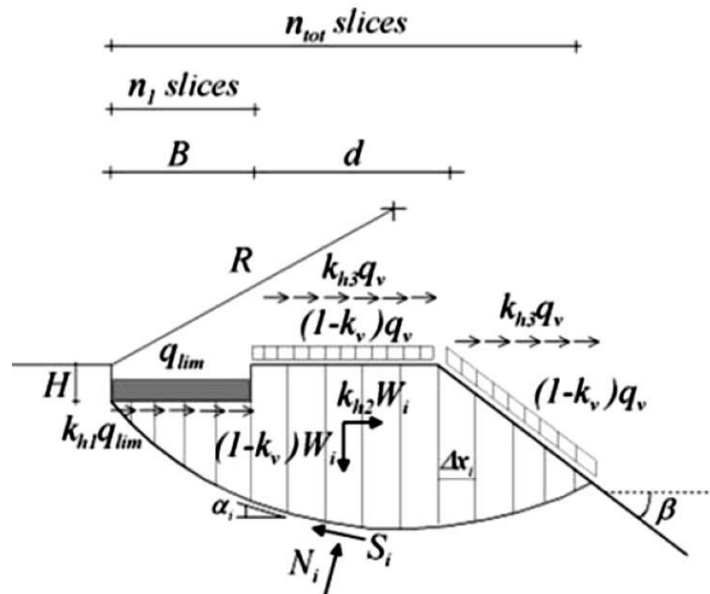


Figure 2.19. The applied forces and the mechanism of failure used in the examination.

(Castelli and Motta, 2010).

When the static conditions are taken into account as  $k_{h1}=k_{h2}=k_{h3}=k_v=0$ , the distance between the footing and slope edge changes among 0 and  $6B$  regarding higher values of internal friction angle. Besides this, angle of inclination ( $\beta$ ) and internal angle of resistance ( $\Phi$ ) change in between  $5^\circ - 35^\circ$  and  $0^\circ - 40^\circ$  respectively.

The ratio of bearing capacity coefficients ( $N_c^*/N_c$ ) changes with the angle of inclination ( $\beta$ ), the normalized interval between the foundation and incline edge ( $d/B$ ) and normalized embedment depth of footing ( $H/B$ ) for undrained conditions. As a result, the ratio of bearing capacity coefficients is computed by using design charts shown in Figure 2.20.

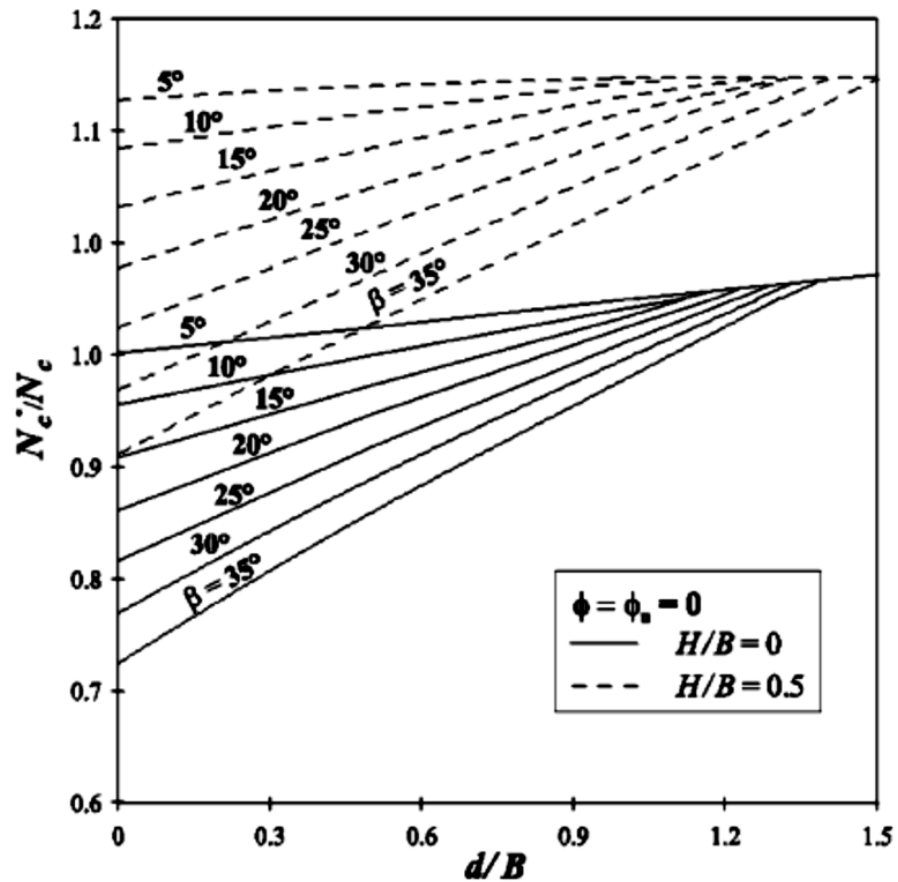


Figure 2.20. Variation of ground factors ( $N_c^*/N_c$ ) in a static condition with the distance of foundation from the edge of the incline (Castelli and Motta, 2010).

When the foundation is located at the edge of the incline, the reduction in the bearing capacity reaches the maximum. As the distance between the slope edge and the foundation increases, the factors of bearing capacity rate ( $N_c^*/N_c$ ) for a foundation near the slope outside and far from the slope decreases. The authors had also concluded that inclination angle ( $\beta$ ) impacts on the distance of the threshold, whilst the embedment of the foundation ( $H$ ) does not influence notably the distance of the threshold  $d/B$  (Castelli and Motta, 2008, 2010). Additionally, these critical distances normalized with footing width change between 1 and 1.4 depending on slope angle ( $\beta$ ). Evidently, the addition in the footing depth only causes an increment in the calculated bearing capacity values.

## 2.2. Seismic Bearing Capacity of Foundations Around Cohesive Slopes

Numerous researchers have pay attention to find a permanent answer for bearing capacity of adjacent to inclines. However, these studies cover the static state while limited studies investigated the resistance of shallow foundations around inclines under earthquake situation. 'Pseudo-static method' is the most popular technique for assessing the impact of an earthquake on the durability of a soil-foundation system. Actually, there are few studies available explaining the seismic impact on the foundations' bearing capacity. In this chapter, different approaches which were suggested a solution method to find the seismic bearing capacity of foundations near inclines will be referred.

The ascertainment of the seismic bearing capacity of footings located horizontally on semi-infinite slopes was determined using the technique of pressure symptoms by Kumar and Rao (2003). The fact that this study is entirely different than presented in the above methods because of the 'semi-infinite slope' assumption. This difference can also be seen in Figure 2.21 and Figure 2.22 clearly. The main reason of addressing to this study in Chapter 2.2 is that it is compared with existing studies approaches, the present analysis describes the change of the factor of undrained  $N_c$  bearing capacity ( $\Phi_u = 0^\circ$ ) with respect to the seismic acceleration coefficient ( $\alpha_h$ ) and the slope angle ( $\beta$ ). Solution tools given in this study would be regarded for the aims of comparison to be given in the following chapter of the dissertation just for the particular case that the footing is at the slope edge ( $\lambda = 0$ ).

Schematic mechanisms of the problem shown in Figure 2.21 and Figure 2.22 were taken into consideration, respectively. The change of  $N_c$  with variations in angle of inclination ( $\beta$ ), the internal frictional, and the horizontal seismic acceleration coefficient ( $\alpha_h$ ) analyzed using failure mechanisms named as the single side and both sides as slope soil material obeys Mohr-Coulomb failure criterion, internal friction angle ( $\beta$ ) used in analyses changes in between  $0^\circ$  and  $50^\circ$ . Additionally, the effect of slope angle ( $\beta$ ) on seismic bearing capacity factors was studied using different slope angles.



following design charts are shown in Figure 2.23, Figure 2.24, and Figure 2.25 that enable to calculate for various cases in which  $\alpha_h \geq 0$  and  $\beta \geq 0$ . Two different curves obtained from the presented design graphs to reflect the effect of various  $N\gamma$  factor concerning to each failure mechanism because of two different failure mechanisms. The results obtained from the presented design graphs, both sides failure mechanism gives more sensible results or smaller values of the seismic acceleration coefficient ( $\alpha_h$ ) and the slope angle ( $\beta$ ). Briefly, when an increment in the seismic acceleration coefficient happens for different slopes, all the factors of bearing capacity decrease significantly.

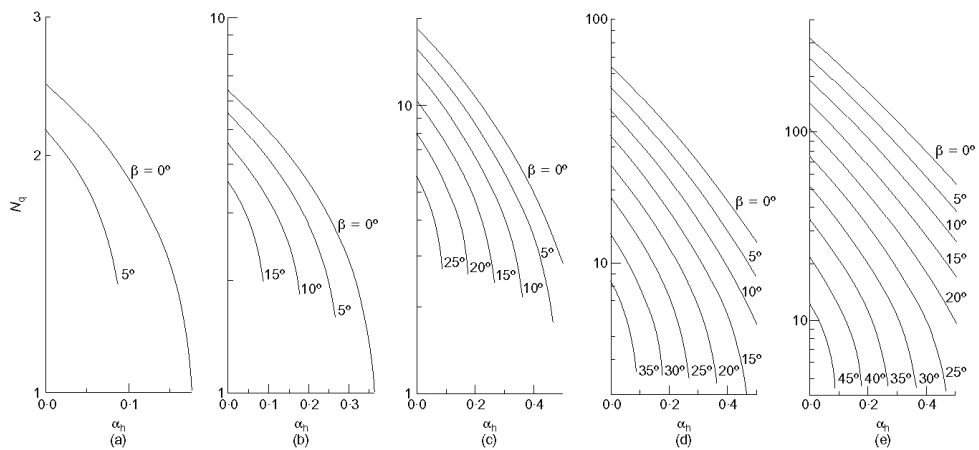


Figure 2.23. Change of  $Nq$  with  $\alpha_h$  for various amounts of  $\Phi$  and  $\beta$ : (a)  $\Phi = 10^\circ$ ; (b)  $\Phi = 20^\circ$ ; (c)  $\Phi = 30^\circ$ ; (d)  $\Phi = 40^\circ$ ; (e)  $\Phi = 50^\circ$  (Kumar and Rao, 2003).

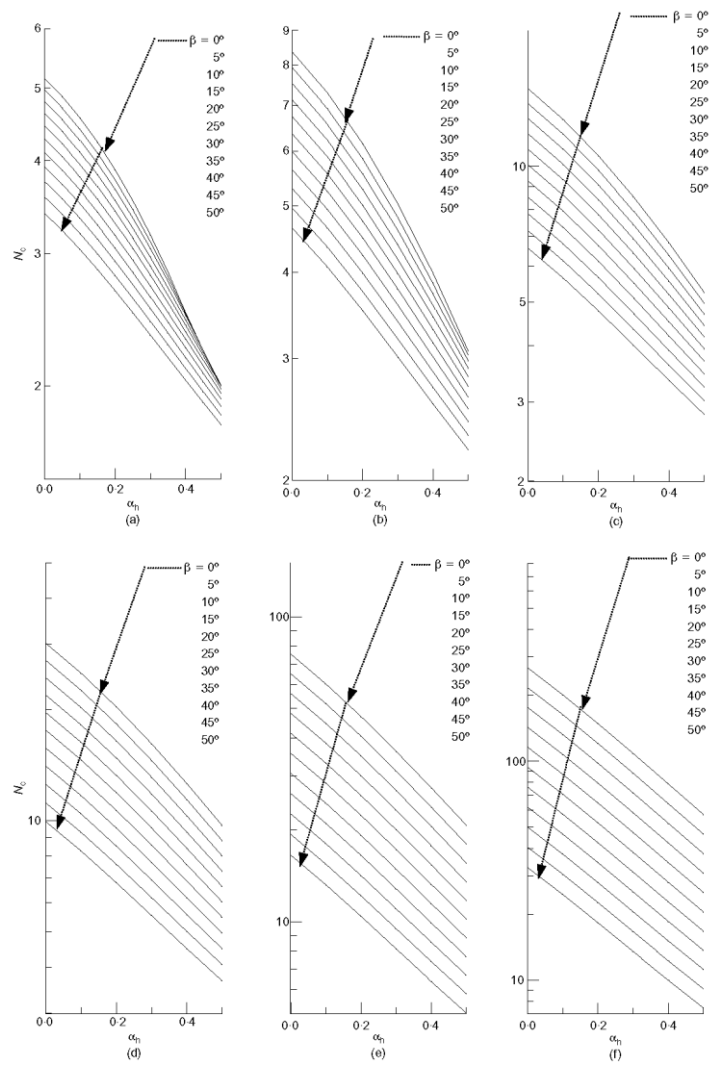


Figure 2.24. Change of  $N_c$  with  $\alpha_h$  for various amounts of  $\Phi$  and  $\beta$ : (a)  $\Phi=0^\circ$ ; (b)  $\Phi=10^\circ$ ; (c)  $\Phi=20^\circ$ ; (d)  $\Phi=30^\circ$ ; (e)  $\Phi=40^\circ$ ; (f)  $\Phi=50^\circ$  (Kumar and Rao, 2003).

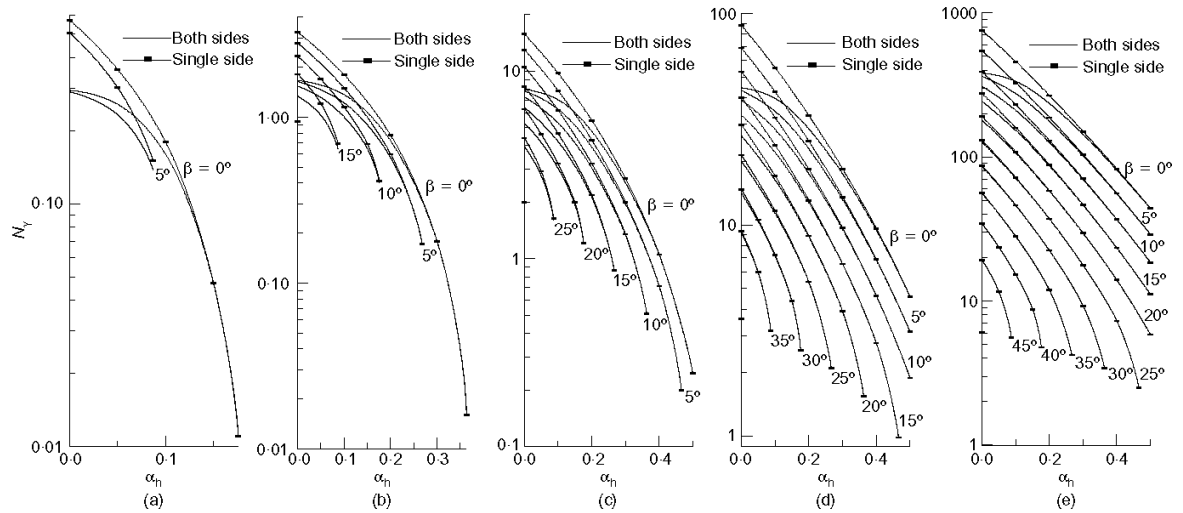


Figure 2.25. Change of  $N_\gamma$  with  $\alpha_h$  for various amounts of  $\Phi$  and  $\beta$ : (a)  $\Phi=10^\circ$ ; (b)  $\Phi=20^\circ$ ; (c)  $\Phi=30^\circ$ ; (d)  $\Phi=40^\circ$ ; (e)  $\Phi=50^\circ$  (Kumar and Rao, 2003).

Shiau *et al.* (2006) proposed a pseudo-static method in conjunction with the limit equilibrium and upper bound limit methods for determining the capacity of the seismic bearing of shallow foundation reclining on  $c-\Phi$  soil. These limitations were defined as being necessary to determine the overall state of the failure facade before the limit equilibrium method and providing higher results than specific limit loads and therefore being non-conservative for the upper bound limit examination.

The authors pointed out that upper and lower bound finite element methods are more confidential methods comparing to the existing methods in the above. As a result, these methods enable the exact limit load from over and under and thus provide a stable load interval to the design engineers for the exact limit load. The fact that the primary purpose of this study was to include the pseudo-static method in the statistical approaches developed at the University of Newcastle based on the upper and lower bound finite element methods. To confirm the results of updated numerical methods, "determination of the seismic bearing capacity of rigid footings on homogenous slopes" was one of the essential criteria chosen in this text.

Schematic diagram of the problem is presented in Figure 2.26. Homogenous soil material obeys the Mohr-Coulomb result in a pattern with the shear strength characteristics cohesion ( $c$ ) and internal friction angle ( $\Phi$ ). Additionally, it is expected that the dynamic quake loading cannot change the shear strength of the soil. Furthermore, the impact of the water pore force is not taken into consideration. The vertical and horizontal acceleration coefficients had been chosen to be equal for slope, structure, and surcharge load, as shown in Figure 2.26. Moreover, the load of the earthquake on the structure footing acts at the foundation level, and the overturning moment due to the inertia of the structure is not considered.

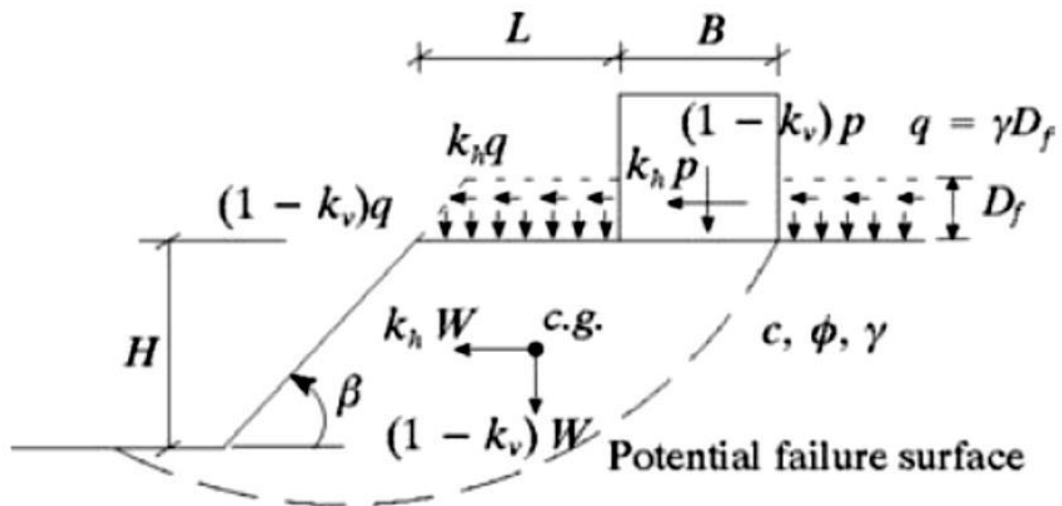


Figure 2.26. Graphical representation of the problem (Shiau *et al.*, 2006).

According to this study, the ultimate bearing capacity of unyielding foundations around inclines can be stated as following given in Equation 2.8.

$$\frac{p}{\gamma B} = f\left(\beta, \frac{L}{B}, \frac{c}{\gamma B}, \phi, \tan \theta\right) \quad (2.8)$$

where  $p$  is the limit pressure average below the foundation,  $\gamma$  is the soil unit mass,  $B$  is the width of foundation,  $\beta$  is the slope angle,  $L$  is the distance from the inclined edge to the edge of the foundation,  $c$  is the cohesion,  $q$  is the surcharge load,  $\Phi$  is the angle of inner resistance of slope soil and  $\tan\theta = k_h/(1-k_v)$ .

As a conclusion of made estimation, it is drawn that the results given in the following have essential influence.

Seismic bearing capacity of such foundations decreases by earthquake forces. Moreover, for any angle of friction, the bearing capacity declines, while the value of  $\tan\theta$  increases. The shaded area is shown in the table Figure 2.27 represents the zone that enclosed with upper and lower bound curve obtained by numerical methods which correct limit load falls into is determined. As shown in the graph given in Figure 2.27, lower and upper bound curves close to each other with the increase of  $\tan\theta$  value and therefore, the efficiency of bonding solutions goes up.

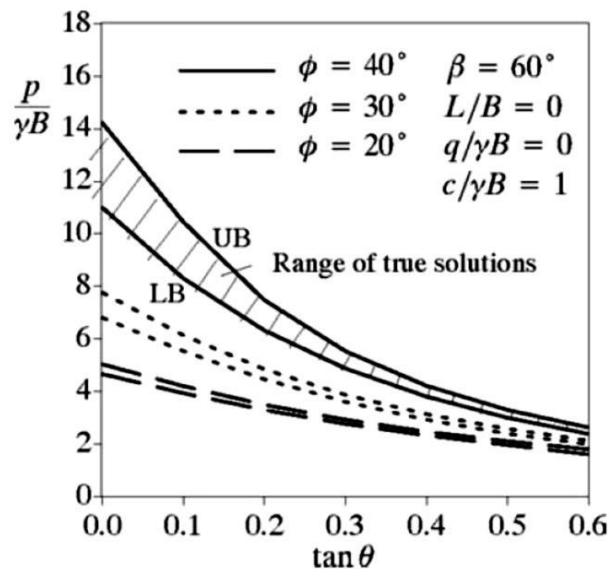


Figure 2.27. Effect of  $\tan\theta$  on  $p/\gamma B$  for various  $\Phi$  (Shiau *et al.*, 2006).

Figure 2.28. explains the change of normalized seismic bearing capacity and upper bound velocity diagrams with different values of  $\tan\theta$ . The velocity fields tend to decrease due to a horizontal earthquake load, and as  $\tan\theta$  increases, a decrease in normalized seismic bearing capacity can be recognized.

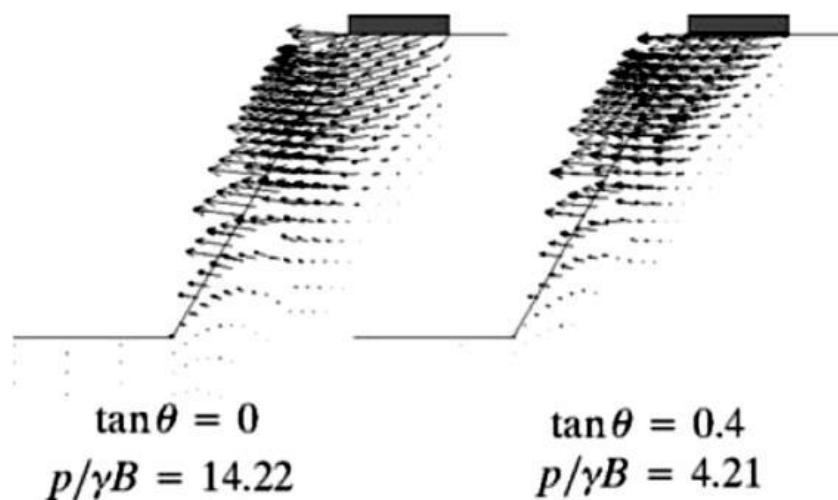


Figure 2.28. Comparison of upper bound velocity diagrams for the effect of inertia forces (Shiau *et al.*, 2006).

The presence of surcharge load on slopes based on  $\beta$ ,  $L/B$ , and  $q/\gamma B$  parameters might reduce, enhance, or does not change the foundation seismic bearing capacity. As can be understood from in the graph given Figure 2.29, a small reduction in  $p/\gamma B$  is seen for a vertical incline. As the overcharge on the inclined surface provides driving energy to the failure of incline, this causes a reduction in the bearing capacity of the foundation. The influence of surcharge load the seismic bearing capacity is remarkably small. Briefly,  $p/\gamma B$  ratio is constant, although the  $q/\gamma B$  ratio increases.

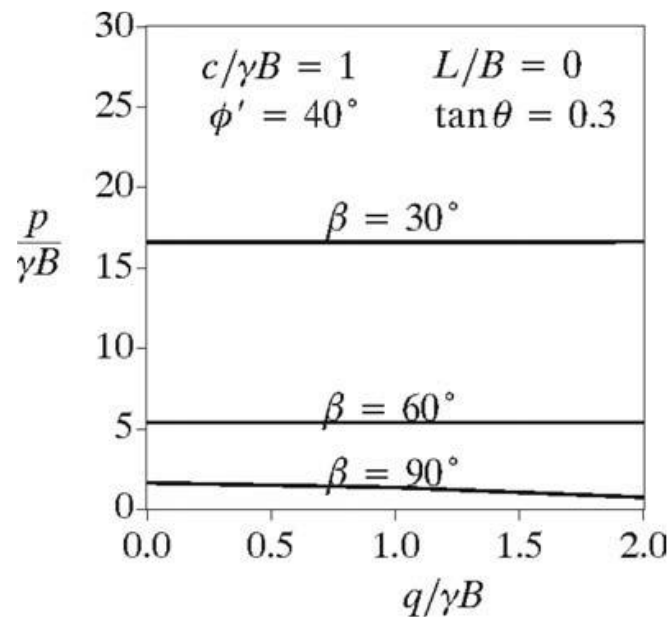


Figure 2.29. Effect of  $q/\gamma B$  on  $p/\gamma B$  for various  $\beta$  (Shiau *et al.*, 2006).

When the impact of inertia force of the soil incline is neglected, an uncertain estimation of the final bearing capacity can be achieved for all inclination angles. The result can be clearly seen in Figure 2.30.

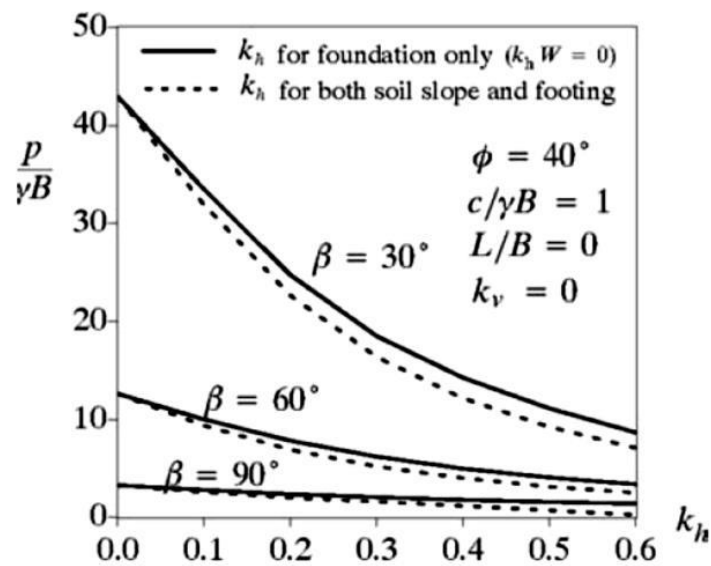


Figure 2.30. Effect of soil inertia  $k_h$  on  $p/\gamma B$  (Shiau *et al.*, 2006).

The results obtained from this study indicated that numerical upper and lower bounds mostly support the right solution by %10 or more. This flow rule showed that solutions of any method have to return outcomes that are placed within upper and lower bounds.

Yamamoto (2010) has stated that Japanese islands have been exposed to severe seismic activities. However, the foundations have to be constructed near slopes. In recent earthquakes, the author reported that the bearing layer under the buildings had destructed and sunk, although the damage of structures was not significantly severe. Hence, he concluded that it is important to investigate both the evaluation of bearing capacity and seismic bearing capacity in such footings design process .

The purpose of this study is to investigate the seismic bearing capacity factors of shallow foundations around inclines by utilizing the upper-bound limit examination. The assumed mechanism of failure in Figure 2.31 consists of a log-spiral shear zone, an active triangular wedge, and passive wedge. The non-symmetrical failure mechanism is determined by just two  $\xi$  and  $\eta$  angular parameters. Furthermore, the author strongly expressed that the developed model can be adopted in the practical applications of geotechnical engineering.

In accordance with material assumptions of limit analysis,  $c-\Phi$  soil is rigid-perfectly plastic material and follows correlated flow rule. Seismic effect determined by the pseudo-static approach consists of a horizontal shear force acting on the footing at the first layer of foundation and an inertia force of the sliding soil mass. In this study, the horizontal seismic acceleration coefficient ( $K_h$ ) was assumed to be equal to calculate inertia force of structure running on the foundation and of the sliding soil mass. The effect of vertical acceleration onto the seismic bearing capacity was neglected.

Shear transfer coefficient ( $f$ ) is introduced to regard variable shear force shift in the foundation base. The impact of footing embedment is also investigated as well.

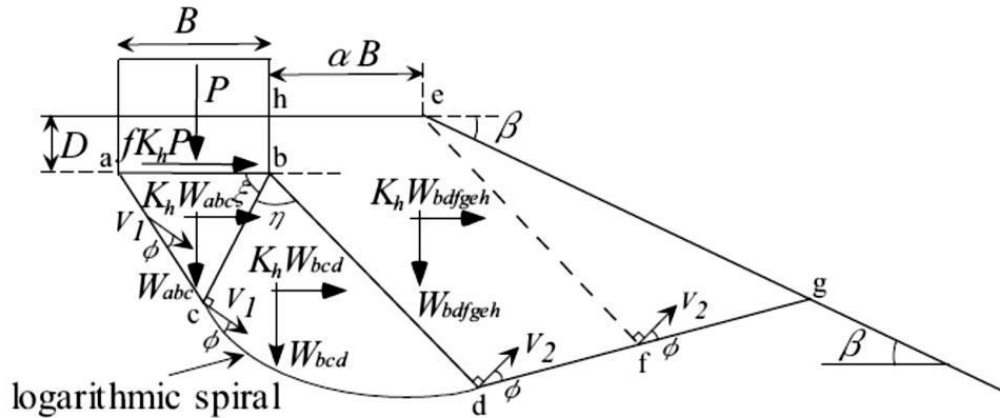


Figure 2.31. Mechanism of failure used in the analysis (Yamamoto, 2010).

Through the solution of the energy balance equation that establishes a base for upper bound limit examination, the upper limit of seismic bearing capacity is obtained through the formula given in Equation 2.9.

$$q_b = cN_{ce} + \frac{1}{2}\gamma BN_{\gamma e} \quad (2.9)$$

where  $c$  is the adherence,  $B$  is the footing width,  $\gamma$  is the specific weight of the soil,  $N_{ce}$  and  $N_{\gamma e}$  are the factors of seismic bearing capacity.

$N_{ce}$  and  $N_{\gamma e}$  seismic bearing capacity factors given in Equation 2.17 are calculated by the equations given in Equation 2.11 and Equation 2.11 respectively.

$$N_{ce} = \frac{1}{\cos \varepsilon + fK_h \sin \varepsilon} (f_7 + f_8 + 2f_9) \quad (2.10)$$

$$N_{\gamma e} = \frac{1}{\cos \varepsilon + f K_h \sin \varepsilon} (f_1 + f_3 + f_5) + K_h (f_2 + f_4 + f_6) \quad (2.11)$$

where  $\xi$  is the angle which defines the geometry of active wedge beneath the footing,  $f$  is the shear transfer coefficient,  $K_h$  is the horizontal seismic coefficient and  $f_i$  ( $i= 1$  to  $9$ ) are the functions of which independent variables are  $\xi$ ,  $\eta$ ,  $\beta$ ,  $\alpha B$ ,  $D/B$  and  $\Phi$ . Since seismic bearing capacity factors obtained in this study are represented by design charts, the expanded forms of  $f_i$  function ( $i= 1$  to  $9$ ) will not be given in detail. Related formulas can also be found in the reference (Yamamoto, 2010).

All possible combinations of  $\xi$  and  $\eta$  variables, providing a kinematically possible swiftness range were considered in this study to get the least amount of two factors ( $N_{ce}$  and  $N_{\gamma e}$ ) individually. Thus, the use of superposition approach is, in fact, on the safe side.

The conclusion drawn in this research compared with the existing researches by earlier scholars after the validity of the method is verified for some cases. Results of the parametric study performed by using this method are summarized as follows :

- The factors of seismic bearing capacity decrease significantly by increasing horizontal seismic coefficient  $K_h$ .
- Increasing the inclination angle causes a decrease in the factors of bearing capacity magnitude.
- Seismic bearing capacity declines by the rise of the coefficient of shear transfer ( $f$ ).
- The factors of bearing capacity quantities rise by the embedment ( $D/B$ ) and the incline peak distance from the start of loading ( $\alpha B$ ).
- As shown in Figure 2.32, as  $K_h$  increases, the angle of active wedge increases, and the angle of the log-spiral zone also decrease. Additionally, by the rise of  $K_h$ , the overall extent of failure mechanism decreases.

Design charts for the bearing capacity factor obtained  $N_{ce}$  and  $N_{\gamma e}$  with  $K_h$  for various amounts of  $\beta$  are presented in Figure 2.33 to 2.40 ( $\Phi= 30^\circ, 40^\circ$ ,  $D/B= 0.0$  and  $1.0$ ,  $\alpha= 0.0$  and  $0.5$ ).

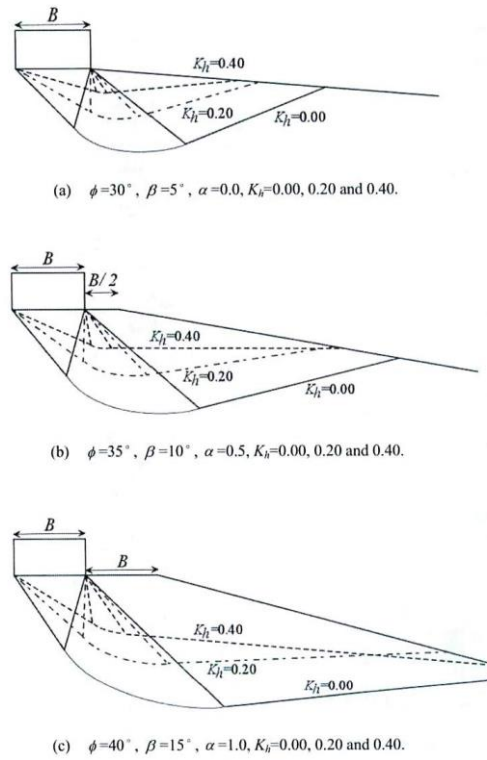


Figure 2.32. Mechanisms of failure for various amounts of  $\Phi$ ,  $\beta$ ,  $\alpha$ , and  $K_h$  (Yamamoto, 2010).

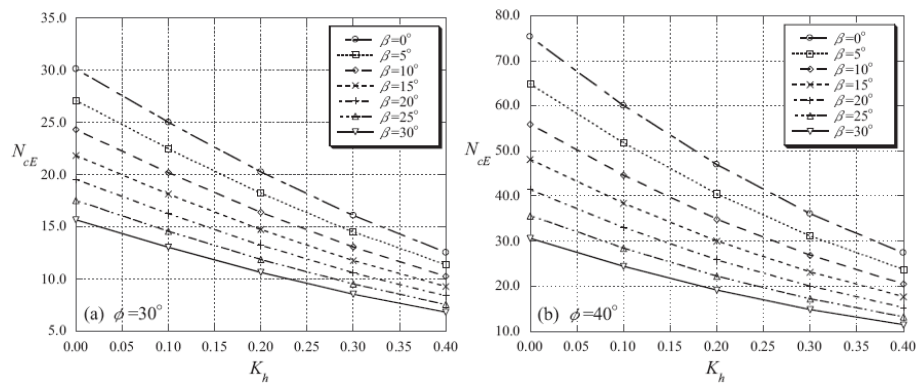


Figure 2.33. Charts of design for  $N_{ce}$  ( $\Phi=30^\circ, 40^\circ$ ,  $D/B=0$ ,  $a=0.0$ ) (Yamamoto, 2010).

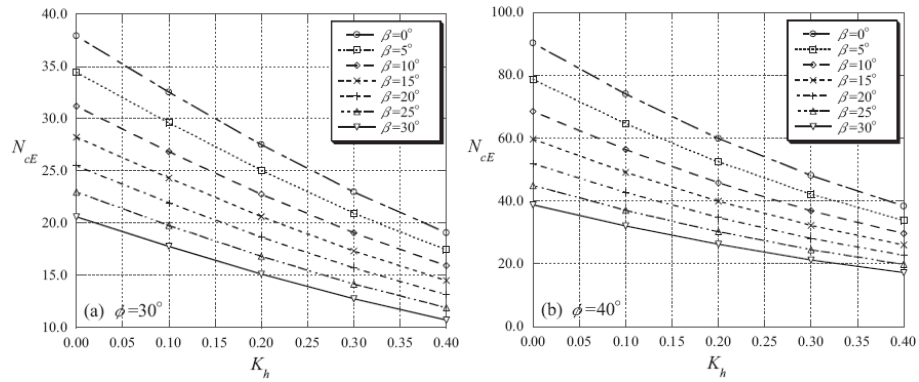


Figure 2.34. Charts of design for  $N_{ce}$  ( $\Phi = 30^\circ, 40^\circ, D/B = 1, a = 0.0$ ) (Yamamoto, 2010).

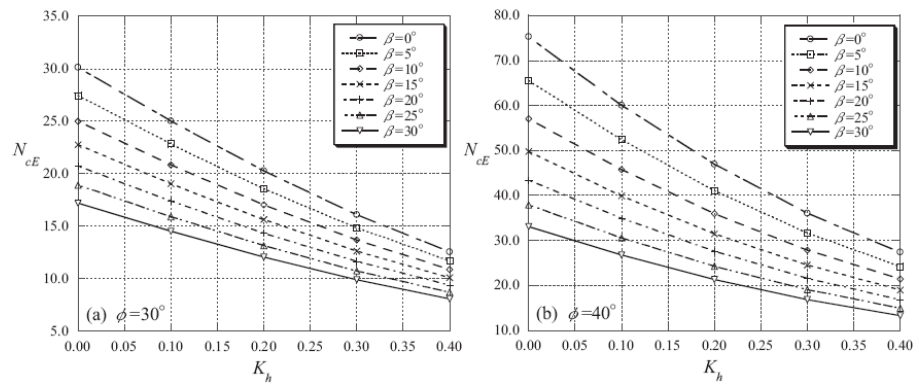


Figure 2.35. Charts of design for  $N_{ce}$  ( $\Phi = 30^\circ, 40^\circ, D/B = 0, a = 0.5$ ) (Yamamoto, 2010).

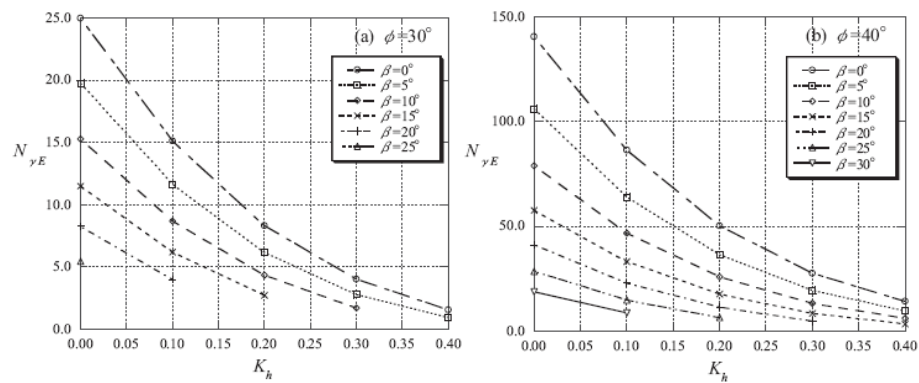


Figure 2.36. Charts of design for  $N_{ye}$  ( $\Phi = 30^\circ, 40^\circ, D/B = 0, a = 0.0$ ) (Yamamoto, 2010).

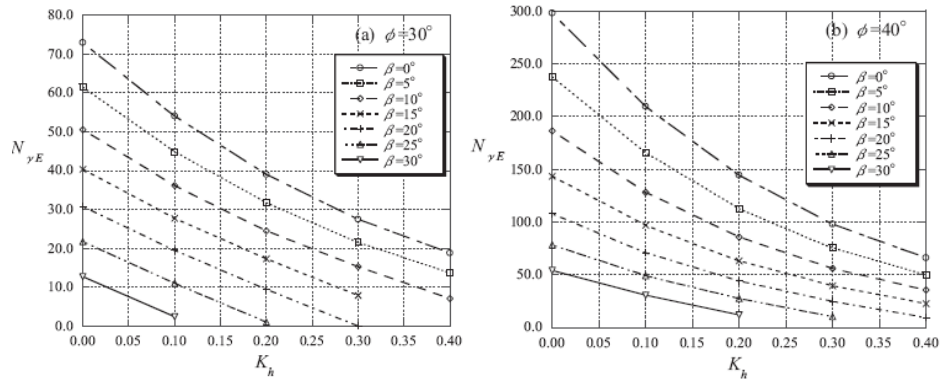


Figure 2.37. Charts of design for  $N_{\gamma E}$  ( $\Phi = 30^\circ, 40^\circ, D/B = 1, a = 0.0$ ) (Yamamoto, 2010).

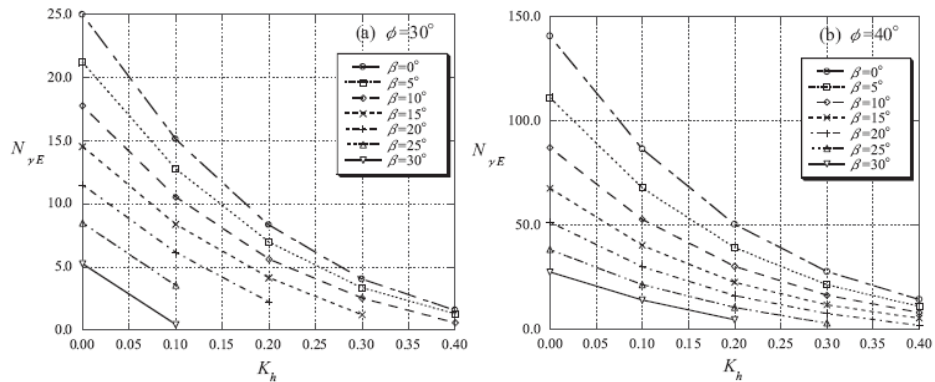


Figure 2.38. Charts of design for  $N_{\gamma E}$  ( $\Phi = 30^\circ, 40^\circ, D/B = 0, a = 0.5$ ) (Yamamoto, 2010).

Castelli and Motta (2010) had expressed that the pseudo-static approach is used to measure the factors of seismic ultimate bearing capacity. Therefore, the study intends to investigate taking into account both the impact of the foundation embedment and the span of the foundation from the inclined edge. According to this method, earthquake forces includes the inertia forces employed on the footing, sliding soil mass and surcharge. The inertia force of the surcharge and structure are computed using equal seismic acceleration coefficients ( $k_{h1}=k_{h3}$ ) to each other. However, the value of the soil mass ( $k_{h2}$ ) was chosen higher than the inertia of the structure because Eurocode 8 supports decreasing the seismic behavior with respect to the flexibility analysis of the constructions. Thus, pseudo-static analysis is performed regarding the subsequent coefficients of seismic as  $k_{h1}=0.1$  and  $0.2$  for the inertia force of the construction,  $k_{h2}=0.2$ , and  $0.4$  for the inertia force of the soil body.

The author concluded that the results obtained from the proposed model are in high consistency with the obtained models of other scholars even though the simplified mechanism. In addition to, the ratio of bearing capacity coefficients in seismic conditions ( $N_c^*/N_c$ ) changes with  $d/B$  ratio, slope angle ( $\beta$ ),  $H/B$  ratio as well as internal friction angle ( $\Phi$ ) and seismic acceleration coefficients ( $k_{h1}$ ,  $k_{h2}$  ve  $k_{h3}$ ). Moreover,  $d/B$  ratio, slope angle ( $\beta$ ),  $H/B$  ratio and  $k_{h1}$  seismic acceleration coefficient plays a significant role on the  $N_c^*/N_c$  ratio in undrained conditions ( $\Phi = \Phi_u = 0^\circ$ ). The rates of seismic bearing capacity  $N_c^*/N_c$  are presented in Figure 2.39 as a function of  $d/B$  for different angles of inclination. The presented charts show that the value of  $k_{h1}$  just takes greater than zero since the decrease in seismic bearing capacity due to the inertia force of the structure is more decisive.

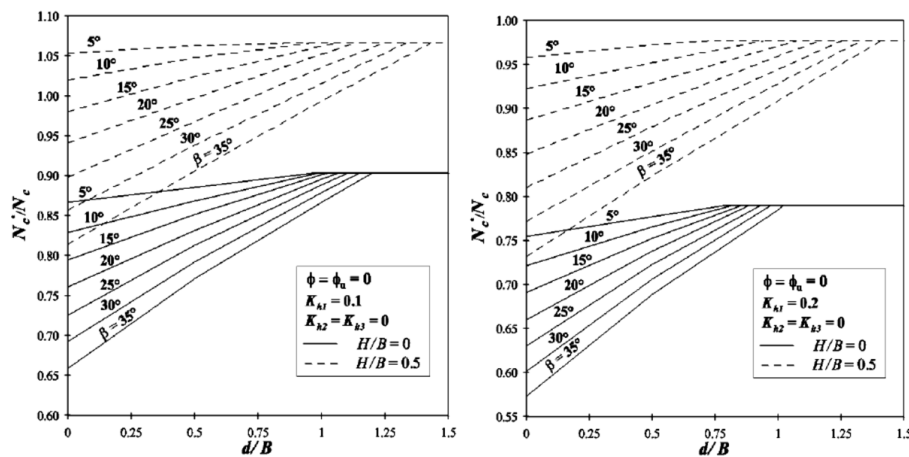


Figure 2.39.  $N_c^*/N_c$  rates as a function of the normalized  $d/B$  distance of incline (Castelli and Motta, 2010).

Results of the developed method are similar to compared with outcomes of static condition; when the foundation is located at the inclined edge, the highest decrease of the bearing capacity is observed. The bearing capacity generally tends to increase with the rise of the distance of foundation from the slope edge. As the footing reaches a certain distance from the slope edge defined as threshold distance, the presence of slope will not affect the failure mechanism. Thus, the ratio no longer takes the constant value that is diminished by the influence of inertia forces only. As shown in Figure 2.39, the threshold distance varies

in between  $0.75B$  and  $1.5B$ . Moreover, this distance increases with the increase of  $k_{h1}$  seismic acceleration coefficient. Besides, it is reported that the threshold distance is not changed by considering either inertia of the structure and of the sliding soil mass separately.

Amin Keshavarz *et al.* (2019) used the finite element method that is named 'FELA' to obtain the seismic bearing capacity of a strip foundation located near homogenous soil slopes. In order to find the under undrained seismic load carrying capacity of a strip footing placed on cohesionless soil, various influential factors were defined respectively; geometrical properties of the slope, the setback distance ratio ( $L/B$ ), and the slope angle, the strength ratio ( $c_{u0}/(\gamma B)$ ), the horizontal earthquake coefficient ( $k_h$ ). Consequently, the functional description of the seismic undrained bearing capacity ( $q_u/\gamma B$ ) and its variables parameters are given briefly in Equation 2.12.

$$\frac{q_u}{\gamma B} = f\left(\frac{L}{B}, \frac{H}{B}, k_h, \frac{c_{u0}}{\gamma B}, \beta, \frac{kB}{c_{u0}}\right) \quad (2.12)$$

In addition with homogeneous soil slope, heterogeneity soil slope effect on the undrained seismic load carrying capacity of a strip footing located close to slope. Therefore, the soil strength heterogeneity ( $kB/c_{u0}$ ) is expressed as a function of seismic bearing capacity.

Graphical representation of the problem is presented in Figure 2.40. Model type is selected as plane strain. Accordingly, the undrained shear strength is assumed as a constant value for the homogeneous soil slope. The soil saturated unit weight is kept constant at 20 kN/m<sup>3</sup>. The dimensions of the model of  $L_x$ ,  $L_y$  and  $L_z$  are arranged  $3B$ ,  $14B$ , and  $13B$ . The reason for choosing these values is to avoid the effect of boundaries on the outcomes.

The effective parameters are chosen: (i)  $c_u/(\gamma B)=0.5, 1.0, 1.5, 2.0, 2.5, 5.0$ ; (ii)  $\beta=10^\circ, 20^\circ, 30^\circ, 40^\circ, 50^\circ$ ; (iii)  $L/B=0, 0.25, 0.50, 1, 2, 3, 4, \text{ and } 5$  for homogeneous soil.

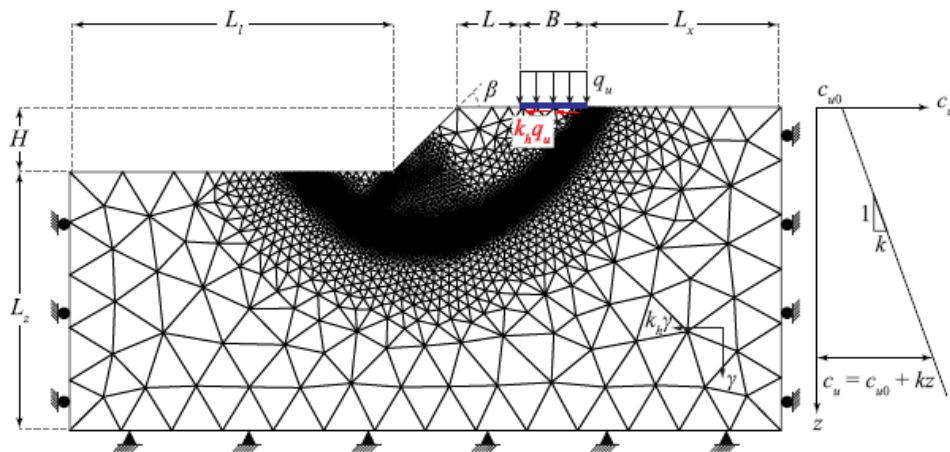


Figure 2.40. Model geometry and a typical FELA mesh.

As mentioned above, computer codes based on FELA have been used to solve the problem of the present study. Even though, FEM and FELA have the same ability to deal with problem, there is a sharp difference regarding the usage methodology. In the FEM, a relatively fine mesh must be taken account in the area where it sustains high deformation to take exact value whereas the FELA adopts automatic adaptive mesh refinement.

The results obtained from this adopted method were compared with other research works. The following outcomes were summarized in the following:

- Figure 2.41 shows that relationship between  $Nc$  and  $L/B$  obtained from the present study shows a good agreement with the finite element results of Georgiadis. On the other hand, the results of Meyerhof and Kusakabe *et al.* are noticeably higher than the results of the present study because of a face failure mechanism in their analysis. However, this hypothesis can't be true because the failure mechanism depends on location of footing from the slope crest.

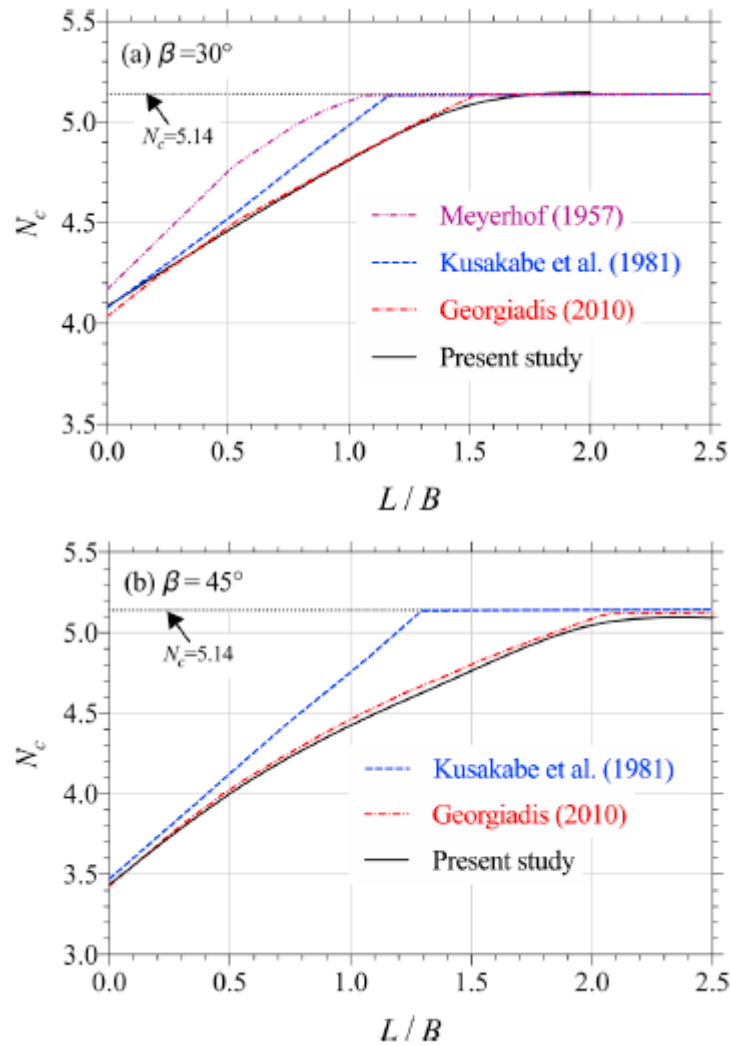


Figure 2.41. Comparison of the results of the present study with those presented by previous researchers (A. Keshavarz *et al.*, 2019).

- As depicted at Figure 2.42, the variation in seismic load carrying capacity was compared for four different values of  $k_h$ ; respectively; 0, 0.1, 0.2 and 0.3. According to the results of present study are good agreement with FEM results of Cinicioglu and Erkli. Only for large values of  $L/B$ , the results are slightly greater than FEM results of Cinicioglu and Erkli.

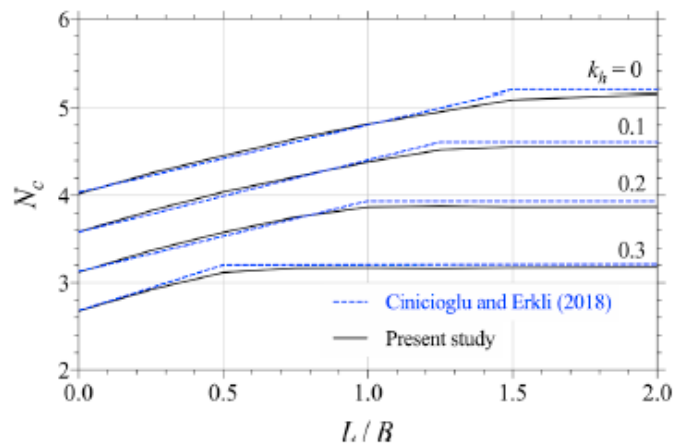


Figure 2.42. Comparison of the variation in  $N_c$  against  $L/B$  for  $\beta = 30^\circ$ ;  $H/B=1, 2, 4$ ; and  $c_{uo}/(\gamma B)=2.5$  (A. Keshavarz *et al.*, 2019).

- As shown in Figure 2.43, the value of  $q_u/(\gamma B)$  decreases as the slope angle increases because of the shape of the failure surface under the footing. Furthermore, Figure 2.44 presents that the impact of  $L/B$  on  $q_u/(\gamma B)$ . The value of  $q_u/(\gamma B)$  increases when footing distance from the slope edge increases and from a constant value of  $L/B$  the value to  $q_u/(\gamma B)$  reaches constant.

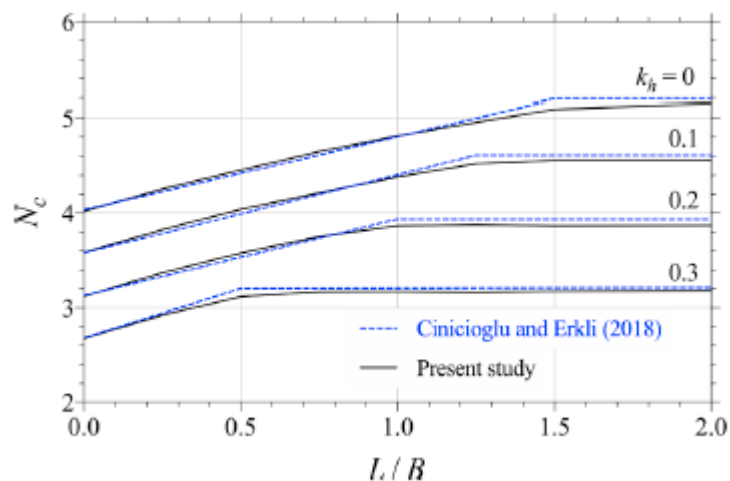


Figure 2.43. Variation of the  $q_u/(\gamma B)$  with  $L/B$  (A. Keshavarz *et al.*, 2019).

- Figure 2.44 shows that the value of  $q_u/(\gamma B)$  decreases as the value of  $k_h$  increases with a constant value  $L/B$ .

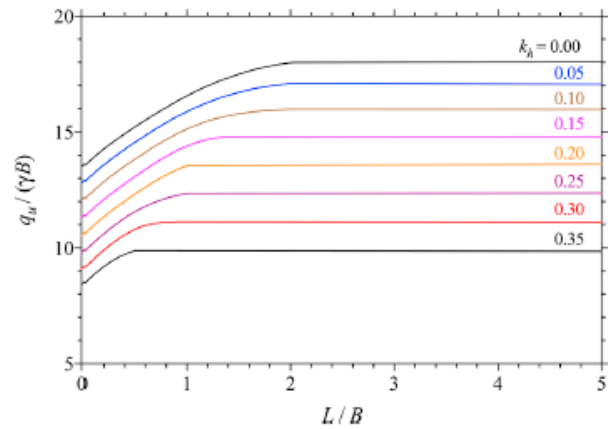


Figure 2.44. The effect of  $k_h$  on  $q_u/(\gamma B)$  ( $H/B=3$ ,  $c_{u0}/(\gamma B)=3.5$ , and  $\beta=35^\circ$ ) (A. Keshavarz *et al.*, 2019).

- As mentioned beginning of the present study, pseudo-static method is used to simulate the earthquake condition. As can be seen in Figure 2.45, for any value of  $k_h \geq 0.38$ ,  $k_h q_u / c_{u0} = 1$ , related with foundation sliding mode of failure.

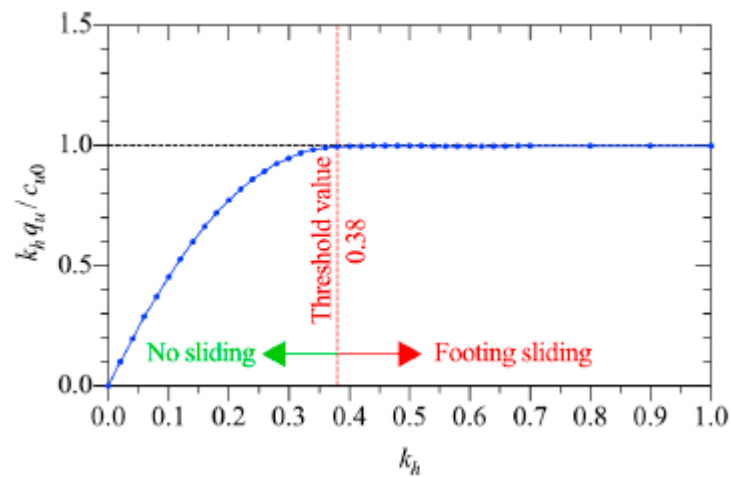


Figure 2.45. Variation of  $k_h q_u / c_{u0}$  against  $k_h$  for the level ground (A. Keshavarz *et al.*, 2019).

- Result of FEM shows that the slope height ratio ( $H/B$ ) has a direct impact on the stability problem for slopes. Based on Taylor approach for the critical value of height of the homogeneous unloaded soil slope ( $H_{cr}$ ), if  $H > H_{cr}$ , the slope isn't stable and can't undergo any load.
- As shown in Figure 2.46, the failure modes at  $L/B = 0$  is overall slope failure which initiates well behind the edge of the footing and creates a failure pattern that covers the entire model.

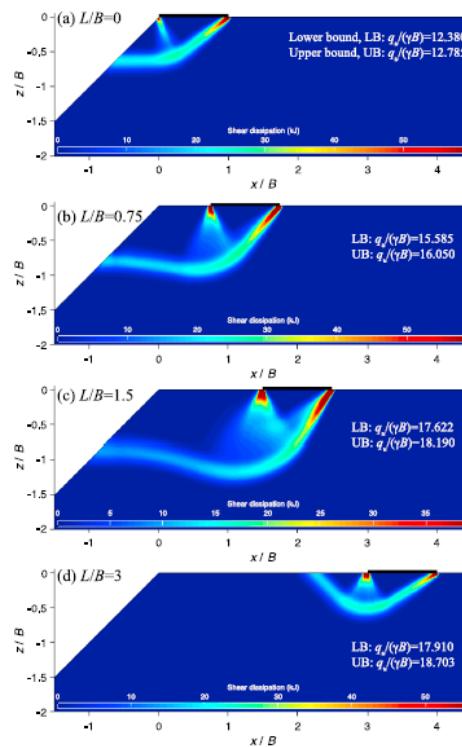


Figure 2.46. Typical foundation failure pattern for  $c_{u0}/(\gamma B)= 4$ ,  $kB/c_{u0}=0$ ,  $k_h=0.1$ ,  $\beta=45^\circ$ , ( $H/B = 4$ ) (A. Keshavarz *et al.*, 2019).

- Contrarily, the failure mode for  $L/B = 3$  changes from face failure to Prandtl-type failure mode. It is also shown in Figure 2.47.
- Another failure mode is called base failure as given in Figure 2.47. Base failure correlates with bearing capacity failure. Conversely, as the value of  $c_{u0}/(\gamma B)$  increases shown in Figure 2.47, the failure modes turns to be the toe failure mode.

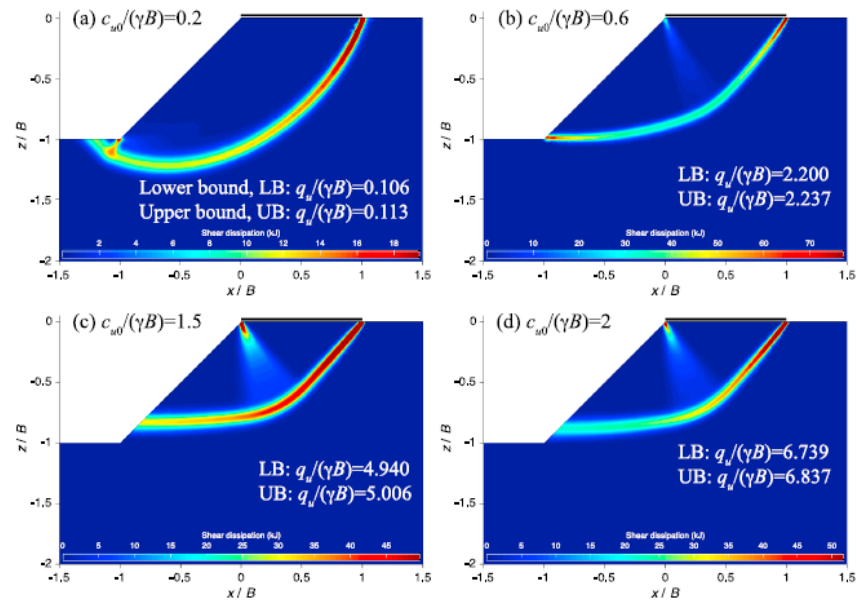


Figure 2.47. The effect of  $c_{u0} / (\gamma B)$  on the failure mode ( $kB/c_{u0}=0$ ,  $k_h=0$ ,  $\beta=45^\circ$ ,  $H/B=1$ ) (A. Keshavarz *et al.*, 2019).

- It is noticed that there is a reverse relationship between  $k_h$  and the volume of failure mode. As shown in Figure 2.48, as  $k_h$  increases, the active thrust increases, the passive thrust decreases, and the wedge angles start smaller.

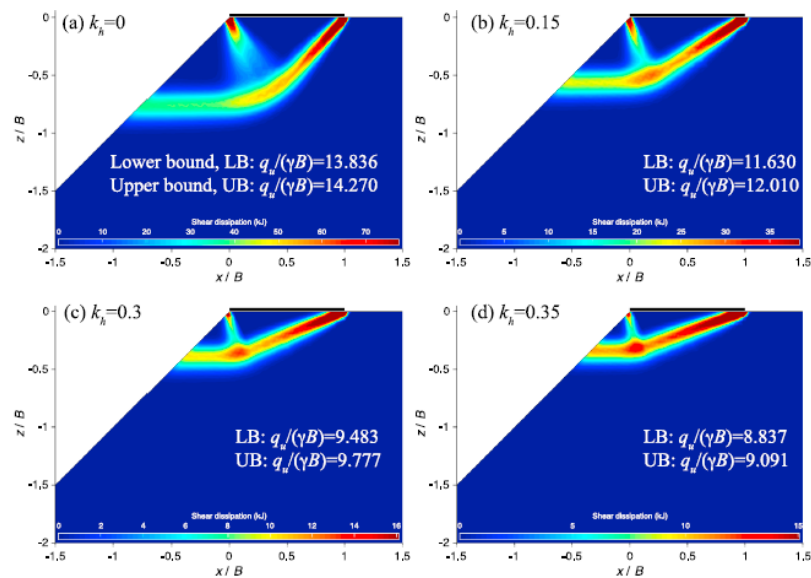


Figure 2.48. The effect of  $k_h$  on the failure mode  $c_{u0} / (\gamma B) = 4$ , ( $kB/c_{u0}=0$ ,  $L/B=0$ ,  $\beta=45^\circ$ ,  $H/B=4$ ) (A. Keshavarz *et al.*, 2019).

- Normalized bearing capacity  $q_u/(\gamma B)$  increases linearly with the increase  $L/B$ . As seen from the graph given in Figure 2.49, due to the failure mode changes from face failure mode to Prandtl-type failure mode, this trend tends to go a certain value.

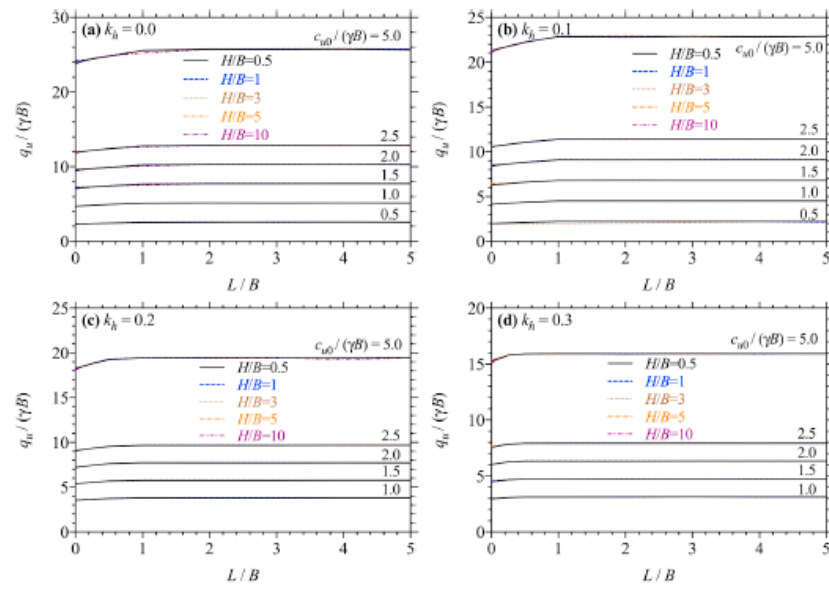


Figure 2.49. Design charts for average values of lower and upper bounds of normalized bearing capacity of a rough strip footing located on slope with  $\beta = 10^0$  (A. Keshavarz *et al.*, 2019).

### 2.3. Shape Effect of Shallow Foundation On Seismic Bearing Capacity

Recently, both numerical and experimental analyses on the final bearing capacity of square and rectangular foundations have attracted the attention of many researchers. However, these studies were mostly performed for the footings placed on the sand. As abovementioned, few researchers have studied to investigate the ultimate loads on square or rectangular foundations resting on frictional-cohesive ( $c-\phi$ ) soil. Notably, five studies (Salgado (2004), Zhu and Michalowski (2005), Gourvenec (2006), Li *et al.* (2009), Yu *et al.* (2011)) suggested a solution to determine the final bearing capacity of footing within the eight studies of research that will be referred to in this section. Contrarily, the reason for

referring the other three research studies is to present brief explanations about their solution methods and their hypotheses.

Yang *et al.* (2003) proposed a technique to calculate the lower bound boundary of rectangular surface foundations' bearing capacity. A perfectly rigid plastic model was integrated to define the feature. The bearing capacity of footing was subjected to the stress boundary condition, stress discontinuity equilibrium state, stress equilibrium state, and yield state. In this study, a rectangular surface footing was taken into consideration depending on the soil internal friction angle and adherence to the bearing capacity.

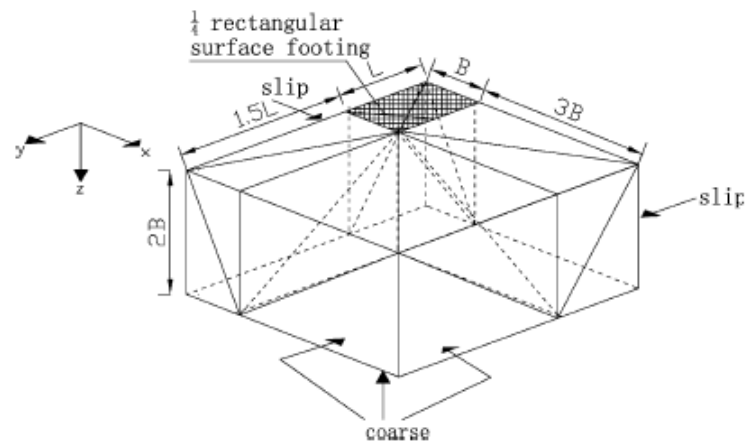


Figure 2.50. Lower bound analysis of finite element coarse mesh (H. Yang *et al.*, 2003).

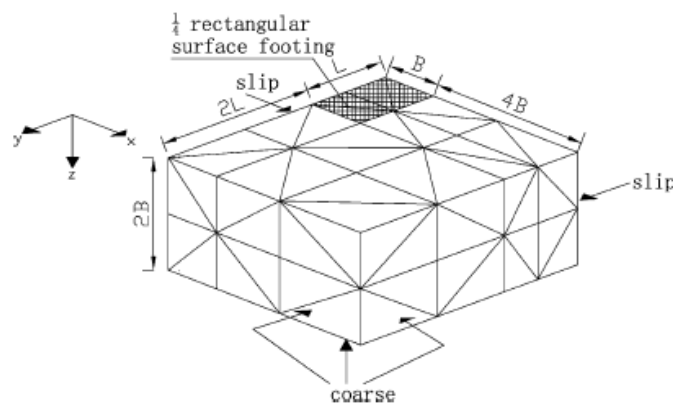


Figure 2.51. Lower bound analysis of finite element fine mesh (H. Yang *et al.*, 2003).

The 3D lower bound examination of the finite element mesh for was shown in Figure 2.50. A quarter of the whole meshes were regarded due to the symmetry. The spreading load on the rectangular foundation given in Figure 2.50 and Figure 2.51 was enlarged by exploring a statically admissible stress discontinuity between the soil underneath the strip foundation.

Within the context of this study, the square element with four nodes was used in all finite element models. It was assumed that more than one node might experience the same coordinates and statically admissible stress discontinuity is allowed at common facades among the neighboring square elements.

| L/B             | Author            |                    |                     | Michalowski |
|-----------------|-------------------|--------------------|---------------------|-------------|
|                 | Yield condition I | Yield condition II | Yield condition III |             |
| (a) Course mesh |                   |                    |                     |             |
| 1               | 5.093             | 5.349              | 5.881               | 6.830       |
| 2               | 4.878             | 5.122              | 5.632               | 6.060       |
| 5               | 4.501             | 4.726              | 5.199               | 5.499       |
| 10              | 4.458             | 4.690              | 5.157               | 5.190       |
| (b) Fine mesh   |                   |                    |                     |             |
| 1               | 5.256             | 5.567              | 6.174               | 6.830       |
| 2               | 5.014             | 5.306              | 5.856               | 6.060       |
| 5               | 4.782             | 4.952              | 5.354               | 5.490       |
| 10              | 4.620             | 4.831              | 5.166               | 5.190       |

Figure 2.52. Comparison of 3-dimensional lower and bound bearing capacity  $N_c$  for strip foundations on a weightless and purely adhesive soil (H. Yang *et al.*, 2003).

As seen from Figure 2.52 and Table 2.1 that coefficient of bearing capacity factor of quadrilateral foundations for utterly cohesive soil was determined by the solution of 3D lower bound. Furthermore, Michalowski (2001) gave the outcome of a similar situation utilizing 3D upper bound approach. A quadrilateral foundations' bearing capacity reduction was observed with an increment of  $L/B$ . As a result of analyses obtained, all results of 3-dimensional lower bound were below the identical Michalowski (2001) upper bound. However, the results should be within the upper and lower bound as the main idea of theory. It was also illustrated in Figure 2.53.

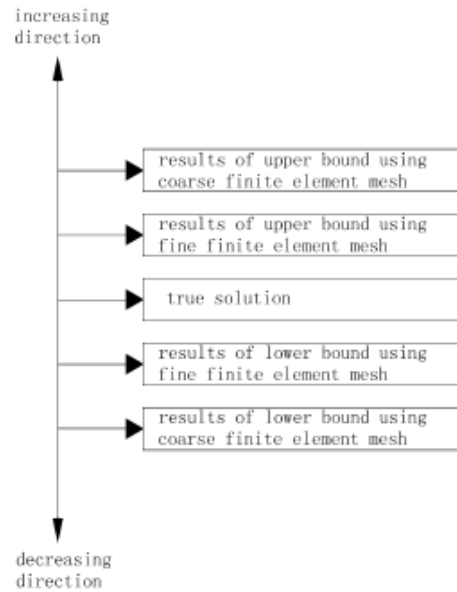


Figure 2.53. Various solutions for 3-dimensional bearing capacity for shallow foundations (H. Yang *et al.*, 2003).

The author had concluded that the accurate results of 3D condition would be more significant than the results of 2-dimensional state. Due to the dimensional outcome in the 3-dimensional state, this kind of impact was ignored entirely in the 2-dimensional state. As seen in Figure 2.53, in the lower bound methods, fine mesh gives a more significant outcome than coarse mesh, because it has matched more to the right solution.

Table 2.1. Comparison of 3-dimensional upper and lower bound coefficient of bearing capacity  $N_c$  for shallow foundations on a weightless and frictional cohesive soil.

| $\phi$ Degrees         | Author    |        |         |           |        |        | Michalowski |           |
|------------------------|-----------|--------|---------|-----------|--------|--------|-------------|-----------|
|                        | $L/B = 1$ |        |         | $L/B = 2$ |        |        | $L/B = 1$   | $L/B = 2$ |
|                        | I         | II     | III     | I         | II     | III    |             |           |
| <i>(a) Coarse mesh</i> |           |        |         |           |        |        |             |           |
| 10                     | 8.651     | 9.489  | 12.037  | 6.011     | 6.647  | 8.363  | 14.365      | 10.733    |
| 15                     | 10.597    | 11.713 | 16.454  | 8.273     | 9.218  | 13.06  | 22.984      | 15.585    |
| 20                     | 15.862    | 18.621 | 29.971  | 10.247    | 12.195 | 20.09  | 39.199      | 23.912    |
| 25                     | 20.179    | 25.734 | 49.912  | 11.653    | 14.277 | 29.424 | 71.397      | 38.312    |
| 30                     | 29.598    | 39.759 | 110.823 | 14.437    | 21.479 | 60.452 | 139.337     | 67.099    |
| <i>(b) Fine mesh</i>   |           |        |         |           |        |        |             |           |
| 10                     | 8.962     | 9.774  | 12.458  | 6.193     | 6.899  | 8.719  | 14.365      | 10.733    |
| 15                     | 10.972    | 12.088 | 17.129  | 8.519     | 9.587  | 13.771 | 22.984      | 15.585    |
| 20                     | 16.385    | 19.465 | 31.460  | 10.668    | 12.717 | 21.115 | 39.199      | 23.912    |
| 25                     | 20.976    | 26.994 | 52.712  | 12.200    | 14.992 | 31.179 | 71.397      | 38.312    |
| 30                     | 31.117    | 42.065 | 116.327 | 15.246    | 22.719 | 64.386 | 139.337     | 67.099    |

The coefficient of bearing capacity  $N_c$  of the exterior foundation for utterly adhesive soil was measured by the of 3-dimensional lower bound technique and compared with the results of identical Michalowski (2001) upper bound, as shown in Table 2.1. According to results, yield condition has a specific effect on 3-dimensional examination of limit lower bound. Moreover, several results can be obtained from different yield criterions. For example, the author's outcome is below Michalowski's method. This variation also grows with the increment of soil inner frictional angle  $\Phi$ .

Salgado *et al.* (2004) developed a solution tool based on finite limit analysis for calculating shallow footings around inclines. These computations were conducted for rough strip, square, circular, and rectangular footings. We can represent the clay as a matter with the  $c=s_u$  and  $\varphi=0$  features, where  $s_u$  is the undrained shear strength of the clay. Therefore, the equation in 2.13 was presented below for a strip footing on the soil surface.

$$q_{bL} = S_u + N_c \quad (2.13)$$

where  $N_c = 2 + \pi \approx 5,14$  (first found by Prandtl 1920, 1921)

The author has modified that equation to calculate the limit base stability of rectangle, circular, or square foundations constructed at various profundities inside the clay, revision determinants converting back to Equation 2.14.

$$q_{bL} = s_c d_c N_c s_u + q_0 \quad (2.14)$$

In accordance with material assumptions of limit analysis,  $c-\varphi$  clay is rigid, completely flexible material and follows correlated flow rule. For clays, the bearing capacity of

foundations of limited design dimension  $B$  and  $L$  have been higher than shallow foundations with breadth  $B$ . As the expressions for shape and depth factors given in Figure 2.54. were illustrated to get the bearing capacity of used in circular, rectangular or square foundations that multiplying  $s_u N_c$ .

| Shape Factors         | Depth Factors   | Author               |
|-----------------------|---|----------------------|
| $s_c = 1 + (0,2) B/L$ | $d_c = 1 + (0,2) D/B$   | Meyerhof (1951)      |
| $s_c = 1 + (0,2) B/L$ | $d_c = 1 +$<br>$(0,4) D/B \text{ for } D/B < 1$<br><br>$d_c$<br>$= 1$<br>$+ (0,4) \tan^{-1} D/B \text{ for } D/B$<br>$\geq 1$ | Brinch Hansen (1970) |

Figure 2.54. Shape and depth factors usually utilized for clays (Salgado *et al.*, 2004).

Although various tables had been presented in this analysis to show the influence of shape and depth effects on ultimate bearing capacity, bearing capacity values depending on ratio of  $B/L$  and  $D/B$  were compared with examination of upper and lower bound limit presented in the following Figure 2.55. They are enough to sum up the essential results of the study. Referring to the table, the corresponding distinction among upper and lower bounds falls to approximately 12% as  $B/L$  declines from 1 to 0.2 for rectangular footings despite the state of  $D/B$ . Computations have been performed according to average amounts and lower bound of  $q_{BL}^{net}$ . However, for employment in design, it is suggested to choose lower values.

| D/B  | Strip |       | Circular |        | Square |        | Rectangular with B/L= |        |        |        |        |        |       |        |
|------|-------|-------|----------|--------|--------|--------|-----------------------|--------|--------|--------|--------|--------|-------|--------|
|      |       |       |          |        |        |        | 0.50                  |        | 0.33   |        | 0.25   |        | 0.20  |        |
|      | L     | U     | L        | U      | L      | U      | L                     | U      | L      | U      | L      | U      | L     | U      |
| 0.00 | 5.132 | 5.203 | 5.856    | 6.227  | 5.5523 | 6.221  | 5.359                 | 6.022  | 5.256  | 5.886  | 5.201  | 5.820  | 5.169 | 5.779  |
| 0.01 | 5.164 | 5.259 | 5.962    | 6.503  | 5.610  | 6.442  | 5.424                 | 6.249  | 5.311  | 6.085  | 5.253  | 6.006  | 5.218 | 5.949  |
| 0.05 | 5.293 | 5.384 | 6.295    | 6.840  | 5.886  | 6.815  | 5.640                 | 6.503  | 5.503  | 6.3003 | 5.430  | 6.203  | 5.389 | 6.126  |
| 0.10 | 5.448 | 5.548 | 6.491    | 7.140  | 6.171  | 7.130  | 5.860                 | 6.756  | 5.697  | 6.533  | 5.614  | 6.413  | 5.565 | 6.321  |
| 0.20 | 5.696 | 5.806 | 6.897    | 7.523  | 6.590  | 7.534  | 6.197                 | 7.116  | 5.997  | 6.867  | 5.895  | 6.731  | 5.836 | 6.637  |
| 0.40 | 6.029 | 6.133 | 7.303    | 8.104  | 7.194  | 8.096  | 6.680                 | 7.574  | 6.408  | 7.271  | 6.272  | 7.113  | 6.190 | 7.003  |
| 0.60 | 6.240 | 6.341 | 7.866    | 8.608  | 7.671  | 8.573  | 7.082                 | 7.993  | 6.740  | 7.608  | 6.567  | 7.412  | 6.465 | 7.299  |
| 0.80 | 6.411 | 6.509 | 8.370    | 9.034  | 8.068  | 8.996  | 7.427                 | 8.377  | 7.030  | 7.936  | 6.817  | 7.706  | 6.695 | 7.370  |
| 1.00 | 6.562 | 6.657 | 8.771    | 9.429  | 8.429  | 9.346  | 7.729                 | 8.724  | 7.297  | 8.240  | 7.048  | 7.976  | 6.904 | 7.819  |
| 2.00 | 7.130 | 7.227 | 9.973    | 11.008 | 9.752  | 10.853 | 8.968                 | 10.055 | 8.447  | 9.476  | 8.109  | 9.086  | 7.860 | 8.835  |
| 3.00 | 7.547 | 7.652 | 10.686   | 12.140 | 10.532 | 12.000 | 9.860                 | 11.076 | 9.296  | 10.473 | 8.920  | 10.026 | 8.607 | 9.696  |
| 4.00 | 7.885 | 7.994 | 10.954   | 13.030 | 10.941 | 12.900 | 10.513                | 11.878 | 10.018 | 11.242 | 9.594  | 10.769 | 9.249 | 10.403 |
| 5.00 | 8.168 | 8.284 | 10.998   | 13.743 | 11.206 | 13.640 | 10.880                | 12.545 | 10.464 | 11.887 | 10.117 | 11.408 | 9.796 | 11.030 |

Figure 2.55. Ratio of net bearing capacity factor to undrained shear strength,  $q_{bl}^{net}/s_u$ , for foundations in clay ( $L$  = lower,  $U$ = upper bound) (Salgado *et al.*, 2004).

The shape factors computed from the average of the upper and lower bound values utilizing the equation given in 2.15.

$$s_c = \frac{q_{bl}^{net}}{d_c[q_{bl}^{net}]} \quad (2.15)$$

The average value at the surface by declining  $B/L$  precisely falls to 1. The values of  $C_1$  and  $C_2$  as a dependent of  $B/L$  is given in Figure 2.56 to provide the best-fit lines with the equation 2.16.

$$s_c = 1 + C_1 \frac{B}{L} + C_2 \sqrt{\frac{D}{B}} \quad (2.16)$$

| B/L       | C <sub>1</sub> | C <sub>2</sub> |
|-----------|----------------|----------------|
| 1(circle) | 0.163          | 0.210          |
| 1(square) | 0.125          | 0.219          |
| 0.5       | 0.156          | 0.173          |
| 0.33      | 0.159          | 0.137          |
| 0.25      | 0.172          | 0.110          |
| 0.2       | 0.190          | 0.090          |

Figure 2.56. Constants of regression in the shape factor equation (Salgado et al., 2004).

Additionally, the estimated factors of form for squared and round footings are varying from the point at  $D/B=4$ , the bound of the graphic. Because of the significant gap among upper and lower limit examination for  $B/L = 1$  and the variation point for  $D/B > 4$ , results for  $D/B > 4$  is not plotted in Figure 2.57.

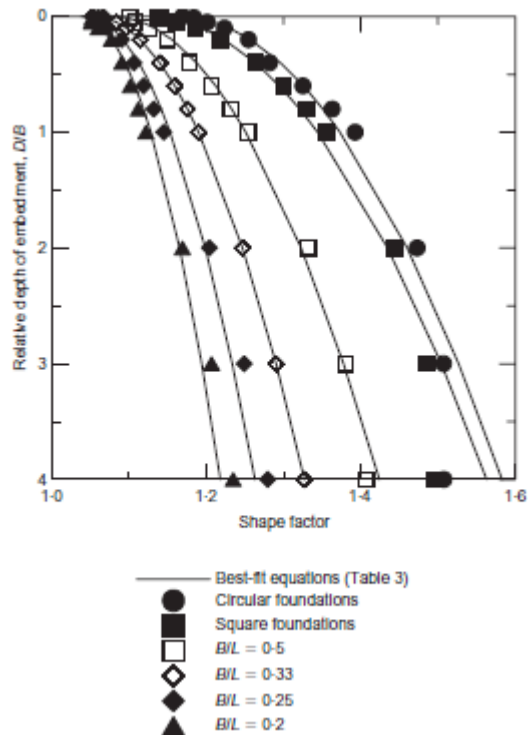


Figure 2.57. Shape factor for foundations of various shapes as a function of relative depth as calculated by limit analysis plotted together with best-fit lines with the form of Equation 2.25 (Salgado *et al.*, 2004).

The author had concluded that the equation utilized in the application for the factors of form perceived to more conservative expect for excessively low  $D/B$ . The equation of Meyerhof (1951) for the factor of depth was also perceived as sensible as well. On the other hand, the Brich Hansen (1970) equation was perceived to be sufficient for extremely low  $D/B$  values and not conservative for higher amounts of  $D/B$ . Based on the presented study, the uncertainties with regard to the equation of bearing capacity may cause lower factors of safety.

In order to investigate the impact of the foundation shape on the bearing capacity of a medium elasto-plastic clay, Zhu and Michalowski (2005) had used the limited element approach. The earlier proposal was according to experimental data for small foundations while a new proposal for these factors is according to the model of elasto-plastic of the clay.

In this study, ABAQUS was used to reach the maximum load of square and rectangular foundations as a finite element system. Twenty-node elements of quadratic brick with a reduced integration plan were adopted in all finite element models prepared within the context of this study. It was depicted in Figure 2.58, there is a schematic description of the finite component mesh.

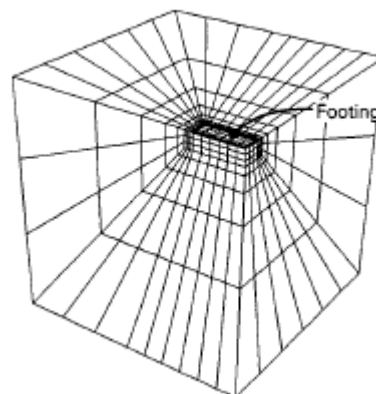


Figure 2.58. Finite element mesh (Zhu and Michalowski, 2005).

A group of computations with finer meshes were performed by the authors. The variation in coefficient of bearing capacity factor gained from computations with the coarse mesh and the fine mesh changed fewer than 1% ( $\phi=10^\circ$ ,  $L/B=2$ ) to not actually 4% ( $\phi=35^\circ$ ,  $L/B=2$ ). The change in  $N_\gamma$  factor was increasing to 8%. Since the coarse mesh was selected for the calculations of finite element and plane strain, the results of these calculations showed that rectangular footings are more dependent on the limit loads than the size of the mesh. The diversity in factors of form calculated for the coarse and fine meshes were quite smaller than 1%.

In essence, the approach adopted in this study is to express the  $N$  factor is the functions of  $\phi$ ,  $c/\gamma B$ , and  $q/\gamma B$ . Eventually, if these three expressions are computed independently, the sum of the three items will be the best upper bound consistent assessment. In this sense, the component of the bearing capacity based on adherence was computed considering no excessive burden ( $q=0$ ) and weightless soil ( $\gamma=0$ ) given in the following Equation 2.17.

$$p = cN'_c = s_c c N_c \quad (2.17)$$

where  $N'_c$  = factor of bearing capacity for the orthogonal foundation. Shape factor  $s_c$  was determined by the formula given in Equation 2.18.

$$s_c = \frac{N'_c}{N_c} \quad (2.18)$$

Where  $N_c$  = factor for the shallow foundation. Shape factor  $s_q$  can be measured in the same method. Hence, the factor  $N'_q$  can be obtained using the Caquot rule of equivalent states as given in Equation 2.19 and Equation 2.20.

$$N'_q = N'_c \tan \phi + 1 \quad (2.19)$$

and

$$s_q = \frac{N'_q}{N_q} \quad (2.20)$$

Therefore,  $s_q$  factor can be obtained if  $s_c$  is identified as given in Equation 2.21.

$$s_q = \frac{N'_q}{N_q} = \frac{N'_c \tan \phi + 1}{N_c \tan \phi + 1} = \frac{s_c N_c \tan \phi + 1}{N_c \tan \phi + 1} \quad (2.21)$$

Results of the developed method were compared with FEM results show clearly that the upper-bound approach limit analysis produces remarkably greater factors of form, especially for small aspect ratios  $L/B$  and great angles of friction  $\phi$ . Outcomes of this study carried out by using the FEM method are summarized in the following:

- When the earlier studies of Meyerhof (1963) and De Beer (1970) are considered, their estimates for  $s_c$  and  $s_q$  are found to be conservative. Particularly smaller amounts of  $s_c$  and  $s_q$  returns for low angles of friction and small aspect ratios of the limited element approach. Additionally, the shape factor  $s_\gamma$  can rise or fall according to the aspect ratio, but it also depends on the angle's internal friction of the clay.
- The shape factors and the bearing capacity computed using FEM had unsatisfactory performance compared to the kinematic boundary examination.

- Meyerhof (1963) or De Beer (1970) approaches are virtually the same, except for small  $\phi$  and low  $L/B$ . Furthermore as shown in the graph given Figure 2.59, their results are lower than those from fine element method.

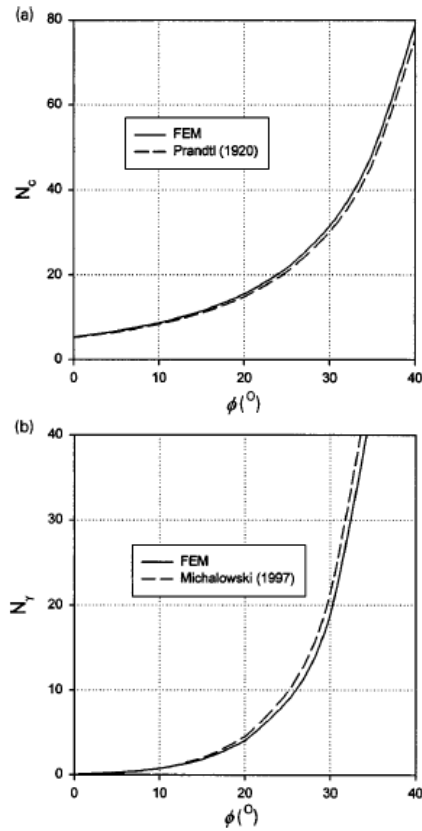


Figure 2.59. The analogy of results: (a) factor  $N_c$  and (b) factor  $N_\gamma$  (Zhu and Michalowski, 2005).

- Factor  $s_\gamma$  results are given in Figure 2.60 somewhat unusual because, by a fall in the aspect ratio for large internal angles of friction,  $s_\gamma$  rises. Besides this, for small angles of friction, it is reduced.  $S_\gamma$  has a bounded top for  $\phi=35^\circ$ .

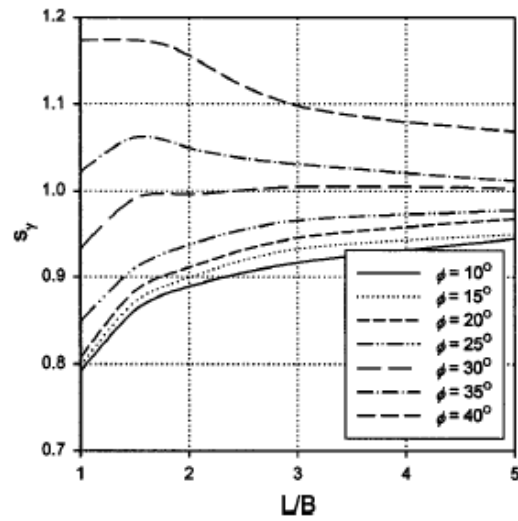


Figure 2.60. Factor  $s_\gamma$  (finite element method) as a function of aspect ratio  $L/B$  and internal friction angle  $\varphi$  (Zhu and Michalowski, 2005).

- As shown in Figure 2.61, the deformation scheme has diagonal symmetry, and the transformation in the zones close to the edges of the squared foundation is not flat.

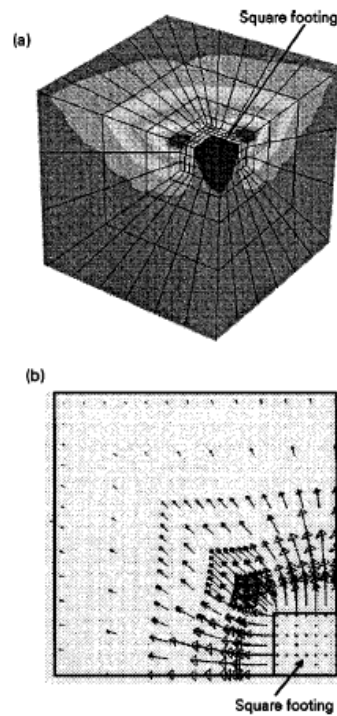


Figure 2.61. Movement in the region of squared foundation: (a) 3-D distribution of vertical displacement intensity and (b) horizontal movement at surface (Zhu and Michalowski, 2005).

Pathak *et al.* (2008) proposed a laboratory model to utilize small scale load tests on footings on  $c-\phi$  clay and to find the bearing capacity of foundation on  $c-\phi$  clay utilizing model test results and compare experimental data with theoretical work. The aim of the study was to investigate the impact of different parameters such as  $L/B$  rate, shape, and size of foundation on bearing capacity.

| Sr. No. | Shape Of Foundation | Footing Designation | Size Of Footing (mm x mm) | L/B Ratio |
|---------|---------------------|---------------------|---------------------------|-----------|
| 1       | Square              | S1                  | 101.6 X 101.6             | 1         |
| 2       | Square              | S2                  | 203.2 X 203.2             | 1         |
| 3       | Rectangular         | R1                  | 50.8 X 152.4              | 3         |
| 4       | Rectangular         | R2                  | 50.8 X 203.2              | 4         |
| 5       | Rectangular         | R3                  | 101.6 X 203.2             | 2         |
| 6       | Rectangular         | R4                  | 101.6 X 304.8             | 3         |
| 7       | Rectangular         | R5                  | 10.6 X 406.4              | 4         |
| 8       | Circular            | C1                  | 114.3 mm dia.             | -         |
| 9       | Circular            | C2                  | 228.6 mm dia.             | -         |

Figure 2.62. Model test programme (Pathak *et al.*, 2008).

The experimental test was conducted in Geotechnical Engineering Laboratory of College of Engineering. In this study, load tests were performed in the lab on two square, two circular, and five rectangular foundations on  $c-\phi$  clay as given Figure 2.62. These tests were performed on square, circular, and rectangular model footings of various sizes located on the surface condition medium, prepared under arranged engineering parameters. Additionally, to show the material employed in the test plan, soil characteristics as listed in Table 2.2.

Table 2.2. Soil characteristics.

| Sr. No. | Test                     | Name<br>Property Name                               | I.S Code No. |
|---------|--------------------------|---|--------------|
| 1       | Sieve Analysis           | Gravel : 0%   | 2720-IV      |
|         |                          | Sand : 56.99 %                                      |              |
|         |                          | Silt : 25.25 %                                      |              |
|         |                          | Clay Content:<br>17.76 %                            |              |
|         |                          | Soil<br>Classification:<br>CL                       |              |
| 2       | Standard Proctor<br>Test | MDD: 1.764<br>g/cc                                  | 2720-VII     |
|         |                          | OMC: 15%  |              |
| 3       | Direct shear test        | C: 4 kN/m <sup>2</sup> ,<br>$\phi$ :34 <sup>o</sup> | 2720-XIII    |
| 4       | Consistency<br>Limits    | Liquid limit:<br>34.20 %                            | 2720-V       |
|         |                          | Plastic limit:<br>22.67 %                           |              |
|         |                          | Plasticity index:<br>11.53%                         |              |

The author compared the results of model test results with a bearing capacity of foundations evaluated by standard techniques such as Vesic's and Terzaghi's technique. As a result of the comparisons, the author concluded that both Vesic's and Terzaghi's approaches underestimate the bearing capacity of both squares as well as rectangular footings. Comparison between bearing capacity obtained from model test and conventional methods is shown in Table 2.3.

Table 2.3. Ultimate bearing capacity (UBC) for footings.

| Footing No. | Footing Size Mm. | L/B Ratio | Measured UBC, kN/m <sup>2</sup> | UBC by Vesic's Approach, Kn/m <sup>2</sup> | UBC by Terzaghi's Approach, Kn/m <sup>2</sup> |
|-------------|------------------|-----------|---------------------------------|--|---|
| S1          | 101.6 x 101.6    | 1         | 377.81                          | 308.88                                     | 299.98  |
| S2          | 203.2 x 203.2    | 1         | 406.87                          | 331.35                                     | 326.24  |
| R1          | 50.8 x 152.4     | 3         | 271.25                          | 224.13                                     | 246.92  |
| R2          | 50.8 x 203.2     | 4         | 244.13                          | 214.94                                     | 241.93  |
| R3          | 101.6 x 203.2    | 2         | 324.43                          | 257.49                                     | 271.68  |
| R4          | 101.6 x 304.8    | 3         | 321.3                           | 240.36                                     | 262.24  |
| R5          | 101.6 x 406.8    | 4         | 319.68                          | 231.79                                     | 257.53  |
| C1          | 114.3 dia.       | -         | 372.28                          | 311.69                                     | 295.87  |
| C2          | 228.6 dia.       | -         | 404.81                          | 336.94                                     | 317.03  |

The author had concluded that by an increment in  $L/B$  rate of foundation, the ultimate bearing capacity values of foundations with the same width decrease. Moreover, limit loads increase with an increase in footing size for the same  $L/B$ .

As anticipated, the ultimate bearing load raises with a rise in the size of the footing. On the other hand, this study based on  $c-\phi$  soil has shown that size effects are minimal for square and circular footings while they are noticeable on rectangular footings.

To assume the forcing answers of squared foundations over soft soils, Yu *et al.* (2011) had proposed that to employ the 3D large deformation finite element examinations during 3D RITSS technique. Additionally, the impacts of surface soil heave and soil layer interface deformation in weightless soil during foundation penetration were examined.

In this study, as being different from foundation failure previously obtained, 'punch-through' failure was considered. It was defined that the foundation drops freely to point A' to balance the load, whenever the preload surpasses the first top capability illustrated at point A in Figure 2.63.

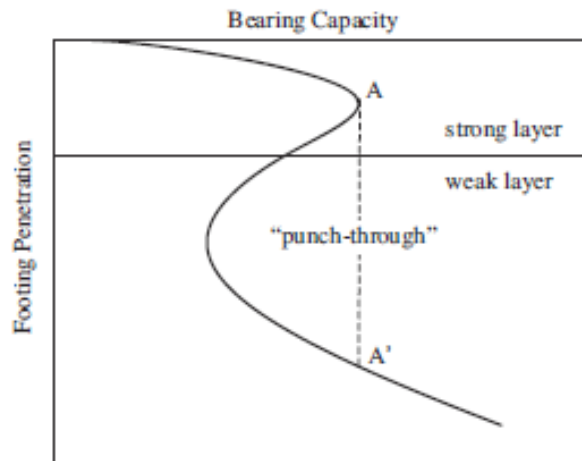


Figure 2.63. Typical penetration response of a footing on strong over weak soils (Yu *et al.*, 2011).

The author also carried out small strain finite element analyses to compare with the available solutions. Using 3D small strain analyses to solve the problem, we can use AFENA finite element computer program (Carter and Balaam 1995). The undrained soil followed Tresca rule. Accordingly, undrained total stress parameters were used. The Poisson's rate was taken  $\nu=0,49$ . Young's modulus' proportion to clay shear strength was set to  $E/c=500$ . The undrained shear strength of the first layer was defined fixed as  $c_1=100\text{kPa}$ , and the strength of underneath layer,  $c_2$ , changed to produce the proper clay layer strength ratio,  $c_2/c_1$ , which is smaller than 1.0.

The soil area was implemented as  $10B$  in width and  $6B$  in depth to prevent boundary effect. A standard mesh representation accepted in this research was depicted in Figure 2.64.

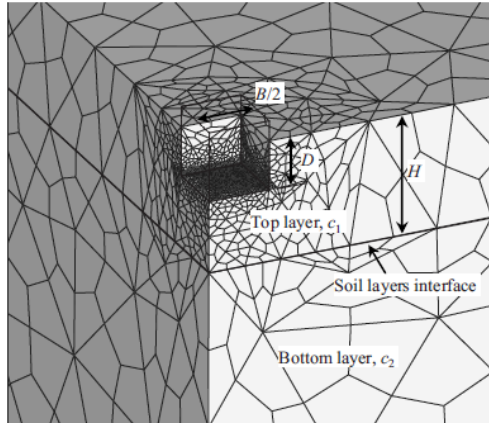


Figure 2.64. Typical finite element mesh (Yu *et al.*, 2011).

The author had also proposed that a useful large deformation method from the inside of the free Lagrangian-Eulerian class called RITSS (remeshing and interpolation method with small strain model). Different 2D plain-strain and axisymmetrical finite element examinations have employed this method (Hu and Randolph 1998a; Wang and Carter 2002; Lu *et al.*, 2004; Thorne *et al.*, 2004; Hossain *et al.* 2005a). Therefore, the 2D RITSS approach has been developed for 3D RITSS FE approach (Yu *et al.* 2008). In order to calculate the factor of bearing capacity of a surface foundation on a uniform, the following Equation 2.31 was used.

$$N_c = \frac{q}{c} = \frac{F}{Axc} \quad (2.31)$$

$q$  is the bearing stress of a foundation near slope;  $c$ =undrained shear strength of the soil;  $F$  is net bearing pressure;  $A$ = foundation space. The area of squared foundations examined in this study. Hence  $A/4=(B'/2)^2$ , where  $B'$ =effective foundation breadth which is extended by half of the least component volume on each edge ( $B'/2=B/2+h_{min}/2$ ).

The author compared the analyses of FE with those of existing solutions presented by previous researchers. As a result of the comparisons, the author concluded that all FE analyses remain within the lower and upper bound methods of Salgado *et al.* (2004).

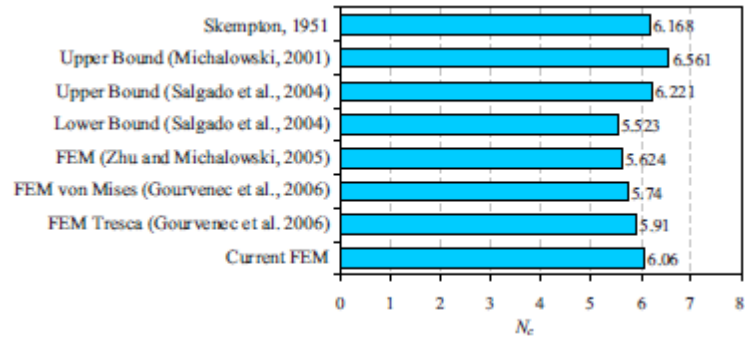


Figure 2.65. Factors of bearing capacity for surface rough squared foundations on smooth soils (Yu *et al.*, 2011).

When the determinant of bearing capacity of an exterior foundation is considered for two-layered clays, it related to the corresponding top layer width,  $H/B$ , and the soils power rate,  $c_2 / c_1$ . The author concluded that the current finite element results were in good agreement with the existing methods of Wang and Carter (2002) and Zhu and Michalowski (2005).

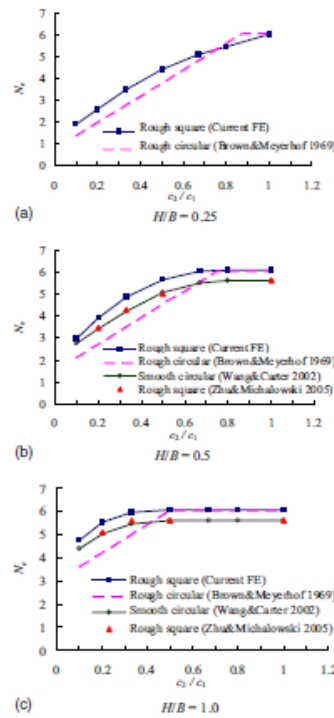


Figure 2.66.  $N_c$  for surface square foundations on two-layer weightless soils (small strain analyses) (Yu *et al.*, 2011).

Li *et al.* (2009) had used a three-dimensional finite difference program to simulate the bearing capacity of rectangular footings. Mohr-Coulomb failure criteria were used to define the soil strength. In the three-dimensional analysis model developed within the scope of this study, according to a dimensionless parameter, soil mass factor, and aspect ratio, calculated outcomes are shown as the function of dimensionless bearing capacity. Additionally, the mechanism of failure in limit conditions is examined.

According to conventional bearing capacity methods for rectangular foundations can be calculated by using empirical modification estimate impacts of foundation form. This equation is represented by Equation 2.22.

$$p_u = cN_c s_c + qN_q s_q + \frac{1}{2} \gamma B N_\gamma s_\gamma \quad (2.22)$$

Where the factors of bearing capacity  $N_c$ ,  $N_q$ , and  $N_\gamma$  shows the impacts of soil adherence  $c$ , overcharge  $q$ , and soil unit mass  $\gamma$ , sequentially;  $s_c$ ,  $s_q$ , and  $s_\gamma$  are shape factors with respect to  $N_c$ ,  $N_q$ , and  $N_\gamma$ , sequentially; and  $B$  is the breadth of the foundation.

In this context, for investigating nonlinear response of elements and associated mechanism of vulnerability and collapse, a computer program named as 'FLAC<sup>3D</sup>' was prepared by authors for three-dimensional analysis. In this study, all three correspondent directions have established the vertical edges and the base. In the general direction, the movements of equal levels are constant. Calculations are carried out for a rough soil foundation interface. Undrained Young's modulus  $E=2 \times 10^5$ , Poisson rate  $\nu= 0.3$  was assumed. Additionally, the dimensionless soil mass factor changed to 100 from 0.1. In order to show the form impact on bearing capacity  $L/B = 1$  (squared), 1.5, 2, 3, and 5 were used in the analyses.

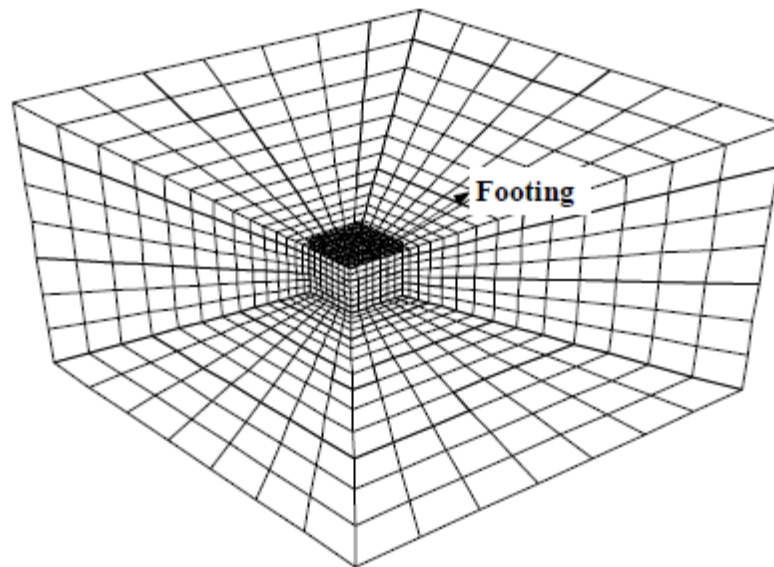


Figure 2.67. The meshing of the computational model (quarter symmetry) (Li *et al.*, 2009).

The normalized soil unit mass is  $G = \frac{\gamma B}{2c}$ . Besides this, soil unit mass and soil adherence are considered as a function of  $G$ . It also shows the kind of soil. Lower  $G$  means the matter adherence is high, while a higher  $G$  means the matter adherence is low. Variation in the normalized vertical bearing capacity factor for a series of foundation aspect ratios

varies from 1 to 5 with the normalized soil mass factor from 0.1 to 100 that is shown in Figure 2.68.

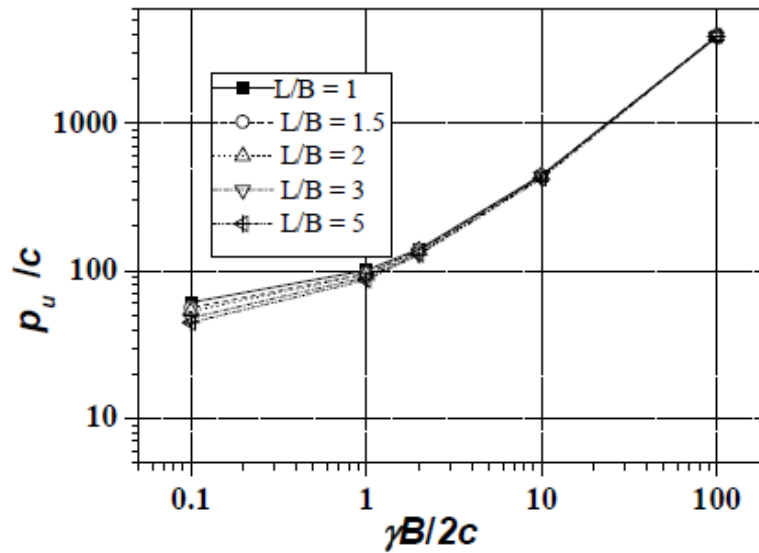


Figure 2.68. Bearing capacity for rectangular foundations of different forms (Li *et al.*, 2009).

Consequently, different shape of footings has a decisive impact on the bearing capacity of the soil, whereas it slightly changes the low adherence clay. The impact scope of the two clays can describe the reason for this effect. This result can easily be seen in Figure 2.69.

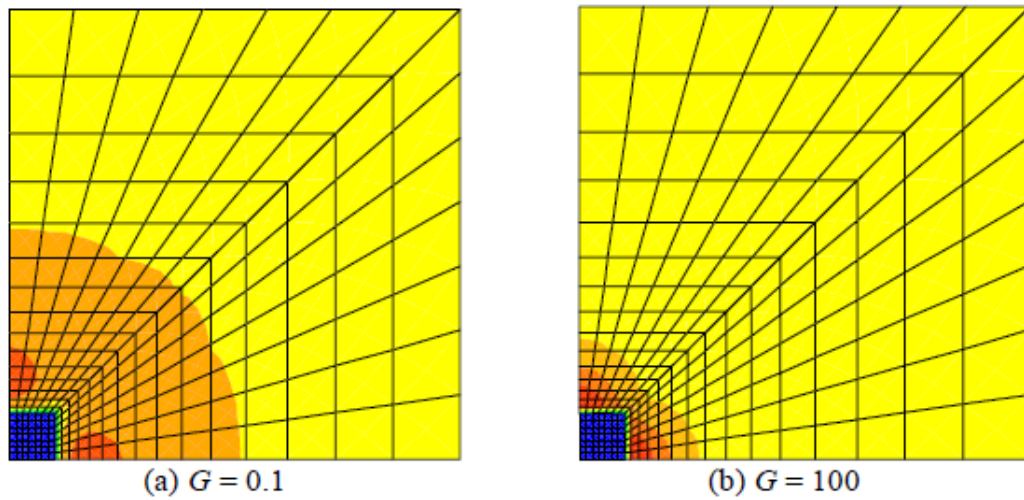


Figure 2.69. Plan representation of the foundation's impact scope (Li *et al.*, 2009).

The author had concluded that the range of failure in less adhesive clay is not as extensive as very adhesive clay; therefore, the failure mechanism is influenced merely through foundation form. Put another way, and a more extensive impact scope has an essential impact on shape effect. Result of the presented method was compared with those presented by Salgado *et al.* (2004), Zhu and Michalowski (2005) and Lyamin *et al.* (2007) then the accuracy of the phenomena was confirmed. As a result of their works,  $s_c$  is influenced by form noticeably and  $s_\gamma$  lead to 1 for any forms. Finally, the sensitivity of form influence on bearing capacity is estimated by influencing range.

Shiau *et al.* (2011) had derived that the undrained bearing capacity of a strip foundation located close to the side of an incline and cohesive slopes. The final bearing capacity of footings on inclines depending on different influential parameter have been computed owing to the finite element examination calculations of the upper and lower bound methods.

The graphical representation given by the author is illustrated in Figure 2.70 to define the problem.  $B$  is the breadth of a wall foundation placed on granular clay with an inclination angle  $\beta$  and inclination altitude  $H$  at a span  $L$  from the side of the incline. In accordance with material assumptions of limit analysis,  $c$ - $\phi$  soil is rigid-perfectly plastic and obeys the Tresca

yield model with a shear strength  $c_u$ .  $H/B$  was chosen as three in all examinations, which leads to 'over the toe collapse' that is discussed in this study.

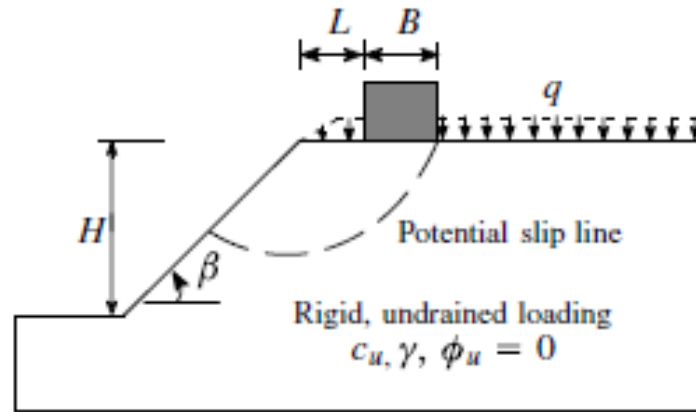


Figure 2.70. Problem notation and potential failure mechanism (Shiau *et al.*, 2011).

As a conclusion, as a function of dimensionless factors, bearing capacity influencing the durability of the system, which is expressed as given in Equation 2.23.

$$\frac{p}{\gamma B} = f\left(\beta, \frac{L}{B}, \frac{c_u}{\gamma B}, \frac{q}{\gamma B}, \frac{H}{B}\right) \quad (2.23)$$

$P$  is the average boundary stress running on the foundation;  $q$  is the overcharge weight for sloping ground. The author compared the results of derived finite-element limit analyses shown in Figure 2.71 with those of calculation analytically presented by Davis and Booker (1973). As a result of the comparisons, the author concluded that the vertical cut has no significant impact on the bearing capacity of the foundation for conditions with  $L/B \geq 4$ . Notably, the bearing capacity is diminished by a factor of 2.5, whereas the aspect ratio of footing  $L/B$  reduced from 4 to 0.

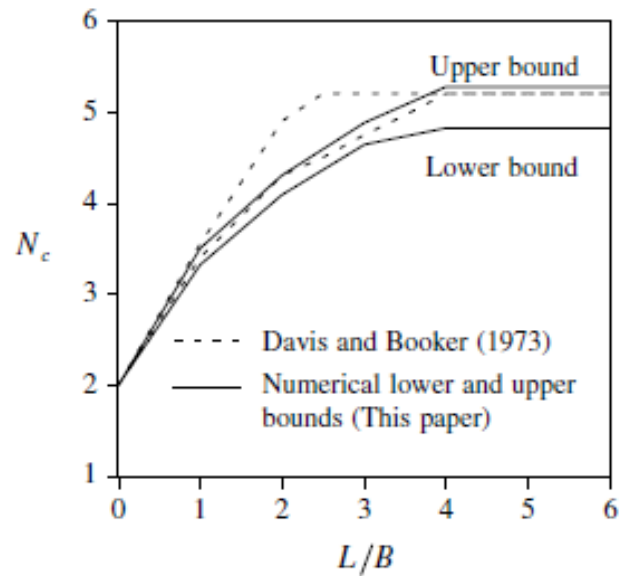


Figure 2.71. Bearing capacity of upper and lower bound for weightless slopes (smooth base,  $\beta=90^\circ$ ) (Shiau *et al.*, 2011).

The author also concluded that curved shapes and swiftness areas depending on different strength rates  $c_u/\gamma B$  of an vertical inclination ( $L/B=0, \beta=90^\circ$ ). Results showed that for both coarse and firm clays, the bearing capacity should be the same, which is presented in Figure 2.72. Whereas for a smaller strength ratio  $c_u/\gamma B = 1$ , the footing may be governed overall slope failure, the mechanism of failure is composed of a rigid triangular wedge for more significant values  $c_u/\gamma B \geq 2$ .

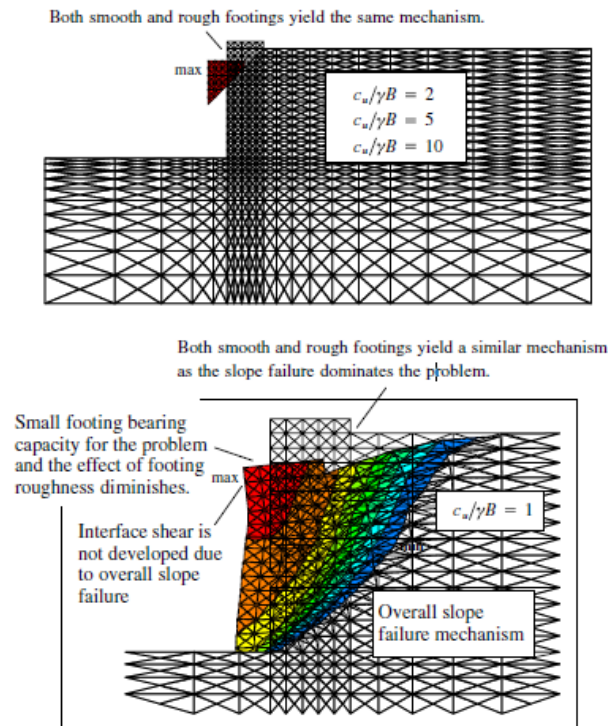


Figure 2.72. The analogy of transformed forms and swiftness profiles for smooth and rough foundations ( $\beta=90^\circ$ ,  $L/B=0$ ) (Shiau *et al.*, 2011).

| $c_u/\gamma B$ | $p/\gamma B$ |       |           |       |           |       |           |       |
|----------------|--------------|-------|-----------|-------|-----------|-------|-----------|-------|
|                | $L/B = 0$    |       | $L/B = 1$ |       | $L/B = 2$ |       | $L/B = 3$ |       |
|                | Smooth       | Rough | Smooth    | Rough | Smooth    | Rough | Smooth    | Rough |
| 10             | 19.95        | 19.95 | 33.75     | 33.79 | 41.31     | 41.33 | 47.30     | 47.32 |
| 5              | 9.50         | 9.50  | 16.12     | 16.17 | 19.64     | 19.65 | 22.73     | 22.74 |
| 3              | 5.50         | 5.50  | 9.01      | 9.01  | 10.85     | 10.88 | 12.72     | 12.78 |
| 1              | 1.32         | 1.32  | 1.20      | 1.20  | 1.46      | 1.46  | 1.99      | 1.99  |

Figure 2.73. Upper Bound Results for Rough and Smooth Foundations ( $\beta=90^\circ$ ) (Shiau *et al.*, 2011).

The average upper and lower bound assumptions of the normalized bearing capacity  $p/\gamma B$  are displayed in Figures 2.74. The dimensionless bearing capacity  $p/\gamma B$  diminishes linearly with the strength rate  $c_u/\gamma B$  until it starts nonlinear and fastly reaches 0 at a specific  $c_u/\gamma B$ .

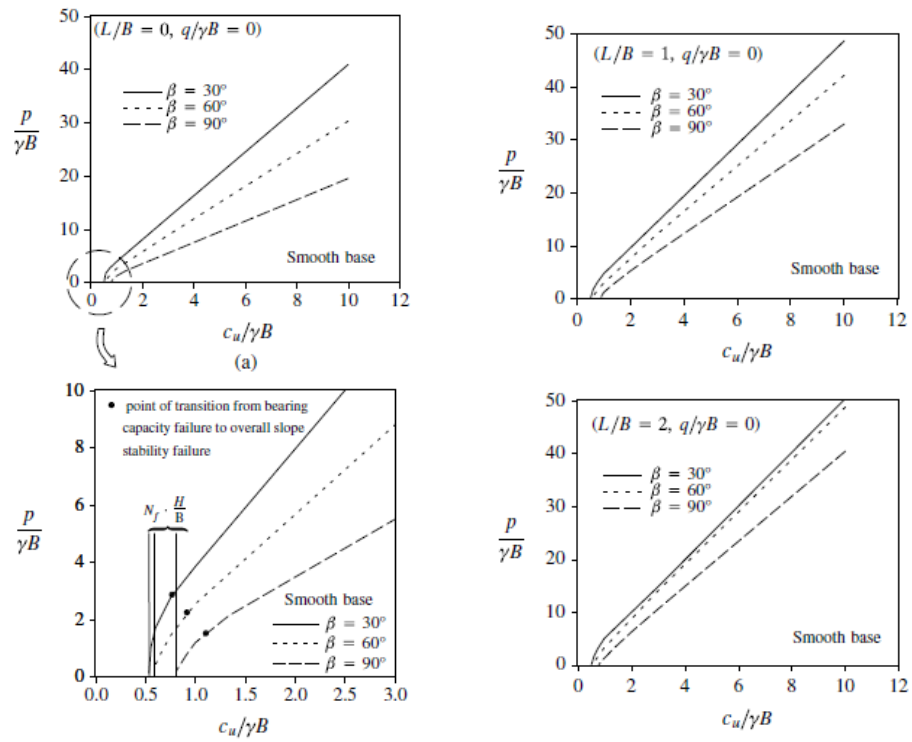


Figure 2.74. Averaged upper and lower bounds for different angles of inclination (Shiau *et al.*, 2011).

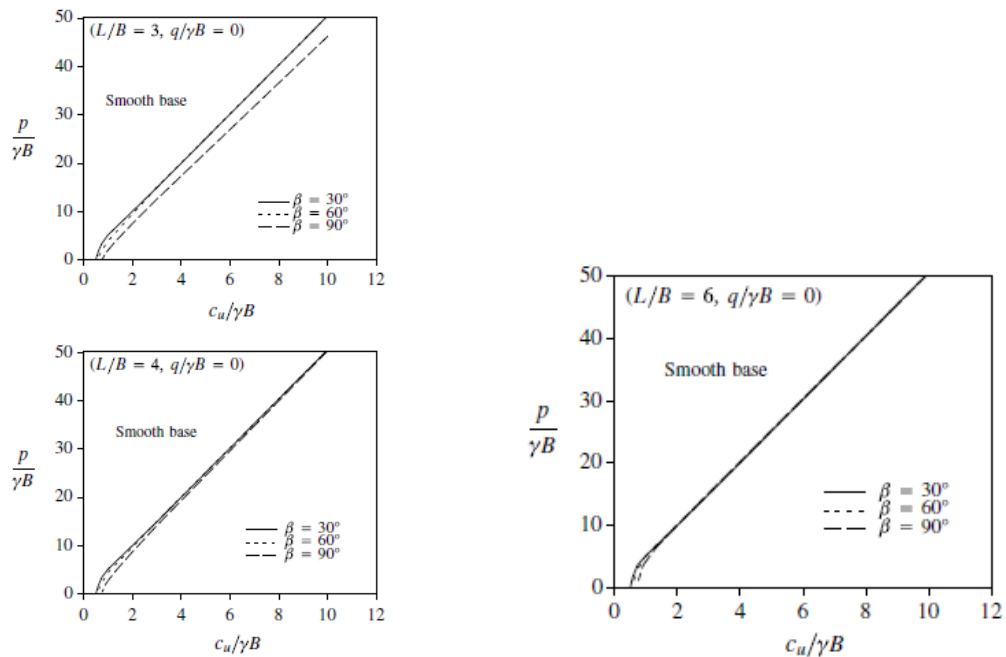


Figure 2.75. Averaged upper and lower bounds for different angles of inclination (Shiau *et al.*, 2011).

Presented design charts are drawn for showing failures of bearing capacity, which is included inside the front of the incline; therefore, the  $H/B$  rate has no impact. The assumed failure mechanism is shown in Figures 2.76 and 2.77.

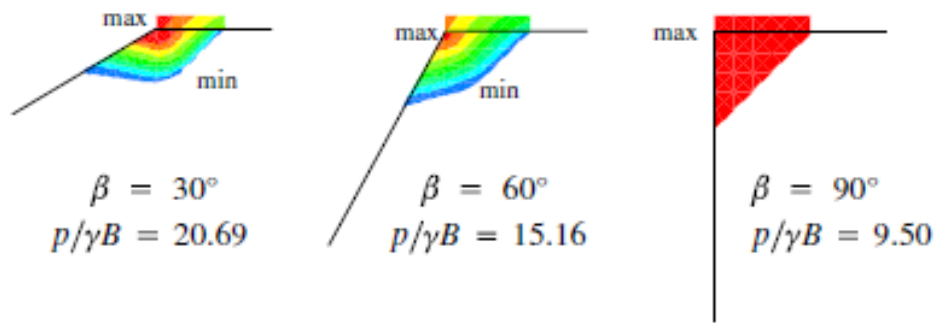


Figure 2.76. Velocity contours for different angles of inclination ( $c_u/\gamma B=5$ ,  $L/B=0$ , flat bottom) (Shiau *et al.*, 2011).

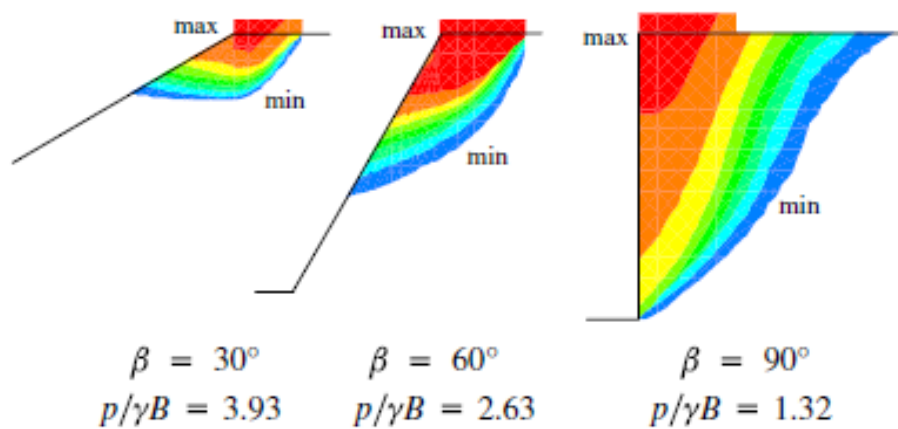


Figure 2.77. Velocity contours for different angles of inclination ( $c_u/\gamma B=1$ ,  $L/B=0$ , flat bottom) (Shiau *et al.*, 2011).

Additionally, the effect of slope angle can be obtained graphically in Figure 2.78 for  $L/B=0$ . As the angle of inclination rises, the footing bearing capacity decreased.

Moreover, it is determined that for all slope angle, the rise in footing capacity prone to hold at a specific point of  $L/B$ . The impact of  $L/B$  is illustrated in Figure 2.78 for examples of an upright portion with  $c_u/\gamma B = 5.0$ . It depicts that at  $L/B=5$ , the figure of the swiftness plan is typically the same for a foundation located on a flat earth. This means that the vertical cut doesn't affect the performance of the foundation.

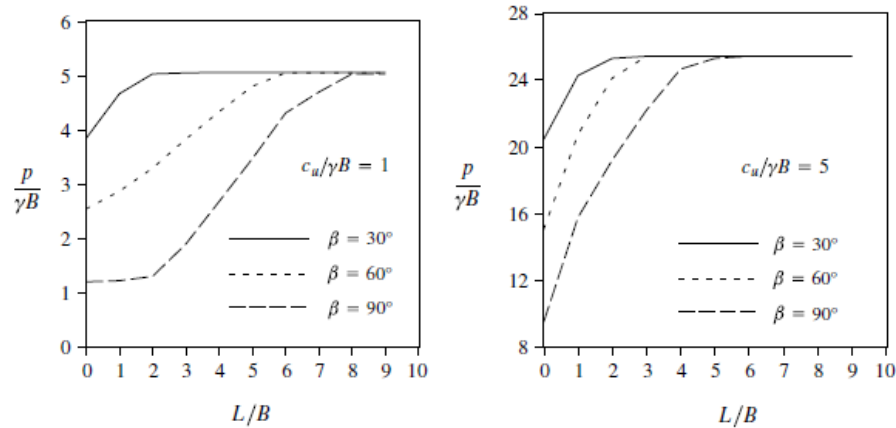


Figure 2.78. Impact of  $L/B$  on the bearing capacity (smooth base ) (Shiau *et al.*, 2011).

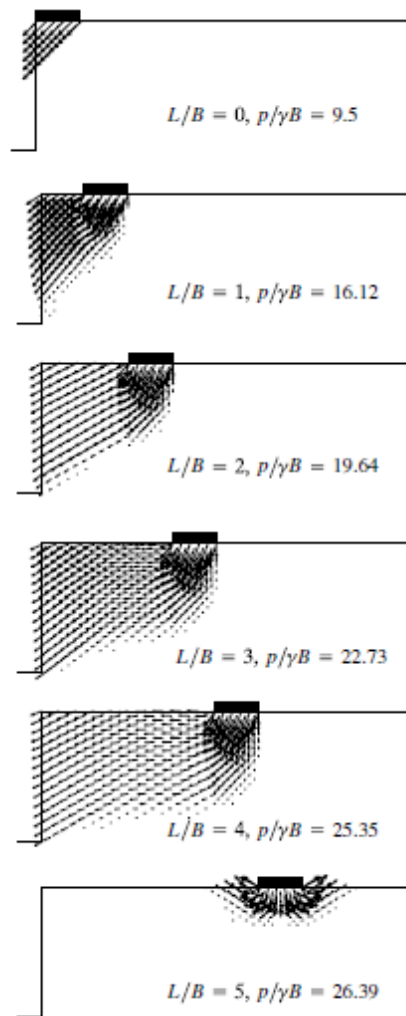


Figure 2.79. Velocity contours for different  $L/B$  (smooth base,  $\beta = 90^\circ$ ,  $c_u/\gamma B = 5$ ) (Shiau *et al.*, 2011).

The author had also examined the influence of  $H/B$ , which was also shown in Figure 2.80. It was observed that all failure mechanisms weren't especially affected by the toe of the incline when the ratio of  $H/B$  more significant than 3. As shown in Figure 2.80, the position of the toe was affected by the collapse load minimal. On the other hand, for minimum amounts of  $H/B$ , the effect of the incline on the failure system becomes trivial, hence the incline would be a portion of the mechanism of the bearing capacity.

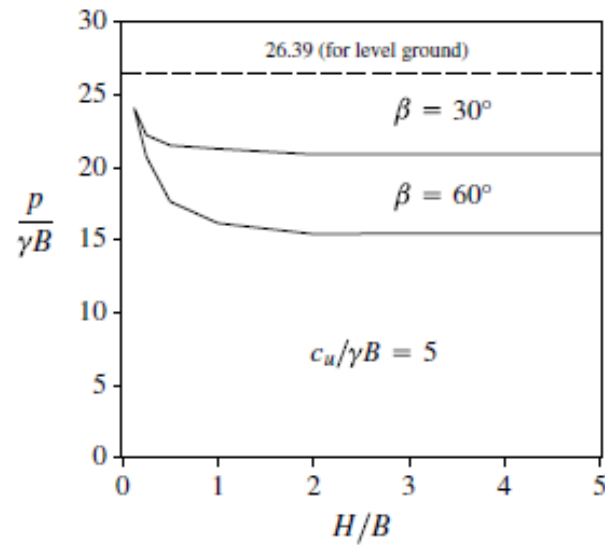


Figure 2.80. Effect of  $H/B$  (flat bottom,  $L/B=0$ ) (Shiau *et al.*, 2011).

Islam *et al.* (2017) had used three-dimensional finite element method including a Mohr-Coulomb elasto-plastic material model that accepted for the consideration of the form impact of the circular and squared surface foundation below upright loading in cohesive soil. In addition that the shape of the failure mechanism and the advanced failure around the foundations were examined with regard to the shape effect. In this study, the finite-element computer program, which is called 'ABAQUS' employed to find the ultimate bearing capacity of square and circular foundations. Finite element mesh used for the examination of the square and circular footings was illustrated in Figure 2.81.

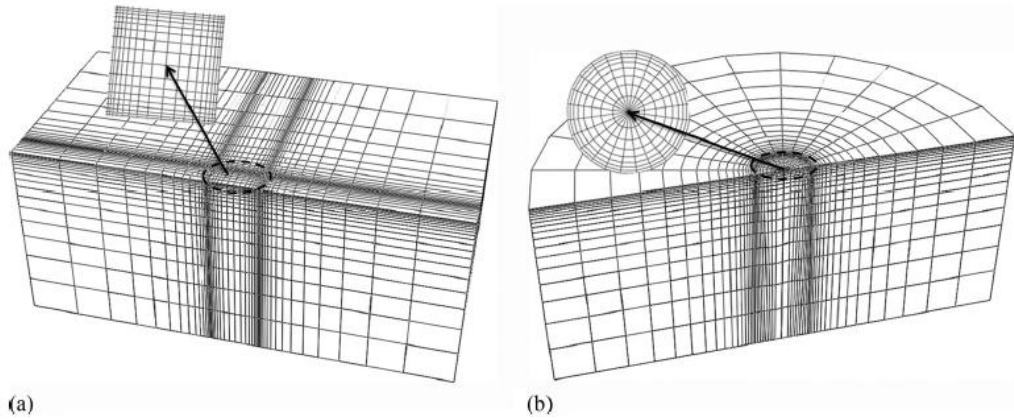


Figure 2.81. FE meshes: (a) half of a square footing; (b) half of a circular footing (Islam *et al.*, 2017).

The author compared the result of the developed method with those presented by previous researchers so far. As a result of the comparisons, the failure load of the square footing was 1.21 times bigger than that of circular footing. The results were also shown in Figure 2.82.

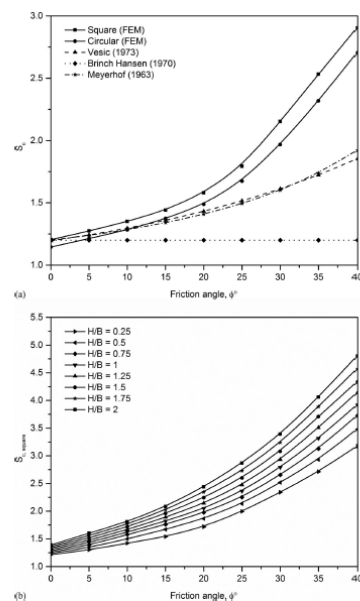


Figure 2.82. Shape factor  $s_c$  as a function of  $\varphi$  and  $D/B$ : (a) comparison with previous studies ( $D/B = 0$ ); (b) square footing; (c) circular footing (Islam *et al.*, 2017).

The assumed failure mechanism is shown in Figure 2.83 presents the plan view of the contours of the resultant displacement of rough circular and square footings at failure and display the change in soil displacement depending on the shape of footing. While the displacement contours of circular footings were created at the side of the foundation and moved to the outward orientation of the footing, the behavior for square footing was created at the corners and moved to the edges. It was concluded that the failure of the circular footing was found to be much shallower than that of the square footing.

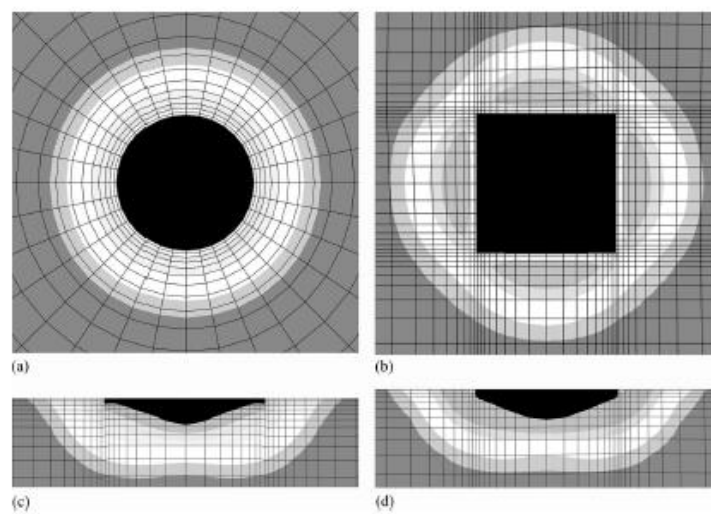


Figure 2.83. The failure mechanism is shown in plan view ( a and b ) and elevational view ( c and d): (a) circular foundation: (b) square foundation: (c) circular foundation: (d) square foundation (Islam *et al.*, 2017).

According to this study, the influence of soil cohesion on the shape factor  $s_c$  can be obtained as given in Equation 2.24.

$$s_c = \frac{N_{c(\text{square or circular})}}{N_{c(\text{strip})}} \quad (2.24)$$

The analysis results also are presented graphically in Figure 2.85. The cohesion shape factors for square and circular footing are calculated by the equations given in Equation 2.25 and Equation 2.26 respectively,

$$s_{c,square} = 1 + (3.5\phi^2 + 0.192) \quad (2.25)$$

$$s_{c,circular} = 1 + (3.1\phi^2 + 0.15) \quad (2.26)$$

The author also stated the impact of soil mass on shape factor. The modified bearing capacity factor ( $N_\gamma$ ) and shape factor ( $s_\gamma$ ) can be computed following Equations 2.27 and 2.28,

$$N_\gamma = \frac{(q_{ult} - cN_c)x2}{\gamma B} \quad (2.27)$$

$$s_\gamma = \frac{N_{\gamma(square\ or\ circular)}}{N_{\gamma(strip)}} \quad (2.28)$$

When the ponderable soil is regarded, the shape modifier can be expressed as given in Figure 2.84 for  $\phi$  ranging from  $5^\circ$  to  $40^\circ$ .

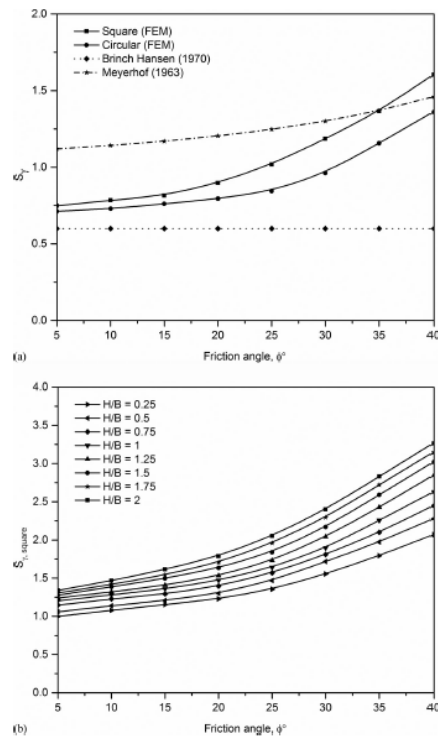


Figure 2.84. Shape factor  $s_g$  as a function of  $\phi$  and  $D/B$ : (a) Comparison with previous studies ( $D/B=0$ ); (b) Square footing; (c) circular footing. (Islam *et al.*, 2017).

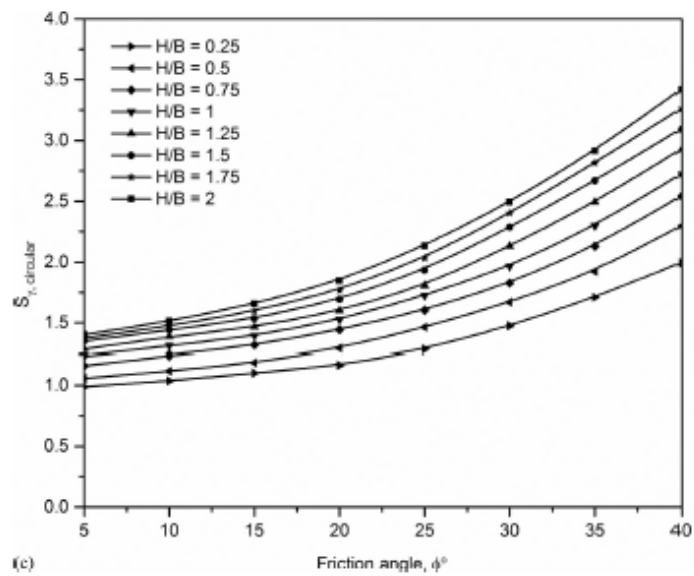


Figure 2.85. Continued (Islam *et al.*, 2017).

The author compared the results of the developed numerical model with those of calculation techniques presented by previous researchers so far. As a result of the comparisons, the author concluded that the results of the proposed method obtained for specific soil and geometrical combinations show a slight difference with those presented by the previous researchers. However, differences between results of the various calculation methods were also found for lower values of friction angle. Therefore, the shape factor  $s_c$  is not only a part of  $\varphi$  but also a function of  $D/B$ . Additionally, the shape factor  $s_\gamma$  is shown in Figure 2.85 also increased with the friction angle.

### 3. METHODOLOGY

The aim of this study is to investigate the effect of the shape effect of foundation which has not been studied in previous studies on the seismic bearing capacity of the shallow foundations constructed on or near the slopes. Numerous finite element models are defined under plane strain conditions and analyzed using Plaxis 3D.

This chapter includes important details regarding to development of the numerical model for determination of seismic bearing capacity of foundations near cohesive slopes. Model geometry, constitutive modelling of slope soil, mesh generation, loading and boundary conditions, material properties and mesh generation will be presented in detail in this chapter. After, the solution expressed by a simplified formula and the stages of the parametric study will be described. Additionally, the numerical approach adopted is the method of finite elements, using a commercial Plaxis 3D software. Therefore, thirdly, steps to be followed in order to make required activities within three Plaxis 3D sub modules (called Initial Phase, Calculation Module and Output) will be addressed with in detail.

At the end of this chapter is presented for verification of results obtained. This validation will be carried out for different shape of foundations. Seismic bearing capacity coefficient obtained by previous researcher for strip footings in undrained conditions will be compared with those obtained by Plaxis 3D. This comparison will be made only for one condition in which the footing is on the slope edge ( $\lambda=0$ ).

#### 3.1 FEM in Geotechnical Engineering and Plaxis 3D

The technique of finite element (FEM) is a numerical method to solve engineering and a wide variety of industries. Therefore, computer codes based on FEM have been designed to deal with difficulties including soil-structure interaction, foundation structures, seepage, and soil dynamics.

Most common methods of analysis generally use approaches that based on presumptions which oversimplify the problem at hand. These methods don't have the ability to consider all of the parameters and factors the design engineer meets and can acutely constrain the results of solution. FEM can deal with many of these deficiencies, therefore it offers many advantages to traditional methods (USACE,1995). Their ability to accurately reflect field conditions essentially depends on the ability of the constitutive model to represent real soil behavior and correctness of the boundary conditions imposed. The user has to describe the model geometry, construction step, soil parameters and boundary conditions. Structural components may be considered during the numerical analysis to model field conditions. Shallow foundations consist of different shape foundations, associated by structural members, can be regarded and, because the soil slope is modelled in the analysis, the relationship between slope angle or slope height and the soil can be taken into consideration. No hypothesized failure instrument or mode of behavior of the problem is not necessary because these are anticipated by the analysis. It enables the background of the boundary condition of problem to be assumed and a single analysis can give information on all design specifications. (Potts *et al.*, 2002)

PLAXIS 3D is a three dimensional finite element computer program that designed for the analysis of various shape foundation structures and stability analyses for different types of geotechnical implementations. The program combines simple graphical input procedures which empower the user to automatically generate complex finite element models. The advanced output facilities give a detailed presentation of computational results. The calculation itself is completely automated and based on robust numerical procedures. (Brinkgreve *et al.*, 2006)

### **3.2 Definition and Assumptions of the Problem**

Graphical representation of the problem is shown in Figure 3.1. The purpose is to obtain seismic bearing capacity ( $q_f$ ) of shallow footings ( $D_f=0$ ) located near cohesive slopes under undrained conditions using pseudo-static approach.

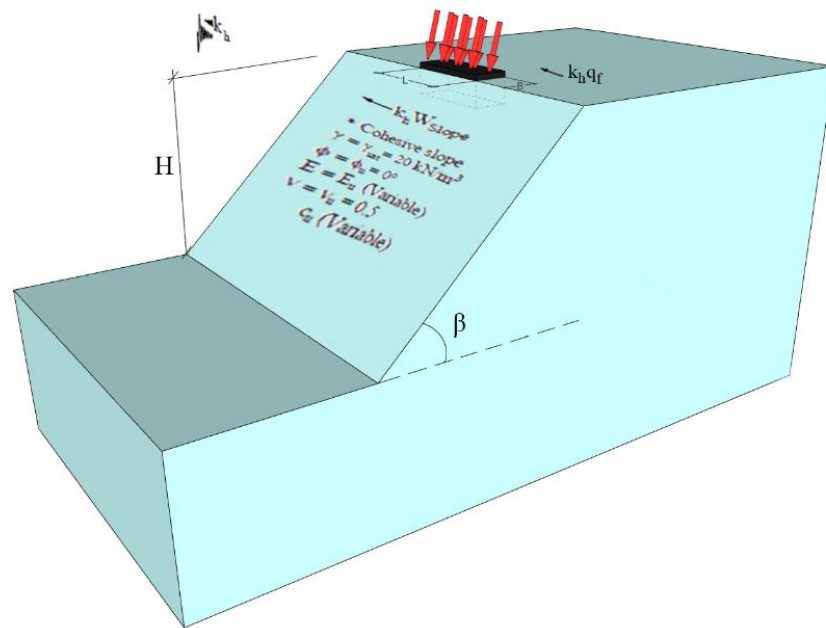


Figure 3.1. Graphical representation of the problem.

Presumptions made for the solution of the problem presented at Figure 3.1, are summed up below. Accordingly;

- The footing is shallow footing. Thus, the effect of embedment depth onto seismic bearing capacity of such footings will not be examined in this study.
- The footing is represented by a rigid plate element and the interface is accepted to be rough.
- Seismic bearing capacity of such footings is determined by using pseudo-static approach. It is estimated that inertia force of structure acts at the base level of footing. Overturning moment due to the inertia force acting on structure is neglected as well.
- Horizontal seismic acceleration coefficients used for calculating the inertia force of structure and of slope soil are chosen to be equal ( $k_h$ ).
- Effect of vertical component of earthquake acceleration onto seismic bearing capacity is neglected ( $k_v = 0$ ).
- Mohr-Coulomb constitutive model is used to define soil behavior.
- Undrained shear strength of soil does not change due to complex, temporary and dynamic earthquake loading.

- Slope soil is uniform and undrained shear strength of soil does not change with depth as well.

### 3.3 Suggested Solution Method

Seismic bearing capacity of shallow foundations can be obtained using Plaxis 3D according to the assumptions abovementioned in Chapter 3.2. Initially, requirement data input should be integrated with input module of the software. Later, calculation module of the software should be performed to interpret the problem at hand. Moreover, failure mechanism will be shaped at the ultimate state that can be observed within Output module of the software while the foundation reaches to the seismic bearing capacity failure.

On the other hand, an available mathematical approach which correlates between seismic bearing capacity ( $q_f$ ) and undrained shear strength of cohesive slope soil ( $c_u$ ) may be described is examined in this study. If the form of equation defined by Skempton (1951) is taken as a reference, seismic bearing capacity of shallow footing can be computed using the formula given in Equation 3.1.

$$q_f = c_u N_{cse} \quad (3.1)$$

where  $q_f$  is the seismic bearing capacity of shallow footings near cohesive slopes,  $c_u$  is the undrained shear strength of cohesive slope soil and  $N_{cse}$  is the seismic bearing capacity factor of shallow footings located near slopes.

Undrained shear strength of cohesive soils can be obtained via several testing methods (UU triaxial compression test, unconfined compression test and etc.) or can be assumed with sufficient certainty using correlations developed for in-situ tests such as vane shear test, standart penetration test (SPT), cone penetration test (CPT) and etc. It will be enough to determine the ultimate footing capacity according to the approach given herein. The only thing to do next is to determine influential parameters on the seismic bearing capacity factor and, if possible, to prepare design charts or to obtain equations for the determination of seismic bearing capacity factor. Therefore, all the details related with parametric study will be given in Chapter 3.4.

### 3.4 Model Geometry

As it was referenced above, it is necessary to constitute a numerical model to set a definite approach and to obtain all influential parameters onto seismic bearing capacity factor. Respectively, parameters that are defined as variables can be classified by three groups.

Initially, it is required to define the geometry of the slope. For this reason, slope height ( $H$ ) and slope angle ( $\beta$ ) are enough to generate the geometry of the slope which foundation is located close. In order to show the influence of the slope angle variation, different slope angles chosen for  $\beta$ ;  $15^\circ, 30^\circ, 45^\circ$ . Moreover, different slope heights were selected for  $H$ ; 2, 4 and 8m. Additionally, ( $\lambda$ ), factor that defines footing distance from the slope edge, is normalized with footing breadth. Besides these, in order to examine the impact of shape effect on foundation, various lengths chosen for  $L$ ; 2, 4, 8, 16 m. The normalized footing distance ( $\lambda$ ) from the slope edge were selected for  $\lambda; 0$ . The relationship between seismic bearing capacity coefficient and normalized footing distance will be represented in the subsequent chapter of this thesis and also to find out threshold distance values as precise as possible for different cases.

Second group is correlated with the strength characteristic of the soil. This factor is taken accounted as variable because the soil strength is described by undrained shear strength according to the material model selected. Undrained shear strength of cohesive slope soil ( $c_u$ ) is 25, 50, 100, 200 kPa.

Lastly, the horizontal seismic acceleration coefficient ( $k_h$ ) is only defined on the models for seismic conditions. Horizontal seismic acceleration coefficient ( $k_h$ ) changes in between 0.1 and 0.3.

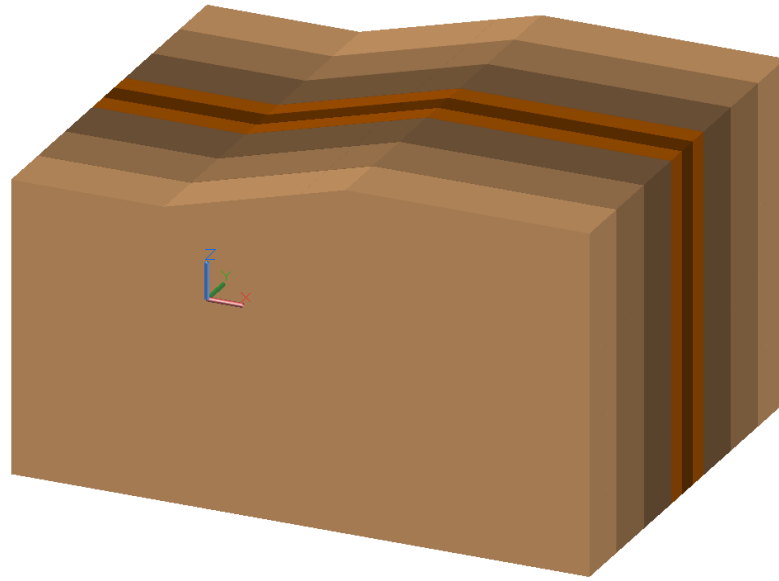


Figure 3.2. Three dimensional model of created finite elements model.

### 3.5 Data Input in Plaxis 3D

As previously noticed that the selected problem in the field of this thesis can be examined by Plaxis 3D software and so, seismic bearing capacity of a shallow foundation located close cohesive soil can be obtained using by a set of geometric, strength and seismic parameters. To deal with the problem, the issues linked with the necessary steps for the Input modules of the software are separated into six subheadings in this section.

#### 3.5.1 General Settings

When a new project has to be defined, the ‘General Settings’ window will be appeared as shown in Figure 3.3. This window consists of two tabs named as ‘Project’ and ‘Dimensions’. If a filename has not been defined in the first tab, this can be done when saving the project. Additionally, a brief description of the problem as the name of the project as well as a more detailed explanation can be given in the ‘Comments’ box.

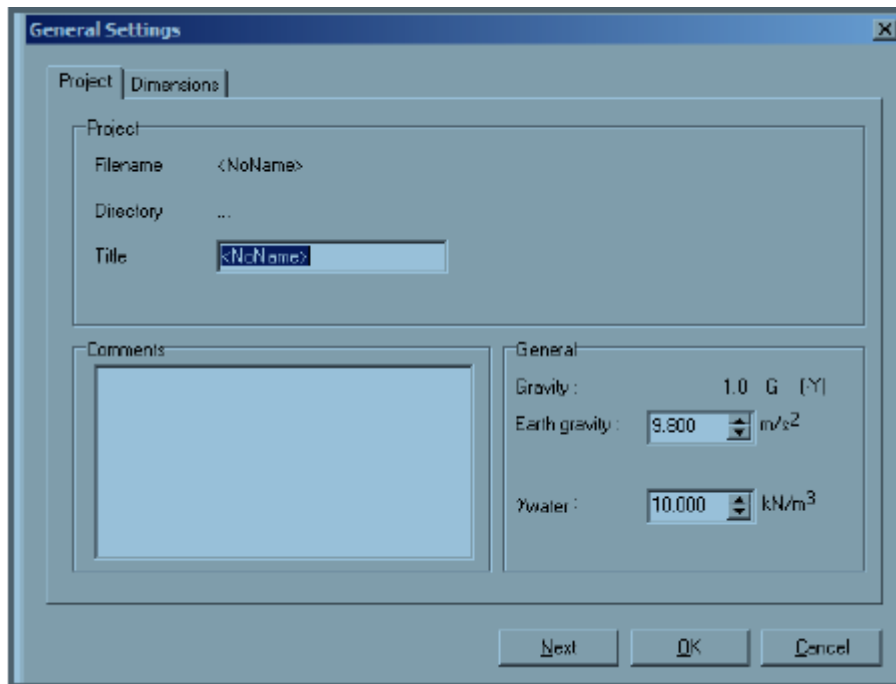


Figure 3.3. 'Project' tab sheet of 'General Settings' window

On the other hand, the basic units of Length, Force and Time, the minimum dimensions of the draw area are shown under 'Dimensions' tab as shown in Figure 3.4. In addition, there are four input data boxes in the same tab sheet that enable the definition of outer boundaries of the drawing area into which the geometry model fits.  $X_{\min}$  is the lowest x-coordinate of model,  $X_{\max}$  the highest x-coordinate,  $Z_{\min}$  the lowest z-coordinate and  $Z_{\max}$  the highest z-coordinate of the model.

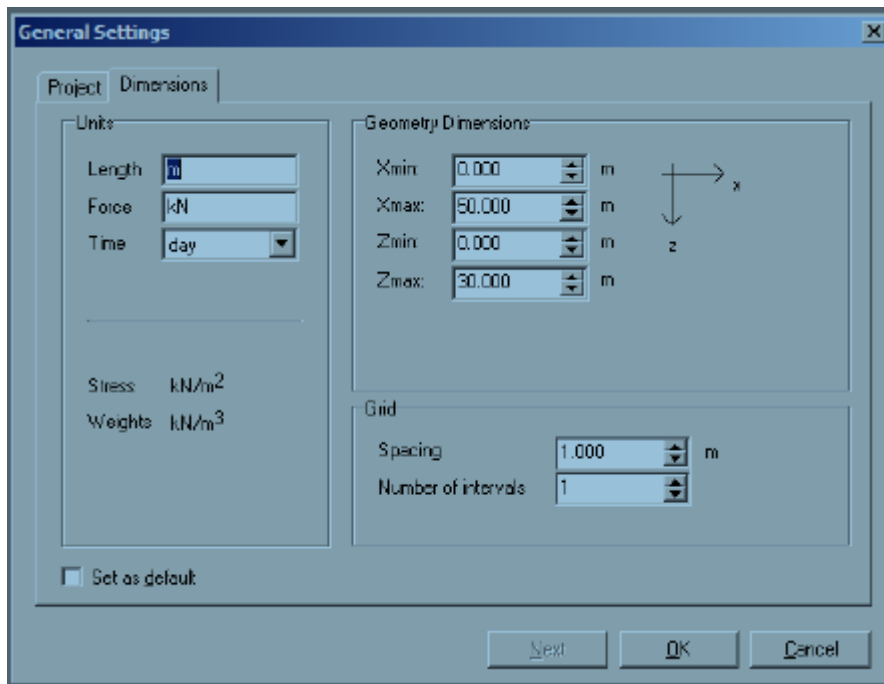


Figure 3.4. 'Dimensions' tab sheet of 'General settings' window

The wedge elements used in Plaxis 3D software consist of 15 nodes. Displacements ( $u_x$ ,  $u_y$  and  $u_z$ ) are computed at the nodes during finite element analysis. Contrary to displacements, stresses and strains are computed at individual Gaussian integration points rather than at the nodes. To obtain more reliable outcomes, 15-node triangular elements were used to generate a finite element as shown in Figure 3.5.

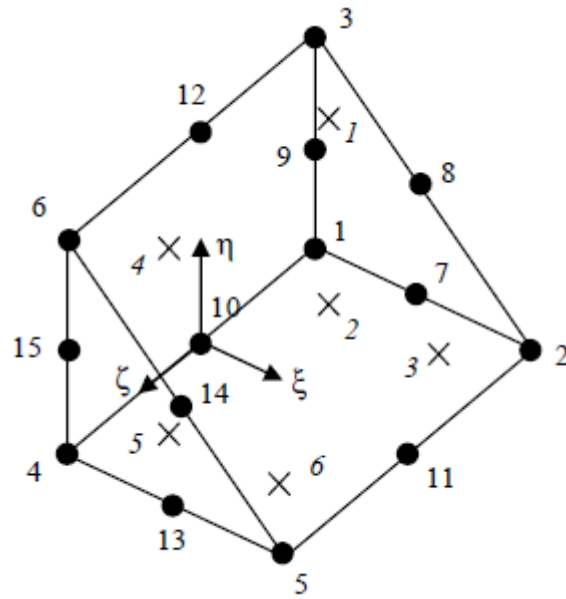


Figure 3.5. Distribution of nodes (.) and stress points (x) in a 15-node wedge element.

### 3.5.2 Numerical Model

While creating the finite element model, the main aspect should be that boundary limits of exterior should not influence footing failure loads computed by computer program. Therefore, exact model shape was obtained by trial and error method. As a conclusion, the model geometry shown in Figure 3.6 is convenient and suitable for all numerical models generated in this present study. According to Figure 3.6, horizontal distance between right footing edge and right vertical boundary changes with breadth of footing ( $8B$ ). On the other hand, the horizontal distance between bottom edge of slope and left vertical boundary and the vertical distance between bottom edge of slope and horizontal bottom boundary were selected as constant, and took the value of 25m and 12m accordingly.

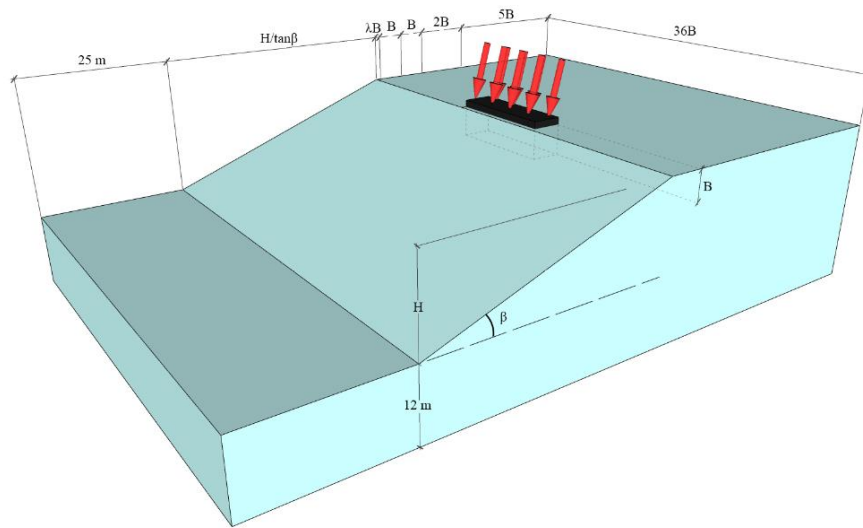


Figure 3.6. Schematic representation of created finite elements model.

Shallow foundation defined by a rigid plate element in finite element models is 2.0 m wide. The plate element is supposed to be weightless and elastic material type is assigned to it. Stiffness parameters that are commonly used for the plate element and equivalent plate thickness ( $d_{eq}$ ) values considered in all analyses are given in Table 3.1. Furthermore, it was noticed that shallow foundation is supposed to be ‘fully rough’.

Table 3.1. Physical and elastic properties of rigid plate element.

| Material Type | Elasticity Modulus E (kN/M) | $d_{eq}$ (m) | Weight, w (kN/m/m) | Poisson ratio, $\nu$ (Unitless) |
|---------------|-----------------------------|--------------|--------------------|---------------------------------|
| Elastic       | $3 \times 10^7$             | 1.0          | 0                  | 0.2                             |

### 3.5.3. Boundary Conditions

‘Standart fixities’ boundary condition is more suitable for geotechnical problems and is used in all prepared finite element analyses. It is easily chosen with a shortcut given on Input menu of the Plaxis 3D. As shown in Figure 3.5, full fixity ( $u_x = u_y = 0$ ) is defined across horizontal geometry line located at the bottom of model y coordinate is minimum while horizontal fixity ( $u_x = 0$ ) is specified across two geometry lines whose x coordinates are minimum and maximum.

### 3.5.4. Loads

The present analyses are made through the pseudo-static approach. The seismic forces are characterized by the horizontal loads applying to the foundation, surcharge and the underlying soil in this method. The multiplication of the horizontal seismic coefficient ( $k_h$ ) by foundation load ( $P$ ), surcharge ( $q$ ), and soil weight ( $W$ ) gives us the horizontal load. The present study explains only the horizontal seismic coefficient ( $k_h$ ). Furthermore, an inclined load placed on the foundation applied with a horizontal component to trigger seismic force, "Soil inertia" ( $k_h W$ ) is the term which means the pseudo-static force applying to the soil mass. Table 3.2 as below presents the schematic diagram of the problem. In this study, horizontal seismic acceleration coefficients were selected as 0.1, 0.2, 0.3.

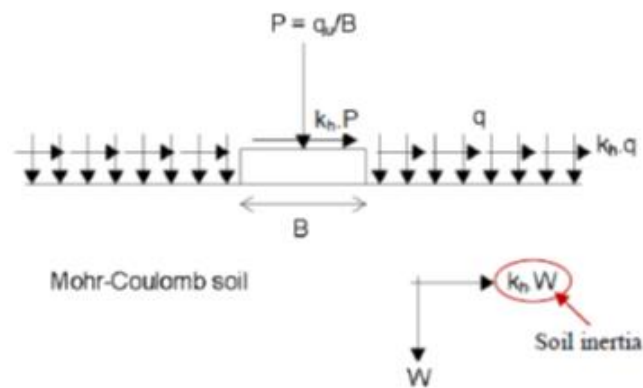


Table 3.2. Schematic diagram of the problem.

As mentioned above, the effect of horizontal earthquake acceleration was considered in this study. Vertical component of the earthquake acceleration was neglected in previous studies as mentioned Chapter 2.2. Only one study in the literature took the influence of vertical earthquake acceleration into consideration. Shiau *et al.* (2006) incorporated the effect of horizontal and vertical earthquake acceleration ( $\tan\theta = k_h/1-k_v$ ). On the other hand, Kramer (1996) noticed that vertical pseudo-static force can decrease or increase at the same time both driving and resisting forces depending on its direction. According to Kramer's results, the effect of vertical pseudo-static force is negligible compared to the effect of horizontal pseudo-static force. For that reason, the effect of vertical earthquake acceleration is generally underestimated in studies when the pseudo-static approach is used.

### 3.5.5. Material Properties

It is essential to recognize drained and undrained conditions. Failure might occur drained and undrained in the event of saturation of the soil pores with water standing on the size of the soil pore, the water saturation's degree and time included. The probability of the undrained failure characteristics increases when the pores are smaller and the loads are applied faster.

An undrained analysis can be made through 3 methods in Plaxis 3D 2018. These are, Undrained A, B and C, can be outlined as follows:

1. Undrained A: Undrained effective stress analysis with effective strength parameters. The undrained shear strength stands on the effective stress state and effective strength parameters.
2. Undrained B: Undrained effective stress analysis with undrained strength parameters. The undrained shear strength is exactly explained by the user and independent of the effective stress state.
3. Undrained C: Undrained total stress analysis with undrained strength parameters. All parameters are pointed out in undrained terms.

As mentioned in Chapter 3.2, all models created in this study are described by Mohr-Coulomb failure criterion under seismic events. Total stress elastic features of the soil ( $E_u$  and  $\nu_u$ ) were considered in the analyses because of the requirement of employing in total stress terms for undrained conditions. The third undrained modelling option enables to monitor the effect of material properties on seismic bearing capacity. Undrained C, therefore, is used in this study.

Due to the necessity of using undrained stiffness and strength parameters, Mohr-Coulomb material model turns into Tresca model. In order to define Tresca model, necessary stiffness and strength parameters are originally undrained elasticity modulus ( $E_u$ ), undrained Poisson ratio ( $\nu_u$ ) and undrained shear strength of cohesive soil ( $c_u$ ). Apart from that,

undrained internal friction angle ( $\Phi_u$ ) and undrained dilation angle ( $\psi_u$ ) should be described as zero. Theoretically, the value of undrained poisson should be 0.5. However, it was selected as 0.35 in all carried out finite element calculation because of the singularity in stiffness matrix.

Four different soil types were employed in this study. These data sets link with different cohesive soil stiffness (soft, medium, stiff, hard). Related parameter details are presented in Table 3.3. Moreover, saturated unit weight of soil ( $\gamma_{sat}$ ) was assigned as constant (20 kN/m<sup>3</sup>). Due to the rough footing assumption, interface strength reduction factor ( $R_{inter}$ ) was assigned as 1.

Table 3.3. Properties of the cohesive slope soils employed in present study.

| Parameter                             |                  |                   | Cohesive Soil Stiffness |                |                |                |
|---------------------------------------|------------------|-------------------|-------------------------|----------------|----------------|----------------|
|                                       |                  |                   | Soft                    | Medium         | Stiff          | Hard           |
|                                       | Name             | Unit              | Value                   | Value          | Value          | Value          |
| Material Model                        | Model            | -                 | MC                      | MC             | MC             | MC             |
| Type of material behavior             | Type             | -                 | Undrained<br>C          | Undrained<br>C | Undrained<br>C | Undrained<br>C |
| Soil unit weight above phreatic level | $\gamma_{unsat}$ | kN/m <sup>3</sup> | 20                      | 20             | 20             | 20             |
| Soil unit weight above phreatic level | $\gamma_{sat}$   | kN/m <sup>3</sup> | -                       | -              | -              | -              |
| Permeability in horizontal direction  | $k_x$            | m/day             | -                       | -              | -              | -              |
| Permeability in horizontal direction  | $k_y$            | m/day             | -                       | -              | -              | -              |
| Undrained elasticity modulus          | $E_u$            | kN/m <sup>2</sup> | 5000                    | 10000          | 20000          | 40000          |
| Undrained Poisson ratio               | $\nu_u$          | -                 | 0.35                    | 0.35           | 0.35           | 0.35           |
| Undrained shear strength              | $c_u$            | kN/m <sup>2</sup> | 25                      | 50             | 100            | 200            |
| Undrained friction angle              | $\Phi_u$         | °                 | 0                       | 0              | 0              | 0              |
| Undrained dilatancy angle             | $\Psi_u$         | °                 | 0                       | 0              | 0              | 0              |
| Interface strength reduction factor   | $R_{inter}$      | -                 | 1                       | 1              | 1              | 1              |

### 3.5.6. Finite Element Mesh Generation

The model used in this study was divided into finite number of elements to achieve finite element examinations. To obtain more reliable results, 15-node triangular elements

were chosen to create a finite element mesh. The soil layer subdivided into three different zones depending on the density of finite elements. The densest mesh zone was placed beneath the footing and bordered along the foundation-soil interfaces and the edge of incline for more exact values. Mesh density decreases as it moves away from the foundation.

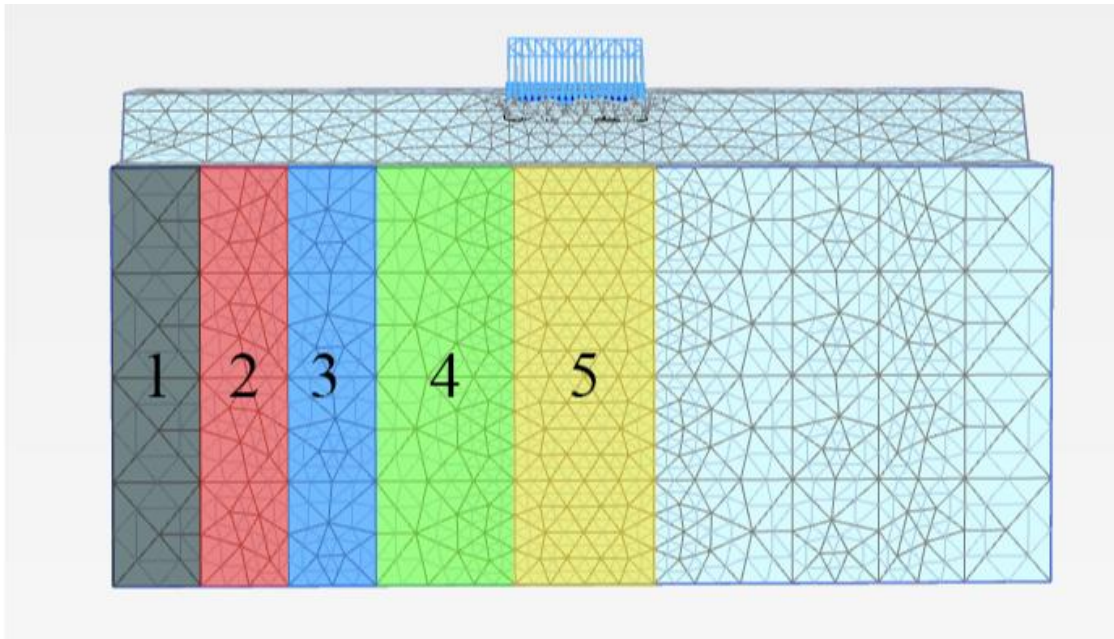


Figure 3.7. Finite element mesh generation.

### 3.6 Design Steps

Design steps consisted of two phases which were respectively the initial phase and second phase which is used for the calculation of undrained seismic bearing capacity of the shallow foundation using by the load factor ( $\Sigma-M_{stage}$ ) until soil body breakdown seems to collapse. First phase includes the activation of inertia force applying on soil clusters.

Typical view of Calculation modules of Plaxis 3D software in which above mentioned calculation steps were defined is given in Figure 3.8 and Figure 3.9, respectively.

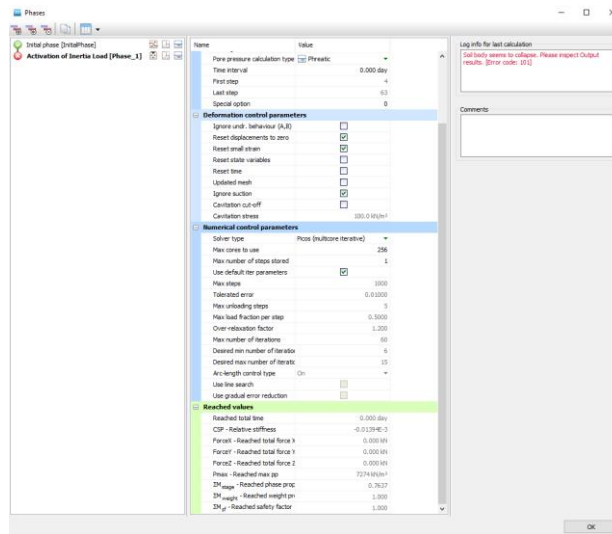


Figure 3.8. Typical view of “Calculation Module” window.

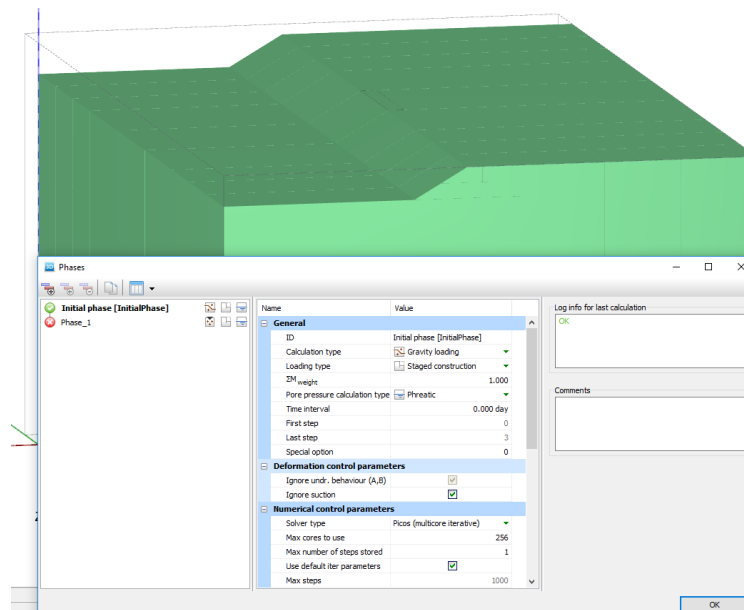


Figure 3.9. Typical View of ‘Initial Phase’ window.

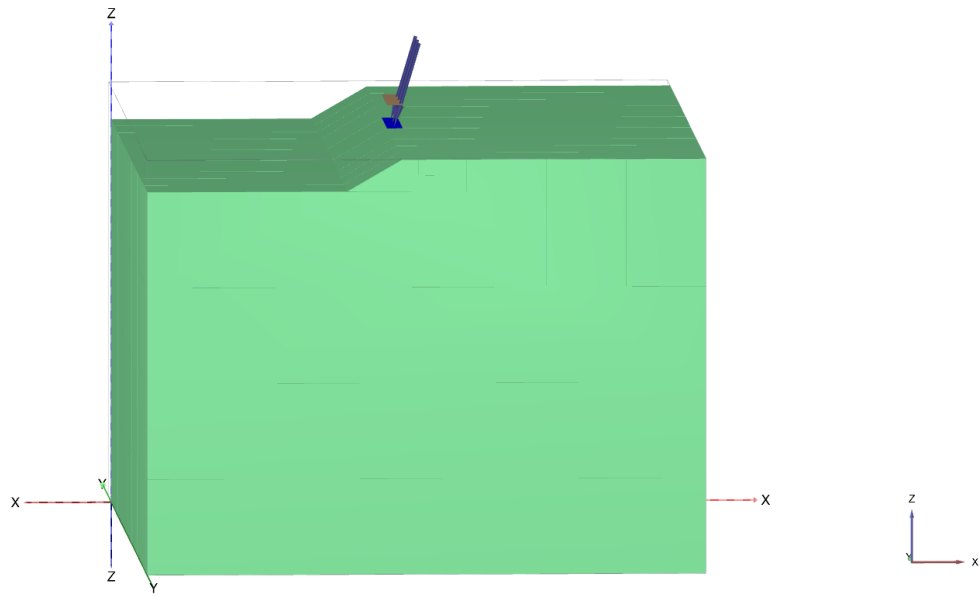


Figure 3.10. Activation of inertia force applying on soil clusters.

Failure was monitored at the initial calculation phase in all numerical examinations generated in this study. Detection of soil failure at the end of the initial stage shows that cohesive slope may not carry its weight under the impact of gravity. Lastly, detection of the failure at the end of the second calculation step shows that a footing located on face of a slope reaches ultimate limit bearing pressure with different foundation failure systems. The ultimate seismic bearing capacity was only computed for all numerical examinations that failure was found at the end of the first calculation phase.

Ultimate seismic bearing pressure coefficient ( $N_{cse}$ ) is obtained by means of the load stage ( $\Sigma M_{stage}$ ) computed by Plaxis 3D. It relates to the magnitude of the applied load on ground. For example, as presented in Figure 3.10, the value of computed load stage at the end of the first calculation phase is 0.424 for the numerical model which is  $C_{45\_2\_0\_2\_25\_0.1\_D}$  ( $\beta=45^\circ$ ,  $H=2.0m$ ,  $L=2$ ,  $\lambda=0$ ,  $c_u=25\text{ kPa}$ ,  $k_h=0.1$ ).

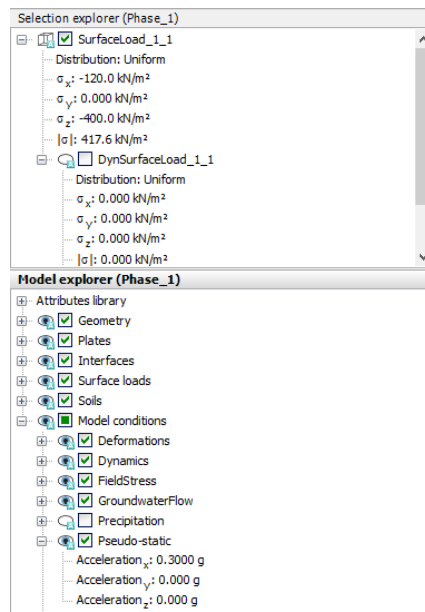


Figure 3.11. The load stage ( $\Sigma$ - $M_{stage}$ ) found by calculations module of Plaxis 3D for the final limit state.

Seismic bearing capacity of footing located on face of slope system ( $q_f$ ),

$q_f$  (kPa) = Magnitude of vertical component of unit load (kPa)  $\times \Sigma$ - $M_{stage}$

$$q_f = 300 \times 0.424 = 127.2 \text{ kPa} \quad (3.2)$$

Based Equation 3.2, seismic bearing capacity factor ( $N_{cse}$ ),

$$N_{cse} = \frac{q_f}{c_u} = \frac{127.2}{25} = 5.09 \quad (3.3)$$

### 3.7 Evaluation of Plaxis 3D Outputs

According to Chapter 3.6, the load stage using Calculations tab of the software can find ultimate seismic bearing pressure and seismic bearing coefficient. On the other hand, shape of failure mechanism and shear surfaces under the foundation should be deeply considered. Different failure systems and shape of shear surfaces can be viewed by selecting ‘Total Deviatoric Strain’ and ‘Incremental Displacements’ from Output results of the software. For example, for the numerical model which is *C\_45\_2\_0\_2\_25\_0.1\_D* ( $\beta=45^\circ$ ,  $H=2.0\text{m}$ ,  $L=2$ ,  $\lambda=0$ ,  $c_u=25\text{ kPa}$ ,  $k_h=0.1$ ), the failure system at the final stage is given in Figure 3.11.

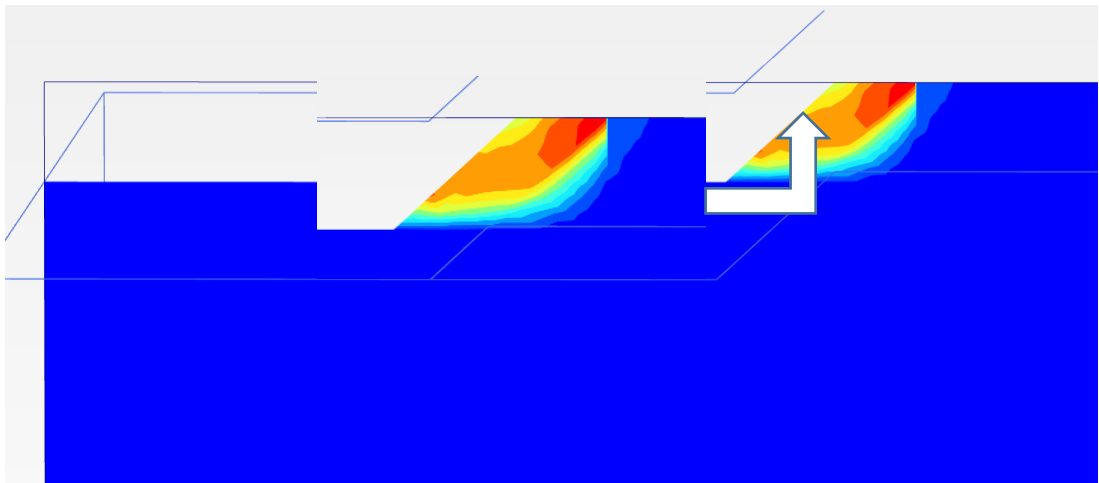


Figure 3.12. Failure mechanism obtained for the finite element model named as *C\_45\_4\_0\_16\_25\_0.1\_D* and enlarged view of the failure mechanism.

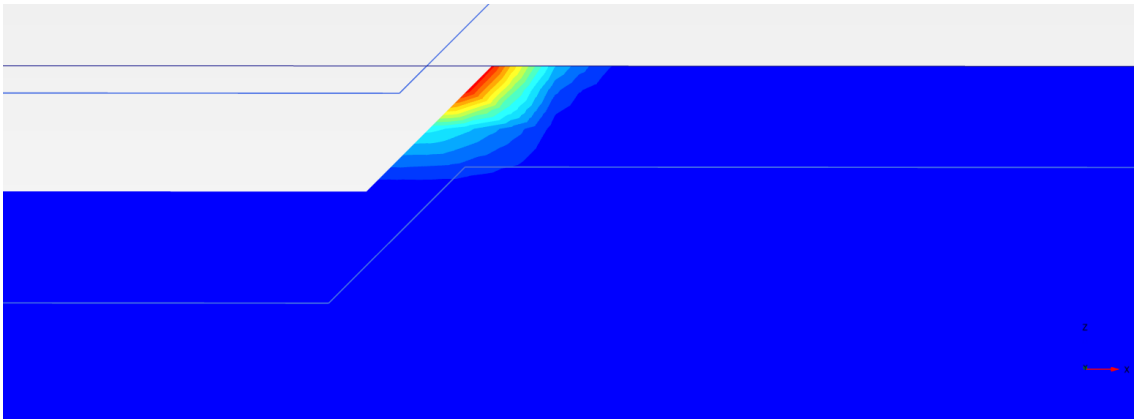


Figure 3.13. Shear surfaces obtained for the finite element model named as C\_45\_4\_0\_16\_25\_0.1\_D.

## 4. RESULTS AND DISCUSSIONS

Outcomes of the parametric study which are conducted will be discussed in this section. The main goal is to reflect the relationship of the parameters with seismic bearing capacity factor ( $N_{cse}$ ) of shallow foundations located close to cohesive slopes. Additionally, seismic bearing capacity coefficient can be defined as a function of different influential factors. With the definition to be made, it would be possible that various types of failure mechanisms that reached the final state by the effect of inertia forces under the foundation or within the cohesive slope.

All numerical models carried out in Plaxis3D were defined systematically. For instance “C\_15\_2\_0\_2\_25\_0.1\_D”, the first capital letter expresses that the soil material type which was the cohesive soil, the second number is the slope angle ( $\beta$ ), the third number is the slope height ( $H$ ), the fourth number is the distance between the footing's near edge, the fifth number is the length of foundation, the sixth number is the undrained strength, and the last number is the horizontal seismic coefficient ( $k_h$ ).

Different from the results mentioned above, shape effects of shallow foundation on seismic bearing capacity will be examined with design charts. Seismic bearing capacity can be determined by design charts given in the next part of this section as well. Also, these design charts will show the relationship between 2D and 3D.

### 4.1 Determination and Influential Parameters

This study is based on various influential parameters. Therefore, these parameters can be effective directly or indirectly on seismic bearing capacity factor. Horizontal seismic acceleration coefficient ( $k_h$ ), normalized slope height ( $H/B$ ), normalized undrained cohesive slope soil strength ( $c_u/\gamma B$ ) and slope angle ( $\beta$ ). The effect of each factor on seismic bearing capacity factor will be explained in a more comprehensive way in the following section.

#### 4.1.1 Influence of Horizontal Seismic Acceleration Coefficient

Seismic bearing capacity factor ( $N_{cse}$ ) drops remarkably with the increase of horizontal seismic acceleration coefficient ( $k_h$ ). As seen from the graph given in Figure 4.1, it is clear that horizontal seismic acceleration factor has a diminishing impact on seismic bearing capacity factor. Additionally, shape effect has become a minor impact on bearing capacity for the values greater than 0.3g.

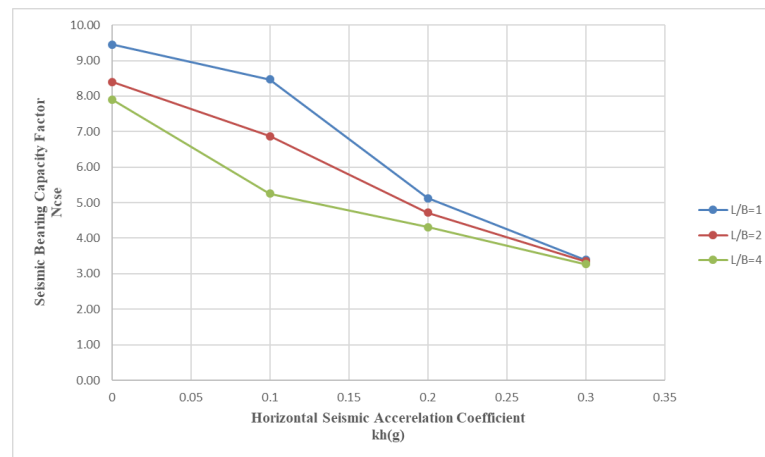


Figure 4.1. Variation of  $N_{cse}$  with  $k_h$  for  $\lambda=0$  ( $\beta=15^\circ$ ,  $c_u/\gamma B = 2.5$ ).

#### 4.1.2 Influence of Slope Angle

Seismic bearing capacity factor ( $N_{cse}$ ) drops dramatically with the increase of slope angle ( $\beta$ ). However, it is obvious that for bigger values of the normalized length of foundation ( $L/B$ ), seismic bearing capacity factor decreases sharply with the increase of slope angle for foundations located close to slope edge. ( $\lambda=0$ )

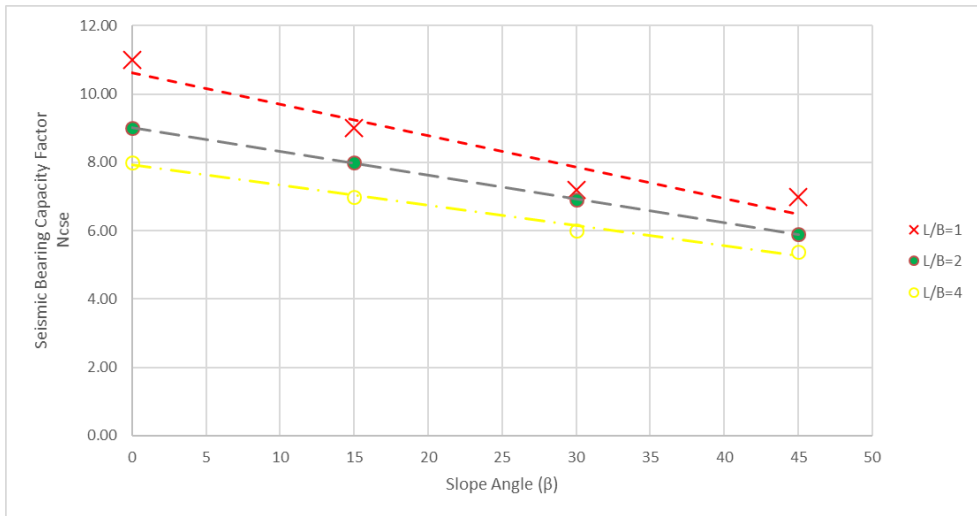


Figure 4.2. Variation of  $N_{cse}$  with  $\beta$  for  $\lambda=0$  ( $k_h=0$ ,  $c_u/\gamma B = 2.5$ ).

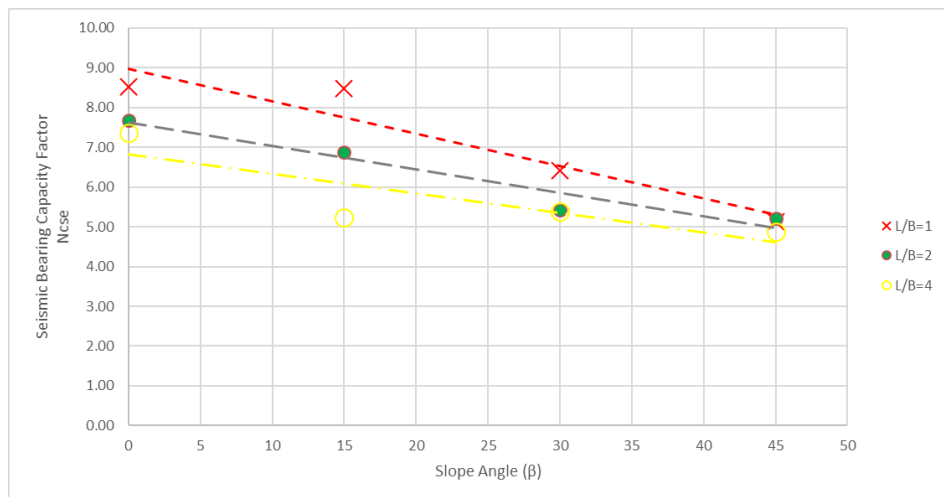


Figure 4.3. Variation of  $N_{cse}$  with  $\beta$  for  $\lambda=0$  ( $k_h=0.1$ ,  $c_u/\gamma B = 2.5$ ).

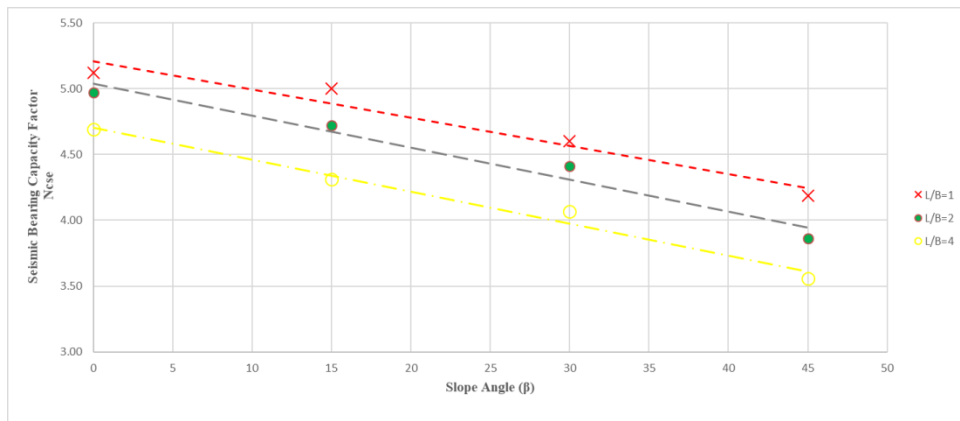


Figure 4.4. Variation of  $N_{cse}$  with  $\beta$  for  $\lambda=0$  ( $k_h=0.2$ ,  $c_u/\gamma B = 2.5$ ).

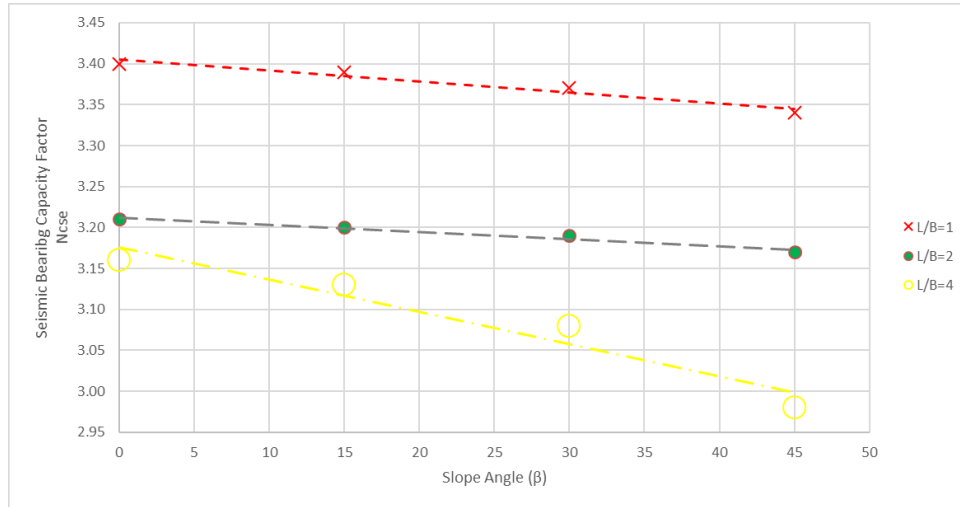


Figure 4.5. Variation of  $N_{cse}$  with  $\beta$  for  $\lambda=0$  ( $k_h=0.3$ ,  $c_u/\gamma B=2.5$ ).

#### 4.1.3 Influence of Slope Height

Additionally, the effect of the  $H/B$  ratio was examined. Actually, the effect of normalized slope height on seismic bearing capacity can be ignored for conditions that the foundation reaches to its ultimate limit bearing pressure with “foundation failure” mode.

On the other hand, the failure mode changes as  $H/B$  ratio raises for the smaller values of  $c_u/\gamma B$  ratio. When  $H/B$  ratio raises, it was firstly observed that failure form changes from “foundation failure” to “base failure due to earthquake”. Later, this evolution continues to another failure form called “base failure due to self-weight of slope”. They are also shown in the lists given in Appendix B.

#### 4.1.4 Influence of Slope Soil Strength

As shown in the chart presented in Figure 4.6, seismic bearing capacity factor ( $N_{cse}$ ) raises with the decrease of  $c_u/\gamma B$  ratio. On the other hand, it is observed from presented chart that the influence of this factor is very limited for the values bigger than 1.25. Due to the effect of  $H/B$  ratio, there is a exact evolution between different failure approaches as  $c_u/\gamma B$  ratio drops.

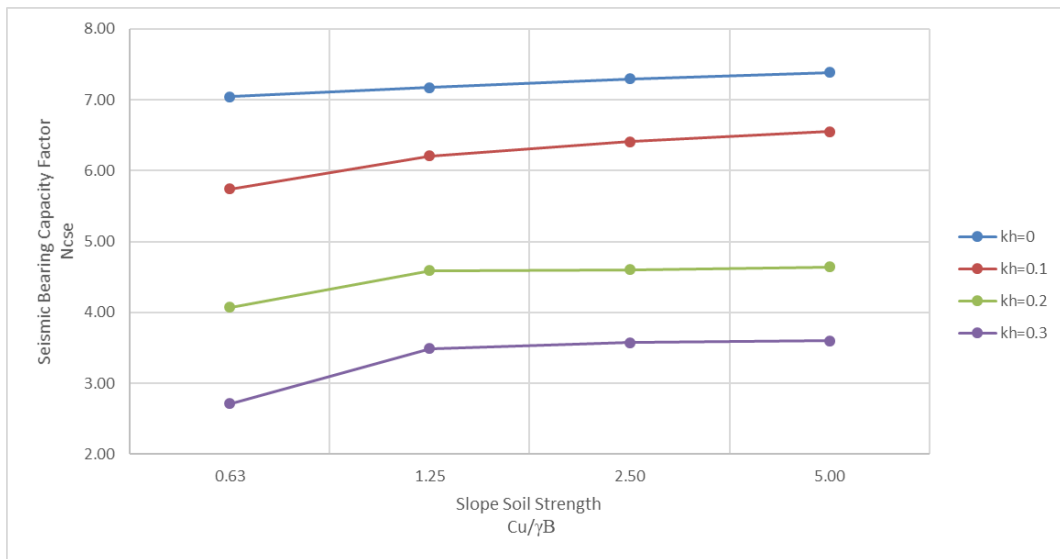


Figure 4.6. Variation of  $N_{cse}$  with  $c_u/\gamma B$  for all  $k_h$  values ( $\beta=30^\circ$ ,  $L/B=1$ ,  $\lambda=0$ ).

## 4.2 Examination of Failure Mechanisms

As a result of numerical examinations which were carried out, it was obtained that there are three major failure shapes that can occur either under the foundation or within cohesive slope at the final state for seismic conditions. As explained before, while the dedication of failure at the end of second phase means that cohesive slope cannot ensure its stability by the effect of earthquake inertia force applying on slope, the dedication of failure at the end of the first phase means that the cohesive slope cannot control its stability under the impact of gravity. These failure modes are described as “base failure” in the present study. Failure mechanism of each of them are given in Figure 4.7 and Figure 4.8 respectively.

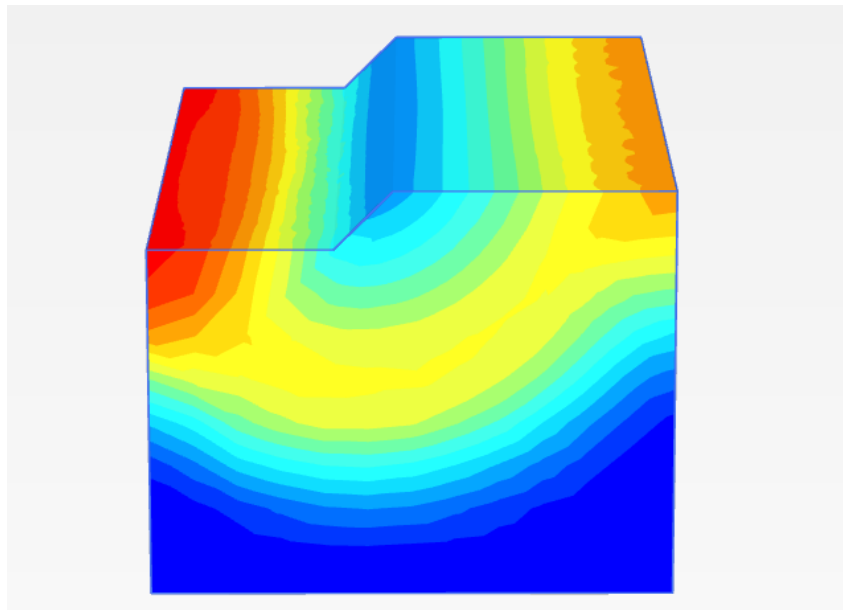


Figure 4.7. Base failure due to self-weight of cohesive slope ( $\beta=45^\circ$ ,  $H/B=4.0$  m and  $c_u/\gamma B=0.625$ ).

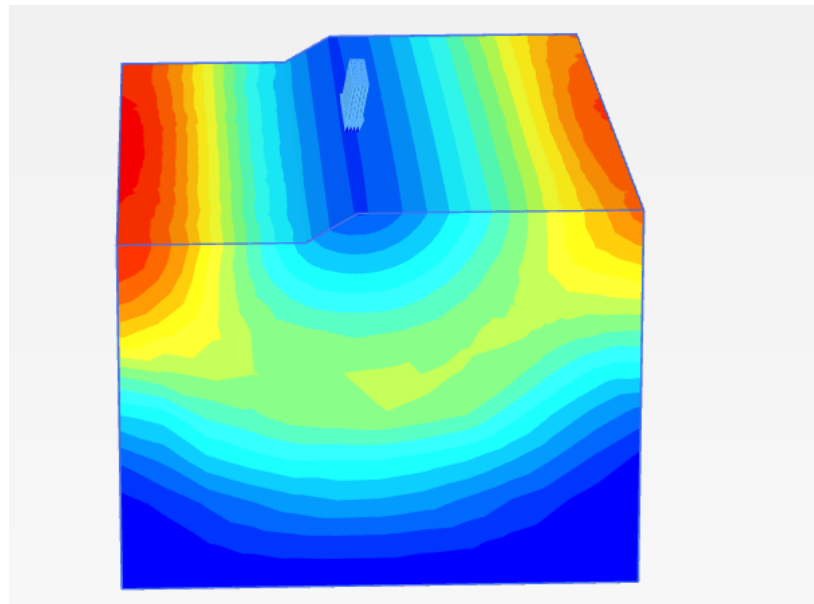


Figure 4.8. Base failure due to self-weight of cohesive slope ( $\beta=45^\circ$ ,  $H/B=4.0$  m,  $c_u/\gamma B=0.625$  and  $k_h=0.2$ ).

Except from failure modes mentioned above, the dedication of failure at the end of the second phase means that the foundation comes to ultimate limit bearing pressure with a failure approach formed under the foundation. It is called as “foundation failure” in all lists given in Appendix B. Failure shapes starts distribution from the foundation edge and afterwad crosses with line of slope, moves from the incline toe or cuts at any point with upper horizontal line of the slope if the foundation is located far enough from the slope edge. This approach is virtually the same with failure mechanism definition made by Meyerhof (1957) and Farzaneh *et al.* (2013).

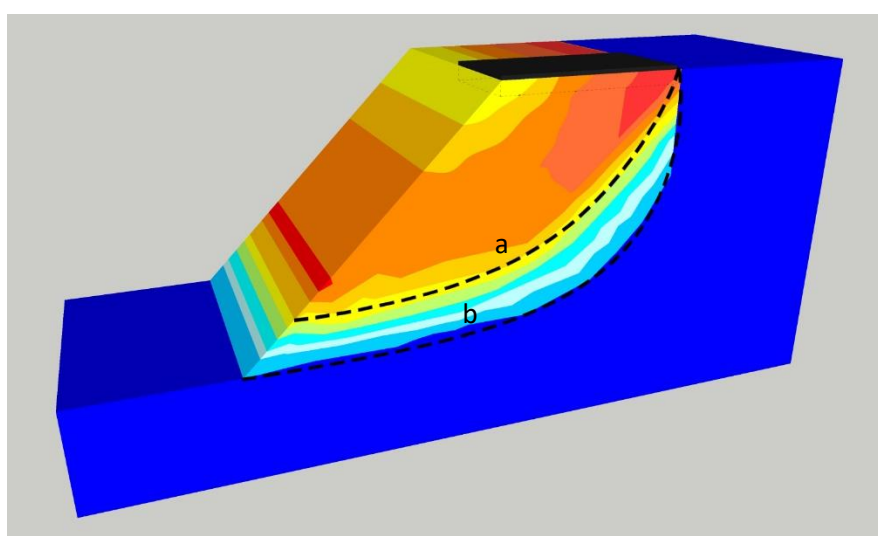


Figure 4.9. Typical “Foundation failure” approaches for  $\lambda=0$  condition (a)  $\beta=45^\circ$ ,  $H/B=1.0$  m,  $c_u/\gamma B = 1.25$  and  $k_h=0.2$ ); (b)  $\beta=45^\circ$ ,  $H/B=2.0$  m,  $c_u/\gamma B = 0.625$  and  $k_h=0.1$ ).

### 4.3 Design Charts

Actually, seismic bearing capacity of shallow foundations located close to cohesive slopes can be obtained from Equation 3.1. Using the outcomes of parametric study, a new approach can be developed by geotechnical engineers and designers. Design charts that will shed light for this approach are given in between Figure 4.10 and Figure 4.43.

According to design charts, it is clearly expressed that the correlation between seismic bearing capacity coefficient ( $N_{cse}$ ) and horizontal seismic acceleration coefficient is drawn as linear. The impact of  $B/L$  will be also examined as given design charts.

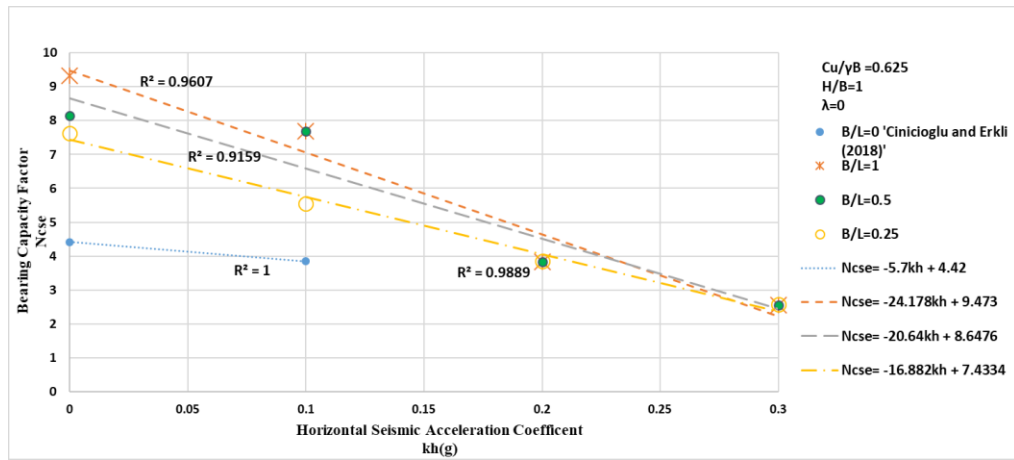


Figure 4.10. Variation of bearing capacity factor with horizontal seismic acceleration coefficient for  $\beta = 15^\circ$ .

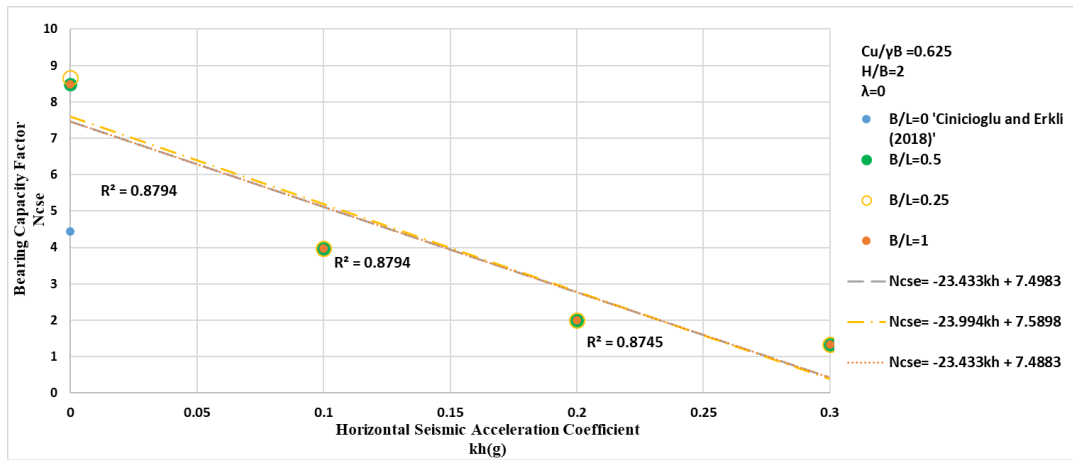


Figure 4.11. Variation of bearing capacity factor with horizontal seismic acceleration coefficient for  $\beta = 15^\circ$ .

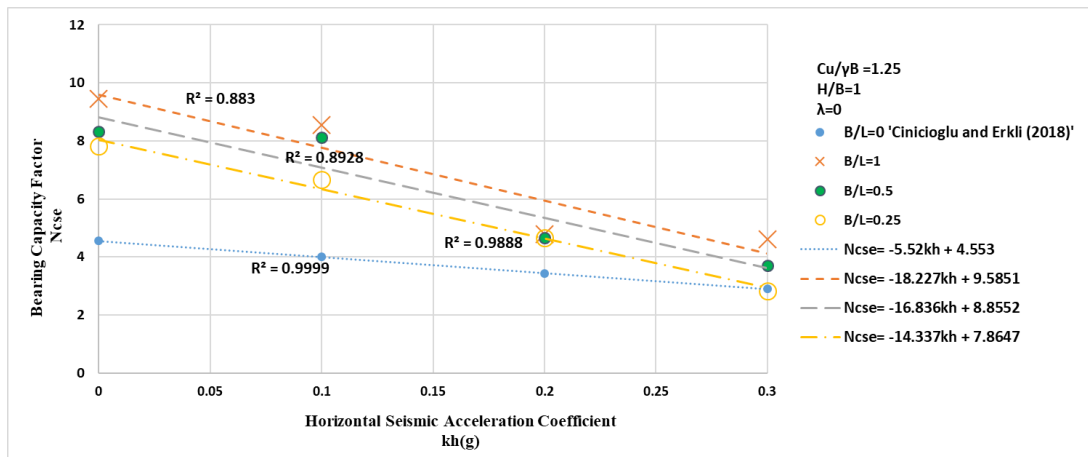


Figure 4.12. Variation of bearing capacity factor with horizontal seismic acceleration coefficient for  $\beta = 15^\circ$ .

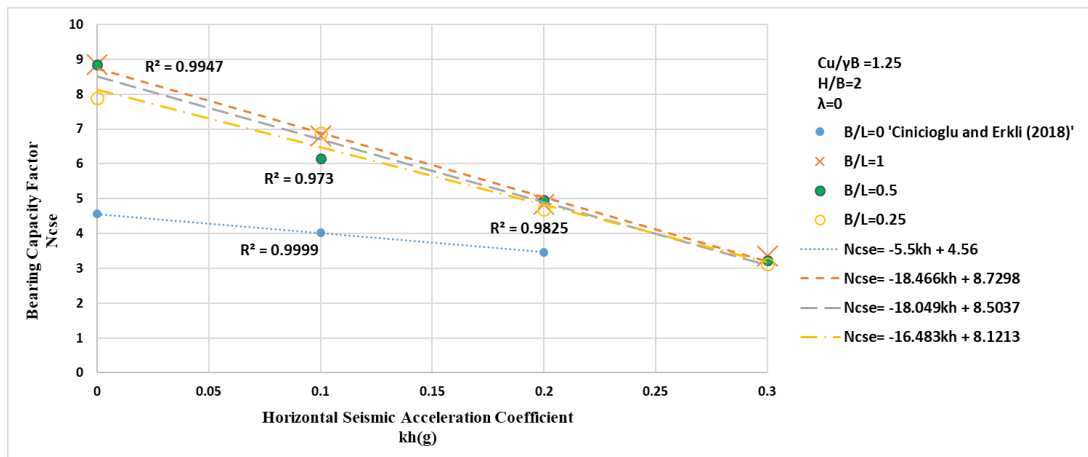


Figure 4.13. Variation of bearing capacity factor with horizontal seismic acceleration coefficient for  $\beta = 15^\circ$ .

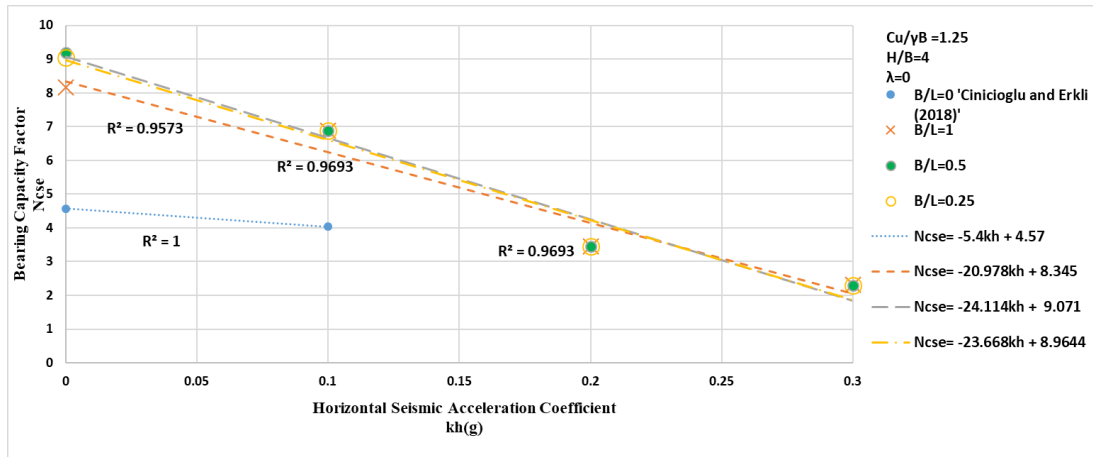


Figure 4.14. Variation of bearing capacity factor with horizontal seismic acceleration coefficient for  $\beta=15^\circ$ .

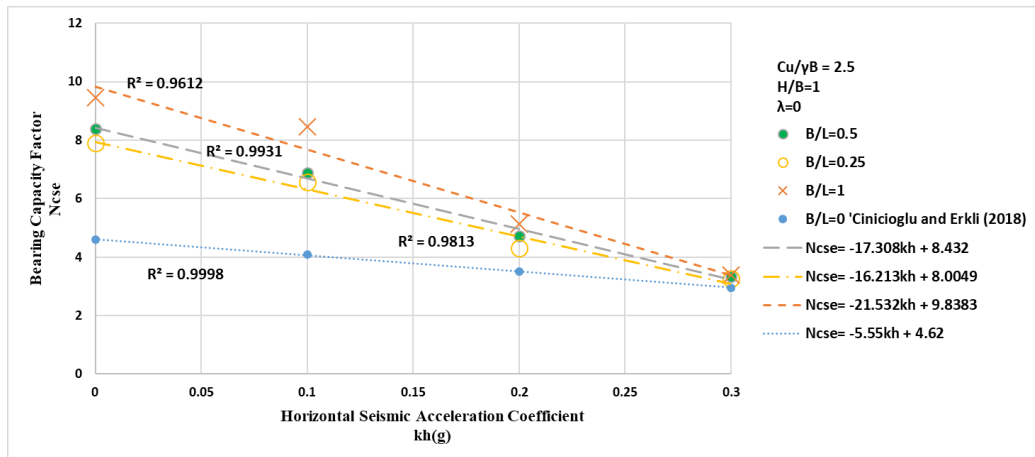


Figure 4.15. Variation of bearing capacity factor with horizontal seismic acceleration coefficient for  $\beta=15^\circ$ .

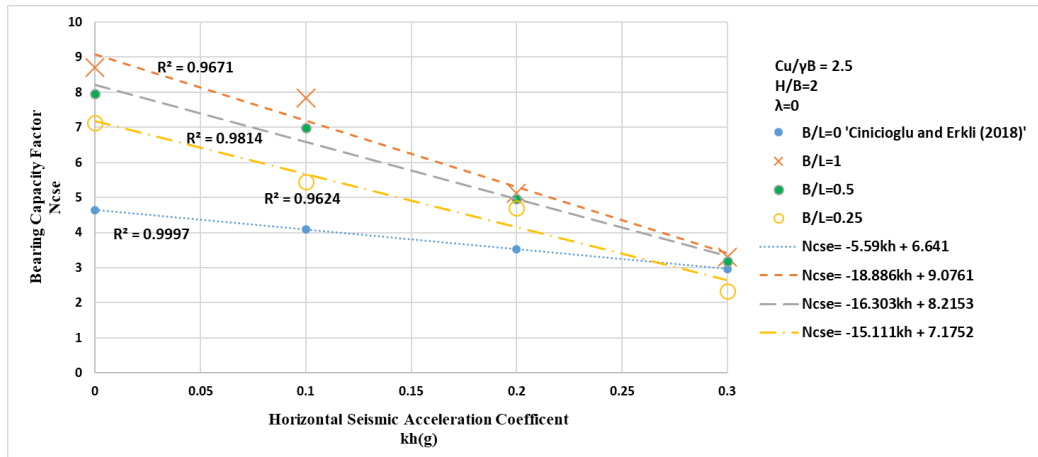


Figure 4.16. Variation of bearing capacity factor with horizontal seismic acceleration coefficient for  $\beta = 15^\circ$ .

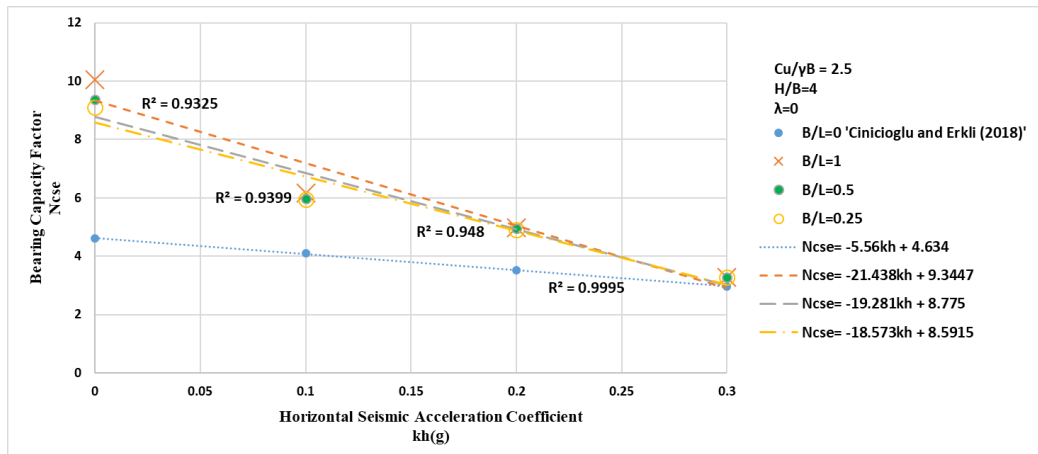


Figure 4.17. Variation of bearing capacity factor with horizontal seismic acceleration coefficient for  $\beta = 15^\circ$ .

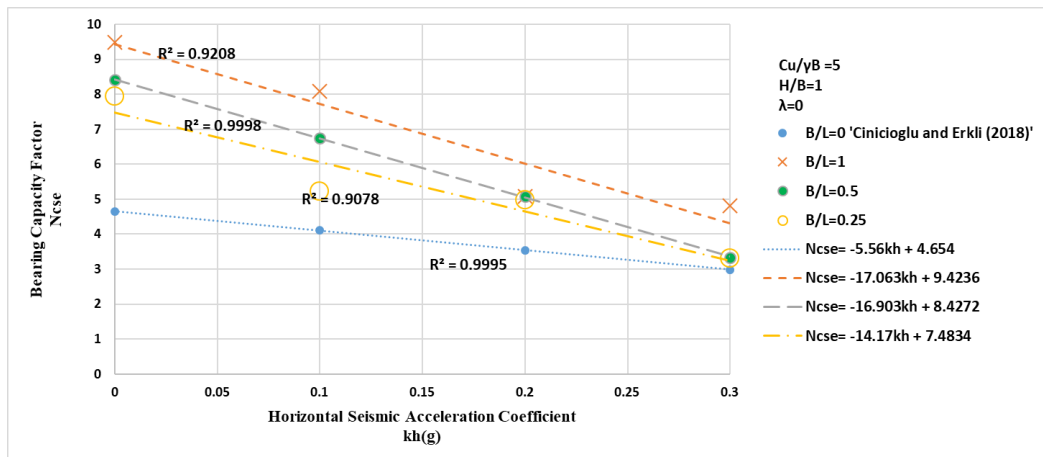


Figure 4.18. Variation of bearing capacity factor with horizontal seismic acceleration coefficient for  $\beta=15^\circ$ .

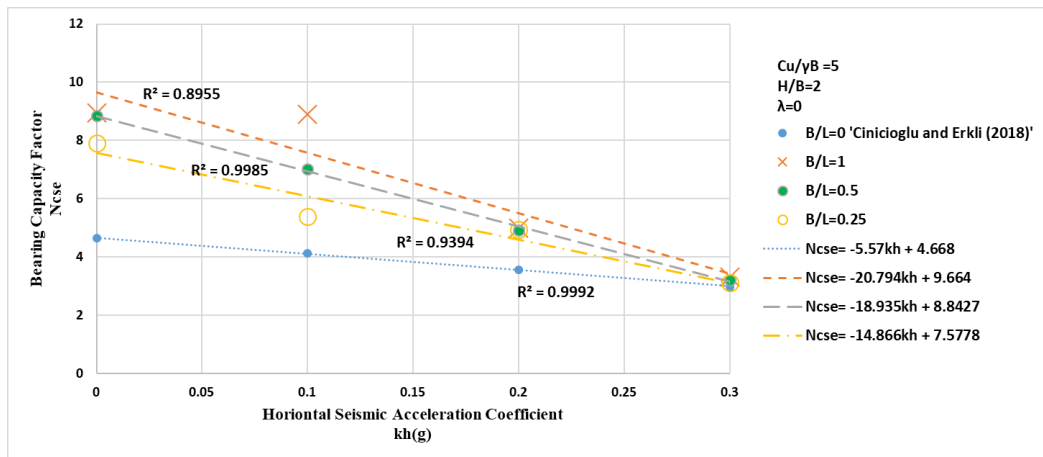


Figure 4.19. Variation of bearing capacity factor with horizontal seismic acceleration coefficient for  $\beta=15^\circ$ .

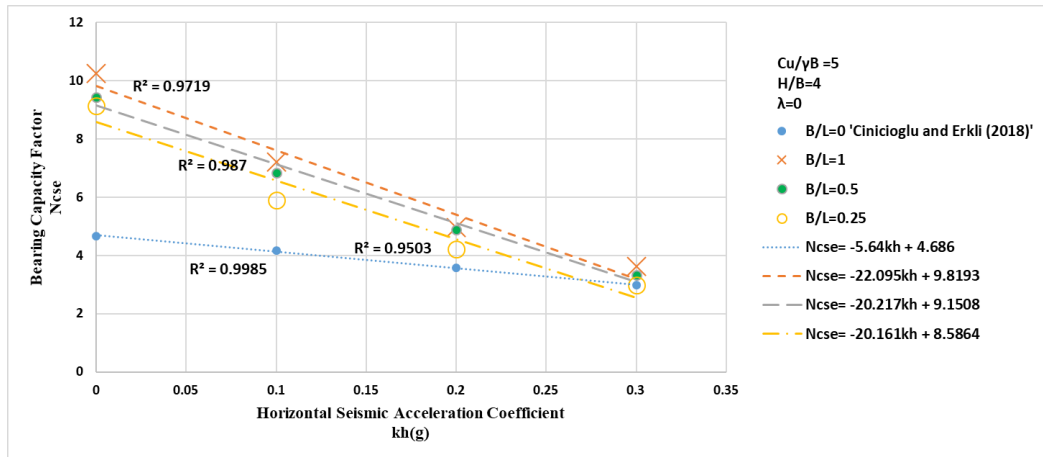


Figure 4.20. Variation of bearing capacity factor with horizontal seismic acceleration coefficient for  $\beta = 15^\circ$ .

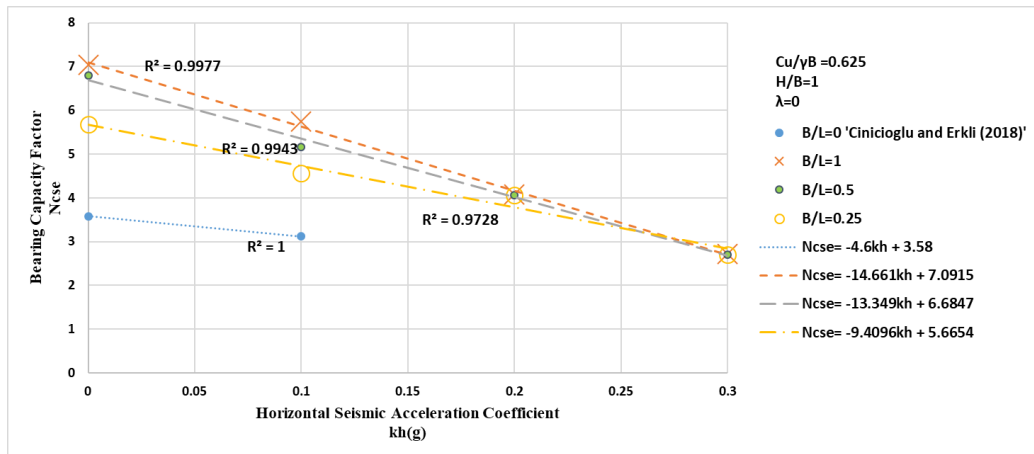


Figure 4.21. Variation of bearing capacity factor with horizontal seismic acceleration coefficient for  $\beta = 30^\circ$ .

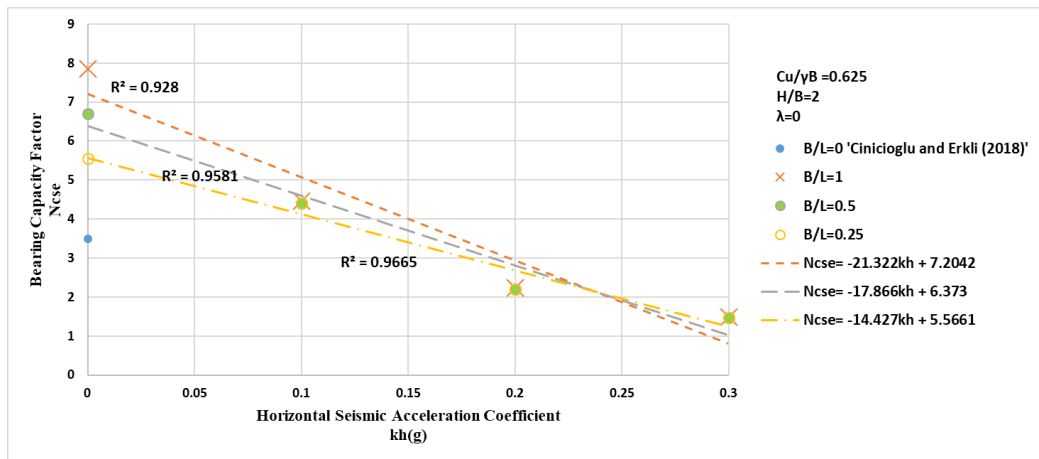


Figure 4.22. Variation of bearing capacity factor with horizontal seismic acceleration coefficient for  $\beta=30^\circ$ .

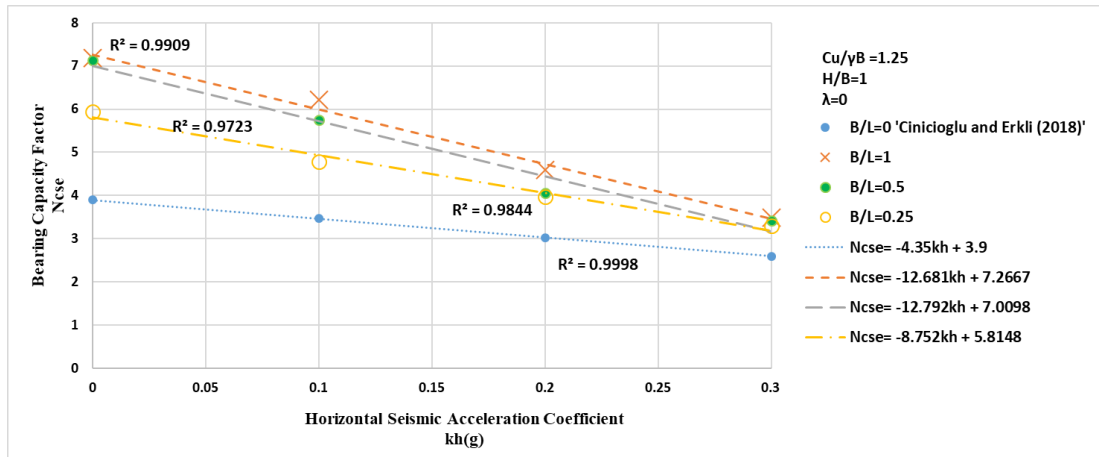


Figure 4.23. Variation of bearing capacity factor with horizontal seismic acceleration coefficient for  $\beta=30^\circ$ .

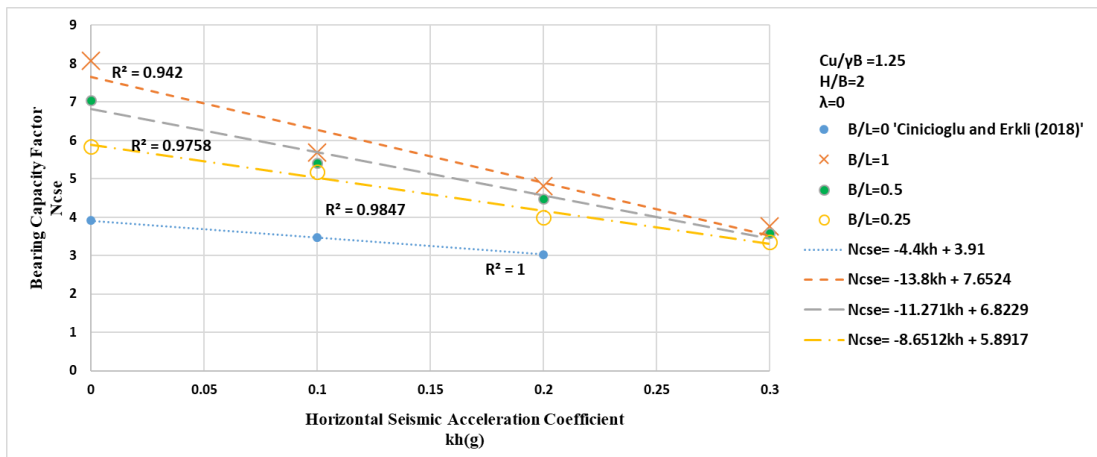


Figure 4.24. Variation of bearing capacity factor with horizontal seismic acceleration coefficient for  $\beta=30^\circ$ .

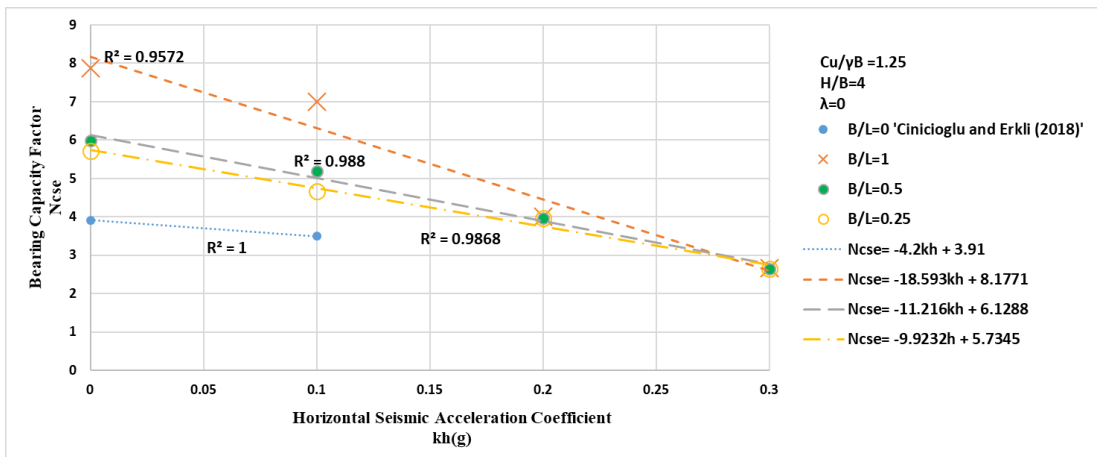


Figure 4.25. Variation of bearing capacity factor with horizontal seismic acceleration coefficient for  $\beta=30^\circ$ .

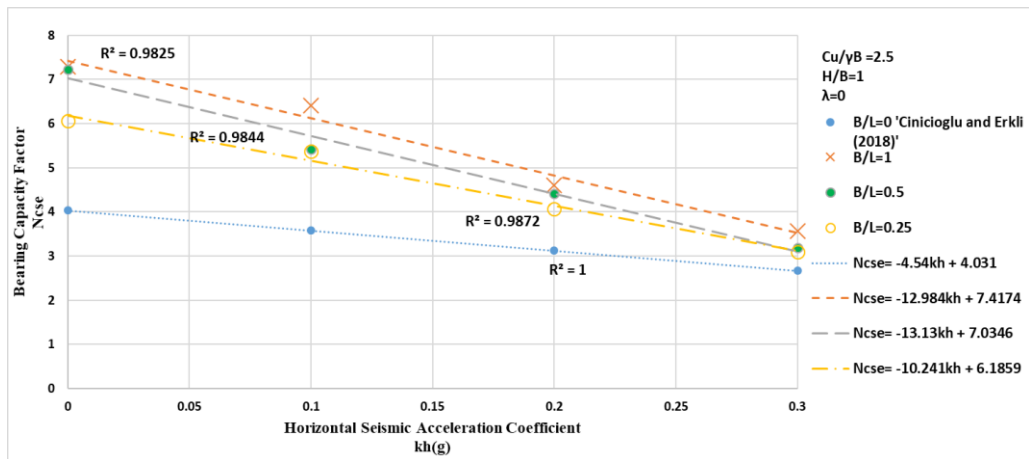


Figure 4.26. Variation of bearing capacity factor with horizontal seismic acceleration coefficient for  $\beta=30^\circ$ .

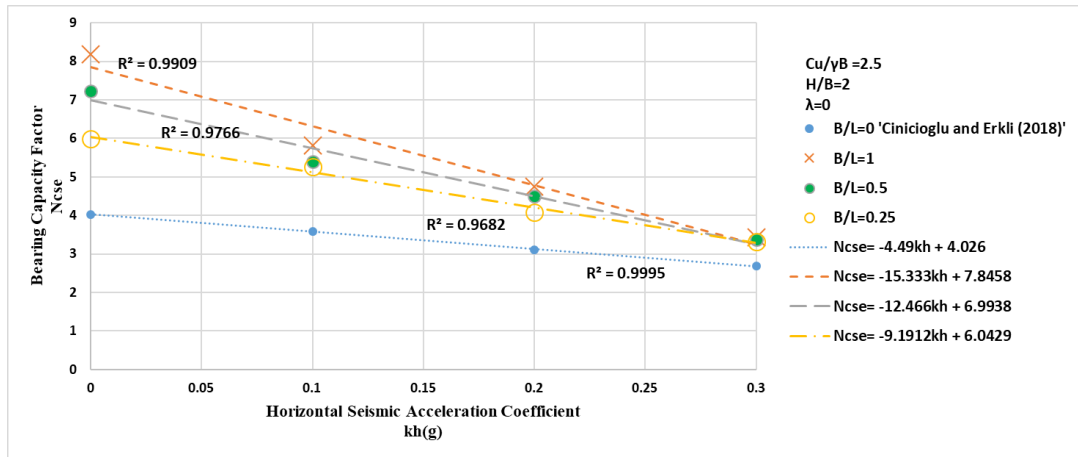


Figure 4.27. variation of bearing capacity factor with horizontal seismic acceleration coefficient for  $\beta=30^\circ$ .

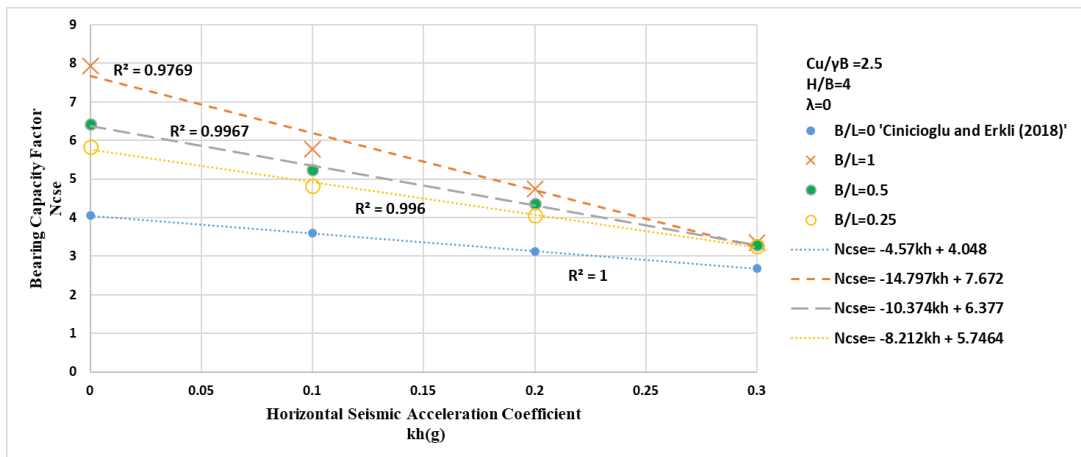


Figure 4.28. Variation of bearing capacity factor with horizontal seismic acceleration coefficient for  $\beta=30^\circ$ .

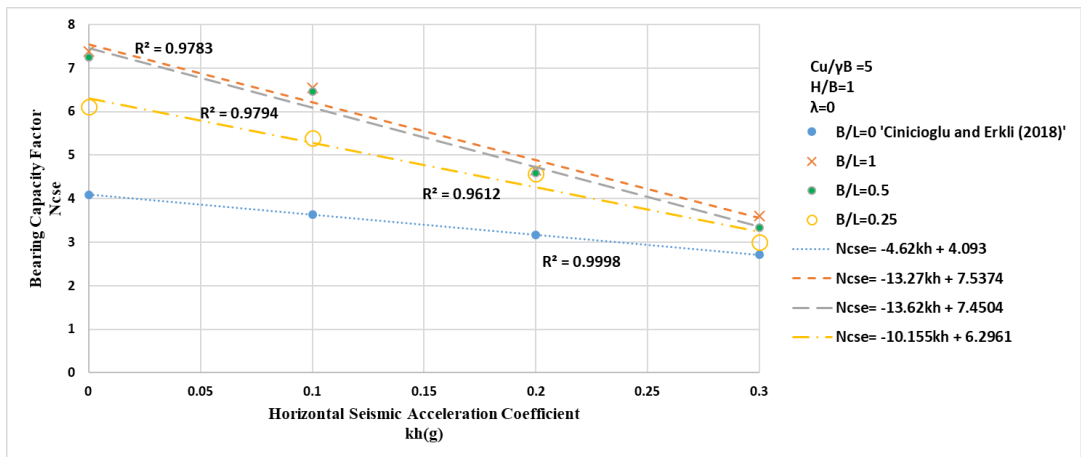


Figure 4.29. Variation of bearing capacity factor with horizontal seismic acceleration coefficient for  $\beta=30^\circ$ .

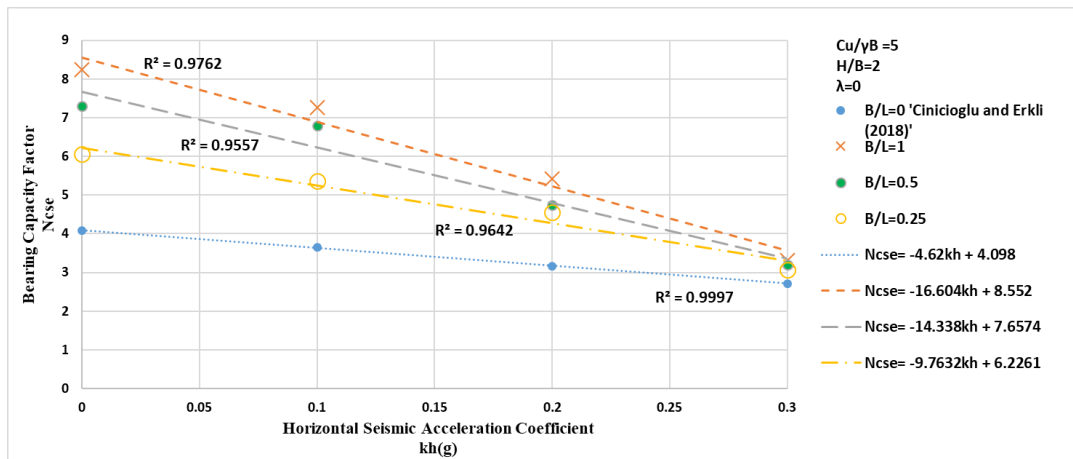


Figure 4.30. Variation of bearing capacity factor with horizontal seismic acceleration coefficient for  $\beta=30^\circ$ .

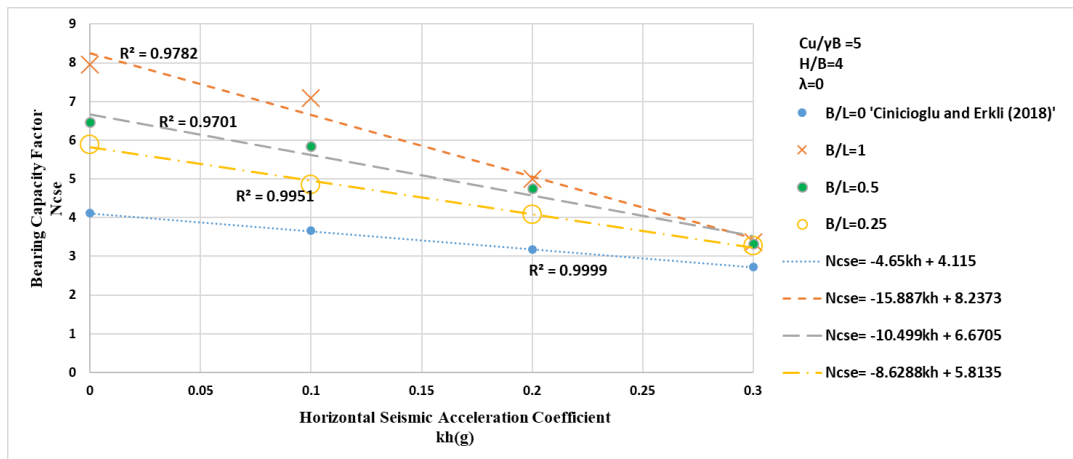


Figure 4.31. Variation of bearing capacity factor with horizontal seismic acceleration coefficient for  $\beta=30^\circ$ .

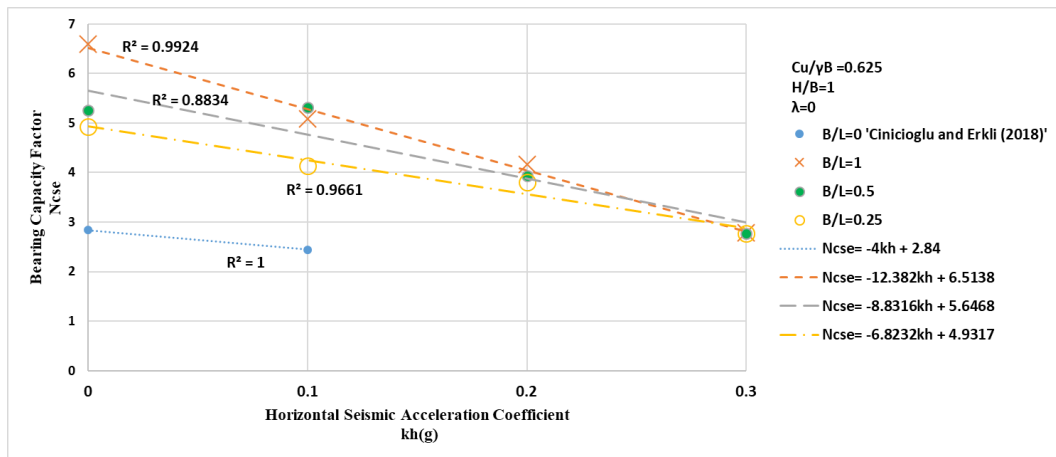


Figure 4.32. Variation of bearing capacity factor with horizontal seismic acceleration coefficient for  $\beta=45^\circ$ .

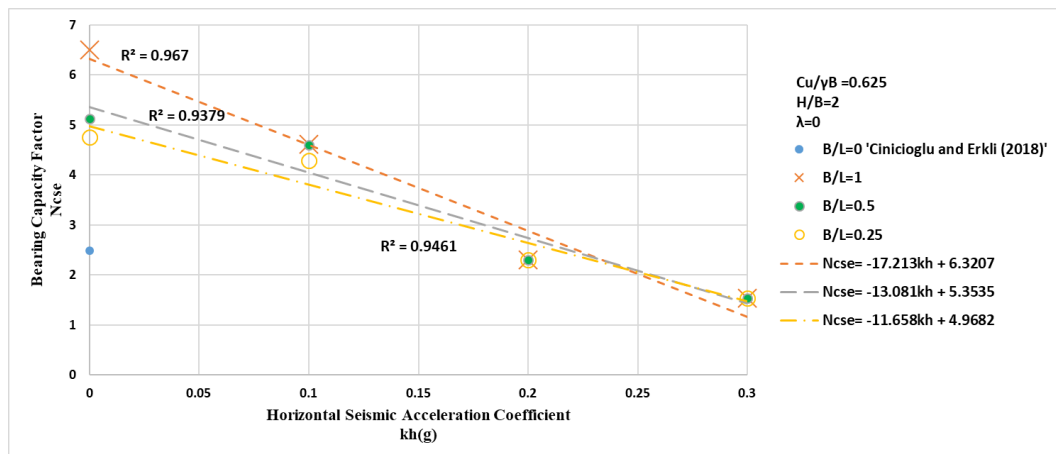


Figure 4.33. Variation of bearing capacity factor with horizontal seismic acceleration coefficient for  $\beta=45^\circ$ .

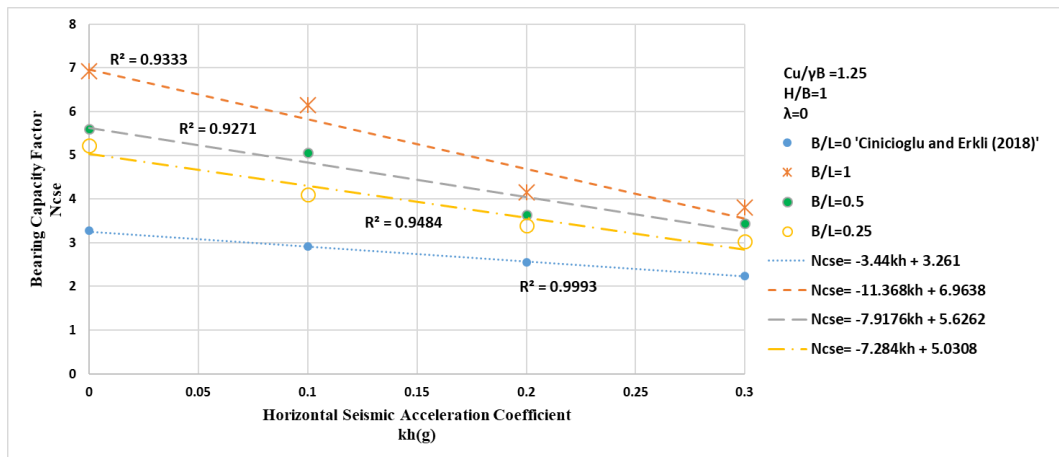


Figure 4.34. Variation of bearing capacity factor with horizontal seismic acceleration coefficient for  $\beta=45^\circ$ .

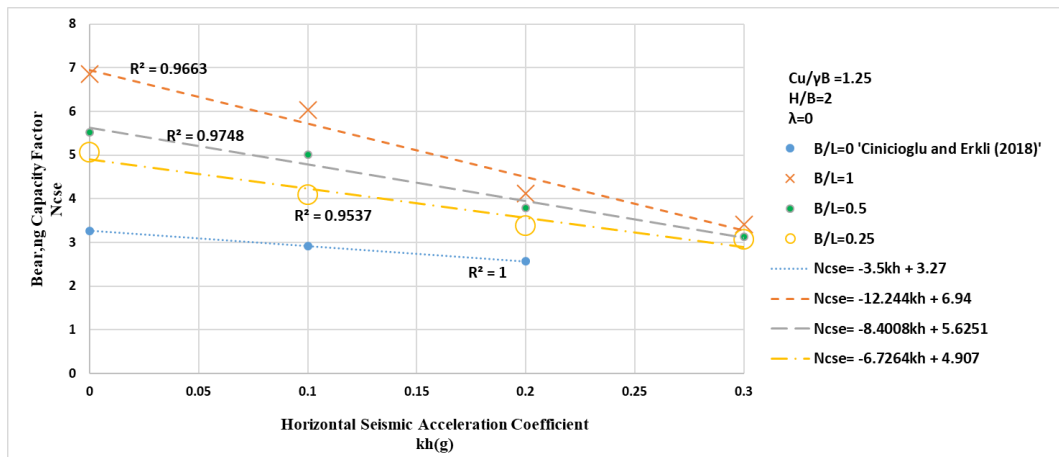


Figure 4.35. Variation of bearing capacity factor with horizontal seismic acceleration coefficient for  $\beta=45^\circ$ .

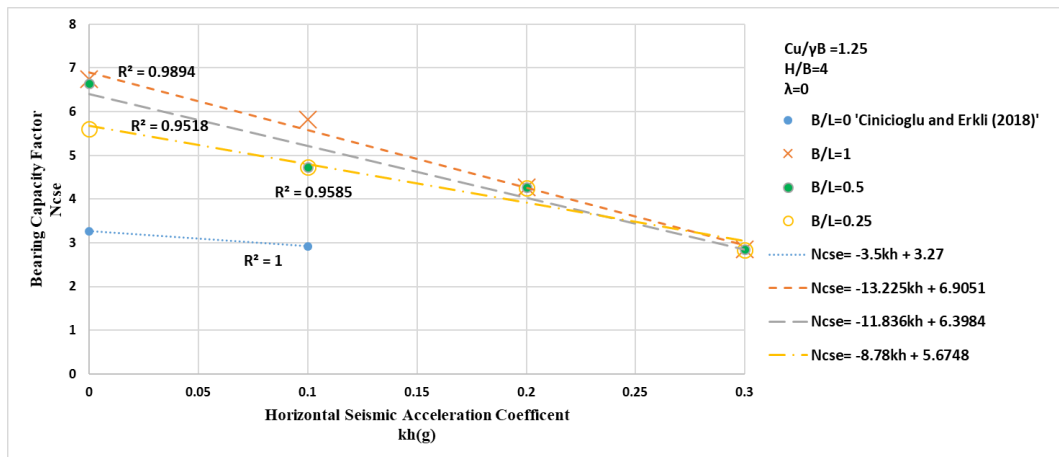


Figure 4.36. Variation of bearing capacity factor with horizontal seismic acceleration coefficient for  $\beta = 45^\circ$ .

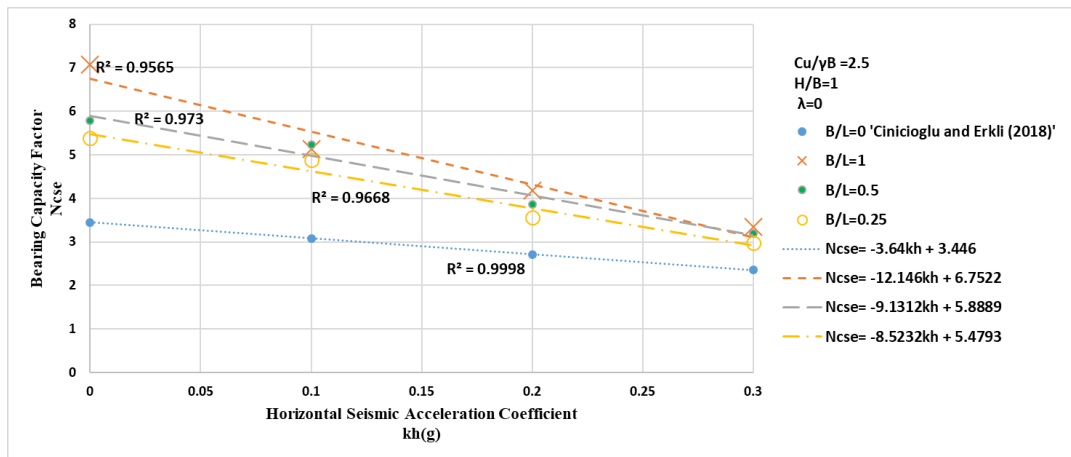


Figure 4.37. Variation of bearing capacity factor with horizontal seismic acceleration coefficient for  $\beta = 45^\circ$ .

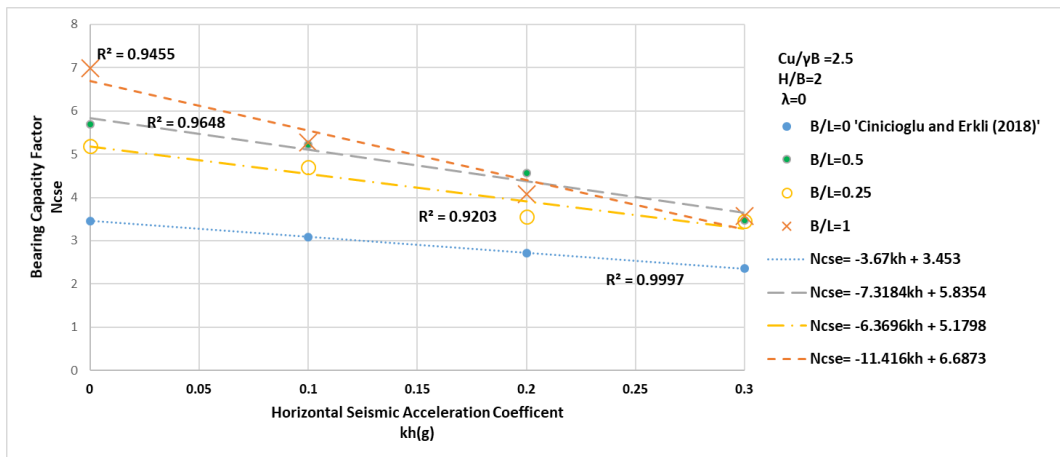


Figure 4.38. Variation of bearing capacity factor with horizontal seismic acceleration coefficient for  $\beta=45^\circ$ .

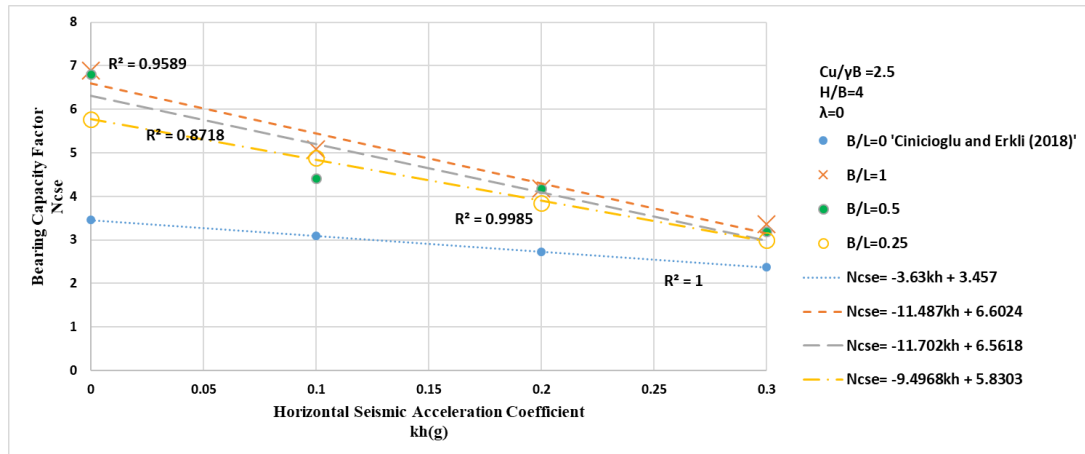


Figure 4.39. Variation of bearing capacity factor with horizontal seismic acceleration coefficient for  $\beta=45^\circ$ .

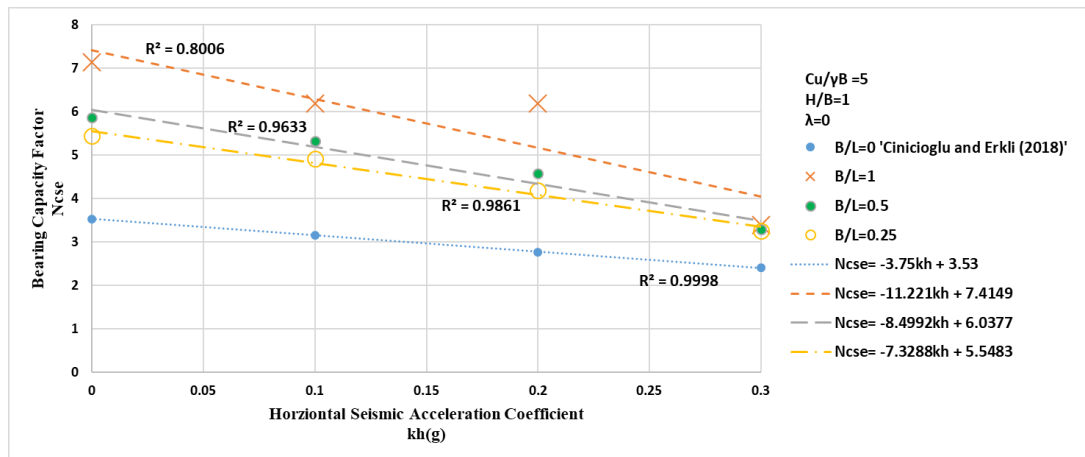


Figure 4.40. Variation of bearing capacity factor with horizontal seismic acceleration coefficient for  $\beta = 45^\circ$ .

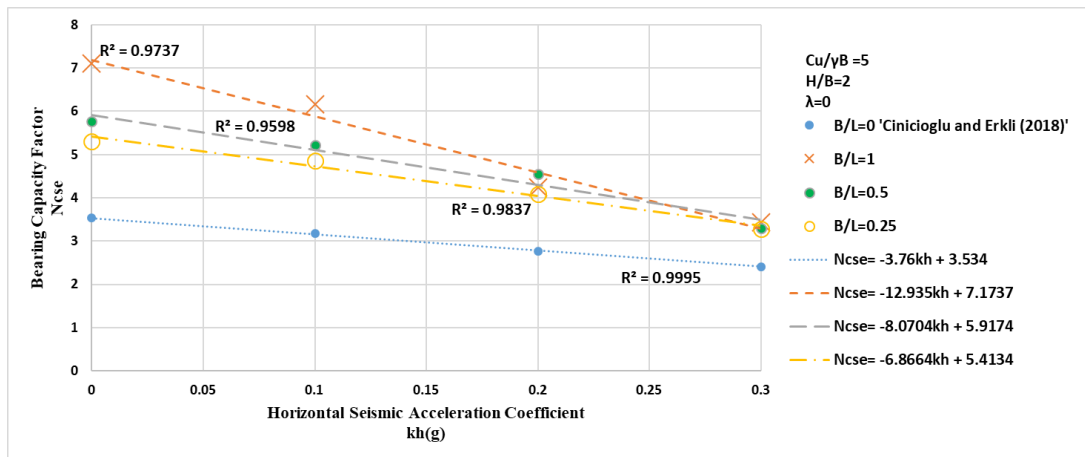


Figure 4.41. Variation of bearing capacity factor with horizontal seismic acceleration coefficient for  $\beta = 45^\circ$ .

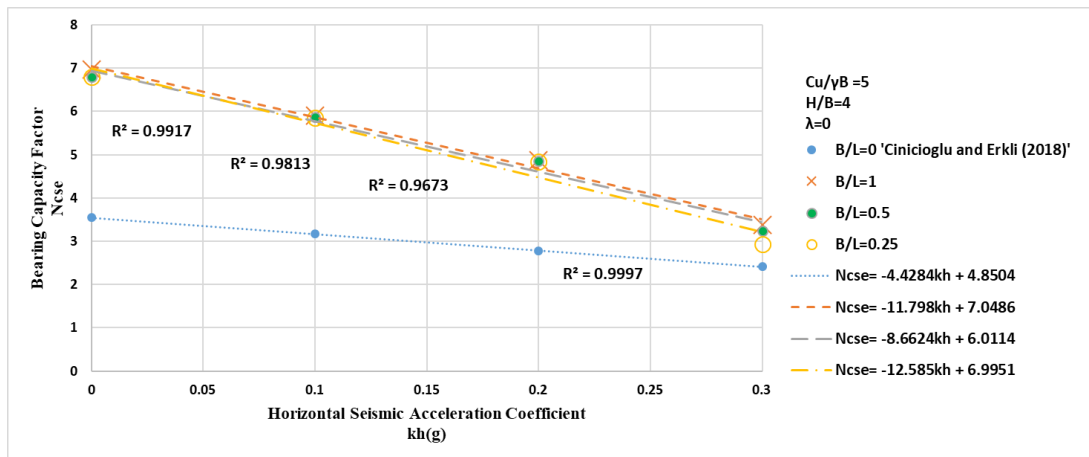


Figure 4.42. Variation of bearing capacity factor with horizontal seismic acceleration coefficient for  $\beta=45^\circ$ .

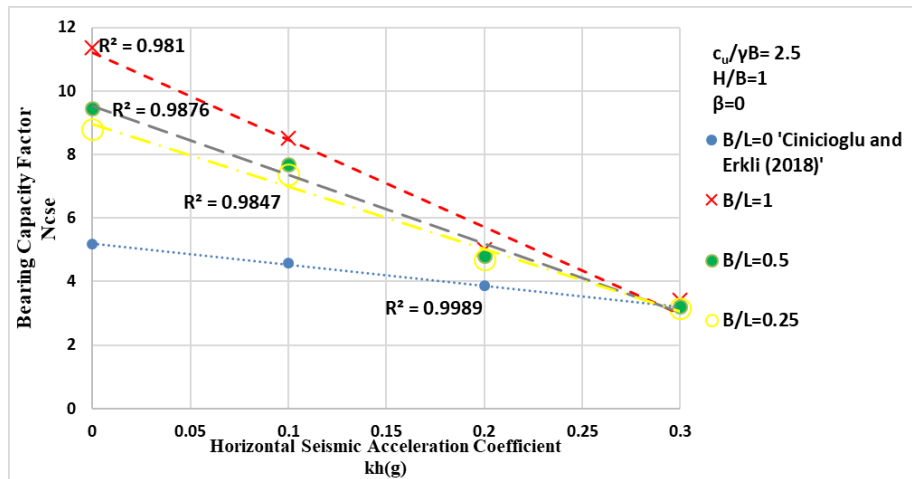


Figure 4.43. Variation of bearing capacity factor with horizontal seismic acceleration coefficient for  $\beta=0^\circ$ .

## 5. CONCLUSIONS

Recently, seismic bearing capacity of shallow foundations located on top of or near slopes has become one of the most critical issues for geotechnical designers and engineers. Numerical methods are more commonly used to solve different geotechnical problems. In this study, the finite element technique is used to evaluate the seismic bearing capacity of shallow footings on soil which provides Mohr-Coulomb soil criterion, for different slope angles, size of foundation and seismic coefficient. Therefore, the commercial available code, called Plaxis 3D, based on FEM is used for finite element examinations.

As a result of numerous analyses that were carried out with PLAXIS 3D, the effect of different influential parameters on the undrained seismic bearing capacity of shallow foundations has been investigated. In this study, different from these parameters, size effect plays an important role to draw the relationship between  $(N_{cse})-k_h$ . Therefore, seismic bearing capacity coefficient  $(N_{cse})$  can be obtained by the design charts given in Chapter 4.3. All the design charts presented are the result of numerical models performed in this field study. As a conclusion of the assessments, it is observed that the issues given below were achieved.

- Seismic bearing capacity factor  $(N_{cse})$  can be considered as a function of  $f(k_h, \beta, c_u/\gamma B, H/B)$ .
- The value of seismic bearing capacity coefficient drops drastically with the increase in horizontal seismic acceleration coefficient. Shape effect has become a minor impact on bearing capacity for the values greater than 0.3g.
- The increase in the slope angle  $(\beta)$  leads to a decrease in seismic bearing capacity factor.
- Due to the increase in size of foundation  $(L)$  with relation to the shape effect and increase in the loading to the system, seismic bearing coefficient decreases.

- According to presented design charts, the slope of each line plotted in graph decreases with the increase in the  $B/L$  ratio. Likewise, zero intercept of each line decreases with the increase in  $B/L$  ratio as linear.

- Three different failure mechanisms (foundation failure, base failure due to inertia effect and base failure due to gravity) were observed.

- For  $c_u/\gamma B = 0.625$  and  $H/B = 4$ , the correlation between seismic bearing capacity factor ( $N_{cse}$ ) and horizontal seismic acceleration coefficient couldn't be drawn because the model failed to reach the final seismic bearing capacity for slope angles. This failure is called 'base failure due to gravity'.

- Normalized slope soil strength ( $c_u/\gamma B$ ) has a slight impact on seismic bearing capacity factor.

- $H/B$  ratio has a small impact on seismic bearing capacity factor when the foundation failure occurs. Seismic bearing capacity factor ( $N_{cse}$ ) raises with the decrease for smaller  $c_u/\gamma B$  ratio values.

- According to accurate results of Plaxis 3D are larger than the results of Plaxis 2D. It should be kept in mind that there is a dimensional effect in Plaxis 3D while this effect completely is ignored in Plaxis 2D.

## REFERENCES

- AASHTO, 1996, *Standard Specifications for Highway Bridges*, American Association of State Highway and Transportation Officials, USA.
- Bowles, J. E., 1996, *Foundation Analysis and Design*, McGraw-Hill, New York, USA.
- Brinkgreve, R. B. J., W. Broere, and D. Waterman, 2006, *Plaxis User's Manual*, Plaxis B. V., Delft, Netherlands.
- Castelli, F, and E. Motta, 2010, "Bearing Capacity of Strip Footings Near Slopes" *Geotech Geol Eng.*, Vol. 28, pp. 187-198.
- Cinicioglu O, and A. Erkli, 2018, "Seismic Bearing Capacity of Surficial Foundations On sloping Cohesive Ground", *Soil Dynamics and Earthquake Engineering*, Vol.111, pp. 53-64.
- Das, B. M., 2010, *Principles of Geotechnical Engineering*, 7th Edition, Cengage Learning, Stamford.
- Das, B. M., and G. V. Ramana, 2011, *Principles of Soil Dynamics*, 2nd Edition, Cengage Learning, Stamford.
- Day, R. W., 2002, *Geotechnical Earthquake Engineering Handbook*, McGraw Hill Professional, New York, USA.
- Erkli, A., and O Çinicioğlu, 2012, "Kohezyonlu Sevlerin Üzerindeki Yüzeysel Şerit Temellerin Sismik Taşıma Gücü", *Zemin Mekaniği ve Temel Muhendisliği 14. Ulusal Kongresi*, Isparta.

- Farzaneh, O, J. Mofidi, and F. Askari, 2013, "Seismic Bearing Capacity of Strip Footings near Cohesive Slopes Using Lower Bound Limit Analysis", *Proceedings of the 18<sup>th</sup> International Conference on Soil Mechanics and Geotechnical Engineering*, Paris, pp. 1467-1470.
- Georgiadis, K., 2010, "Undrained Bearing Capacity of Strip Footings on Slopes", *Journal of Geotechnical and Geoenvironmental Engineering*, Vol. 136, No. 5, pp. 677-685.
- Hansen, J. B., 1961, "A General Formula for Bearing Capacity". *Danish Geotechnical Institute Bulletin 11*, Copenhagen, Denmark, pp.38-46.
- Islam, M. S., M. Rokouzzaman, and T. Sakai, 2017, "Shape Effect of Square and Circular Footing under Vertical Loading: Experimental and Numerical Studies", *International Journal of Geomechanics*, Vol.17, No.9, pp. 1-9.
- Keshavarz, A., M. Beygi, and R. Vali, 2019, "Undrained Seismic Bearing Capacity of Strip Footing Placed on Homogeneous and Heterogeneous Soil Slopes by Finite Element Limit Analysis", *Computers and Geotechnics*, Vol.113, pp. 1-13.
- Koppula, S. D, 1984, "On Stability of Slopes on Clays with Linearly Increasing Strength", *Canadian Geotechnical Journal*, Vol. 21, No. 3, pp. 557-581.
- Kramer, S. L., 1996, *Geotechnical Earthquake Engineering*, Prentice Hall, New Jersey.
- Kumar, J., and M. Rao, 2003, "Seismic Bearing Capacity of Foundations on Slopes", *Geotechnique*, Vol. 53, No.3, pp. 347-361.
- Kusakabe, O., T. Kimura, and H. Yamaguchi, 1981, "Bearing Capacity of Slopes under Strip Loads on the Top Surfaces", *Soils and Foundations*, Vol. 21, No. 4, pp. 29-40.
- Li, J.-P., L.-Y. Chen, and F.Y. Liang, 2009, "Effect of Footing Shape on Bearing Capacity of Rectangular Footings", *International Foundation Congress and Equipment Expo*, Orlando, Florida, United States.

- Merlos, J., and M. P. Romo, 2006, "Fluctuant Bearing Capacity of Shallow Foundations During Earthquakes", *Soil Dynamics and Earthquake Engineering*, Vol. 26, pp. 103-114
- Meyerhof, G. G., 1957, "The Ultimate Bearing Capacity of Foundation on Slopes", *Proceedings of the Fourth International Conference on Soil Mechanics*, London, pp. 384-386.
- Pathak, S. R., S. N. Kamat, and D. R. Phatak, 2008, "Study of Behaviour of Square and Rectangular Footings Resting on Cohesive Soils Based on Model Tests", *International Conference on Case Histories in Geotechnical Engineering*, p.31.
- Potts, D. M., and L. Zdravkovic, 1999, *Finite Element Analysis in Geotechnical Engineering: Theory*, Thomas Telford, London.
- Potts, D. M., and L. Zdravkovic, 2001, *Finite Element Analysis in Geotechnical Engineering: Application*, Thomas Telford, London.
- Potts, D. M., K. Axelsson, L. Grande, H. Schweiger, and M. Long, 2002, *Guidelines for the Use of Advanced Numerical Analysis*, Thomas Telford, London.
- Prandtl, L., 1920, "Uber die Harte Plastischer Korper", *Nachrichten von der Koniglichen Gesellschaft der Wissenschaften*, Gottingen, Math. Phys., Klasse, pp. 74-85.
- Salgado, R., A. V. Lyamin, S. W. Sloan, and H. S. Yu, 2004, "Two and Three Dimensional Bearing Capacity of Foundations in Clay." *Geotechnique*, Vol. 54 No.5, pp. 297-306.
- Shiau, J., A. Lyamin, and S. Sloan, 2006, "Application of Pseudo-Static Limit Analysis in Geotechnical Earthquake Design", *Numerical Methods in Geotechnical Engineering-Schweiger (ed)*, Taylor&Francis Group, LLC., London.
- Shiau, J., R. S. Merifield, A. V. Lyamin, and S. Sloan, 2011, "Undrained Stability of Footings on Slopes", *International Journal of Geomechanics*, Vol.11, pp. 381-390.

- Skempton, A. W., 1951, "The Bearing Capacity of Clays", *Building Research Congress*, London, pp. 180-189.
- Sloan, S. W., 1988, "Lower Bound Limit Analysis Using Finite Elements and Linear Programming", *International Journal for Numerical and Analytical Methods in Geomechanics*, Vol. 12, pp. 61-67.
- Taiebat, H. A., and J. P. Carter, 2008, "Flow Rule Effects in the Tresca Model", *Computers and Geotechnics*, Vol. 35, pp. 500-503.
- Taylor, D. W., 1937, "Stability of Earth Slopes", *Journal of the Boston Society of Civil Engineers*, Vol. 24, pp. 197-246.
- Terzaghi, K., 1943, *Theoretical Soil Mechanics*, John Wiley & Sons, Inc., New York, USA.
- U.S. Army Corps of Engineers, 1995, *Engineering and Design: Geotechnical Analysis by The Finite Element Method*, Washington, DC.
- Vesic, A.S., 1975, *Foundation Engineering Handbook*, H.F. Winterkorn and H. Y Fang, eds., Van Nostrand Reinhold, New York, USA.
- Washington State Department of Transportation, 2005, *Geotechnical Design Manual*, Washington, DC.
- Yamamoto, K., 2010 "Seismic Bearing Capacity of Shallow Foundations near Slopes Using the Upper-Bound Method", *International Journal of Geotechnical Engineering*, Vol. 4, No. 2, pp. 255-267.
- Yang, H., Z. Shen, and J. Wang, 2003, "3D Lower Bound Bearing Capacity of Smooth Rectangular Surface Footings", *Mechanics Research Communications*, Vol.30, No.5, pp. 481-492.

- Yu, L., J. Liu, X.-J. Kong, and Y. Hu, M. ASCE, 2011, “Three-dimensional Large Deformation FE Analysis of Square Footings in Two-Layered Clays”, *Journal of Geotechnical and Geoenvironmental Engineering*, Vol.137, No.1, pp. 52-58.
- Zhu, M., and R. L. Michalowski, 2005, “Shape Factors For Limit Loads on Square and Rectangular Footings”, *Journal of Geotechnical and Geoenvironmental Engineering*, Vol.131, No.2, pp. 223–231.

**APPENDIX A: LIST OF RESULTS OF FINITE ELEMENTS MODELS  
CREATED FOR STATIC CONDITION**

List of results for finite element models created for static condition is given in Table A.1, Table A.2 and Table A.3.

Table A.1. List of results of finite elements models created for static condition ( $\beta= 15^\circ$ ).

| Model No. | GEOTECHNICAL PROPERTIES |       |           |       |       | SLOPE SOIL PROPERTIES         |                            |              |             |       | SEISMIC EFFECT |                   | ANALYSIS RESULTS FOR STATIC LOADING |             |      |         |             |        |       |                    |
|-----------|-------------------------|-------|-----------|-------|-------|-------------------------------|----------------------------|--------------|-------------|-------|----------------|-------------------|-------------------------------------|-------------|------|---------|-------------|--------|-------|--------------------|
|           | $\beta$ (°)             | H (m) | $\lambda$ | B (m) | L (m) | $\gamma$ (kN/m <sup>3</sup> ) | $c_u$ (kN/m <sup>2</sup> ) | $\phi_u$ (°) | $E_u$ (kPa) | $v_u$ | $k_b$          | FILE NAME         | H/B                                 | $\beta$ (°) | Load | M stage | $q_t$ (kPa) | $N_s$  | cu/vB | Failure Mode       |
| 1         | 0                       | 2     | 0         | 2     | 4     | 20                            | 100                        | 0            | 20000       | 0.35  | 0              | C.0.2.0.2.100.S   | 1                                   | 0           | 2000 | 0.5688  | 1138        | 11.376 | 2.5   | Foundation Failure |
| 2         | 0                       | 2     | 0         | 2     | 4     | 20                            | 100                        | 0            | 20000       | 0.35  | 0              | C.0.2.0.4.100.S   | 1                                   | 0           | 2000 | 0.4724  | 945         | 9.448  | 2.5   | Foundation Failure |
| 3         | 0                       | 2     | 0         | 2     | 8     | 20                            | 100                        | 0            | 20000       | 0.35  | 0              | C.0.2.0.8.100.S   | 1                                   | 0           | 2000 | 0.4396  | 879         | 8.792  | 2.5   | Foundation Failure |
| 4         | 0                       | 2     | 0         | 2     | 16    | 20                            | 100                        | 0            | 20000       | 0.35  | 0              | C.0.2.0.16.100.S  | 1                                   | 0           | 2000 | 0.3882  | 776         | 7.764  | 2.5   | Foundation Failure |
| 5         | 15                      | 2     | 0         | 2     | 2     | 20                            | 25                         | 0            | 5000        | 0.35  | 0              | C.15.2.0.2.25.S   | 1                                   | 15          | 300  | 0.7768  | 233.04      | 9      | 0.63  | Foundation Failure |
| 6         | 15                      | 4     | 0         | 2     | 2     | 20                            | 25                         | 0            | 5000        | 0.35  | 0              | C.15.4.0.2.25.S   | 2                                   | 15          | 300  | 0.7066  | 212         | 8.48   | 0.63  | Foundation Failure |
| 7         | 15                      | 8     | 0         | 2     | 2     | 20                            | 25                         | 0            | 5000        | 0.35  | 0              | C.15.8.0.2.25.S   | 4                                   | 15          | 200  | N.F.    | N.F.        | N.F.   | 0.63  | Base failure_GR    |
| 8         | 15                      | 2     | 0         | 2     | 4     | 20                            | 25                         | 0            | 5000        | 0.35  | 0              | C.15.2.0.4.25.S   | 1                                   | 15          | 300  | 0.6788  | 204         | 8.15   | 0.63  | Foundation Failure |
| 9         | 15                      | 4     | 0         | 2     | 4     | 20                            | 25                         | 0            | 5000        | 0.35  | 0              | C.15.4.0.4.25.S   | 2                                   | 15          | 300  | 0.7219  | 217         | 8.66   | 0.63  | Foundation Failure |
| 10        | 15                      | 8     | 0         | 2     | 4     | 20                            | 25                         | 0            | 5000        | 0.35  | 0              | C.15.8.0.4.25.S   | 4                                   | 15          | 200  | N.F.    | N.F.        | N.F.   | 0.63  | Base failure_GR    |
| 11        | 15                      | 2     | 0         | 2     | 8     | 20                            | 25                         | 0            | 5000        | 0.35  | 0              | C.15.2.0.8.25.S   | 1                                   | 15          | 200  | 0.9542  | 191         | 7.63   | 0.63  | Foundation Failure |
| 12        | 15                      | 4     | 0         | 2     | 8     | 20                            | 25                         | 0            | 5000        | 0.35  | 0              | C.15.4.0.8.25.S   | 2                                   | 15          | 200  | 0.9704  | 194         | 7.76   | 0.63  | Foundation Failure |
| 13        | 15                      | 8     | 0         | 2     | 8     | 20                            | 25                         | 0            | 5000        | 0.35  | 0              | C.15.8.0.8.25.S   | 4                                   | 15          | 200  | N.F.    | N.F.        | N.F.   | 0.63  | Base failure_GR    |
| 14        | 15                      | 2     | 0         | 2     | 16    | 20                            | 25                         | 0            | 5000        | 0.35  | 0              | C.15.2.0.16.25.S  | 1                                   | 15          | 300  | 0.6834  | 205         | 8.20   | 0.63  | Foundation Failure |
| 15        | 15                      | 4     | 0         | 2     | 16    | 20                            | 25                         | 0            | 5000        | 0.35  | 0              | C.15.4.0.16.25.S  | 2                                   | 15          | 200  | 0.9823  | 196         | 7.86   | 0.63  | Foundation Failure |
| 16        | 15                      | 8     | 0         | 2     | 16    | 20                            | 25                         | 0            | 5000        | 0.35  | 0              | C.15.8.0.16.25.S  | 4                                   | 15          | 200  | N.F.    | N.F.        | N.F.   | 0.63  | Base failure_GR    |
| 17        | 15                      | 2     | 0         | 2     | 2     | 20                            | 50                         | 0            | 10000       | 0.35  | 0              | C.15.2.0.2.50.S   | 1                                   | 15          | 600  | 0.7868  | 472         | 9.44   | 1.25  | Foundation Failure |
| 18        | 15                      | 4     | 0         | 2     | 2     | 20                            | 50                         | 0            | 10000       | 0.35  | 0              | C.15.4.0.2.50.S   | 2                                   | 15          | 600  | 0.7377  | 443         | 8.85   | 1.25  | Foundation Failure |
| 19        | 15                      | 8     | 0         | 2     | 2     | 20                            | 50                         | 0            | 10000       | 0.35  | 0              | C.15.8.0.2.50.S   | 4                                   | 15          | 600  | 0.6798  | 408         | 8.16   | 1.25  | Foundation Failure |
| 20        | 15                      | 2     | 0         | 2     | 4     | 20                            | 50                         | 0            | 10000       | 0.35  | 0              | C.15.2.0.4.50.S   | 1                                   | 15          | 600  | 0.6944  | 417         | 8.33   | 1.25  | Foundation Failure |
| 21        | 15                      | 4     | 0         | 2     | 4     | 20                            | 50                         | 0            | 10000       | 0.35  | 0              | C.15.4.0.4.50.S   | 2                                   | 15          | 600  | 0.7376  | 443         | 8.85   | 1.25  | Foundation Failure |
| 22        | 15                      | 8     | 0         | 2     | 4     | 20                            | 50                         | 0            | 10000       | 0.35  | 0              | C.15.8.0.4.50.S   | 4                                   | 15          | 600  | 0.7661  | 460         | 9.19   | 1.25  | Foundation Failure |
| 23        | 15                      | 2     | 0         | 2     | 8     | 20                            | 50                         | 0            | 10000       | 0.35  | 0              | C.15.2.0.8.50.S   | 1                                   | 15          | 400  | 0.9781  | 391         | 7.82   | 1.25  | Foundation Failure |
| 24        | 15                      | 4     | 0         | 2     | 8     | 20                            | 50                         | 0            | 10000       | 0.35  | 0              | C.15.4.0.8.50.S   | 2                                   | 15          | 400  | 0.9866  | 395         | 7.89   | 1.25  | Foundation Failure |
| 25        | 15                      | 8     | 0         | 2     | 8     | 20                            | 50                         | 0            | 10000       | 0.35  | 0              | C.15.8.0.8.50.S   | 4                                   | 15          | 600  | 0.7535  | 452         | 9.04   | 1.25  | Foundation Failure |
| 26        | 15                      | 2     | 0         | 2     | 16    | 20                            | 50                         | 0            | 10000       | 0.35  | 0              | C.15.2.0.16.50.S  | 1                                   | 15          | 600  | 0.708   | 425         | 8.50   | 1.25  | Foundation Failure |
| 27        | 15                      | 4     | 0         | 2     | 16    | 20                            | 50                         | 0            | 10000       | 0.35  | 0              | C.15.4.0.16.50.S  | 2                                   | 15          | 600  | 0.6711  | 403         | 8.05   | 1.25  | Foundation Failure |
| 28        | 15                      | 8     | 0         | 2     | 16    | 20                            | 50                         | 0            | 10000       | 0.35  | 0              | C.15.8.0.16.50.S  | 4                                   | 15          | 400  | 0.9295  | 372         | 7.44   | 1.25  | Foundation Failure |
| 29        | 15                      | 2     | 0         | 2     | 2     | 20                            | 100                        | 0            | 20000       | 0.35  | 0              | C.15.2.0.2.100.S  | 1                                   | 15          | 1000 | 0.9451  | 945         | 9.45   | 2.50  | Foundation Failure |
| 30        | 15                      | 4     | 0         | 2     | 2     | 20                            | 100                        | 0            | 20000       | 0.35  | 0              | C.15.4.0.2.100.S  | 2                                   | 15          | 1000 | 0.8702  | 870         | 8.70   | 2.50  | Foundation Failure |
| 31        | 15                      | 8     | 0         | 2     | 2     | 20                            | 100                        | 0            | 20000       | 0.35  | 0              | C.15.8.0.2.100.S  | 4                                   | 15          | 1200 | 0.8366  | 1004        | 10.04  | 2.50  | Foundation Failure |
| 32        | 15                      | 2     | 0         | 2     | 4     | 20                            | 100                        | 0            | 20000       | 0.35  | 0              | C.15.2.0.4.100.S  | 1                                   | 15          | 1000 | 0.8398  | 840         | 8.40   | 2.50  | Foundation Failure |
| 33        | 15                      | 4     | 0         | 2     | 4     | 20                            | 100                        | 0            | 20000       | 0.35  | 0              | C.15.4.0.4.100.S  | 2                                   | 15          | 800  | 0.9933  | 795         | 7.95   | 2.50  | Foundation Failure |
| 34        | 15                      | 8     | 0         | 2     | 4     | 20                            | 100                        | 0            | 20000       | 0.35  | 0              | C.15.8.0.4.100.S  | 4                                   | 15          | 1000 | 0.9357  | 936         | 9.36   | 2.50  | Foundation Failure |
| 35        | 15                      | 2     | 0         | 2     | 8     | 20                            | 100                        | 0            | 20000       | 0.35  | 0              | C.15.2.0.8.100.S  | 1                                   | 15          | 800  | 0.9875  | 790         | 7.90   | 2.50  | Foundation Failure |
| 36        | 15                      | 4     | 0         | 2     | 8     | 20                            | 100                        | 0            | 20000       | 0.35  | 0              | C.15.4.0.8.100.S  | 2                                   | 15          | 800  | 0.8912  | 713         | 7.13   | 2.50  | Foundation Failure |
| 37        | 15                      | 8     | 0         | 2     | 8     | 20                            | 100                        | 0            | 20000       | 0.35  | 0              | C.15.8.0.8.100.S  | 4                                   | 15          | 1000 | 0.9109  | 911         | 9.11   | 2.50  | Foundation Failure |
| 38        | 15                      | 2     | 0         | 2     | 16    | 20                            | 100                        | 0            | 20000       | 0.35  | 0              | C.15.2.0.16.100.S | 1                                   | 15          | 1000 | 0.8629  | 863         | 8.63   | 2.50  | Foundation Failure |
| 39        | 15                      | 4     | 0         | 2     | 16    | 20                            | 100                        | 0            | 20000       | 0.35  | 0              | C.15.4.0.16.100.S | 2                                   | 15          | 1000 | 0.8151  | 815         | 8.15   | 2.50  | Foundation Failure |
| 40        | 15                      | 8     | 0         | 2     | 16    | 20                            | 100                        | 0            | 20000       | 0.35  | 0              | C.15.8.0.16.100.S | 4                                   | 15          | 800  | 0.9425  | 754         | 7.54   | 2.50  | Foundation Failure |
| 41        | 15                      | 2     | 0         | 2     | 2     | 20                            | 200                        | 0            | 40000       | 0.35  | 0              | C.15.2.0.2.200.S  | 1                                   | 15          | 2000 | 0.949   | 1898        | 9.49   | 5.00  | Foundation Failure |
| 42        | 15                      | 4     | 0         | 2     | 2     | 20                            | 200                        | 0            | 40000       | 0.35  | 0              | C.15.4.0.2.200.S  | 2                                   | 15          | 2000 | 0.8954  | 1791        | 8.95   | 5.00  | Foundation Failure |
| 43        | 15                      | 8     | 0         | 2     | 2     | 20                            | 200                        | 0            | 40000       | 0.35  | 0              | C.15.8.0.2.200.S  | 4                                   | 15          | 2200 | 0.9304  | 2047        | 10.23  | 5.00  | Foundation Failure |
| 44        | 15                      | 2     | 0         | 2     | 4     | 20                            | 200                        | 0            | 40000       | 0.35  | 0              | C.15.2.0.4.200.S  | 1                                   | 15          | 2000 | 0.841   | 1682        | 8.41   | 5.00  | Foundation Failure |
| 45        | 15                      | 4     | 0         | 2     | 4     | 20                            | 200                        | 0            | 40000       | 0.35  | 0              | C.15.4.0.4.200.S  | 2                                   | 15          | 2000 | 0.8843  | 1769        | 8.84   | 5.00  | Foundation Failure |
| 46        | 15                      | 8     | 0         | 2     | 4     | 20                            | 200                        | 0            | 40000       | 0.35  | 0              | C.15.8.0.4.200.S  | 4                                   | 15          | 2000 | 0.942   | 1884        | 9.42   | 5.00  | Foundation Failure |
| 47        | 15                      | 2     | 0         | 2     | 8     | 20                            | 200                        | 0            | 40000       | 0.35  | 0              | C.15.2.0.8.200.S  | 1                                   | 15          | 1600 | 0.9923  | 1588        | 7.94   | 5.00  | Foundation Failure |
| 48        | 15                      | 4     | 0         | 2     | 8     | 20                            | 200                        | 0            | 40000       | 0.35  | 0              | C.15.4.0.8.200.S  | 2                                   | 15          | 1600 | 0.9898  | 1588        | 7.92   | 5.00  | Foundation Failure |
| 49        | 15                      | 8     | 0         | 2     | 8     | 20                            | 200                        | 0            | 40000       | 0.35  | 0              | C.15.8.0.8.200.S  | 4                                   | 15          | 2000 | 0.9142  | 1828        | 9.14   | 5.00  | Foundation Failure |
| 50        | 15                      | 2     | 0         | 2     | 16    | 20                            | 200                        | 0            | 40000       | 0.35  | 0              | C.15.2.0.16.200.S | 1                                   | 15          | 2000 | 0.8697  | 1739        | 8.70   | 5.00  | Foundation Failure |
| 51        | 15                      | 4     | 0         | 2     | 16    | 20                            | 200                        | 0            | 40000       | 0.35  | 0              | C.15.4.0.16.200.S | 2                                   | 15          | 2000 | 0.8131  | 1626        | 8.13   | 5.00  | Foundation Failure |
| 52        | 15                      | 8     | 0         | 2     | 16    | 20                            | 200                        | 0            | 40000       | 0.35  | 0              | C.15.8.0.16.200.S | 4                                   | 15          | 1600 | 0.9525  | 1524        | 7.62   | 5.00  | Foundation Failure |

N.F.:Not found.  
 Base failure\_EQ:Failed due to earthquake.  
 Base failure\_GR:Failed due to gravity.

Table A.2. List of results of finite elements models created for static condition ( $\beta= 30^\circ$ ).

| Model No. | GEOTECHNICAL PROPERTIES |       |           |       |       |                               |                            | SLOPE SOIL PROPERTIES |             |       |       |     |             |      | SEISMI C EFFECT | FILE NAME | ANALYSIS RESULTS FOR STATIC LOADING |                 |                    |       |              |  |  |
|-----------|-------------------------|-------|-----------|-------|-------|-------------------------------|----------------------------|-----------------------|-------------|-------|-------|-----|-------------|------|-----------------|-----------|-------------------------------------|-----------------|--------------------|-------|--------------|--|--|
|           | $\beta$ (°)             | H (m) | $\lambda$ | B (m) | L (m) | $\gamma$ (kN/m <sup>3</sup> ) | $c_u$ (kN/m <sup>2</sup> ) | $\phi_u$ (°)          | $E_u$ (kPa) | $v_u$ | $k_b$ | H/B | $\beta$ (°) | Load |                 |           | Mistage                             | $q_r$ (kPa)     | $N_{cs}$           | cu/yB | Failure Mode |  |  |
| 1         | 30                      | 2     | 0         | 2     | 2     | 20                            | 25                         | 0                     | 5000        | 0.35  | 0     | 1   | 30          | 200  | 0.8803          | 176       | 7.04                                | 0.63            | Foundation Failure |       |              |  |  |
| 2         | 30                      | 4     | 0         | 2     | 2     | 20                            | 25                         | 0                     | 5000        | 0.35  | 0     | 2   | 30          | 200  | 0.9814          | 196       | 7.85                                | 0.63            | Foundation Failure |       |              |  |  |
| 3         | 30                      | 8     | 0         | 2     | 2     | 20                            | 25                         | 0                     | 5000        | 0.35  | 0     | 4   | 30          | 200  | N.F.            | N.F.      | N.F.                                | Base failure_GR |                    |       |              |  |  |
| 4         | 30                      | 2     | 0         | 2     | 4     | 20                            | 25                         | 0                     | 5000        | 0.35  | 0     | 1   | 30          | 200  | 0.8492          | 170       | 6.79                                | 0.63            | Foundation Failure |       |              |  |  |
| 5         | 30                      | 4     | 0         | 2     | 4     | 20                            | 25                         | 0                     | 5000        | 0.35  | 0     | 2   | 30          | 200  | 0.8364          | 167       | 6.69                                | 0.63            | Foundation Failure |       |              |  |  |
| 6         | 30                      | 8     | 0         | 2     | 4     | 20                            | 25                         | 0                     | 5000        | 0.35  | 0     | 4   | 30          | 200  | N.F.            | N.F.      | N.F.                                | Base failure_GR |                    |       |              |  |  |
| 7         | 30                      | 2     | 0         | 2     | 8     | 20                            | 25                         | 0                     | 5000        | 0.35  | 0     | 1   | 30          | 200  | 0.7098          | 142       | 5.68                                | 0.63            | Foundation Failure |       |              |  |  |
| 8         | 30                      | 4     | 0         | 2     | 8     | 20                            | 25                         | 0                     | 5000        | 0.35  | 0     | 2   | 30          | 200  | 0.6929          | 139       | 5.54                                | 0.63            | Foundation Failure |       |              |  |  |
| 9         | 30                      | 8     | 0         | 2     | 8     | 20                            | 25                         | 0                     | 5000        | 0.35  | 0     | 4   | 30          | 200  | N.F.            | N.F.      | N.F.                                | Base failure_GR |                    |       |              |  |  |
| 10        | 30                      | 2     | 0         | 2     | 16    | 20                            | 25                         | 0                     | 5000        | 0.35  | 0     | 1   | 30          | 200  | 0.7457          | 149       | 5.97                                | 0.63            | Foundation Failure |       |              |  |  |
| 11        | 30                      | 4     | 0         | 2     | 16    | 20                            | 25                         | 0                     | 5000        | 0.35  | 0     | 2   | 30          | 200  | 0.7173          | 143       | 5.74                                | 0.63            | Foundation Failure |       |              |  |  |
| 12        | 30                      | 8     | 0         | 2     | 16    | 20                            | 25                         | 0                     | 5000        | 0.35  | 0     | 4   | 30          | 200  | N.F.            | N.F.      | N.F.                                | Base failure_GR |                    |       |              |  |  |
| 13        | 30                      | 2     | 0         | 2     | 2     | 20                            | 50                         | 0                     | 10000       | 0.35  | 0     | 1   | 30          | 400  | 0.8968          | 359       | 7.17                                | 1.25            | Foundation Failure |       |              |  |  |
| 14        | 30                      | 4     | 0         | 2     | 2     | 20                            | 50                         | 0                     | 10000       | 0.35  | 0     | 2   | 30          | 400  | 0.6725          | 404       | 8.07                                | 1.25            | Foundation Failure |       |              |  |  |
| 15        | 30                      | 8     | 0         | 2     | 2     | 20                            | 50                         | 0                     | 10000       | 0.35  | 0     | 4   | 30          | 400  | 0.9838          | 394       | 7.87                                | 1.25            | Foundation Failure |       |              |  |  |
| 16        | 30                      | 2     | 0         | 2     | 4     | 20                            | 50                         | 0                     | 10000       | 0.35  | 0     | 1   | 30          | 400  | 0.891           | 356       | 7.13                                | 1.25            | Foundation Failure |       |              |  |  |
| 17        | 30                      | 4     | 0         | 2     | 4     | 20                            | 50                         | 0                     | 10000       | 0.35  | 0     | 2   | 30          | 400  | 0.88            | 352       | 7.04                                | 1.25            | Foundation Failure |       |              |  |  |
| 18        | 30                      | 8     | 0         | 2     | 4     | 20                            | 50                         | 0                     | 10000       | 0.35  | 0     | 4   | 30          | 400  | 0.7474          | 299       | 5.98                                | 1.25            | Foundation Failure |       |              |  |  |
| 19        | 30                      | 2     | 0         | 2     | 8     | 20                            | 50                         | 0                     | 10000       | 0.35  | 0     | 1   | 30          | 400  | 0.7432          | 297       | 5.95                                | 1.25            | Foundation Failure |       |              |  |  |
| 20        | 30                      | 4     | 0         | 2     | 8     | 20                            | 50                         | 0                     | 10000       | 0.35  | 0     | 2   | 30          | 400  | 0.7309          | 292       | 5.85                                | 1.25            | Foundation Failure |       |              |  |  |
| 21        | 30                      | 8     | 0         | 2     | 8     | 20                            | 50                         | 0                     | 10000       | 0.35  | 0     | 4   | 30          | 400  | 0.7146          | 286       | 5.72                                | 1.25            | Foundation Failure |       |              |  |  |
| 22        | 30                      | 2     | 0         | 2     | 16    | 20                            | 50                         | 0                     | 10000       | 0.35  | 0     | 1   | 30          | 400  | 0.78            | 312       | 6.24                                | 1.25            | Foundation Failure |       |              |  |  |
| 23        | 30                      | 4     | 0         | 2     | 16    | 20                            | 50                         | 0                     | 10000       | 0.35  | 0     | 2   | 30          | 400  | 0.7637          | 305       | 6.11                                | 1.25            | Foundation Failure |       |              |  |  |
| 24        | 30                      | 8     | 0         | 2     | 16    | 20                            | 50                         | 0                     | 10000       | 0.35  | 0     | 4   | 30          | 400  | 0.7974          | 319       | 6.38                                | 1.25            | Foundation Failure |       |              |  |  |
| 25        | 30                      | 2     | 0         | 2     | 2     | 20                            | 100                        | 0                     | 20000       | 0.35  | 0     | 1   | 30          | 800  | 0.9121          | 730       | 7.30                                | 2.50            | Foundation Failure |       |              |  |  |
| 26        | 30                      | 4     | 0         | 2     | 2     | 20                            | 100                        | 0                     | 20000       | 0.35  | 0     | 2   | 30          | 1000 | 0.8181          | 818       | 8.18                                | 2.50            | Foundation Failure |       |              |  |  |
| 27        | 30                      | 8     | 0         | 2     | 2     | 20                            | 100                        | 0                     | 20000       | 0.35  | 0     | 4   | 30          | 800  | 0.9924          | 794       | 7.94                                | 2.50            | Foundation Failure |       |              |  |  |
| 28        | 30                      | 2     | 0         | 2     | 4     | 20                            | 100                        | 0                     | 20000       | 0.35  | 0     | 1   | 30          | 800  | 0.904           | 723       | 7.23                                | 2.50            | Foundation Failure |       |              |  |  |
| 29        | 30                      | 4     | 0         | 2     | 4     | 20                            | 100                        | 0                     | 20000       | 0.35  | 0     | 2   | 30          | 800  | 0.903           | 722       | 7.22                                | 2.50            | Foundation Failure |       |              |  |  |
| 30        | 30                      | 8     | 0         | 2     | 4     | 20                            | 100                        | 0                     | 20000       | 0.35  | 0     | 4   | 30          | 800  | 0.8033          | 643       | 6.43                                | 2.50            | Foundation Failure |       |              |  |  |
| 31        | 30                      | 2     | 0         | 2     | 8     | 20                            | 100                        | 0                     | 20000       | 0.35  | 0     | 1   | 30          | 800  | 0.758           | 606       | 6.06                                | 2.50            | Foundation Failure |       |              |  |  |
| 32        | 30                      | 4     | 0         | 2     | 8     | 20                            | 100                        | 0                     | 20000       | 0.35  | 0     | 2   | 30          | 800  | 0.749           | 599       | 5.99                                | 2.50            | Foundation Failure |       |              |  |  |
| 33        | 30                      | 8     | 0         | 2     | 8     | 20                            | 100                        | 0                     | 20000       | 0.35  | 0     | 4   | 30          | 800  | 0.7289          | 583       | 5.83                                | 2.50            | Foundation Failure |       |              |  |  |
| 34        | 30                      | 2     | 0         | 2     | 16    | 20                            | 100                        | 0                     | 20000       | 0.35  | 0     | 1   | 30          | 800  | 0.8053          | 644       | 6.44                                | 2.50            | Foundation Failure |       |              |  |  |
| 35        | 30                      | 4     | 0         | 2     | 16    | 20                            | 100                        | 0                     | 20000       | 0.35  | 0     | 2   | 30          | 800  | 0.7815          | 625       | 6.25                                | 2.50            | Foundation Failure |       |              |  |  |
| 36        | 30                      | 8     | 0         | 2     | 16    | 20                            | 100                        | 0                     | 20000       | 0.35  | 0     | 4   | 30          | 800  | 0.8204          | 656       | 6.56                                | 2.50            | Foundation Failure |       |              |  |  |
| 37        | 30                      | 2     | 0         | 2     | 2     | 20                            | 200                        | 0                     | 40000       | 0.35  | 0     | 1   | 30          | 1600 | 0.9236          | 1478      | 7.39                                | 5.00            | Foundation Failure |       |              |  |  |
| 38        | 30                      | 4     | 0         | 2     | 2     | 20                            | 200                        | 0                     | 40000       | 0.35  | 0     | 2   | 30          | 2000 | 0.824           | 1648      | 8.24                                | 5.00            | Foundation Failure |       |              |  |  |
| 39        | 30                      | 8     | 0         | 2     | 2     | 20                            | 200                        | 0                     | 40000       | 0.35  | 0     | 4   | 30          | 1600 | 0.9955          | 1593      | 7.96                                | 5.00            | Foundation Failure |       |              |  |  |
| 40        | 30                      | 2     | 0         | 2     | 4     | 20                            | 200                        | 0                     | 40000       | 0.35  | 0     | 1   | 30          | 1600 | 0.9061          | 1450      | 7.25                                | 5.00            | Foundation Failure |       |              |  |  |
| 41        | 30                      | 4     | 0         | 2     | 4     | 20                            | 200                        | 0                     | 40000       | 0.35  | 0     | 2   | 30          | 1600 | 0.912           | 1459      | 7.30                                | 5.00            | Foundation Failure |       |              |  |  |
| 42        | 30                      | 8     | 0         | 2     | 4     | 20                            | 200                        | 0                     | 40000       | 0.35  | 0     | 4   | 30          | 1600 | 0.8075          | 1292      | 6.46                                | 5.00            | Foundation Failure |       |              |  |  |
| 43        | 30                      | 2     | 0         | 2     | 8     | 20                            | 200                        | 0                     | 40000       | 0.35  | 0     | 1   | 30          | 1600 | 0.7642          | 1223      | 6.11                                | 5.00            | Foundation Failure |       |              |  |  |
| 44        | 30                      | 4     | 0         | 2     | 8     | 20                            | 200                        | 0                     | 40000       | 0.35  | 0     | 2   | 30          | 1600 | 0.7564          | 1210      | 6.05                                | 5.00            | Foundation Failure |       |              |  |  |
| 45        | 30                      | 8     | 0         | 2     | 8     | 20                            | 200                        | 0                     | 40000       | 0.35  | 0     | 4   | 30          | 1600 | 0.7359          | 1177      | 5.89                                | 5.00            | Foundation Failure |       |              |  |  |
| 46        | 30                      | 2     | 0         | 2     | 16    | 20                            | 200                        | 0                     | 40000       | 0.35  | 0     | 1   | 30          | 1600 | 0.8148          | 1304      | 6.52                                | 5.00            | Foundation Failure |       |              |  |  |
| 47        | 30                      | 4     | 0         | 2     | 16    | 20                            | 200                        | 0                     | 40000       | 0.35  | 0     | 2   | 30          | 1600 | 0.7919          | 1267      | 6.34                                | 5.00            | Foundation Failure |       |              |  |  |
| 48        | 30                      | 8     | 0         | 2     | 16    | 20                            | 200                        | 0                     | 40000       | 0.35  | 0     | 4   | 30          | 1600 | 0.8306          | 1329      | 6.64                                | 5.00            | Foundation Failure |       |              |  |  |

N.F.:Not found.  
 Base failure\_EQ:Failed due to earthquake.  
 Base failure\_GR:Failed due to gravity.

Table A.3. List of results of finite elements models created for static condition ( $\beta= 45^\circ$ ).

| Model No. | GEOTECHNICAL PROPERTIES |       |           |       |       |                               | SLOPE SOIL PROPERTIES      |              |             |         |       |                   | SEISMIC EFFECT | FILE NAME | ANALYSIS RESULTS FOR STATIC LOADING |        |        |             |       |                    | Failure Mode |
|-----------|-------------------------|-------|-----------|-------|-------|-------------------------------|----------------------------|--------------|-------------|---------|-------|-------------------|----------------|-----------|-------------------------------------|--------|--------|-------------|-------|--------------------|--------------|
|           | $\beta$ (°)             | H (m) | $\lambda$ | B (m) | L (m) | $\gamma$ (kN/m <sup>3</sup> ) | $c_u$ (kN/m <sup>2</sup> ) | $\phi_u$ (°) | $E_u$ (kPa) | $\nu_u$ | $k_h$ | H/B               |                |           | $\beta$ (°)                         | Load   | Mstage | $q_r$ (kPa) | $N_s$ | cu/yB              |              |
| 1         | 45                      | 2     | 0         | 2     | 2     | 20                            | 25                         | 0            | 5000        | 0.35    | 0     | C_45_2_0_2_25_S   | 1              | 45        | 200                                 | 0.8246 | 165    | 6.60        | 0.63  | Foundation Failure |              |
| 2         | 45                      | 4     | 0         | 2     | 2     | 20                            | 25                         | 0            | 5000        | 0.35    | 0     | C_45_4_0_2_25_S   | 2              | 45        | 200                                 | 0.8129 | 163    | 6.50        | 0.63  | Foundation Failure |              |
| 3         | 45                      | 8     | 0         | 2     | 2     | 20                            | 25                         | 0            | 5000        | 0.35    | 0     | C_45_8_0_2_25_S   | 4              | 45        | 200                                 | N.F.   | N.F.   | 0.63        | 0.63  | Base failure_ GR   |              |
| 4         | 45                      | 2     | 0         | 2     | 4     | 20                            | 25                         | 0            | 5000        | 0.35    | 0     | C_45_2_0_4_25_S   | 1              | 45        | 200                                 | 0.6871 | 131    | 5.26        | 0.63  | Foundation Failure |              |
| 5         | 45                      | 4     | 0         | 2     | 4     | 20                            | 25                         | 0            | 5000        | 0.35    | 0     | C_45_4_0_4_25_S   | 2              | 45        | 200                                 | 0.6409 | 128    | 5.13        | 0.63  | Foundation Failure |              |
| 6         | 45                      | 8     | 0         | 2     | 4     | 20                            | 25                         | 0            | 5000        | 0.35    | 0     | C_45_8_0_4_25_S   | 4              | 45        | 200                                 | N.F.   | N.F.   | 0.63        | 0.63  | Base failure_ GR   |              |
| 7         | 45                      | 2     | 0         | 2     | 8     | 20                            | 25                         | 0            | 5000        | 0.35    | 0     | C_45_2_0_8_25_S   | 1              | 45        | 200                                 | 0.616  | 123    | 4.93        | 0.63  | Foundation Failure |              |
| 8         | 45                      | 4     | 0         | 2     | 8     | 20                            | 25                         | 0            | 5000        | 0.35    | 0     | C_45_4_0_8_25_S   | 2              | 45        | 200                                 | 0.5952 | 119    | 4.76        | 0.63  | Foundation Failure |              |
| 9         | 45                      | 8     | 0         | 2     | 8     | 20                            | 25                         | 0            | 5000        | 0.35    | 0     | C_45_8_0_8_25_S   | 4              | 45        | 200                                 | N.F.   | N.F.   | 0.63        | 0.63  | Base failure_ GR   |              |
| 10        | 45                      | 2     | 0         | 2     | 16    | 20                            | 25                         | 0            | 5000        | 0.35    | 0     | C_45_2_0_16_25_S  | 1              | 45        | 200                                 | 0.6716 | 134    | 5.37        | 0.63  | Foundation Failure |              |
| 11        | 45                      | 4     | 0         | 2     | 16    | 20                            | 25                         | 0            | 5000        | 0.35    | 0     | C_45_4_0_16_25_S  | 2              | 45        | 200                                 | 0.561  | 112    | 4.49        | 0.63  | Foundation Failure |              |
| 12        | 45                      | 8     | 0         | 2     | 16    | 20                            | 25                         | 0            | 5000        | 0.35    | 0     | C_45_8_0_16_25_S  | 4              | 45        | 200                                 | N.F.   | N.F.   | 0.63        | 0.63  | Base failure_ GR   |              |
| 13        | 45                      | 2     | 0         | 2     | 2     | 20                            | 50                         | 0            | 10000       | 0.35    | 0     | C_45_2_0_2_50_S   | 1              | 45        | 400                                 | 0.8655 | 346    | 6.92        | 1.25  | Foundation Failure |              |
| 14        | 45                      | 4     | 0         | 2     | 2     | 20                            | 50                         | 0            | 10000       | 0.35    | 0     | C_45_4_0_2_50_S   | 2              | 45        | 400                                 | 0.8562 | 342    | 6.85        | 1.25  | Foundation Failure |              |
| 15        | 45                      | 8     | 0         | 2     | 2     | 20                            | 50                         | 0            | 10000       | 0.35    | 0     | C_45_8_0_2_50_S   | 4              | 45        | 400                                 | 0.8425 | 337    | 6.74        | 1.25  | Foundation Failure |              |
| 16        | 45                      | 2     | 0         | 2     | 4     | 20                            | 50                         | 0            | 10000       | 0.35    | 0     | C_45_2_0_4_50_S   | 1              | 45        | 400                                 | 0.7013 | 281    | 5.61        | 1.25  | Foundation Failure |              |
| 17        | 45                      | 4     | 0         | 2     | 4     | 20                            | 50                         | 0            | 10000       | 0.35    | 0     | C_45_4_0_4_50_S   | 2              | 45        | 400                                 | 0.6905 | 276    | 5.52        | 1.25  | Foundation Failure |              |
| 18        | 45                      | 8     | 0         | 2     | 4     | 20                            | 50                         | 0            | 10000       | 0.35    | 0     | C_45_8_0_4_50_S   | 4              | 45        | 400                                 | 0.8303 | 332    | 6.64        | 1.25  | Foundation Failure |              |
| 19        | 45                      | 2     | 0         | 2     | 8     | 20                            | 50                         | 0            | 10000       | 0.35    | 0     | C_45_2_0_8_50_S   | 1              | 45        | 400                                 | 0.6529 | 261    | 5.22        | 1.25  | Foundation Failure |              |
| 20        | 45                      | 4     | 0         | 2     | 8     | 20                            | 50                         | 0            | 10000       | 0.35    | 0     | C_45_4_0_8_50_S   | 2              | 45        | 400                                 | 0.6333 | 253    | 5.07        | 1.25  | Foundation Failure |              |
| 21        | 45                      | 8     | 0         | 2     | 8     | 20                            | 50                         | 0            | 10000       | 0.35    | 0     | C_45_8_0_8_50_S   | 4              | 45        | 400                                 | 0.7009 | 280    | 5.61        | 1.25  | Foundation Failure |              |
| 22        | 45                      | 2     | 0         | 2     | 16    | 20                            | 50                         | 0            | 10000       | 0.35    | 0     | C_45_2_0_16_50_S  | 1              | 45        | 400                                 | 0.7254 | 290    | 5.80        | 1.25  | Foundation Failure |              |
| 23        | 45                      | 4     | 0         | 2     | 16    | 20                            | 50                         | 0            | 10000       | 0.35    | 0     | C_45_4_0_16_50_S  | 2              | 45        | 400                                 | 0.6533 | 261    | 5.23        | 1.25  | Foundation Failure |              |
| 24        | 45                      | 8     | 0         | 2     | 16    | 20                            | 50                         | 0            | 10000       | 0.35    | 0     | C_45_8_0_16_50_S  | 4              | 45        | 400                                 | 0.6899 | 276    | 5.52        | 1.25  | Foundation Failure |              |
| 25        | 45                      | 2     | 0         | 2     | 2     | 20                            | 100                        | 0            | 20000       | 0.35    | 0     | C_45_2_0_2_100_S  | 1              | 45        | 800                                 | 0.8836 | 707    | 7.07        | 2.50  | Foundation Failure |              |
| 26        | 45                      | 4     | 0         | 2     | 2     | 20                            | 100                        | 0            | 20000       | 0.35    | 0     | C_45_4_0_2_100_S  | 2              | 45        | 800                                 | 0.8729 | 698    | 6.98        | 2.50  | Foundation Failure |              |
| 27        | 45                      | 8     | 0         | 2     | 2     | 20                            | 100                        | 0            | 20000       | 0.35    | 0     | C_45_8_0_2_100_S  | 4              | 45        | 800                                 | 0.8616 | 689    | 6.89        | 2.50  | Foundation Failure |              |
| 28        | 45                      | 2     | 0         | 2     | 4     | 20                            | 100                        | 0            | 20000       | 0.35    | 0     | C_45_2_0_4_100_S  | 1              | 45        | 800                                 | 0.7236 | 579    | 5.79        | 2.50  | Foundation Failure |              |
| 29        | 45                      | 4     | 0         | 2     | 4     | 20                            | 100                        | 0            | 20000       | 0.35    | 0     | C_45_4_0_4_100_S  | 2              | 45        | 800                                 | 0.7113 | 569    | 5.69        | 2.50  | Foundation Failure |              |
| 30        | 45                      | 8     | 0         | 2     | 4     | 20                            | 100                        | 0            | 20000       | 0.35    | 0     | C_45_8_0_4_100_S  | 4              | 45        | 800                                 | 0.8498 | 680    | 6.80        | 2.50  | Foundation Failure |              |
| 31        | 45                      | 2     | 0         | 2     | 8     | 20                            | 100                        | 0            | 20000       | 0.35    | 0     | C_45_2_0_8_100_S  | 1              | 45        | 800                                 | 0.6726 | 538    | 5.38        | 2.50  | Foundation Failure |              |
| 32        | 45                      | 4     | 0         | 2     | 8     | 20                            | 100                        | 0            | 20000       | 0.35    | 0     | C_45_4_0_8_100_S  | 2              | 45        | 800                                 | 0.6487 | 519    | 5.19        | 2.50  | Foundation Failure |              |
| 33        | 45                      | 8     | 0         | 2     | 8     | 20                            | 100                        | 0            | 20000       | 0.35    | 0     | C_45_8_0_8_100_S  | 4              | 45        | 800                                 | 0.7212 | 577    | 5.77        | 2.50  | Foundation Failure |              |
| 34        | 45                      | 2     | 0         | 2     | 16    | 20                            | 100                        | 0            | 20000       | 0.35    | 0     | C_45_2_0_16_100_S | 1              | 45        | 800                                 | 0.7419 | 594    | 5.94        | 2.50  | Foundation Failure |              |
| 35        | 45                      | 4     | 0         | 2     | 16    | 20                            | 100                        | 0            | 20000       | 0.35    | 0     | C_45_4_0_16_100_S | 2              | 45        | 800                                 | 0.692  | 554    | 5.54        | 2.50  | Foundation Failure |              |
| 36        | 45                      | 8     | 0         | 2     | 16    | 20                            | 100                        | 0            | 20000       | 0.35    | 0     | C_45_8_0_16_100_S | 4              | 45        | 800                                 | 0.7267 | 581    | 5.81        | 2.50  | Foundation Failure |              |
| 37        | 45                      | 2     | 0         | 2     | 2     | 20                            | 200                        | 0            | 40000       | 0.35    | 0     | C_45_2_0_2_200_S  | 1              | 45        | 1600                                | 0.892  | 1427   | 7.14        | 5.00  | Foundation Failure |              |
| 38        | 45                      | 4     | 0         | 2     | 2     | 20                            | 200                        | 0            | 40000       | 0.35    | 0     | C_45_4_0_2_200_S  | 2              | 45        | 1600                                | 0.8874 | 1420   | 7.10        | 5.00  | Foundation Failure |              |
| 39        | 45                      | 8     | 0         | 2     | 2     | 20                            | 200                        | 0            | 40000       | 0.35    | 0     | C_45_8_0_2_200_S  | 4              | 45        | 1600                                | 0.8705 | 1393   | 6.96        | 5.00  | Foundation Failure |              |
| 40        | 45                      | 2     | 0         | 2     | 4     | 20                            | 200                        | 0            | 40000       | 0.35    | 0     | C_45_2_0_4_200_S  | 1              | 45        | 1600                                | 0.7341 | 1175   | 5.87        | 5.00  | Foundation Failure |              |
| 41        | 45                      | 4     | 0         | 2     | 4     | 20                            | 200                        | 0            | 40000       | 0.35    | 0     | C_45_4_0_4_200_S  | 2              | 45        | 1600                                | 0.7208 | 1153   | 5.77        | 5.00  | Foundation Failure |              |
| 42        | 45                      | 8     | 0         | 2     | 4     | 20                            | 200                        | 0            | 40000       | 0.35    | 0     | C_45_8_0_4_200_S  | 4              | 45        | 1600                                | 0.8505 | 1361   | 6.80        | 5.00  | Foundation Failure |              |
| 43        | 45                      | 2     | 0         | 2     | 8     | 20                            | 200                        | 0            | 40000       | 0.35    | 0     | C_45_2_0_8_200_S  | 1              | 45        | 1600                                | 0.6814 | 1090   | 5.45        | 5.00  | Foundation Failure |              |
| 44        | 45                      | 4     | 0         | 2     | 8     | 20                            | 200                        | 0            | 40000       | 0.35    | 0     | C_45_4_0_8_200_S  | 2              | 45        | 1600                                | 0.6632 | 1061   | 5.31        | 5.00  | Foundation Failure |              |
| 45        | 45                      | 8     | 0         | 2     | 8     | 20                            | 200                        | 0            | 40000       | 0.35    | 0     | C_45_8_0_8_200_S  | 4              | 45        | 1600                                | 0.849  | 1358   | 6.79        | 5.00  | Foundation Failure |              |
| 46        | 45                      | 2     | 0         | 2     | 16    | 20                            | 200                        | 0            | 40000       | 0.35    | 0     | C_45_2_0_16_200_S | 1              | 45        | 1600                                | 0.7616 | 1219   | 6.09        | 5.00  | Foundation Failure |              |
| 47        | 45                      | 4     | 0         | 2     | 16    | 20                            | 200                        | 0            | 40000       | 0.35    | 0     | C_45_4_0_16_200_S | 2              | 45        | 1600                                | 0.7091 | 1135   | 5.67        | 5.00  | Foundation Failure |              |
| 48        | 45                      | 8     | 0         | 2     | 16    | 20                            | 200                        | 0            | 40000       | 0.35    | 0     | C_45_8_0_16_200_S | 4              | 45        | 1600                                | 0.7377 | 1180   | 5.90        | 5.00  | Foundation Failure |              |

N.F.:Not found.  
 Base failure\_EQ:Failed due to earthquake.  
 Base failure\_GR:Failed due to gravity.

**APPENDIX B: LIST OF RESULTS OF FINITE ELEMENTS MODELS  
CREATED FOR SEISMIC CONDITION**

List of results for finite element models created for seismic condition is given in Table B.1, Table B.2 and Table B.3.

Table B.1. List of results of finite elements models created for seismic condition ( $\beta=15^\circ$ ).

| Model No. | GEOTECHNICAL PROPERTIES |       |           |       |       | SLOPE SOIL PROPERTIES         |                            |              |             |       | SEISMIC EFFECT |                       |     | ANALYSIS RESULTS FOR SEISMIC LOADING |      |        |             |       |       |                    |
|-----------|-------------------------|-------|-----------|-------|-------|-------------------------------|----------------------------|--------------|-------------|-------|----------------|-----------------------|-----|--------------------------------------|------|--------|-------------|-------|-------|--------------------|
|           | $\beta$ (°)             | H (m) | $\lambda$ | B (m) | L (m) | $\gamma$ (kN/m <sup>3</sup> ) | $c_u$ (kN/m <sup>2</sup> ) | $\phi_u$ (°) | $E_u$ (kPa) | $v_u$ | $k_b$          | FILE NAME             | H/B | $\beta$ (°)                          | Load | Mstage | $q_f$ (kPa) | $N_s$ | cu/yB | Failure Mode       |
| 1         | 0                       | 2     | 0         | 2     | 2     | 20                            | 100                        | 0            | 20000       | 0.35  | 0.1            | C_0_2_0_2_100_0.1_D   | 1   | 0                                    | 2000 | 0.4261 | 852.2       | 8.522 | 2.5   | Foundation Failure |
| 2         | 0                       | 2     | 0         | 2     | 4     | 20                            | 100                        | 0            | 20000       | 0.35  | 0.1            | C_0_2_0_4_100_0.1_D   | 1   | 0                                    | 2000 | 0.3841 | 768.2       | 7.682 | 2.5   | Foundation Failure |
| 3         | 0                       | 2     | 0         | 2     | 8     | 20                            | 100                        | 0            | 20000       | 0.35  | 0.1            | C_0_2_0_8_100_0.1_D   | 1   | 0                                    | 2000 | 0.3688 | 737.6       | 7.376 | 2.5   | Foundation Failure |
| 4         | 0                       | 2     | 0         | 2     | 16    | 20                            | 100                        | 0            | 20000       | 0.35  | 0.1            | C_0_2_0_16_100_0.1_D  | 1   | 0                                    | 2000 | 0.3574 | 714.8       | 7.148 | 2.5   | Foundation Failure |
| 5         | 15                      | 2     | 0         | 2     | 2     | 20                            | 25                         | 0            | 5000        | 0.35  | 0.1            | C_15_2_0_2_25_0.1_D   | 1   | 15                                   | 200  | 0.9611 | 192.22      | 7.69  | 0.63  | Base failure_EQ    |
| 6         | 15                      | 4     | 0         | 2     | 2     | 20                            | 25                         | 0            | 5000        | 0.35  | 0.1            | C_15_4_0_2_25_0.1_D   | 2   | 15                                   | 200  | 0.4968 | 99.36       | 3.97  | 0.63  | Base failure_EQ    |
| 7         | 15                      | 8     | 0         | 2     | 2     | 20                            | 25                         | 0            | 5000        | 0.35  | 0.1            | C_15_8_0_2_25_0.1_D   | 4   | 15                                   | 200  | N.F.   | N.F.        | N.F.  | 0.63  | Base failure_GR    |
| 8         | 15                      | 2     | 0         | 2     | 4     | 20                            | 25                         | 0            | 5000        | 0.35  | 0.1            | C_15_2_0_4_25_0.1_D   | 1   | 15                                   | 200  | 0.9605 | 192.1       | 7.68  | 0.63  | Base failure_EQ    |
| 9         | 15                      | 4     | 0         | 2     | 4     | 20                            | 25                         | 0            | 5000        | 0.35  | 0.1            | C_15_4_0_4_25_0.1_D   | 2   | 15                                   | 200  | 0.4976 | 99.52       | 3.98  | 0.63  | Base failure_EQ    |
| 10        | 15                      | 8     | 0         | 2     | 4     | 20                            | 25                         | 0            | 5000        | 0.35  | 0.1            | C_15_8_0_4_25_0.1_D   | 4   | 15                                   | 200  | N.F.   | N.F.        | N.F.  | 0.63  | Base failure_GR    |
| 11        | 15                      | 2     | 0         | 2     | 8     | 20                            | 25                         | 0            | 5000        | 0.35  | 0.1            | C_15_2_0_8_25_0.1_D   | 1   | 15                                   | 200  | 0.932  | 138.64      | 5.55  | 0.63  | Foundation Failure |
| 12        | 15                      | 4     | 0         | 2     | 8     | 20                            | 25                         | 0            | 5000        | 0.35  | 0.1            | C_15_4_0_8_25_0.1_D   | 2   | 15                                   | 200  | 0.5037 | 100.74      | 4.03  | 0.63  | Base failure_EQ    |
| 13        | 15                      | 8     | 0         | 2     | 8     | 20                            | 25                         | 0            | 5000        | 0.35  | 0.1            | C_15_8_0_8_25_0.1_D   | 4   | 15                                   | 200  | N.F.   | N.F.        | N.F.  | 0.63  | Base failure_GR    |
| 14        | 15                      | 2     | 0         | 2     | 16    | 20                            | 25                         | 0            | 5000        | 0.35  | 0.1            | C_15_2_0_16_25_0.1_D  | 1   | 15                                   | 200  | 0.882  | 176.4       | 7.06  | 0.63  | Foundation Failure |
| 15        | 15                      | 4     | 0         | 2     | 16    | 20                            | 25                         | 0            | 5000        | 0.35  | 0.1            | C_15_4_0_16_25_0.1_D  | 2   | 15                                   | 200  | 0.5033 | 100.66      | 4.03  | 0.63  | Base failure_EQ    |
| 16        | 15                      | 8     | 0         | 2     | 16    | 20                            | 25                         | 0            | 5000        | 0.35  | 0.1            | C_15_8_0_16_25_0.1_D  | 4   | 15                                   | 200  | N.F.   | N.F.        | N.F.  | 0.63  | Base failure_GR    |
| 17        | 15                      | 2     | 0         | 2     | 2     | 20                            | 50                         | 0            | 10000       | 0.35  | 0.1            | C_15_2_0_2_50_0.1_D   | 1   | 15                                   | 600  | 0.7125 | 427.5       | 8.55  | 1.25  | Foundation Failure |
| 18        | 15                      | 4     | 0         | 2     | 2     | 20                            | 50                         | 0            | 10000       | 0.35  | 0.1            | C_15_4_0_2_50_0.1_D   | 2   | 15                                   | 600  | 0.5668 | 340.08      | 6.80  | 1.25  | Foundation Failure |
| 19        | 15                      | 8     | 0         | 2     | 2     | 20                            | 50                         | 0            | 10000       | 0.35  | 0.1            | C_15_8_0_2_50_0.1_D   | 4   | 15                                   | 600  | 0.8596 | 343.84      | 6.88  | 1.25  | Base failure_EQ    |
| 20        | 15                      | 2     | 0         | 2     | 4     | 20                            | 50                         | 0            | 10000       | 0.35  | 0.1            | C_15_2_0_4_50_0.1_D   | 1   | 15                                   | 600  | 0.6772 | 406.32      | 8.13  | 1.25  | Foundation Failure |
| 21        | 15                      | 4     | 0         | 2     | 4     | 20                            | 50                         | 0            | 10000       | 0.35  | 0.1            | C_15_4_0_4_50_0.1_D   | 2   | 15                                   | 600  | 0.8605 | 516.3       | 10.33 | 1.25  | Foundation Failure |
| 22        | 15                      | 8     | 0         | 2     | 4     | 20                            | 50                         | 0            | 10000       | 0.35  | 0.1            | C_15_8_0_4_50_0.1_D   | 4   | 15                                   | 600  | 0.8327 | 343.72      | 6.87  | 1.25  | Base failure_EQ    |
| 23        | 15                      | 2     | 0         | 2     | 8     | 20                            | 50                         | 0            | 10000       | 0.35  | 0.1            | C_15_2_0_8_50_0.1_D   | 1   | 15                                   | 400  | 0.8327 | 333.08      | 6.66  | 1.25  | Foundation Failure |
| 24        | 15                      | 4     | 0         | 2     | 8     | 20                            | 50                         | 0            | 10000       | 0.35  | 0.1            | C_15_4_0_8_50_0.1_D   | 2   | 15                                   | 400  | 0.5121 | 204.84      | 4.10  | 1.25  | Foundation Failure |
| 25        | 15                      | 8     | 0         | 2     | 8     | 20                            | 50                         | 0            | 10000       | 0.35  | 0.1            | C_15_8_0_8_50_0.1_D   | 4   | 15                                   | 400  | 0.8597 | 343.88      | 6.88  | 1.25  | Foundation Failure |
| 26        | 15                      | 2     | 0         | 2     | 16    | 20                            | 50                         | 0            | 10000       | 0.35  | 0.1            | C_15_2_0_16_50_0.1_D  | 1   | 15                                   | 400  | 0.918  | 367.2       | 7.34  | 1.25  | Foundation Failure |
| 27        | 15                      | 4     | 0         | 2     | 16    | 20                            | 50                         | 0            | 10000       | 0.35  | 0.1            | C_15_4_0_16_50_0.1_D  | 2   | 15                                   | 400  | 0.8934 | 357.36      | 7.15  | 1.25  | Foundation Failure |
| 28        | 15                      | 8     | 0         | 2     | 16    | 20                            | 50                         | 0            | 10000       | 0.35  | 0.1            | C_15_8_0_16_50_0.1_D  | 4   | 15                                   | 400  | 0.7424 | 296.96      | 5.94  | 1.25  | Foundation Failure |
| 29        | 15                      | 2     | 0         | 2     | 2     | 20                            | 100                        | 0            | 20000       | 0.35  | 0.1            | C_15_2_0_2_100_0.1_D  | 1   | 15                                   | 1000 | 0.8471 | 847.1       | 8.47  | 2.50  | Foundation Failure |
| 30        | 15                      | 4     | 0         | 2     | 2     | 20                            | 100                        | 0            | 20000       | 0.35  | 0.1            | C_15_4_0_2_100_0.1_D  | 2   | 15                                   | 1000 | 0.9839 | 983.9       | 9.84  | 2.50  | Foundation Failure |
| 31        | 15                      | 8     | 0         | 2     | 2     | 20                            | 100                        | 0            | 20000       | 0.35  | 0.1            | C_15_8_0_2_100_0.1_D  | 4   | 15                                   | 1000 | 0.6177 | 617.7       | 6.18  | 2.50  | Foundation Failure |
| 32        | 15                      | 2     | 0         | 2     | 4     | 20                            | 100                        | 0            | 20000       | 0.35  | 0.1            | C_15_2_0_4_100_0.1_D  | 1   | 15                                   | 1000 | 0.6876 | 687.6       | 6.88  | 2.50  | Foundation Failure |
| 33        | 15                      | 4     | 0         | 2     | 4     | 20                            | 100                        | 0            | 20000       | 0.35  | 0.1            | C_15_4_0_4_100_0.1_D  | 2   | 15                                   | 1000 | 0.8733 | 873.3       | 8.73  | 2.50  | Foundation Failure |
| 34        | 15                      | 8     | 0         | 2     | 4     | 20                            | 100                        | 0            | 20000       | 0.35  | 0.1            | C_15_8_0_4_100_0.1_D  | 4   | 15                                   | 1000 | 0.597  | 597         | 5.97  | 2.50  | Foundation Failure |
| 35        | 15                      | 2     | 0         | 2     | 8     | 20                            | 100                        | 0            | 20000       | 0.35  | 0.1            | C_15_2_0_8_100_0.1_D  | 1   | 15                                   | 800  | 0.6561 | 656.1       | 6.56  | 2.50  | Foundation Failure |
| 36        | 15                      | 4     | 0         | 2     | 8     | 20                            | 100                        | 0            | 20000       | 0.35  | 0.1            | C_15_4_0_8_100_0.1_D  | 2   | 15                                   | 800  | 0.6818 | 681.8       | 6.82  | 2.50  | Foundation Failure |
| 37        | 15                      | 8     | 0         | 2     | 8     | 20                            | 100                        | 0            | 20000       | 0.35  | 0.1            | C_15_8_0_8_100_0.1_D  | 4   | 15                                   | 800  | 0.595  | 595         | 5.95  | 2.50  | Foundation Failure |
| 38        | 15                      | 2     | 0         | 2     | 16    | 20                            | 100                        | 0            | 20000       | 0.35  | 0.1            | C_15_2_0_16_100_0.1_D | 1   | 15                                   | 800  | 0.9347 | 934.7       | 9.35  | 2.50  | Foundation Failure |
| 39        | 15                      | 4     | 0         | 2     | 16    | 20                            | 100                        | 0            | 20000       | 0.35  | 0.1            | C_15_4_0_16_100_0.1_D | 2   | 15                                   | 800  | 0.9006 | 900.6       | 9.01  | 2.50  | Foundation Failure |
| 40        | 15                      | 8     | 0         | 2     | 16    | 20                            | 100                        | 0            | 20000       | 0.35  | 0.1            | C_15_8_0_16_100_0.1_D | 4   | 15                                   | 800  | 0.8588 | 858.8       | 8.59  | 2.50  | Foundation Failure |
| 41        | 15                      | 2     | 0         | 2     | 2     | 20                            | 200                        | 0            | 40000       | 0.35  | 0.1            | C_15_2_0_2_200_0.1_D  | 1   | 15                                   | 2000 | 0.8083 | 808.3       | 8.08  | 5.00  | Foundation Failure |
| 42        | 15                      | 4     | 0         | 2     | 2     | 20                            | 200                        | 0            | 40000       | 0.35  | 0.1            | C_15_4_0_2_200_0.1_D  | 2   | 15                                   | 2000 | 0.8906 | 890.6       | 8.91  | 5.00  | Foundation Failure |
| 43        | 15                      | 8     | 0         | 2     | 2     | 20                            | 200                        | 0            | 40000       | 0.35  | 0.1            | C_15_8_0_2_200_0.1_D  | 4   | 15                                   | 2000 | 0.9006 | 900.6       | 9.01  | 5.00  | Foundation Failure |
| 44        | 15                      | 2     | 0         | 2     | 4     | 20                            | 200                        | 0            | 40000       | 0.35  | 0.1            | C_15_2_0_4_200_0.1_D  | 1   | 15                                   | 2000 | 0.6743 | 674.3       | 6.74  | 5.00  | Foundation Failure |
| 45        | 15                      | 4     | 0         | 2     | 4     | 20                            | 200                        | 0            | 40000       | 0.35  | 0.1            | C_15_4_0_4_200_0.1_D  | 2   | 15                                   | 2000 | 0.877  | 877         | 8.77  | 5.00  | Foundation Failure |
| 46        | 15                      | 8     | 0         | 2     | 4     | 20                            | 200                        | 0            | 40000       | 0.35  | 0.1            | C_15_8_0_4_200_0.1_D  | 4   | 15                                   | 2000 | 0.6837 | 683.7       | 6.84  | 5.00  | Foundation Failure |
| 47        | 15                      | 2     | 0         | 2     | 8     | 20                            | 200                        | 0            | 40000       | 0.35  | 0.1            | C_15_2_0_8_200_0.1_D  | 1   | 15                                   | 1600 | 0.6532 | 653.2       | 6.53  | 5.00  | Foundation Failure |
| 48        | 15                      | 4     | 0         | 2     | 8     | 20                            | 200                        | 0            | 40000       | 0.35  | 0.1            | C_15_4_0_8_200_0.1_D  | 2   | 15                                   | 1600 | 0.6755 | 675.5       | 6.76  | 5.00  | Foundation Failure |
| 49        | 15                      | 8     | 0         | 2     | 8     | 20                            | 200                        | 0            | 40000       | 0.35  | 0.1            | C_15_8_0_8_200_0.1_D  | 4   | 15                                   | 1600 | 0.5904 | 590.4       | 5.90  | 5.00  | Foundation Failure |
| 50        | 15                      | 2     | 0         | 2     | 16    | 20                            | 200                        | 0            | 40000       | 0.35  | 0.1            | C_15_2_0_16_200_0.1_D | 1   | 15                                   | 1600 | 0.9559 | 955.9       | 9.56  | 5.00  | Foundation Failure |
| 51        | 15                      | 4     | 0         | 2     | 16    | 20                            | 200                        | 0            | 40000       | 0.35  | 0.1            | C_15_4_0_16_200_0.1_D | 2   | 15                                   | 1600 | 0.91   | 91          | 9.1   | 5.00  | Foundation Failure |
| 52        | 15                      | 8     | 0         | 2     | 16    | 20                            | 200                        | 0            | 40000       | 0.35  | 0.1            | C_15_8_0_16_200_0.1_D | 4   | 15                                   | 1600 | 0.8722 | 872.2       | 8.73  | 5.00  | Foundation Failure |

N.F.: Not found.  
 Base failure\_EQ: Failed due to earthquake.  
 Base failure\_GR: Failed due to gravity.

Table B.1. List of results of finite elements models created for seismic condition ( $\beta= 15^\circ$ )  
(Cont.).

| Model No. | GEOTECHNICAL PROPERTIES |       |           |       |       |                               | SLOPE SOIL PROPERTIES      |              |             |       |       |       | SEISMIC EFFECT |             | ANALYSIS RESULTS FOR SEISMIC LOADING |        |             |          |      |                    |
|-----------|-------------------------|-------|-----------|-------|-------|-------------------------------|----------------------------|--------------|-------------|-------|-------|-------|----------------|-------------|--------------------------------------|--------|-------------|----------|------|--------------------|
|           | $\beta$ (°)             | H (m) | $\lambda$ | B (m) | L (m) | $\gamma$ (kN/m <sup>3</sup> ) | $c_u$ (kN/m <sup>2</sup> ) | $\phi_u$ (°) | $E_u$ (kPa) | $v_u$ | $F_b$ | $F_h$ | H/B            | $\beta$ (°) | Load                                 | Mstage | $q_t$ (kPa) | $N_{cs}$ | cu/B | Failure Mode       |
| 53        | 0                       | 2     | 0         | 2     | 2     | 20                            | 100                        | 0            | 20000       | 0.35  | 0.2   | 0.2   | 1              | 0           | 2000                                 | 0.256  | 512         | 5.12     | 2.5  | Foundation Failure |
| 54        | 0                       | 2     | 0         | 2     | 4     | 20                            | 100                        | 0            | 20000       | 0.35  | 0.2   | 0.2   | 1              | 0           | 2000                                 | 0.256  | 480         | 4.8      | 2.5  | Foundation Failure |
| 55        | 0                       | 2     | 0         | 2     | 8     | 20                            | 100                        | 0            | 20000       | 0.35  | 0.2   | 0.2   | 1              | 0           | 2000                                 | 0.2345 | 469         | 4.69     | 2.5  | Foundation Failure |
| 56        | 0                       | 2     | 0         | 2     | 16    | 20                            | 100                        | 0            | 20000       | 0.35  | 0.2   | 0.2   | 1              | 0           | 2000                                 | 0.2497 | 499.4       | 4.994    | 2.5  | Foundation Failure |
| 57        | 15                      | 2     | 0         | 2     | 2     | 20                            | 25                         | 0            | 5000        | 0.35  | 0.2   | 0.2   | 1              | 15          | 200                                  | 0.4781 | 95.62       | 3.82     | 0.63 | Base failure_EQ    |
| 58        | 15                      | 4     | 0         | 2     | 2     | 20                            | 25                         | 0            | 5000        | 0.35  | 0.2   | 0.2   | 2              | 15          | 200                                  | 0.2488 | 49.76       | 1.99     | 0.63 | Base failure_EQ    |
| 59        | 15                      | 8     | 0         | 2     | 2     | 20                            | 25                         | 0            | 5000        | 0.35  | 0.2   | 0.2   | 4              | 15          | 200                                  | N.F.   | N.F.        | N.F.     | 0.63 | Base failure_GR    |
| 60        | 15                      | 4     | 0         | 2     | 4     | 20                            | 25                         | 0            | 5000        | 0.35  | 0.2   | 0.2   | 1              | 15          | 200                                  | 0.4781 | 95.62       | 3.82     | 0.63 | Base failure_EQ    |
| 61        | 15                      | 4     | 0         | 2     | 4     | 20                            | 25                         | 0            | 5000        | 0.35  | 0.2   | 0.2   | 2              | 15          | 200                                  | 0.2489 | 49.78       | 1.99     | 0.63 | Base failure_EQ    |
| 62        | 15                      | 8     | 0         | 2     | 4     | 20                            | 25                         | 0            | 5000        | 0.35  | 0.2   | 0.2   | 4              | 15          | 200                                  | N.F.   | N.F.        | N.F.     | 0.63 | Base failure_GR    |
| 63        | 15                      | 2     | 0         | 2     | 8     | 20                            | 25                         | 0            | 5000        | 0.35  | 0.2   | 0.2   | 1              | 15          | 200                                  | 0.482  | 96.4        | 3.86     | 0.63 | Base failure_EQ    |
| 64        | 15                      | 4     | 0         | 2     | 8     | 20                            | 25                         | 0            | 5000        | 0.35  | 0.2   | 0.2   | 2              | 15          | 200                                  | 0.2524 | 50.48       | 2.02     | 0.63 | Base failure_EQ    |
| 65        | 15                      | 8     | 0         | 2     | 8     | 20                            | 25                         | 0            | 5000        | 0.35  | 0.2   | 0.2   | 4              | 15          | 200                                  | N.F.   | N.F.        | N.F.     | 0.63 | Base failure_GR    |
| 66        | 15                      | 2     | 0         | 2     | 16    | 20                            | 25                         | 0            | 5000        | 0.35  | 0.2   | 0.2   | 1              | 15          | 200                                  | 0.4825 | 96.5        | 3.86     | 0.63 | Base failure_EQ    |
| 67        | 15                      | 4     | 0         | 2     | 16    | 20                            | 25                         | 0            | 5000        | 0.35  | 0.2   | 0.2   | 2              | 15          | 200                                  | 0.2517 | 50.34       | 2.01     | 0.63 | Base failure_EQ    |
| 68        | 15                      | 8     | 0         | 2     | 16    | 20                            | 25                         | 0            | 5000        | 0.35  | 0.2   | 0.2   | 4              | 15          | 200                                  | N.F.   | N.F.        | N.F.     | 0.63 | Base failure_GR    |
| 69        | 15                      | 2     | 0         | 2     | 4     | 20                            | 50                         | 0            | 10000       | 0.35  | 0.2   | 0.2   | 1              | 15          | 600                                  | 0.3996 | 239.76      | 4.80     | 1.25 | Foundation Failure |
| 70        | 15                      | 4     | 0         | 2     | 8     | 20                            | 50                         | 0            | 10000       | 0.35  | 0.2   | 0.2   | 2              | 15          | 400                                  | 0.604  | 241.6       | 4.83     | 1.25 | Base failure_EQ    |
| 71        | 15                      | 8     | 0         | 2     | 8     | 20                            | 50                         | 0            | 10000       | 0.35  | 0.2   | 0.2   | 4              | 15          | 400                                  | 0.4316 | 172.64      | 3.45     | 1.25 | Base failure_EQ    |
| 72        | 15                      | 2     | 0         | 2     | 4     | 20                            | 50                         | 0            | 10000       | 0.35  | 0.2   | 0.2   | 1              | 15          | 600                                  | 0.3888 | 233.28      | 4.67     | 1.25 | Foundation Failure |
| 73        | 15                      | 4     | 0         | 2     | 4     | 20                            | 50                         | 0            | 10000       | 0.35  | 0.2   | 0.2   | 2              | 15          | 400                                  | 0.6198 | 247.92      | 4.96     | 1.25 | Foundation Failure |
| 74        | 15                      | 8     | 0         | 2     | 4     | 20                            | 50                         | 0            | 10000       | 0.35  | 0.2   | 0.2   | 4              | 15          | 400                                  | 0.4316 | 172.64      | 3.45     | 1.25 | Base failure_EQ    |
| 75        | 15                      | 2     | 0         | 2     | 8     | 20                            | 50                         | 0            | 10000       | 0.35  | 0.2   | 0.2   | 1              | 15          | 400                                  | 0.582  | 232.8       | 4.66     | 1.25 | Foundation Failure |
| 76        | 15                      | 4     | 0         | 2     | 8     | 20                            | 50                         | 0            | 10000       | 0.35  | 0.2   | 0.2   | 2              | 15          | 400                                  | 0.586  | 234.4       | 4.69     | 1.25 | Foundation Failure |
| 77        | 15                      | 8     | 0         | 2     | 8     | 20                            | 50                         | 0            | 10000       | 0.35  | 0.2   | 0.2   | 4              | 15          | 400                                  | 0.4306 | 172.24      | 3.44     | 1.25 | Base failure_EQ    |
| 78        | 15                      | 2     | 0         | 2     | 16    | 20                            | 50                         | 0            | 10000       | 0.35  | 0.2   | 0.2   | 1              | 15          | 400                                  | 0.6184 | 247.36      | 4.95     | 1.25 | Foundation Failure |
| 79        | 15                      | 4     | 0         | 2     | 16    | 20                            | 50                         | 0            | 10000       | 0.35  | 0.2   | 0.2   | 2              | 15          | 400                                  | 0.6175 | 247         | 4.94     | 1.25 | Foundation Failure |
| 80        | 15                      | 8     | 0         | 2     | 16    | 20                            | 50                         | 0            | 10000       | 0.35  | 0.2   | 0.2   | 4              | 15          | 400                                  | 0.4336 | 173.44      | 3.47     | 1.25 | Base failure_EQ    |
| 81        | 15                      | 2     | 0         | 2     | 2     | 20                            | 100                        | 0            | 20000       | 0.35  | 0.2   | 0.2   | 1              | 15          | 1000                                 | 0.4912 | 491.2       | 4.91     | 2.50 | Foundation Failure |
| 82        | 15                      | 4     | 0         | 2     | 2     | 20                            | 100                        | 0            | 20000       | 0.35  | 0.2   | 0.2   | 2              | 15          | 1000                                 | 0.5    | 500         | 5.00     | 2.50 | Foundation Failure |
| 83        | 15                      | 8     | 0         | 2     | 2     | 20                            | 100                        | 0            | 20000       | 0.35  | 0.2   | 0.2   | 4              | 15          | 1200                                 | 0.4155 | 498.6       | 4.99     | 2.50 | Foundation Failure |
| 84        | 15                      | 2     | 0         | 2     | 4     | 20                            | 100                        | 0            | 20000       | 0.35  | 0.2   | 0.2   | 1              | 15          | 800                                  | 0.5903 | 472.24      | 4.72     | 2.50 | Base failure_EQ    |
| 85        | 15                      | 4     | 0         | 2     | 4     | 20                            | 100                        | 0            | 20000       | 0.35  | 0.2   | 0.2   | 2              | 15          | 800                                  | 0.6198 | 495.84      | 4.96     | 2.50 | Foundation Failure |
| 86        | 15                      | 8     | 0         | 2     | 4     | 20                            | 100                        | 0            | 20000       | 0.35  | 0.2   | 0.2   | 4              | 15          | 800                                  | 0.6177 | 494.16      | 4.94     | 2.50 | Foundation Failure |
| 87        | 15                      | 2     | 0         | 2     | 8     | 20                            | 100                        | 0            | 20000       | 0.35  | 0.2   | 0.2   | 1              | 15          | 800                                  | 0.5383 | 430.64      | 4.31     | 2.50 | Foundation Failure |
| 88        | 15                      | 4     | 0         | 2     | 8     | 20                            | 100                        | 0            | 20000       | 0.35  | 0.2   | 0.2   | 2              | 15          | 800                                  | 0.5886 | 470.88      | 4.71     | 2.50 | Foundation Failure |
| 89        | 15                      | 8     | 0         | 2     | 8     | 20                            | 100                        | 0            | 20000       | 0.35  | 0.2   | 0.2   | 4              | 15          | 800                                  | 0.6116 | 489.28      | 4.89     | 2.50 | Foundation Failure |
| 90        | 15                      | 2     | 0         | 2     | 16    | 20                            | 100                        | 0            | 20000       | 0.35  | 0.2   | 0.2   | 1              | 15          | 800                                  | 0.6825 | 546         | 5.46     | 2.50 | Base failure_EQ    |
| 91        | 15                      | 4     | 0         | 2     | 16    | 20                            | 100                        | 0            | 20000       | 0.35  | 0.2   | 0.2   | 2              | 15          | 800                                  | 0.6776 | 542.08      | 5.42     | 2.50 | Base failure_EQ    |
| 92        | 15                      | 8     | 0         | 2     | 16    | 20                            | 100                        | 0            | 20000       | 0.35  | 0.2   | 0.2   | 4              | 15          | 800                                  | 0.6057 | 484.56      | 4.85     | 2.50 | Base failure_EQ    |
| 93        | 15                      | 2     | 0         | 2     | 2     | 20                            | 200                        | 0            | 40000       | 0.35  | 0.2   | 0.2   | 1              | 15          | 1600                                 | 0.6351 | 1016.16     | 5.08     | 5.00 | Foundation Failure |
| 94        | 15                      | 4     | 0         | 2     | 2     | 20                            | 200                        | 0            | 40000       | 0.35  | 0.2   | 0.2   | 2              | 15          | 1600                                 | 0.6241 | 998.56      | 4.99     | 5.00 | Foundation Failure |
| 95        | 15                      | 8     | 0         | 2     | 2     | 20                            | 200                        | 0            | 40000       | 0.35  | 0.2   | 0.2   | 4              | 15          | 2000                                 | 0.4965 | 993         | 4.97     | 5.00 | Foundation Failure |
| 96        | 15                      | 2     | 0         | 2     | 4     | 20                            | 200                        | 0            | 40000       | 0.35  | 0.2   | 0.2   | 1              | 15          | 1600                                 | 0.6358 | 1017.28     | 5.09     | 5.00 | Foundation Failure |
| 97        | 15                      | 4     | 0         | 2     | 4     | 20                            | 200                        | 0            | 40000       | 0.35  | 0.2   | 0.2   | 2              | 15          | 1600                                 | 0.6152 | 984.32      | 4.92     | 5.00 | Base failure_EQ    |
| 98        | 15                      | 8     | 0         | 2     | 4     | 20                            | 200                        | 0            | 40000       | 0.35  | 0.2   | 0.2   | 4              | 15          | 1600                                 | 0.6105 | 976.8       | 4.88     | 5.00 | Foundation Failure |
| 99        | 15                      | 2     | 0         | 2     | 8     | 20                            | 200                        | 0            | 40000       | 0.35  | 0.2   | 0.2   | 1              | 15          | 1600                                 | 0.6208 | 993.28      | 4.97     | 5.00 | Foundation Failure |
| 100       | 15                      | 4     | 0         | 2     | 8     | 20                            | 200                        | 0            | 40000       | 0.35  | 0.2   | 0.2   | 2              | 15          | 1600                                 | 0.6197 | 991.52      | 4.96     | 5.00 | Base failure_EQ    |
| 101       | 15                      | 8     | 0         | 2     | 8     | 20                            | 200                        | 0            | 40000       | 0.35  | 0.2   | 0.2   | 4              | 15          | 1600                                 | 0.5275 | 844         | 4.22     | 5.00 | Base failure_EQ    |
| 102       | 15                      | 2     | 0         | 2     | 16    | 20                            | 200                        | 0            | 40000       | 0.35  | 0.2   | 0.2   | 1              | 15          | 1600                                 | 0.5626 | 900.16      | 4.50     | 5.00 | Foundation Failure |
| 103       | 15                      | 4     | 0         | 2     | 16    | 20                            | 200                        | 0            | 40000       | 0.35  | 0.2   | 0.2   | 2              | 15          | 1600                                 | 0.6219 | 995.04      | 4.98     | 5.00 | Base failure_EQ    |
| 104       | 15                      | 8     | 0         | 2     | 16    | 20                            | 200                        | 0            | 40000       | 0.35  | 0.2   | 0.2   | 4              | 15          | 1600                                 | 0.6151 | 984.16      | 4.92     | 5.00 | Base failure_EQ    |

N.F. :Not found.  
Base failure EQ:Failed due to earthquake.  
Base failure GR:Failed due to gravity.

Table B.1. List of results of finite elements models created for seismic condition ( $\beta= 15^\circ$ )

(Cont.).

| Model No. | GEOTECHNICAL PROPERTIES |       |           |       |       |                               | SLOPE SOIL PROPERTIES      |              |             |       |       |                       | SEISMIC EFFECT |             | ANALYSIS RESULTS FOR SEISMIC LOADING |        |             |        |       |                    |
|-----------|-------------------------|-------|-----------|-------|-------|-------------------------------|----------------------------|--------------|-------------|-------|-------|-----------------------|----------------|-------------|--------------------------------------|--------|-------------|--------|-------|--------------------|
|           | $\beta$ (°)             | H (m) | $\lambda$ | B (m) | L (m) | $\gamma$ (kN/m <sup>3</sup> ) | $c_u$ (kN/m <sup>2</sup> ) | $\phi_h$ (°) | $E_u$ (kPa) | $v_u$ | $k_h$ | FILE NAME             | H/B            | $\beta$ (°) | Load                                 | Mstage | $q_r$ (kPa) | $N_s$  | cu/yB | Failure Mode       |
| 105       | 0                       | 2     | 0         | 2     | 2     | 20                            | 100                        | 0            | 20000       | 0.35  | 0.3   | C_0_2_0_2_100_0_3_D   | 1              | 0           | 2000                                 | 0.17   | 340         | 3.4    | 2.5   | Foundation Failure |
| 106       | 0                       | 2     | 0         | 2     | 4     | 20                            | 100                        | 0            | 20000       | 0.35  | 0.3   | C_0_2_0_4_100_0_3_D   | 1              | 0           | 2000                                 | 0.16   | 320         | 3.2    | 2.5   | Foundation Failure |
| 107       | 0                       | 2     | 0         | 2     | 8     | 20                            | 100                        | 0            | 20000       | 0.35  | 0.3   | C_0_2_0_8_100_0_3_D   | 1              | 0           | 2000                                 | 0.158  | 316         | 3.16   | 2.5   | Foundation Failure |
| 108       | 0                       | 2     | 0         | 2     | 16    | 20                            | 100                        | 0            | 20000       | 0.35  | 0.3   | C_0_2_0_16_100_0_3_D  | 1              | 0           | 2000                                 | 0.15   | 300         | 3      | 2.5   | Foundation Failure |
| 109       | 15                      | 2     | 0         | 2     | 2     | 20                            | 25                         | 0            | 5000        | 0.35  | 0.3   | C_15_2_0_2_25_0_3_D   | 1              | 15          | 200                                  | 0.3188 | 65.76       | 2.5504 | 0.63  | Base failure_EQ    |
| 110       | 15                      | 4     | 0         | 2     | 2     | 20                            | 25                         | 0            | 5000        | 0.35  | 0.3   | C_15_4_0_2_25_0_3_D   | 2              | 15          | 200                                  | 0.1662 | 33.24       | 1.33   | 0.63  | Base failure_EQ    |
| 111       | 15                      | 8     | 0         | 2     | 2     | 20                            | 25                         | 0            | 5000        | 0.35  | 0.3   | C_15_8_0_2_25_0_3_D   | 4              | 15          | 200                                  | N.F.   | N.F.        | N.F.   | 0.63  | Base failure_GR    |
| 112       | 15                      | 2     | 0         | 2     | 4     | 20                            | 25                         | 0            | 5000        | 0.35  | 0.3   | C_15_2_0_4_25_0_3_D   | 1              | 15          | 200                                  | 0.319  | 63.8        | 2.55   | 0.63  | Base failure_EQ    |
| 113       | 15                      | 4     | 0         | 2     | 4     | 20                            | 25                         | 0            | 5000        | 0.35  | 0.3   | C_15_4_0_4_25_0_3_D   | 2              | 15          | 200                                  | 0.166  | 33.2        | 1.33   | 0.63  | Base failure_EQ    |
| 114       | 15                      | 8     | 0         | 2     | 4     | 20                            | 25                         | 0            | 5000        | 0.35  | 0.3   | C_15_8_0_4_25_0_3_D   | 4              | 15          | 200                                  | N.F.   | N.F.        | N.F.   | 0.63  | Base failure_GR    |
| 115       | 15                      | 2     | 0         | 2     | 8     | 20                            | 25                         | 0            | 5000        | 0.35  | 0.3   | C_15_2_0_8_25_0_3_D   | 1              | 15          | 200                                  | 0.3212 | 64.24       | 2.57   | 0.63  | Base failure_EQ    |
| 116       | 15                      | 4     | 0         | 2     | 8     | 20                            | 25                         | 0            | 5000        | 0.35  | 0.3   | C_15_4_0_8_25_0_3_D   | 2              | 15          | 200                                  | 0.1682 | 33.64       | 1.35   | 0.63  | Base failure_EQ    |
| 117       | 15                      | 8     | 0         | 2     | 8     | 20                            | 25                         | 0            | 5000        | 0.35  | 0.3   | C_15_8_0_8_25_0_3_D   | 4              | 15          | 200                                  | N.F.   | N.F.        | N.F.   | 0.63  | Base failure_GR    |
| 118       | 15                      | 2     | 0         | 2     | 16    | 20                            | 25                         | 0            | 5000        | 0.35  | 0.3   | C_15_2_0_16_25_0_3_D  | 1              | 15          | 200                                  | 0.3216 | 64.32       | 2.57   | 0.63  | Base failure_EQ    |
| 119       | 15                      | 4     | 0         | 2     | 16    | 20                            | 25                         | 0            | 5000        | 0.35  | 0.3   | C_15_4_0_16_25_0_3_D  | 2              | 15          | 200                                  | 0.1678 | 33.56       | 1.34   | 0.63  | Base failure_EQ    |
| 120       | 15                      | 8     | 0         | 2     | 16    | 20                            | 25                         | 0            | 5000        | 0.35  | 0.3   | C_15_8_0_16_25_0_3_D  | 4              | 15          | 200                                  | N.F.   | N.F.        | N.F.   | 0.63  | Base failure_GR    |
| 121       | 15                      | 2     | 0         | 2     | 2     | 20                            | 50                         | 0            | 10000       | 0.35  | 0.3   | C_15_2_0_2_50_0_3_D   | 1              | 15          | 300                                  | 0.7696 | 230.88      | 4.62   | 1.25  | Base failure_EQ    |
| 122       | 15                      | 4     | 0         | 2     | 2     | 20                            | 50                         | 0            | 10000       | 0.35  | 0.3   | C_15_4_0_2_50_0_3_D   | 2              | 15          | 400                                  | 0.4192 | 167.68      | 3.35   | 1.25  | Base failure_EQ    |
| 123       | 15                      | 8     | 0         | 2     | 2     | 20                            | 50                         | 0            | 10000       | 0.35  | 0.3   | C_15_8_0_2_50_0_3_D   | 4              | 15          | 400                                  | 0.2883 | 115.32      | 2.31   | 1.25  | Base failure_EQ    |
| 124       | 15                      | 2     | 0         | 2     | 4     | 20                            | 50                         | 0            | 10000       | 0.35  | 0.3   | C_15_2_0_4_50_0_3_D   | 1              | 15          | 400                                  | 0.4643 | 185.72      | 3.71   | 1.25  | Base failure_EQ    |
| 125       | 15                      | 4     | 0         | 2     | 4     | 20                            | 50                         | 0            | 10000       | 0.35  | 0.3   | C_15_4_0_4_50_0_3_D   | 2              | 15          | 400                                  | 0.4038 | 161.52      | 3.23   | 1.25  | Base failure_EQ    |
| 126       | 15                      | 8     | 0         | 2     | 4     | 20                            | 50                         | 0            | 10000       | 0.35  | 0.3   | C_15_8_0_4_50_0_3_D   | 4              | 15          | 400                                  | 0.2874 | 114.96      | 2.30   | 1.25  | Base failure_EQ    |
| 127       | 15                      | 2     | 0         | 2     | 8     | 20                            | 50                         | 0            | 10000       | 0.35  | 0.3   | C_15_2_0_8_50_0_3_D   | 1              | 15          | 400                                  | 0.3526 | 141.04      | 2.82   | 1.25  | Base failure_EQ    |
| 128       | 15                      | 4     | 0         | 2     | 8     | 20                            | 50                         | 0            | 10000       | 0.35  | 0.3   | C_15_4_0_8_50_0_3_D   | 2              | 15          | 400                                  | 0.3913 | 156.52      | 3.13   | 1.25  | Base failure_EQ    |
| 129       | 15                      | 8     | 0         | 2     | 8     | 20                            | 50                         | 0            | 10000       | 0.35  | 0.3   | C_15_8_0_8_50_0_3_D   | 4              | 15          | 400                                  | 0.287  | 114.8       | 2.30   | 1.25  | Base failure_EQ    |
| 130       | 15                      | 2     | 0         | 2     | 16    | 20                            | 50                         | 0            | 10000       | 0.35  | 0.3   | C_15_2_0_16_50_0_3_D  | 1              | 15          | 400                                  | 0.6179 | 247.16      | 4.94   | 1.25  | Base failure_EQ    |
| 131       | 15                      | 4     | 0         | 2     | 16    | 20                            | 50                         | 0            | 10000       | 0.35  | 0.3   | C_15_4_0_16_50_0_3_D  | 2              | 15          | 400                                  | 0.4277 | 171.08      | 3.42   | 1.25  | Base failure_EQ    |
| 132       | 15                      | 8     | 0         | 2     | 16    | 20                            | 50                         | 0            | 10000       | 0.35  | 0.3   | C_15_8_0_16_50_0_3_D  | 4              | 15          | 400                                  | 0.2892 | 115.68      | 2.31   | 1.25  | Base failure_EQ    |
| 133       | 15                      | 2     | 0         | 2     | 2     | 20                            | 100                        | 0            | 20000       | 0.35  | 0.3   | C_15_2_0_2_100_0_3_D  | 1              | 15          | 1000                                 | 0.359  | 359         | 3.59   | 2.50  | Base failure_EQ    |
| 134       | 15                      | 4     | 0         | 2     | 2     | 20                            | 100                        | 0            | 20000       | 0.35  | 0.3   | C_15_4_0_2_100_0_3_D  | 2              | 15          | 800                                  | 0.4142 | 331.36      | 3.31   | 2.50  | Base failure_EQ    |
| 135       | 15                      | 8     | 0         | 2     | 2     | 20                            | 100                        | 0            | 20000       | 0.35  | 0.3   | C_15_8_0_2_100_0_3_D  | 4              | 15          | 800                                  | 0.4098 | 327.84      | 3.28   | 2.50  | Base failure_EQ    |
| 136       | 15                      | 2     | 0         | 2     | 4     | 20                            | 100                        | 0            | 20000       | 0.35  | 0.3   | C_15_2_0_4_100_0_3_D  | 1              | 15          | 800                                  | 0.4    | 320         | 3.20   | 2.50  | Base failure_EQ    |
| 137       | 15                      | 4     | 0         | 2     | 4     | 20                            | 100                        | 0            | 20000       | 0.35  | 0.3   | C_15_4_0_4_100_0_3_D  | 2              | 15          | 800                                  | 0.3985 | 318.8       | 3.19   | 2.50  | Base failure_EQ    |
| 138       | 15                      | 8     | 0         | 2     | 4     | 20                            | 100                        | 0            | 20000       | 0.35  | 0.3   | C_15_8_0_4_100_0_3_D  | 4              | 15          | 800                                  | 0.4091 | 327.28      | 3.27   | 2.50  | Base failure_EQ    |
| 139       | 15                      | 2     | 0         | 2     | 8     | 20                            | 100                        | 0            | 20000       | 0.35  | 0.3   | C_15_2_0_8_100_0_3_D  | 1              | 15          | 800                                  | 0.3912 | 312.96      | 3.13   | 2.50  | Base failure_EQ    |
| 140       | 15                      | 4     | 0         | 2     | 8     | 20                            | 100                        | 0            | 20000       | 0.35  | 0.3   | C_15_4_0_8_100_0_3_D  | 2              | 15          | 1000                                 | 0.2341 | 234.1       | 2.34   | 2.50  | Base failure_EQ    |
| 141       | 15                      | 8     | 0         | 2     | 8     | 20                            | 100                        | 0            | 20000       | 0.35  | 0.3   | C_15_8_0_8_100_0_3_D  | 4              | 15          | 800                                  | 0.4088 | 327.04      | 3.27   | 2.50  | Base failure_EQ    |
| 142       | 15                      | 2     | 0         | 2     | 16    | 20                            | 100                        | 0            | 20000       | 0.35  | 0.3   | C_15_2_0_16_100_0_3_D | 1              | 15          | 800                                  | 0.3847 | 307.76      | 3.08   | 2.50  | Base failure_EQ    |
| 143       | 15                      | 4     | 0         | 2     | 16    | 20                            | 100                        | 0            | 20000       | 0.35  | 0.3   | C_15_4_0_16_100_0_3_D | 2              | 15          | 800                                  | 0.4193 | 335.44      | 3.35   | 2.50  | Base failure_EQ    |
| 144       | 15                      | 8     | 0         | 2     | 16    | 20                            | 100                        | 0            | 20000       | 0.35  | 0.3   | C_15_8_0_16_100_0_3_D | 4              | 15          | 800                                  | 0.5515 | 441.2       | 4.41   | 2.50  | Base failure_EQ    |
| 145       | 15                      | 2     | 0         | 2     | 2     | 20                            | 200                        | 0            | 40000       | 0.35  | 0.3   | C_15_2_0_2_200_0_3_D  | 1              | 15          | 1600                                 | 0.6004 | 960.64      | 4.80   | 5.00  | Base failure_EQ    |
| 146       | 15                      | 4     | 0         | 2     | 2     | 20                            | 200                        | 0            | 40000       | 0.35  | 0.3   | C_15_4_0_2_200_0_3_D  | 2              | 15          | 1600                                 | 0.4159 | 665.44      | 3.33   | 5.00  | Base failure_EQ    |
| 147       | 15                      | 8     | 0         | 2     | 2     | 20                            | 200                        | 0            | 40000       | 0.35  | 0.3   | C_15_8_0_2_200_0_3_D  | 4              | 15          | 2000                                 | 0.3616 | 723.2       | 3.62   | 5.00  | Base failure_EQ    |
| 148       | 15                      | 2     | 0         | 2     | 4     | 20                            | 200                        | 0            | 40000       | 0.35  | 0.3   | C_15_2_0_4_200_0_3_D  | 1              | 15          | 1600                                 | 0.416  | 665.6       | 3.33   | 5.00  | Base failure_EQ    |
| 149       | 15                      | 4     | 0         | 2     | 4     | 20                            | 200                        | 0            | 40000       | 0.35  | 0.3   | C_15_4_0_4_200_0_3_D  | 2              | 15          | 1600                                 | 0.4057 | 645.92      | 3.23   | 5.00  | Base failure_EQ    |
| 150       | 15                      | 8     | 0         | 2     | 4     | 20                            | 200                        | 0            | 40000       | 0.35  | 0.3   | C_15_8_0_4_200_0_3_D  | 4              | 15          | 1600                                 | 0.4165 | 666.4       | 3.33   | 5.00  | Base failure_EQ    |
| 151       | 15                      | 2     | 0         | 2     | 8     | 20                            | 200                        | 0            | 40000       | 0.35  | 0.3   | C_15_2_0_8_200_0_3_D  | 1              | 15          | 1600                                 | 0.4127 | 660.32      | 3.30   | 5.00  | Base failure_EQ    |
| 152       | 15                      | 4     | 0         | 2     | 8     | 20                            | 200                        | 0            | 40000       | 0.35  | 0.3   | C_15_4_0_8_200_0_3_D  | 2              | 15          | 1600                                 | 0.389  | 622.4       | 3.11   | 5.00  | Base failure_EQ    |
| 153       | 15                      | 8     | 0         | 2     | 8     | 20                            | 200                        | 0            | 40000       | 0.35  | 0.3   | C_15_8_0_8_200_0_3_D  | 4              | 15          | 2000                                 | 0.2983 | 596.6       | 2.98   | 5.00  | Base failure_EQ    |
| 154       | 15                      | 2     | 0         | 2     | 16    | 20                            | 200                        | 0            | 40000       | 0.35  | 0.3   | C_15_2_0_16_200_0_3_D | 1              | 15          | 1600                                 | 0.4097 | 655.52      | 3.28   | 5.00  | Base failure_EQ    |
| 155       | 15                      | 4     | 0         | 2     | 16    | 20                            | 200                        | 0            | 40000       | 0.35  | 0.3   | C_15_4_0_16_200_0_3_D | 2              | 15          | 1600                                 | 0.4106 | 656.96      | 3.28   | 5.00  | Base failure_EQ    |
| 156       | 15                      | 8     | 0         | 2     | 16    | 20                            | 200                        | 0            | 40000       | 0.35  | 0.3   | C_15_8_0_16_200_0_3_D | 4              | 15          | 1600                                 | 0.4099 | 641.44      | 3.21   | 5.00  | Base failure_EQ    |

N.F.: Not found.  
 Base failure EQ: Failed due to earthquake.  
 Base failure\_GR: Failed due to gravity.

Table B.2. List of results of finite elements models created for seismic condition ( $\beta= 30^\circ$ )

| Model No. | GEOTECHNICAL PROPERTIES |       |           |       |       |                               | SLOPE SOIL PROPERTIES      |              |             |       |       |  | SEISMIC EFFECT          |             | FILE NAME | ANALYSIS RESULTS FOR SEISMIC LOADING |             |       |       |                    |  |
|-----------|-------------------------|-------|-----------|-------|-------|-------------------------------|----------------------------|--------------|-------------|-------|-------|--|-------------------------|-------------|-----------|--------------------------------------|-------------|-------|-------|--------------------|--|
|           | $\beta$ (°)             | H (m) | $\lambda$ | B (m) | L (m) | $\gamma$ (kN/m <sup>3</sup> ) | $c_u$ (kN/m <sup>2</sup> ) | $\phi_u$ (°) | $E_u$ (kPa) | $V_u$ | $k_h$ |  | H/B                     | $\beta$ (°) | Load      | Mstage                               | $q_r$ (kPa) | $N_s$ | cu/yB | Failure Mode       |  |
| 1         | 30                      | 2     | 0         | 2     | 2     | 20                            | 25                         | 0            | 5000        | 0.35  | 0.1   |  | C_30_2_0_2_25_0.1_1.D   | 30          | 200       | 0.718                                | 143.6       | 5.74  | 0.63  | Foundation Failure |  |
| 2         | 30                      | 4     | 0         | 2     | 2     | 20                            | 25                         | 0            | 5000        | 0.35  | 0.1   |  | C_30_4_0_2_25_0.1_1.D   | 30          | 200       | 0.571                                | 111.42      | 4.46  | 0.63  | Base failure_EQ    |  |
| 3         | 30                      | 8     | 0         | 2     | 2     | 20                            | 25                         | 0            | 5000        | 0.35  | 0.1   |  | C_30_8_0_2_25_0.1_1.D   | 30          | 200       | N.F.                                 | N.F.        | N.F.  | 0.63  | Base failure_GR    |  |
| 4         | 30                      | 2     | 0         | 2     | 4     | 20                            | 25                         | 0            | 5000        | 0.35  | 0.1   |  | C_30_2_0_4_25_0.1_1.D   | 30          | 200       | 0.6451                               | 129.02      | 5.16  | 0.63  | Foundation Failure |  |
| 5         | 30                      | 4     | 0         | 2     | 4     | 20                            | 25                         | 0            | 5000        | 0.35  | 0.1   |  | C_30_4_0_4_25_0.1_1.D   | 30          | 200       | 0.5498                               | 109.96      | 4.40  | 0.63  | Base failure_EQ    |  |
| 6         | 30                      | 8     | 0         | 2     | 4     | 20                            | 25                         | 0            | 5000        | 0.35  | 0.1   |  | C_30_8_0_4_25_0.1_1.D   | 30          | 200       | N.F.                                 | N.F.        | N.F.  | 0.63  | Base failure_GR    |  |
| 7         | 30                      | 2     | 0         | 2     | 8     | 20                            | 25                         | 0            | 5000        | 0.35  | 0.1   |  | C_30_2_0_8_25_0.1_1.D   | 30          | 200       | 0.5705                               | 114.1       | 4.56  | 0.63  | Base failure_EQ    |  |
| 8         | 30                      | 4     | 0         | 2     | 8     | 20                            | 25                         | 0            | 5000        | 0.35  | 0.1   |  | C_30_4_0_8_25_0.1_1.D   | 30          | 200       | 0.5498                               | 109.96      | 4.40  | 0.63  | Base failure_EQ    |  |
| 9         | 30                      | 8     | 0         | 2     | 8     | 20                            | 25                         | 0            | 5000        | 0.35  | 0.1   |  | C_30_8_0_8_25_0.1_1.D   | 30          | 200       | N.F.                                 | N.F.        | N.F.  | 0.63  | Base failure_GR    |  |
| 10        | 30                      | 2     | 0         | 2     | 16    | 20                            | 25                         | 0            | 5000        | 0.35  | 0.1   |  | C_30_2_0_16_25_0.1_1.D  | 30          | 200       | 0.574                                | 114.8       | 4.59  | 0.63  | Foundation Failure |  |
| 11        | 30                      | 4     | 0         | 2     | 16    | 20                            | 25                         | 0            | 5000        | 0.35  | 0.1   |  | C_30_4_0_16_25_0.1_1.D  | 30          | 200       | 0.5635                               | 112.7       | 4.51  | 0.63  | Base failure_EQ    |  |
| 12        | 30                      | 8     | 0         | 2     | 16    | 20                            | 25                         | 0            | 5000        | 0.35  | 0.1   |  | C_30_8_0_16_25_0.1_1.D  | 30          | 200       | N.F.                                 | N.F.        | N.F.  | 0.63  | Base failure_GR    |  |
| 13        | 30                      | 2     | 0         | 2     | 2     | 20                            | 50                         | 0            | 10000       | 0.35  | 0.1   |  | C_30_2_0_2_50_0.1_1.D   | 30          | 600       | 0.5174                               | 310.44      | 6.21  | 1.25  | Foundation Failure |  |
| 14        | 30                      | 4     | 0         | 2     | 2     | 20                            | 50                         | 0            | 10000       | 0.35  | 0.1   |  | C_30_4_0_2_50_0.1_1.D   | 30          | 600       | 0.4738                               | 284.28      | 5.69  | 1.25  | Foundation Failure |  |
| 15        | 30                      | 8     | 0         | 2     | 2     | 20                            | 50                         | 0            | 10000       | 0.35  | 0.1   |  | C_30_8_0_2_50_0.1_1.D   | 30          | 600       | 0.8754                               | 350.16      | 7.00  | 1.25  | Base failure_EQ    |  |
| 16        | 30                      | 2     | 0         | 2     | 4     | 20                            | 50                         | 0            | 10000       | 0.35  | 0.1   |  | C_30_2_0_4_50_0.1_1.D   | 30          | 600       | 0.4791                               | 287.46      | 5.75  | 1.25  | Foundation Failure |  |
| 17        | 30                      | 4     | 0         | 2     | 4     | 20                            | 50                         | 0            | 10000       | 0.35  | 0.1   |  | C_30_4_0_4_50_0.1_1.D   | 30          | 600       | 0.4512                               | 270.72      | 5.41  | 1.25  | Foundation Failure |  |
| 18        | 30                      | 8     | 0         | 2     | 4     | 20                            | 50                         | 0            | 10000       | 0.35  | 0.1   |  | C_30_8_0_4_50_0.1_1.D   | 30          | 600       | 0.6485                               | 259.4       | 5.19  | 1.25  | Foundation Failure |  |
| 19        | 30                      | 2     | 0         | 2     | 8     | 20                            | 50                         | 0            | 10000       | 0.35  | 0.1   |  | C_30_2_0_8_50_0.1_1.D   | 30          | 400       | 0.5987                               | 239.48      | 4.79  | 1.25  | Foundation Failure |  |
| 20        | 30                      | 4     | 0         | 2     | 8     | 20                            | 50                         | 0            | 10000       | 0.35  | 0.1   |  | C_30_4_0_8_50_0.1_1.D   | 30          | 400       | 0.6473                               | 258.92      | 5.18  | 1.25  | Foundation Failure |  |
| 21        | 30                      | 8     | 0         | 2     | 8     | 20                            | 50                         | 0            | 10000       | 0.35  | 0.1   |  | C_30_8_0_8_50_0.1_1.D   | 30          | 400       | 0.5827                               | 233.08      | 4.66  | 1.25  | Foundation Failure |  |
| 22        | 30                      | 2     | 0         | 2     | 16    | 20                            | 50                         | 0            | 10000       | 0.35  | 0.1   |  | C_30_2_0_16_50_0.1_1.D  | 30          | 400       | 0.7021                               | 280.84      | 5.62  | 1.25  | Foundation Failure |  |
| 23        | 30                      | 4     | 0         | 2     | 16    | 20                            | 50                         | 0            | 10000       | 0.35  | 0.1   |  | C_30_4_0_16_50_0.1_1.D  | 30          | 400       | 0.6818                               | 272.72      | 5.45  | 1.25  | Foundation Failure |  |
| 24        | 30                      | 8     | 0         | 2     | 16    | 20                            | 50                         | 0            | 10000       | 0.35  | 0.1   |  | C_30_8_0_16_50_0.1_1.D  | 30          | 400       | 0.6818                               | 272.72      | 5.45  | 1.25  | Foundation Failure |  |
| 25        | 30                      | 2     | 0         | 2     | 2     | 20                            | 100                        | 0            | 20000       | 0.35  | 0.1   |  | C_30_2_0_2_100_0.1_1.D  | 30          | 1000      | 0.6441                               | 641         | 6.41  | 2.50  | Foundation Failure |  |
| 26        | 30                      | 4     | 0         | 2     | 2     | 20                            | 100                        | 0            | 20000       | 0.35  | 0.1   |  | C_30_4_0_2_100_0.1_1.D  | 30          | 1000      | 0.5821                               | 582.1       | 5.82  | 2.50  | Foundation Failure |  |
| 27        | 30                      | 8     | 0         | 2     | 2     | 20                            | 100                        | 0            | 20000       | 0.35  | 0.1   |  | C_30_8_0_2_100_0.1_1.D  | 30          | 1000      | 0.5777                               | 577.7       | 5.78  | 2.50  | Foundation Failure |  |
| 28        | 30                      | 2     | 0         | 2     | 4     | 20                            | 100                        | 0            | 20000       | 0.35  | 0.1   |  | C_30_2_0_4_100_0.1_1.D  | 30          | 800       | 0.6781                               | 542.48      | 5.42  | 2.50  | Foundation Failure |  |
| 29        | 30                      | 4     | 0         | 2     | 4     | 20                            | 100                        | 0            | 20000       | 0.35  | 0.1   |  | C_30_4_0_4_100_0.1_1.D  | 30          | 800       | 0.675                                | 540         | 5.40  | 2.50  | Foundation Failure |  |
| 30        | 30                      | 8     | 0         | 2     | 4     | 20                            | 100                        | 0            | 20000       | 0.35  | 0.1   |  | C_30_8_0_4_100_0.1_1.D  | 30          | 800       | 0.6543                               | 523.44      | 5.23  | 2.50  | Foundation Failure |  |
| 31        | 30                      | 2     | 0         | 2     | 8     | 20                            | 100                        | 0            | 20000       | 0.35  | 0.1   |  | C_30_2_0_8_100_0.1_1.D  | 30          | 800       | 0.6725                               | 538         | 5.38  | 2.50  | Foundation Failure |  |
| 32        | 30                      | 4     | 0         | 2     | 8     | 20                            | 100                        | 0            | 20000       | 0.35  | 0.1   |  | C_30_4_0_8_100_0.1_1.D  | 30          | 800       | 0.6578                               | 526.24      | 5.26  | 2.50  | Foundation Failure |  |
| 33        | 30                      | 8     | 0         | 2     | 8     | 20                            | 100                        | 0            | 20000       | 0.35  | 0.1   |  | C_30_8_0_8_100_0.1_1.D  | 30          | 800       | 0.6031                               | 482.48      | 4.82  | 2.50  | Foundation Failure |  |
| 34        | 30                      | 2     | 0         | 2     | 16    | 20                            | 100                        | 0            | 20000       | 0.35  | 0.1   |  | C_30_2_0_16_100_0.1_1.D | 30          | 800       | 0.7196                               | 575.68      | 5.76  | 2.50  | Foundation Failure |  |
| 35        | 30                      | 4     | 0         | 2     | 16    | 20                            | 100                        | 0            | 20000       | 0.35  | 0.1   |  | C_30_4_0_16_100_0.1_1.D | 30          | 800       | 0.7105                               | 568.4       | 5.68  | 2.50  | Foundation Failure |  |
| 36        | 30                      | 8     | 0         | 2     | 16    | 20                            | 100                        | 0            | 20000       | 0.35  | 0.1   |  | C_30_8_0_16_100_0.1_1.D | 30          | 800       | 0.7326                               | 586.08      | 5.86  | 2.50  | Foundation Failure |  |
| 37        | 30                      | 2     | 0         | 2     | 2     | 20                            | 200                        | 0            | 40000       | 0.35  | 0.1   |  | C_30_2_0_2_200_0.1_1.D  | 30          | 1600      | 0.8189                               | 1310.24     | 6.55  | 5.00  | Foundation Failure |  |
| 38        | 30                      | 4     | 0         | 2     | 2     | 20                            | 200                        | 0            | 40000       | 0.35  | 0.1   |  | C_30_4_0_2_200_0.1_1.D  | 30          | 1600      | 0.908                                | 1452.8      | 7.26  | 5.00  | Foundation Failure |  |
| 39        | 30                      | 8     | 0         | 2     | 2     | 20                            | 200                        | 0            | 40000       | 0.35  | 0.1   |  | C_30_8_0_2_200_0.1_1.D  | 30          | 1600      | 0.8858                               | 1417.28     | 7.09  | 5.00  | Foundation Failure |  |
| 40        | 30                      | 2     | 0         | 2     | 4     | 20                            | 200                        | 0            | 40000       | 0.35  | 0.1   |  | C_30_2_0_4_200_0.1_1.D  | 30          | 1600      | 0.8071                               | 1291.36     | 6.46  | 5.00  | Foundation Failure |  |
| 41        | 30                      | 4     | 0         | 2     | 4     | 20                            | 200                        | 0            | 40000       | 0.35  | 0.1   |  | C_30_4_0_4_200_0.1_1.D  | 30          | 1600      | 0.8486                               | 1357.76     | 6.79  | 5.00  | Foundation Failure |  |
| 42        | 30                      | 8     | 0         | 2     | 4     | 20                            | 200                        | 0            | 40000       | 0.35  | 0.1   |  | C_30_8_0_4_200_0.1_1.D  | 30          | 1600      | 0.73                                 | 1168        | 5.84  | 5.00  | Foundation Failure |  |
| 43        | 30                      | 2     | 0         | 2     | 8     | 20                            | 200                        | 0            | 40000       | 0.35  | 0.1   |  | C_30_2_0_8_200_0.1_1.D  | 30          | 1600      | 0.6746                               | 1079.36     | 5.40  | 5.00  | Foundation Failure |  |
| 44        | 30                      | 4     | 0         | 2     | 8     | 20                            | 200                        | 0            | 40000       | 0.35  | 0.1   |  | C_30_4_0_8_200_0.1_1.D  | 30          | 1600      | 0.6714                               | 1074.24     | 5.37  | 5.00  | Foundation Failure |  |
| 45        | 30                      | 8     | 0         | 2     | 8     | 20                            | 200                        | 0            | 40000       | 0.35  | 0.1   |  | C_30_8_0_8_200_0.1_1.D  | 30          | 1600      | 0.6055                               | 968.8       | 4.84  | 5.00  | Foundation Failure |  |
| 46        | 30                      | 2     | 0         | 2     | 16    | 20                            | 200                        | 0            | 40000       | 0.35  | 0.1   |  | C_30_2_0_16_200_0.1_1.D | 30          | 1600      | 0.7345                               | 1175.2      | 5.88  | 5.00  | Foundation Failure |  |
| 47        | 30                      | 4     | 0         | 2     | 16    | 20                            | 200                        | 0            | 40000       | 0.35  | 0.1   |  | C_30_4_0_16_200_0.1_1.D | 30          | 1600      | 0.7177                               | 1148.32     | 5.74  | 5.00  | Foundation Failure |  |
| 48        | 30                      | 8     | 0         | 2     | 16    | 20                            | 200                        | 0            | 40000       | 0.35  | 0.1   |  | C_30_8_0_16_200_0.1_1.D | 30          | 1600      | 0.7641                               | 1222.56     | 6.11  | 5.00  | Foundation Failure |  |

N.F.: Not found.  
 Base failure\_EQ: Failed due to earthquake.  
 Base failure\_GR: Failed due to gravity.

Table B.2. List of results of finite elements models created for seismic condition ( $\beta= 30^\circ$ )

(Cont.).

| Model No. | GEOTECHNICAL PROPERTIES |       |           |       |       |                               | SLOPE SOIL PROPERTIES      |              |             |       |       |  | SEISMIC EFFECT        |     | ANALYSIS RESULTS FOR SEISMIC LOADING |      |         |             |       |       |                    |
|-----------|-------------------------|-------|-----------|-------|-------|-------------------------------|----------------------------|--------------|-------------|-------|-------|--|-----------------------|-----|--------------------------------------|------|---------|-------------|-------|-------|--------------------|
|           | $\beta$ (°)             | H (m) | $\lambda$ | B (m) | L (m) | $\gamma$ (kN/m <sup>3</sup> ) | $c_u$ (kN/m <sup>2</sup> ) | $\phi_u$ (°) | $E_u$ (kPa) | $v_u$ | $k_h$ |  | FILE NAME             | H/B | $\beta$ (°)                          | Load | Mstage  | $q_r$ (kPa) | $N_e$ | cu/yB | Failure Mode       |
| 49        | 30                      | 2     | 0         | 2     | 2     | 20                            | 25                         | 0            | 5000        | 0.35  | 0.2   |  | C_30_2_0_2_25_0_2_D   | 1   | 30                                   | 200  | 0.5087  | 101.74      | 4.07  | 0.63  | Base failure_EQ    |
| 50        | 30                      | 4     | 0         | 2     | 2     | 20                            | 25                         | 0            | 5000        | 0.35  | 0.2   |  | C_30_4_0_2_25_0_2_D   | 2   | 30                                   | 200  | 0.2786  | 55.72       | 2.23  | 0.63  | Base failure_EQ    |
| 51        | 30                      | 8     | 0         | 2     | 2     | 20                            | 25                         | 0            | 5000        | 0.35  | 0.2   |  | C_30_8_0_2_25_0_2_D   | 4   | 30                                   | 200  | N.F.    | N.F.        | N.F.  | 0.63  | Base failure_GR    |
| 52        | 30                      | 2     | 0         | 2     | 4     | 20                            | 25                         | 0            | 5000        | 0.35  | 0.2   |  | C_30_2_0_4_25_0_2_D   | 1   | 30                                   | 200  | 0.5083  | 101.66      | 4.07  | 0.63  | Base failure_EQ    |
| 53        | 30                      | 4     | 0         | 2     | 4     | 20                            | 25                         | 0            | 5000        | 0.35  | 0.2   |  | C_30_4_0_4_25_0_2_D   | 2   | 30                                   | 200  | 0.2754  | 55.08       | 2.20  | 0.63  | Base failure_EQ    |
| 54        | 30                      | 8     | 0         | 2     | 4     | 20                            | 25                         | 0            | 5000        | 0.35  | 0.2   |  | C_30_8_0_4_25_0_2_D   | 4   | 30                                   | 200  | N.F.    | N.F.        | N.F.  | 0.63  | Base failure_GR    |
| 55        | 30                      | 2     | 0         | 2     | 8     | 20                            | 25                         | 0            | 5000        | 0.35  | 0.2   |  | C_30_2_0_8_25_0_2_D   | 1   | 30                                   | 200  | 0.5082  | 101.64      | 4.07  | 0.63  | Base failure_EQ    |
| 56        | 30                      | 4     | 0         | 2     | 8     | 20                            | 25                         | 0            | 5000        | 0.35  | 0.2   |  | C_30_4_0_8_25_0_2_D   | 2   | 30                                   | 200  | 0.2749  | 54.98       | 2.20  | 0.63  | Base failure_EQ    |
| 57        | 30                      | 8     | 0         | 2     | 8     | 20                            | 25                         | 0            | 5000        | 0.35  | 0.2   |  | C_30_8_0_8_25_0_2_D   | 4   | 30                                   | 200  | N.F.    | N.F.        | N.F.  | 0.63  | Base failure_GR    |
| 58        | 30                      | 2     | 0         | 2     | 16    | 20                            | 25                         | 0            | 5000        | 0.35  | 0.2   |  | C_30_2_0_16_25_0_2_D  | 1   | 30                                   | 200  | 0.5145  | 102.9       | 4.12  | 0.63  | Base failure_EQ    |
| 59        | 30                      | 4     | 0         | 2     | 16    | 20                            | 25                         | 0            | 5000        | 0.35  | 0.2   |  | C_30_4_0_16_25_0_2_D  | 2   | 30                                   | 200  | 0.2819  | 56.38       | 2.26  | 0.63  | Base failure_EQ    |
| 60        | 30                      | 8     | 0         | 2     | 16    | 20                            | 25                         | 0            | 5000        | 0.35  | 0.2   |  | C_30_8_0_16_25_0_2_D  | 4   | 30                                   | 200  | N.F.    | N.F.        | N.F.  | 0.63  | Base failure_GR    |
| 61        | 30                      | 2     | 0         | 2     | 2     | 20                            | 50                         | 0            | 10000       | 0.35  | 0.2   |  | C_30_2_0_2_50_0_2_D   | 1   | 30                                   | 750  | 0.3058  | 229.35      | 4.59  | 1.25  | Foundation Failure |
| 62        | 30                      | 4     | 0         | 2     | 2     | 20                            | 50                         | 0            | 10000       | 0.35  | 0.2   |  | C_30_4_0_2_50_0_2_D   | 2   | 30                                   | 400  | 0.6016  | 240.64      | 4.81  | 1.25  | Foundation Failure |
| 63        | 30                      | 8     | 0         | 2     | 2     | 20                            | 50                         | 0            | 10000       | 0.35  | 0.2   |  | C_30_8_0_2_50_0_2_D   | 4   | 30                                   | 400  | 0.501   | 200.4       | 4.01  | 1.25  | Base failure_EQ    |
| 64        | 30                      | 2     | 0         | 2     | 4     | 20                            | 50                         | 0            | 10000       | 0.35  | 0.2   |  | C_30_2_0_4_50_0_2_D   | 1   | 30                                   | 400  | 0.5074  | 202.96      | 4.06  | 1.25  | Foundation Failure |
| 65        | 30                      | 4     | 0         | 2     | 4     | 20                            | 50                         | 0            | 10000       | 0.35  | 0.2   |  | C_30_4_0_4_50_0_2_D   | 2   | 30                                   | 400  | 0.56    | 224         | 4.48  | 1.25  | Foundation Failure |
| 66        | 30                      | 8     | 0         | 2     | 4     | 20                            | 50                         | 0            | 10000       | 0.35  | 0.2   |  | C_30_8_0_4_50_0_2_D   | 4   | 30                                   | 400  | 0.4966  | 198.64      | 3.97  | 1.25  | Base failure_EQ    |
| 67        | 30                      | 2     | 0         | 2     | 8     | 20                            | 50                         | 0            | 10000       | 0.35  | 0.2   |  | C_30_2_0_8_50_0_2_D   | 1   | 30                                   | 400  | 0.4965  | 198.6       | 3.97  | 1.25  | Foundation Failure |
| 68        | 30                      | 4     | 0         | 2     | 8     | 20                            | 50                         | 0            | 10000       | 0.35  | 0.2   |  | C_30_4_0_8_50_0_2_D   | 2   | 30                                   | 400  | 0.4989  | 199.56      | 3.99  | 1.25  | Foundation Failure |
| 69        | 30                      | 8     | 0         | 2     | 8     | 20                            | 50                         | 0            | 10000       | 0.35  | 0.2   |  | C_30_8_0_8_50_0_2_D   | 4   | 30                                   | 400  | 0.4955  | 198.2       | 3.96  | 1.25  | Base failure_EQ    |
| 70        | 30                      | 2     | 0         | 2     | 16    | 20                            | 50                         | 0            | 10000       | 0.35  | 0.2   |  | C_30_2_0_16_50_0_2_D  | 1   | 30                                   | 400  | 0.5085  | 203.4       | 4.07  | 1.25  | Foundation Failure |
| 71        | 30                      | 4     | 0         | 2     | 16    | 20                            | 50                         | 0            | 10000       | 0.35  | 0.2   |  | C_30_4_0_16_50_0_2_D  | 2   | 30                                   | 400  | 0.5099  | 205.96      | 4.08  | 1.25  | Foundation Failure |
| 72        | 30                      | 8     | 0         | 2     | 16    | 20                            | 50                         | 0            | 10000       | 0.35  | 0.2   |  | C_30_8_0_16_50_0_2_D  | 4   | 30                                   | 400  | 0.5035  | 201.4       | 4.03  | 1.25  | Base failure_EQ    |
| 73        | 30                      | 2     | 0         | 2     | 2     | 20                            | 100                        | 0            | 20000       | 0.35  | 0.2   |  | C_30_2_0_2_100_0_2_D  | 1   | 30                                   | 1000 | 0.46    | 460         | 4.60  | 2.50  | Foundation Failure |
| 74        | 30                      | 4     | 0         | 2     | 2     | 20                            | 100                        | 0            | 20000       | 0.35  | 0.2   |  | C_30_4_0_2_100_0_2_D  | 2   | 30                                   | 1000 | 0.4757  | 475.7       | 4.76  | 2.50  | Foundation Failure |
| 75        | 30                      | 8     | 0         | 2     | 2     | 20                            | 100                        | 0            | 20000       | 0.35  | 0.2   |  | C_30_8_0_2_100_0_2_D  | 4   | 30                                   | 1000 | 0.4742  | 474.2       | 4.74  | 2.50  | Foundation Failure |
| 76        | 30                      | 2     | 0         | 2     | 4     | 20                            | 100                        | 0            | 20000       | 0.35  | 0.2   |  | C_30_2_0_4_100_0_2_D  | 1   | 30                                   | 800  | 0.55125 | 441         | 4.41  | 2.50  | Foundation Failure |
| 77        | 30                      | 4     | 0         | 2     | 4     | 20                            | 100                        | 0            | 20000       | 0.35  | 0.2   |  | C_30_4_0_4_100_0_2_D  | 2   | 30                                   | 800  | 0.5631  | 450.48      | 4.50  | 2.50  | Foundation Failure |
| 78        | 30                      | 8     | 0         | 2     | 4     | 20                            | 100                        | 0            | 20000       | 0.35  | 0.2   |  | C_30_8_0_4_100_0_2_D  | 4   | 30                                   | 800  | 0.5455  | 436.4       | 4.36  | 2.50  | Foundation Failure |
| 79        | 30                      | 2     | 0         | 2     | 8     | 20                            | 100                        | 0            | 20000       | 0.35  | 0.2   |  | C_30_2_0_8_100_0_2_D  | 1   | 30                                   | 800  | 0.5084  | 406.72      | 4.07  | 2.50  | Foundation Failure |
| 80        | 30                      | 4     | 0         | 2     | 8     | 20                            | 100                        | 0            | 20000       | 0.35  | 0.2   |  | C_30_4_0_8_100_0_2_D  | 2   | 30                                   | 800  | 0.51    | 408         | 4.08  | 2.50  | Foundation Failure |
| 81        | 30                      | 8     | 0         | 2     | 8     | 20                            | 100                        | 0            | 20000       | 0.35  | 0.2   |  | C_30_8_0_8_100_0_2_D  | 4   | 30                                   | 800  | 0.5063  | 405.04      | 4.05  | 2.50  | Foundation Failure |
| 82        | 30                      | 2     | 0         | 2     | 16    | 20                            | 100                        | 0            | 20000       | 0.35  | 0.2   |  | C_30_2_0_16_100_0_2_D | 1   | 30                                   | 800  | 0.6213  | 497.04      | 4.97  | 2.50  | Foundation Failure |
| 83        | 30                      | 4     | 0         | 2     | 16    | 20                            | 100                        | 0            | 20000       | 0.35  | 0.2   |  | C_30_4_0_16_100_0_2_D | 2   | 30                                   | 800  | 0.5214  | 417.12      | 4.17  | 2.50  | Foundation Failure |
| 84        | 30                      | 8     | 0         | 2     | 16    | 20                            | 100                        | 0            | 20000       | 0.35  | 0.2   |  | C_30_8_0_16_100_0_2_D | 4   | 30                                   | 800  | 0.5158  | 412.64      | 4.13  | 2.50  | Foundation Failure |
| 85        | 30                      | 2     | 0         | 2     | 2     | 20                            | 200                        | 0            | 40000       | 0.35  | 0.2   |  | C_30_2_0_2_200_0_2_D  | 1   | 30                                   | 1600 | 0.581   | 929.6       | 4.65  | 5.00  | Foundation Failure |
| 86        | 30                      | 4     | 0         | 2     | 2     | 20                            | 200                        | 0            | 40000       | 0.35  | 0.2   |  | C_30_4_0_2_200_0_2_D  | 2   | 30                                   | 1600 | 0.6778  | 1084.48     | 5.42  | 5.00  | Foundation Failure |
| 87        | 30                      | 8     | 0         | 2     | 2     | 20                            | 200                        | 0            | 40000       | 0.35  | 0.2   |  | C_30_8_0_2_200_0_2_D  | 4   | 30                                   | 1600 | 0.6255  | 1000.8      | 5.00  | 5.00  | Foundation Failure |
| 88        | 30                      | 2     | 0         | 2     | 4     | 20                            | 200                        | 0            | 40000       | 0.35  | 0.2   |  | C_30_2_0_4_200_0_2_D  | 1   | 30                                   | 1600 | 0.5743  | 918.88      | 4.59  | 5.00  | Foundation Failure |
| 89        | 30                      | 4     | 0         | 2     | 4     | 20                            | 200                        | 0            | 40000       | 0.35  | 0.2   |  | C_30_4_0_4_200_0_2_D  | 2   | 30                                   | 1600 | 0.593   | 948.8       | 4.74  | 5.00  | Foundation Failure |
| 90        | 30                      | 8     | 0         | 2     | 4     | 20                            | 200                        | 0            | 40000       | 0.35  | 0.2   |  | C_30_8_0_4_200_0_2_D  | 4   | 30                                   | 2000 | 0.4763  | 952.6       | 4.76  | 5.00  | Foundation Failure |
| 91        | 30                      | 2     | 0         | 2     | 8     | 20                            | 200                        | 0            | 40000       | 0.35  | 0.2   |  | C_30_2_0_8_200_0_2_D  | 1   | 30                                   | 1600 | 0.5725  | 916         | 4.58  | 5.00  | Foundation Failure |
| 92        | 30                      | 4     | 0         | 2     | 8     | 20                            | 200                        | 0            | 40000       | 0.35  | 0.2   |  | C_30_4_0_8_200_0_2_D  | 2   | 30                                   | 1600 | 0.5694  | 911.04      | 4.56  | 5.00  | Foundation Failure |
| 93        | 30                      | 8     | 0         | 2     | 8     | 20                            | 200                        | 0            | 40000       | 0.35  | 0.2   |  | C_30_8_0_8_200_0_2_D  | 4   | 30                                   | 1600 | 0.51    | 816         | 4.08  | 5.00  | Foundation Failure |
| 94        | 30                      | 2     | 0         | 2     | 16    | 20                            | 200                        | 0            | 40000       | 0.35  | 0.2   |  | C_30_2_0_16_200_0_2_D | 1   | 30                                   | 1600 | 0.6216  | 994.56      | 4.97  | 5.00  | Foundation Failure |
| 95        | 30                      | 4     | 0         | 2     | 16    | 20                            | 200                        | 0            | 40000       | 0.35  | 0.2   |  | C_30_4_0_16_200_0_2_D | 2   | 30                                   | 1600 | 0.6098  | 975.68      | 4.88  | 5.00  | Foundation Failure |
| 96        | 30                      | 8     | 0         | 2     | 16    | 20                            | 200                        | 0            | 40000       | 0.35  | 0.2   |  | C_30_8_0_16_200_0_2_D | 4   | 30                                   | 1600 | 0.6349  | 1015.84     | 5.08  | 5.00  | Foundation Failure |

N.F.: Not found.  
 Base failure EQ: Failed due to earthquake.  
 Base failure GR: Failed due to gravity.

Table B.2. List of results of finite elements models created for seismic condition ( $\beta= 30^\circ$ )

(Cont.).

| Model No. | GEOTECHNICAL PROPERTIES |       |           |       |       |                               | SLOPE SOIL PROPERTIES      |              |             |       |       |                         | SEISMIC EFFECT |             | ANALYSIS RESULTS FOR SEISMIC LOADING |         |             |          |       |                    |
|-----------|-------------------------|-------|-----------|-------|-------|-------------------------------|----------------------------|--------------|-------------|-------|-------|-------------------------|----------------|-------------|--------------------------------------|---------|-------------|----------|-------|--------------------|
|           | $\beta$ (°)             | H (m) | $\lambda$ | B (m) | L (m) | $\gamma$ (kN/m <sup>3</sup> ) | $c_u$ (kN/m <sup>2</sup> ) | $\phi_b$ (°) | $E_u$ (kPa) | $v_u$ | $k_b$ | FILE NAME               | H/B            | $\beta$ (°) | Load                                 | Mstage  | $q_r$ (kPa) | $N_{se}$ | cu/yB | Failure Mode       |
| 97        | 30                      | 2     | 0         | 2     | 2     | 20                            | 25                         | 0            | 5000        | 0.35  | 0.3   | C_30_2_0_2_25_0_3_3_D   | 1              | 30          | 200                                  | 0.3392  | 67.84       | 2.71     | 0.63  | Base failure_EQ    |
| 98        | 30                      | 4     | 0         | 2     | 2     | 20                            | 25                         | 0            | 5000        | 0.35  | 0.3   | C_30_4_0_2_25_0_3_3_D   | 2              | 30          | 200                                  | 0.1858  | 37.16       | 1.49     | 0.63  | Base failure_EQ    |
| 99        | 30                      | 8     | 0         | 2     | 2     | 20                            | 25                         | 0            | 5000        | 0.35  | 0.3   | C_30_8_0_2_25_0_3_3_D   | 4              | 30          | 200                                  | N.F.    | N.F.        | N.F.     | 0.63  | Base failure_GR    |
| 100       | 30                      | 2     | 0         | 2     | 4     | 20                            | 25                         | 0            | 5000        | 0.35  | 0.3   | C_30_2_0_4_25_0_3_3_D   | 1              | 30          | 200                                  | 0.3386  | 67.72       | 1.71     | 0.63  | Base failure_EQ    |
| 101       | 30                      | 4     | 0         | 2     | 4     | 20                            | 25                         | 0            | 5000        | 0.35  | 0.3   | C_30_4_0_4_25_0_3_3_D   | 2              | 30          | 200                                  | 0.1838  | 36.76       | 1.47     | 0.63  | Base failure_EQ    |
| 102       | 30                      | 8     | 0         | 2     | 4     | 20                            | 25                         | 0            | 5000        | 0.35  | 0.3   | C_30_8_0_4_25_0_3_3_D   | 4              | 30          | 200                                  | N.F.    | N.F.        | N.F.     | 0.63  | Base failure_GR    |
| 103       | 30                      | 2     | 0         | 2     | 8     | 20                            | 25                         | 0            | 5000        | 0.35  | 0.3   | C_30_2_0_8_25_0_3_3_D   | 1              | 30          | 200                                  | 0.3385  | 67.7        | 2.71     | 0.63  | Base failure_EQ    |
| 104       | 30                      | 4     | 0         | 2     | 8     | 20                            | 25                         | 0            | 5000        | 0.35  | 0.3   | C_30_4_0_8_25_0_3_3_D   | 2              | 30          | 200                                  | 0.1834  | 36.68       | 1.47     | 0.63  | Base failure_EQ    |
| 105       | 30                      | 8     | 0         | 2     | 8     | 20                            | 25                         | 0            | 5000        | 0.35  | 0.3   | C_30_8_0_8_25_0_3_3_D   | 4              | 30          | 200                                  | N.F.    | N.F.        | N.F.     | 0.63  | Base failure_GR    |
| 106       | 30                      | 2     | 0         | 2     | 16    | 20                            | 25                         | 0            | 5000        | 0.35  | 0.3   | C_30_2_0_16_25_0_3_3_D  | 1              | 30          | 200                                  | 0.343   | 68.6        | 2.74     | 0.63  | Base failure_EQ    |
| 107       | 30                      | 4     | 0         | 2     | 16    | 20                            | 25                         | 0            | 5000        | 0.35  | 0.3   | C_30_4_0_16_25_0_3_3_D  | 2              | 30          | 200                                  | 0.1879  | 37.58       | 1.50     | 0.63  | Base failure_EQ    |
| 108       | 30                      | 8     | 0         | 2     | 16    | 20                            | 25                         | 0            | 5000        | 0.35  | 0.3   | C_30_8_0_16_25_0_3_3_D  | 4              | 30          | 200                                  | N.F.    | N.F.        | N.F.     | 0.63  | Base failure_GR    |
| 109       | 30                      | 2     | 0         | 2     | 2     | 20                            | 50                         | 0            | 10000       | 0.35  | 0.3   | C_30_2_0_2_50_0_3_3_D   | 1              | 30          | 400                                  | 0.436   | 174.4       | 3.49     | 1.25  | Foundation failure |
| 110       | 30                      | 4     | 0         | 2     | 2     | 20                            | 50                         | 0            | 10000       | 0.35  | 0.3   | C_30_4_0_2_50_0_3_3_D   | 2              | 30          | 400                                  | 0.4701  | 188.04      | 3.76     | 1.25  | Foundation failure |
| 111       | 30                      | 8     | 0         | 2     | 2     | 20                            | 50                         | 0            | 10000       | 0.35  | 0.3   | C_30_8_0_2_50_0_3_3_D   | 4              | 30          | 400                                  | 0.3307  | 132.28      | 2.65     | 1.25  | Base failure_EQ    |
| 112       | 30                      | 2     | 0         | 2     | 4     | 20                            | 50                         | 0            | 10000       | 0.35  | 0.3   | C_30_2_0_4_50_0_3_3_D   | 1              | 30          | 400                                  | 0.4284  | 171.36      | 3.43     | 1.25  | Foundation failure |
| 113       | 30                      | 4     | 0         | 2     | 4     | 20                            | 50                         | 0            | 10000       | 0.35  | 0.3   | C_30_4_0_4_50_0_3_3_D   | 2              | 30          | 400                                  | 0.4493  | 179.72      | 3.59     | 1.25  | Foundation failure |
| 114       | 30                      | 8     | 0         | 2     | 4     | 20                            | 50                         | 0            | 10000       | 0.35  | 0.3   | C_30_8_0_4_50_0_3_3_D   | 4              | 30          | 400                                  | 0.3302  | 132.08      | 2.64     | 1.25  | Base failure_EQ    |
| 115       | 30                      | 2     | 0         | 2     | 8     | 20                            | 50                         | 0            | 10000       | 0.35  | 0.3   | C_30_2_0_8_50_0_3_3_D   | 1              | 30          | 400                                  | 0.4126  | 165.04      | 3.30     | 1.25  | Foundation failure |
| 116       | 30                      | 4     | 0         | 2     | 8     | 20                            | 50                         | 0            | 10000       | 0.35  | 0.3   | C_30_4_0_8_50_0_3_3_D   | 2              | 30          | 400                                  | 0.4199  | 167.96      | 3.36     | 1.25  | Foundation failure |
| 117       | 30                      | 8     | 0         | 2     | 8     | 20                            | 50                         | 0            | 10000       | 0.35  | 0.3   | C_30_8_0_8_50_0_3_3_D   | 4              | 30          | 400                                  | 0.3339  | 133.56      | 2.67     | 1.25  | Base failure_EQ    |
| 118       | 30                      | 2     | 0         | 2     | 16    | 20                            | 50                         | 0            | 10000       | 0.35  | 0.3   | C_30_2_0_16_50_0_3_3_D  | 1              | 30          | 400                                  | 0.4241  | 169.64      | 3.39     | 1.25  | Foundation failure |
| 119       | 30                      | 4     | 0         | 2     | 16    | 20                            | 50                         | 0            | 10000       | 0.35  | 0.3   | C_30_4_0_16_50_0_3_3_D  | 2              | 30          | 400                                  | 0.4179  | 167.16      | 3.34     | 1.25  | Base failure_EQ    |
| 120       | 30                      | 8     | 0         | 2     | 16    | 20                            | 50                         | 0            | 10000       | 0.35  | 0.3   | C_30_8_0_16_50_0_3_3_D  | 4              | 30          | 400                                  | 0.3358  | 134.32      | 2.69     | 1.25  | Base failure_EQ    |
| 121       | 30                      | 2     | 0         | 2     | 2     | 20                            | 100                        | 0            | 20000       | 0.35  | 0.3   | C_30_2_0_2_100_0_3_3_D  | 1              | 30          | 800                                  | 0.42125 | 337         | 3.37     | 2.50  | Base failure_EQ    |
| 122       | 30                      | 4     | 0         | 2     | 2     | 20                            | 100                        | 0            | 20000       | 0.35  | 0.3   | C_30_4_0_2_100_0_3_3_D  | 2              | 30          | 800                                  | 0.4281  | 342.48      | 3.42     | 2.50  | Foundation failure |
| 123       | 30                      | 8     | 0         | 2     | 2     | 20                            | 100                        | 0            | 20000       | 0.35  | 0.3   | C_30_8_0_2_100_0_3_3_D  | 4              | 30          | 800                                  | 0.419   | 335.2       | 3.35     | 2.50  | Foundation failure |
| 124       | 30                      | 2     | 0         | 2     | 4     | 20                            | 100                        | 0            | 20000       | 0.35  | 0.3   | C_30_2_0_4_100_0_3_3_D  | 1              | 30          | 800                                  | 0.3992  | 319.56      | 3.19     | 2.50  | Foundation failure |
| 125       | 30                      | 4     | 0         | 2     | 4     | 20                            | 100                        | 0            | 20000       | 0.35  | 0.3   | C_30_4_0_4_100_0_3_3_D  | 2              | 30          | 800                                  | 0.4209  | 336.72      | 3.37     | 2.50  | Foundation failure |
| 126       | 30                      | 8     | 0         | 2     | 4     | 20                            | 100                        | 0            | 20000       | 0.35  | 0.3   | C_30_8_0_4_100_0_3_3_D  | 4              | 30          | 800                                  | 0.4121  | 329.68      | 3.30     | 2.50  | Foundation failure |
| 127       | 30                      | 2     | 0         | 2     | 8     | 20                            | 100                        | 0            | 20000       | 0.35  | 0.3   | C_30_2_0_8_100_0_3_3_D  | 1              | 30          | 800                                  | 0.38625 | 309         | 3.09     | 2.50  | Base failure_EQ    |
| 128       | 30                      | 4     | 0         | 2     | 8     | 20                            | 100                        | 0            | 20000       | 0.35  | 0.3   | C_30_4_0_8_100_0_3_3_D  | 2              | 30          | 800                                  | 0.4153  | 332.24      | 3.32     | 2.50  | Foundation failure |
| 129       | 30                      | 8     | 0         | 2     | 8     | 20                            | 100                        | 0            | 20000       | 0.35  | 0.3   | C_30_8_0_8_100_0_3_3_D  | 4              | 30          | 800                                  | 0.4073  | 325.84      | 3.26     | 2.50  | Foundation failure |
| 130       | 30                      | 2     | 0         | 2     | 16    | 20                            | 100                        | 0            | 20000       | 0.35  | 0.3   | C_30_2_0_16_100_0_3_3_D | 1              | 30          | 800                                  | 0.425   | 340         | 3.40     | 2.50  | Foundation failure |
| 131       | 30                      | 4     | 0         | 2     | 16    | 20                            | 100                        | 0            | 20000       | 0.35  | 0.3   | C_30_4_0_16_100_0_3_3_D | 2              | 30          | 800                                  | 0.3982  | 318.56      | 3.19     | 2.50  | Base failure_EQ    |
| 132       | 30                      | 8     | 0         | 2     | 16    | 20                            | 100                        | 0            | 20000       | 0.35  | 0.3   | C_30_8_0_16_100_0_3_3_D | 4              | 30          | 800                                  | 0.3942  | 315.36      | 3.15     | 2.50  | Base failure_EQ    |
| 133       | 30                      | 2     | 0         | 2     | 2     | 20                            | 200                        | 0            | 40000       | 0.35  | 0.3   | C_30_2_0_2_200_0_3_3_D  | 1              | 30          | 1600                                 | 0.45    | 720         | 3.60     | 5.00  | Base failure_EQ    |
| 134       | 30                      | 4     | 0         | 2     | 2     | 20                            | 200                        | 0            | 40000       | 0.35  | 0.3   | C_30_4_0_2_200_0_3_3_D  | 2              | 30          | 1600                                 | 0.4149  | 663.84      | 3.32     | 5.00  | Base failure_EQ    |
| 135       | 30                      | 8     | 0         | 2     | 2     | 20                            | 200                        | 0            | 40000       | 0.35  | 0.3   | C_30_8_0_2_200_0_3_3_D  | 4              | 30          | 1600                                 | 0.4203  | 672.48      | 3.36     | 5.00  | Base failure_EQ    |
| 136       | 30                      | 2     | 0         | 2     | 4     | 20                            | 200                        | 0            | 40000       | 0.35  | 0.3   | C_30_2_0_4_200_0_3_3_D  | 1              | 30          | 1600                                 | 0.4162  | 665.92      | 3.33     | 5.00  | Base failure_EQ    |
| 137       | 30                      | 4     | 0         | 2     | 4     | 20                            | 200                        | 0            | 40000       | 0.35  | 0.3   | C_30_4_0_4_200_0_3_3_D  | 2              | 30          | 1600                                 | 0.3998  | 639.68      | 3.20     | 5.00  | Base failure_EQ    |
| 138       | 30                      | 8     | 0         | 2     | 4     | 20                            | 200                        | 0            | 40000       | 0.35  | 0.3   | C_30_8_0_4_200_0_3_3_D  | 4              | 30          | 1600                                 | 0.4149  | 663.84      | 3.32     | 5.00  | Base failure_EQ    |
| 139       | 30                      | 2     | 0         | 2     | 8     | 20                            | 200                        | 0            | 40000       | 0.35  | 0.3   | C_30_2_0_8_200_0_3_3_D  | 1              | 30          | 1600                                 | 0.3751  | 600.16      | 3.00     | 5.00  | Base failure_EQ    |
| 140       | 30                      | 4     | 0         | 2     | 8     | 20                            | 200                        | 0            | 40000       | 0.35  | 0.3   | C_30_4_0_8_200_0_3_3_D  | 2              | 30          | 1600                                 | 0.3836  | 613.76      | 3.07     | 5.00  | Base failure_EQ    |
| 141       | 30                      | 8     | 0         | 2     | 8     | 20                            | 200                        | 0            | 40000       | 0.35  | 0.3   | C_30_8_0_8_200_0_3_3_D  | 4              | 30          | 1600                                 | 0.4082  | 653.12      | 3.27     | 5.00  | Base failure_EQ    |
| 142       | 30                      | 2     | 0         | 2     | 16    | 20                            | 200                        | 0            | 40000       | 0.35  | 0.3   | C_30_2_0_16_200_0_3_3_D | 1              | 30          | 1600                                 | 0.4099  | 655.84      | 3.28     | 5.00  | Base failure_EQ    |
| 143       | 30                      | 4     | 0         | 2     | 16    | 20                            | 200                        | 0            | 40000       | 0.35  | 0.3   | C_30_4_0_16_200_0_3_3_D | 2              | 30          | 1600                                 | 0.4096  | 655.36      | 3.28     | 5.00  | Base failure_EQ    |
| 144       | 30                      | 8     | 0         | 2     | 16    | 20                            | 200                        | 0            | 40000       | 0.35  | 0.3   | C_30_8_0_16_200_0_3_3_D | 4              | 30          | 1600                                 | 0.4114  | 658.24      | 3.29     | 5.00  | Base failure_EQ    |

N.F.:Not found.

Base failure\_EQ:Failed due to earthquake.

Base failure\_GR:Failed due to gravity.

Table B.3. List of results of finite elements models created for seismic condition ( $\beta=45^\circ$ )

| Model No. | GEOTECHNICAL PROPERTIES |       |           |       |       |                               | SLOPE SOIL PROPERTIES      |              |             |       |       |                       | SEISMIC EFFECT |             | ANALYSIS RESULTS FOR SEISMIC LOADING |        |             |          |       |                    |
|-----------|-------------------------|-------|-----------|-------|-------|-------------------------------|----------------------------|--------------|-------------|-------|-------|-----------------------|----------------|-------------|--------------------------------------|--------|-------------|----------|-------|--------------------|
|           | $\beta$                 | H (m) | $\lambda$ | B (m) | L (m) | $\gamma$ (kN/m <sup>3</sup> ) | $c_u$ (kN/m <sup>2</sup> ) | $\phi_u$ (°) | $E_u$ (kPa) | $v_u$ | $k_h$ | FILE NAME             | H/B            | $\beta$ (°) | Load                                 | Mstage | $q_r$ (kPa) | $N_{cs}$ | cu/yB | Failure Mode       |
| 1         | 45                      | 2     | 0         | 2     | 2     | 20                            | 25                         | 0            | 5000        | 0.35  | 0.1   | C_45_2_0_2_25_0.1_D   | 1              | 45          | 300                                  | 0.424  | 127.2       | 5.09     | 0.63  | Foundation Failure |
| 2         | 45                      | 4     | 0         | 2     | 2     | 20                            | 25                         | 0            | 5000        | 0.35  | 0.1   | C_45_4_0_2_25_0.1_D   | 2              | 45          | 200                                  | 0.5766 | 115.52      | 4.61     | 0.63  | Base failure_EQ    |
| 3         | 45                      | 8     | 0         | 2     | 2     | 20                            | 25                         | 0            | 5000        | 0.35  | 0.1   | C_45_8_0_2_25_0.1_D   | 4              | 45          | 200                                  | N.F.   | N.F.        | N.F.     | 0.63  | Base failure_GR    |
| 4         | 45                      | 2     | 0         | 2     | 4     | 20                            | 25                         | 0            | 5000        | 0.35  | 0.1   | C_45_2_0_4_25_0.1_D   | 1              | 45          | 200                                  | 0.6649 | 132.98      | 5.32     | 0.63  | Foundation Failure |
| 5         | 45                      | 4     | 0         | 2     | 4     | 20                            | 25                         | 0            | 5000        | 0.35  | 0.1   | C_45_4_0_4_25_0.1_D   | 2              | 45          | 200                                  | 0.5755 | 115.1       | 4.60     | 0.63  | Base failure_EQ    |
| 6         | 45                      | 8     | 0         | 2     | 4     | 20                            | 25                         | 0            | 5000        | 0.35  | 0.1   | C_45_8_0_4_25_0.1_D   | 4              | 45          | 200                                  | N.F.   | N.F.        | N.F.     | 0.63  | Base failure_GR    |
| 7         | 45                      | 2     | 0         | 2     | 8     | 20                            | 25                         | 0            | 5000        | 0.35  | 0.1   | C_45_2_0_8_25_0.1_D   | 1              | 45          | 200                                  | 0.5172 | 103.44      | 4.14     | 0.63  | Foundation Failure |
| 8         | 45                      | 4     | 0         | 2     | 8     | 20                            | 25                         | 0            | 5000        | 0.35  | 0.1   | C_45_4_0_8_25_0.1_D   | 2              | 45          | 200                                  | 0.5335 | 107         | 4.28     | 0.63  | Foundation Failure |
| 9         | 45                      | 8     | 0         | 2     | 8     | 20                            | 25                         | 0            | 5000        | 0.35  | 0.1   | C_45_8_0_8_25_0.1_D   | 4              | 45          | 200                                  | N.F.   | N.F.        | N.F.     | 0.63  | Base failure_GR    |
| 10        | 45                      | 2     | 0         | 2     | 16    | 20                            | 25                         | 0            | 5000        | 0.35  | 0.1   | C_45_2_0_16_25_0.1_D  | 1              | 45          | 200                                  | 0.4842 | 96.84       | 3.87     | 0.63  | Foundation Failure |
| 11        | 45                      | 4     | 0         | 2     | 16    | 20                            | 25                         | 0            | 5000        | 0.35  | 0.1   | C_45_4_0_16_25_0.1_D  | 2              | 45          | 200                                  | 0.5078 | 101.56      | 4.06     | 0.63  | Foundation Failure |
| 12        | 45                      | 8     | 0         | 2     | 16    | 20                            | 25                         | 0            | 5000        | 0.35  | 0.1   | C_45_8_0_16_25_0.1_D  | 4              | 45          | 200                                  | N.F.   | N.F.        | N.F.     | 0.63  | Base failure_GR    |
| 13        | 45                      | 2     | 0         | 2     | 2     | 20                            | 50                         | 0            | 10000       | 0.35  | 0.1   | C_45_2_0_2_50_0.1_D   | 1              | 45          | 600                                  | 0.513  | 307.8       | 6.16     | 1.25  | Foundation Failure |
| 14        | 45                      | 4     | 0         | 2     | 2     | 20                            | 50                         | 0            | 10000       | 0.35  | 0.1   | C_45_4_0_2_50_0.1_D   | 2              | 45          | 600                                  | 0.5028 | 301.68      | 6.03     | 1.25  | Foundation Failure |
| 15        | 45                      | 8     | 0         | 2     | 2     | 20                            | 50                         | 0            | 10000       | 0.35  | 0.1   | C_45_8_0_2_50_0.1_D   | 4              | 45          | 600                                  | 0.728  | 291.2       | 5.82     | 1.25  | Foundation Failure |
| 16        | 45                      | 2     | 0         | 2     | 4     | 20                            | 50                         | 0            | 10000       | 0.35  | 0.1   | C_45_2_0_4_50_0.1_D   | 1              | 45          | 600                                  | 0.4215 | 252.9       | 5.06     | 1.25  | Foundation Failure |
| 17        | 45                      | 4     | 0         | 2     | 4     | 20                            | 50                         | 0            | 10000       | 0.35  | 0.1   | C_45_4_0_4_50_0.1_D   | 2              | 45          | 600                                  | 0.6272 | 250.88      | 5.02     | 1.25  | Foundation Failure |
| 18        | 45                      | 8     | 0         | 2     | 4     | 20                            | 50                         | 0            | 10000       | 0.35  | 0.1   | C_45_8_0_4_50_0.1_D   | 4              | 45          | 600                                  | 0.7145 | 285.8       | 5.72     | 1.25  | Foundation Failure |
| 19        | 45                      | 2     | 0         | 2     | 8     | 20                            | 50                         | 0            | 10000       | 0.35  | 0.1   | C_45_2_0_8_50_0.1_D   | 1              | 45          | 400                                  | 0.5131 | 205.24      | 4.10     | 1.25  | Foundation Failure |
| 20        | 45                      | 4     | 0         | 2     | 8     | 20                            | 50                         | 0            | 10000       | 0.35  | 0.1   | C_45_4_0_8_50_0.1_D   | 2              | 45          | 400                                  | 0.5108 | 204.32      | 4.09     | 1.25  | Foundation Failure |
| 21        | 45                      | 8     | 0         | 2     | 8     | 20                            | 50                         | 0            | 10000       | 0.35  | 0.1   | C_45_8_0_8_50_0.1_D   | 4              | 45          | 400                                  | 0.591  | 236.4       | 4.73     | 1.25  | Foundation Failure |
| 22        | 45                      | 2     | 0         | 2     | 16    | 20                            | 50                         | 0            | 10000       | 0.35  | 0.1   | C_45_2_0_16_50_0.1_D  | 1              | 45          | 1000                                 | 0.6573 | 262.92      | 5.26     | 1.25  | Foundation Failure |
| 23        | 45                      | 4     | 0         | 2     | 16    | 20                            | 50                         | 0            | 10000       | 0.35  | 0.1   | C_45_4_0_16_50_0.1_D  | 2              | 45          | 1000                                 | 0.6016 | 240.64      | 4.81     | 1.25  | Foundation Failure |
| 24        | 45                      | 8     | 0         | 2     | 16    | 20                            | 50                         | 0            | 10000       | 0.35  | 0.1   | C_45_8_0_16_50_0.1_D  | 4              | 45          | 1000                                 | 0.6341 | 253.64      | 5.07     | 1.25  | Foundation Failure |
| 25        | 45                      | 2     | 0         | 2     | 2     | 20                            | 100                        | 0            | 20000       | 0.35  | 0.1   | C_45_2_0_2_100_0.1_D  | 1              | 45          | 1000                                 | 0.5131 | 513.1       | 5.13     | 2.50  | Foundation Failure |
| 26        | 45                      | 4     | 0         | 2     | 2     | 20                            | 100                        | 0            | 20000       | 0.35  | 0.1   | C_45_4_0_2_100_0.1_D  | 2              | 45          | 1000                                 | 0.5269 | 526.9       | 5.27     | 2.50  | Foundation Failure |
| 27        | 45                      | 8     | 0         | 2     | 2     | 20                            | 100                        | 0            | 20000       | 0.35  | 0.1   | C_45_8_0_2_100_0.1_D  | 4              | 45          | 1000                                 | 0.5083 | 508.3       | 5.08     | 2.50  | Foundation Failure |
| 28        | 45                      | 2     | 0         | 2     | 4     | 20                            | 100                        | 0            | 20000       | 0.35  | 0.1   | C_45_2_0_4_100_0.1_D  | 1              | 45          | 800                                  | 0.6533 | 522.64      | 5.23     | 2.50  | Foundation Failure |
| 29        | 45                      | 4     | 0         | 2     | 4     | 20                            | 100                        | 0            | 20000       | 0.35  | 0.1   | C_45_4_0_4_100_0.1_D  | 2              | 45          | 800                                  | 0.6536 | 522.88      | 5.23     | 2.50  | Foundation Failure |
| 30        | 45                      | 8     | 0         | 2     | 4     | 20                            | 100                        | 0            | 20000       | 0.35  | 0.1   | C_45_8_0_4_100_0.1_D  | 4              | 45          | 800                                  | 0.5525 | 442         | 4.42     | 2.50  | Foundation Failure |
| 31        | 45                      | 2     | 0         | 2     | 8     | 20                            | 100                        | 0            | 20000       | 0.35  | 0.1   | C_45_2_0_8_100_0.1_D  | 1              | 45          | 800                                  | 0.6103 | 488.24      | 4.88     | 2.50  | Foundation Failure |
| 32        | 45                      | 4     | 0         | 2     | 8     | 20                            | 100                        | 0            | 20000       | 0.35  | 0.1   | C_45_4_0_8_100_0.1_D  | 2              | 45          | 800                                  | 0.5876 | 470.08      | 4.70     | 2.50  | Foundation Failure |
| 33        | 45                      | 8     | 0         | 2     | 8     | 20                            | 100                        | 0            | 20000       | 0.35  | 0.1   | C_45_8_0_8_100_0.1_D  | 4              | 45          | 800                                  | 0.6103 | 488.24      | 4.88     | 2.50  | Foundation Failure |
| 34        | 45                      | 2     | 0         | 2     | 16    | 20                            | 100                        | 0            | 20000       | 0.35  | 0.1   | C_45_2_0_16_100_0.1_D | 1              | 45          | 800                                  | 0.6731 | 538.48      | 5.38     | 2.50  | Foundation Failure |
| 35        | 45                      | 4     | 0         | 2     | 16    | 20                            | 100                        | 0            | 20000       | 0.35  | 0.1   | C_45_4_0_16_100_0.1_D | 2              | 45          | 800                                  | 0.6364 | 509.12      | 5.09     | 2.50  | Foundation Failure |
| 36        | 45                      | 8     | 0         | 2     | 16    | 20                            | 100                        | 0            | 20000       | 0.35  | 0.1   | C_45_8_0_16_100_0.1_D | 4              | 45          | 800                                  | 0.6621 | 529.68      | 5.30     | 2.50  | Foundation Failure |
| 37        | 45                      | 2     | 0         | 2     | 2     | 20                            | 200                        | 0            | 40000       | 0.35  | 0.1   | C_45_2_0_2_200_0.1_D  | 1              | 45          | 1600                                 | 0.7747 | 1239.52     | 6.20     | 5.00  | Foundation Failure |
| 38        | 45                      | 4     | 0         | 2     | 2     | 20                            | 200                        | 0            | 40000       | 0.35  | 0.1   | C_45_4_0_2_200_0.1_D  | 2              | 45          | 1600                                 | 0.7707 | 1233.12     | 6.17     | 5.00  | Foundation Failure |
| 39        | 45                      | 8     | 0         | 2     | 2     | 20                            | 200                        | 0            | 40000       | 0.35  | 0.1   | C_45_8_0_2_200_0.1_D  | 4              | 45          | 1600                                 | 0.7383 | 1181.28     | 5.91     | 5.00  | Foundation Failure |
| 40        | 45                      | 2     | 0         | 2     | 4     | 20                            | 200                        | 0            | 40000       | 0.35  | 0.1   | C_45_2_0_4_200_0.1_D  | 1              | 45          | 1600                                 | 0.6649 | 1063.84     | 5.32     | 5.00  | Foundation Failure |
| 41        | 45                      | 4     | 0         | 2     | 4     | 20                            | 200                        | 0            | 40000       | 0.35  | 0.1   | C_45_4_0_4_200_0.1_D  | 2              | 45          | 1600                                 | 0.6514 | 1042.24     | 5.21     | 5.00  | Foundation Failure |
| 42        | 45                      | 8     | 0         | 2     | 4     | 20                            | 200                        | 0            | 40000       | 0.35  | 0.1   | C_45_8_0_4_200_0.1_D  | 4              | 45          | 1600                                 | 0.7333 | 1173.28     | 5.87     | 5.00  | Foundation Failure |
| 43        | 45                      | 2     | 0         | 2     | 8     | 20                            | 200                        | 0            | 40000       | 0.35  | 0.1   | C_45_2_0_8_200_0.1_D  | 1              | 45          | 1600                                 | 0.614  | 982.4       | 4.91     | 5.00  | Foundation Failure |
| 44        | 45                      | 4     | 0         | 2     | 8     | 20                            | 200                        | 0            | 40000       | 0.35  | 0.1   | C_45_4_0_8_200_0.1_D  | 2              | 45          | 1600                                 | 0.6078 | 972.48      | 4.86     | 5.00  | Foundation Failure |
| 45        | 45                      | 8     | 0         | 2     | 8     | 20                            | 200                        | 0            | 40000       | 0.35  | 0.1   | C_45_8_0_8_200_0.1_D  | 4              | 45          | 1600                                 | 0.7325 | 1172        | 5.86     | 5.00  | Foundation Failure |
| 46        | 45                      | 2     | 0         | 2     | 16    | 20                            | 200                        | 0            | 40000       | 0.35  | 0.1   | C_45_2_0_16_200_0.1_D | 1              | 45          | 1600                                 | 0.6935 | 1109.6      | 5.55     | 5.00  | Foundation Failure |
| 47        | 45                      | 4     | 0         | 2     | 16    | 20                            | 200                        | 0            | 40000       | 0.35  | 0.1   | C_45_4_0_16_200_0.1_D | 2              | 45          | 1600                                 | 0.6526 | 1044.16     | 5.22     | 5.00  | Foundation Failure |
| 48        | 45                      | 8     | 0         | 2     | 16    | 20                            | 200                        | 0            | 40000       | 0.35  | 0.1   | C_45_8_0_16_200_0.1_D | 4              | 45          | 1600                                 | 0.6728 | 1076.48     | 5.38     | 5.00  | Foundation Failure |

N.F.: Not found.

Base failure EQ: Failed due to earthquake.

Base failure GR: Failed due to gravity.

Table B.3. List of results of finite elements models created for seismic condition ( $\beta= 45^\circ$ )

(Cont.).

| Model No. | GEOTECHNICAL PROPERTIES |       |           |       |       |                               |                            |              |             |       | SLOPE SOIL PROPERTIES |                       |     |             |      | SEISMIC EFFECT |             | ANALYSIS RESULTS FOR SEISMIC LOADING |       |                    |  |  |  |  |
|-----------|-------------------------|-------|-----------|-------|-------|-------------------------------|----------------------------|--------------|-------------|-------|-----------------------|-----------------------|-----|-------------|------|----------------|-------------|--------------------------------------|-------|--------------------|--|--|--|--|
|           | $\beta$ (°)             | H (m) | $\lambda$ | B (m) | L (m) | $\gamma$ (kN/m <sup>3</sup> ) | $c_u$ (kN/m <sup>2</sup> ) | $\phi_h$ (°) | $E_u$ (kPa) | $v_u$ | $k_h$                 | FILE NAME             | H/B | $\beta$ (°) | Load | Mstage         | $q_r$ (kPa) | $N_e$                                | cu/yB | Failure Mode       |  |  |  |  |
| 49        | 45                      | 2     | 0         | 2     | 2     | 20                            | 25                         | 0            | 5000        | 0.35  | 0.2                   | C_45_2_0_2_25_0_2_D   | 1   | 45          | 200  | 0.5204         | 104.08      | 4.16                                 | 0.63  | Base failure_EQ    |  |  |  |  |
| 50        | 45                      | 4     | 0         | 2     | 2     | 20                            | 25                         | 0            | 5000        | 0.35  | 0.2                   | C_45_4_0_2_25_0_2_D   | 2   | 45          | 200  | 0.288          | 57.6        | 2.30                                 | 0.63  | Base failure_EQ    |  |  |  |  |
| 51        | 45                      | 8     | 0         | 2     | 2     | 20                            | 25                         | 0            | 5000        | 0.35  | 0.2                   | C_45_8_0_2_25_0_2_D   | 4   | 45          | 200  | N.F.           | N.F.        | N.F.                                 | 0.63  | Base failure_GR    |  |  |  |  |
| 52        | 45                      | 2     | 0         | 2     | 4     | 20                            | 25                         | 0            | 5000        | 0.35  | 0.2                   | C_45_2_0_4_25_0_2_D   | 1   | 45          | 300  | 0.3283         | 98.49       | 3.94                                 | 0.63  | Foundation Failure |  |  |  |  |
| 53        | 45                      | 4     | 0         | 2     | 4     | 20                            | 25                         | 0            | 5000        | 0.35  | 0.2                   | C_45_4_0_4_25_0_2_D   | 2   | 45          | 200  | 0.2874         | 57.48       | 2.30                                 | 0.63  | Base failure_EQ    |  |  |  |  |
| 54        | 45                      | 8     | 0         | 2     | 4     | 20                            | 25                         | 0            | 5000        | 0.35  | 0.2                   | C_45_8_0_4_25_0_2_D   | 4   | 45          | 200  | N.F.           | N.F.        | N.F.                                 | 0.63  | Base failure_GR    |  |  |  |  |
| 55        | 45                      | 2     | 0         | 2     | 8     | 20                            | 25                         | 0            | 5000        | 0.35  | 0.2                   | C_45_2_0_8_25_0_2_D   | 1   | 45          | 200  | 0.4752         | 95.04       | 3.80                                 | 0.63  | Foundation Failure |  |  |  |  |
| 56        | 45                      | 4     | 0         | 2     | 8     | 20                            | 25                         | 0            | 5000        | 0.35  | 0.2                   | C_45_4_0_8_25_0_2_D   | 2   | 45          | 200  | 0.2877         | 57.54       | 2.30                                 | 0.63  | Base failure_EQ    |  |  |  |  |
| 57        | 45                      | 8     | 0         | 2     | 8     | 20                            | 25                         | 0            | 5000        | 0.35  | 0.2                   | C_45_8_0_8_25_0_2_D   | 4   | 45          | 200  | N.F.           | N.F.        | N.F.                                 | 0.63  | Base failure_GR    |  |  |  |  |
| 58        | 45                      | 2     | 0         | 2     | 16    | 20                            | 25                         | 0            | 5000        | 0.35  | 0.2                   | C_45_2_0_16_25_0_2_D  | 1   | 45          | 200  | 0.5253         | 105.06      | 4.20                                 | 0.63  | Base failure_EQ    |  |  |  |  |
| 59        | 45                      | 4     | 0         | 2     | 16    | 20                            | 25                         | 0            | 5000        | 0.35  | 0.2                   | C_45_4_0_16_25_0_2_D  | 2   | 45          | 200  | 0.2931         | 58.62       | 2.34                                 | 0.63  | Base failure_EQ    |  |  |  |  |
| 60        | 45                      | 8     | 0         | 2     | 16    | 20                            | 25                         | 0            | 5000        | 0.35  | 0.2                   | C_45_8_0_16_25_0_2_D  | 4   | 45          | 200  | N.F.           | N.F.        | N.F.                                 | 0.63  | Base failure_GR    |  |  |  |  |
| 61        | 45                      | 2     | 0         | 2     | 2     | 20                            | 50                         | 0            | 10000       | 0.35  | 0.2                   | C_45_2_0_2_50_0_2_D   | 1   | 45          | 600  | 0.346          | 207.6       | 4.15                                 | 1.25  | Foundation Failure |  |  |  |  |
| 62        | 45                      | 4     | 0         | 2     | 2     | 20                            | 50                         | 0            | 10000       | 0.35  | 0.2                   | C_45_4_0_2_50_0_2_D   | 2   | 45          | 400  | 0.5188         | 206.32      | 4.13                                 | 1.25  | Foundation Failure |  |  |  |  |
| 63        | 45                      | 8     | 0         | 2     | 2     | 20                            | 50                         | 0            | 10000       | 0.35  | 0.2                   | C_45_8_0_2_50_0_2_D   | 4   | 45          | 400  | 0.5341         | 213.64      | 4.27                                 | 1.25  | Base failure_EQ    |  |  |  |  |
| 64        | 45                      | 2     | 0         | 2     | 4     | 20                            | 50                         | 0            | 10000       | 0.35  | 0.2                   | C_45_2_0_4_50_0_2_D   | 1   | 45          | 400  | 0.4554         | 182.16      | 3.64                                 | 1.25  | Foundation Failure |  |  |  |  |
| 65        | 45                      | 4     | 0         | 2     | 4     | 20                            | 50                         | 0            | 10000       | 0.35  | 0.2                   | C_45_4_0_4_50_0_2_D   | 2   | 45          | 400  | 0.4729         | 189.16      | 3.78                                 | 1.25  | Foundation Failure |  |  |  |  |
| 66        | 45                      | 8     | 0         | 2     | 4     | 20                            | 50                         | 0            | 10000       | 0.35  | 0.2                   | C_45_8_0_4_50_0_2_D   | 4   | 45          | 400  | 0.5341         | 213.64      | 4.27                                 | 1.25  | Base failure_EQ    |  |  |  |  |
| 67        | 45                      | 2     | 0         | 2     | 8     | 20                            | 50                         | 0            | 10000       | 0.35  | 0.2                   | C_45_2_0_8_50_0_2_D   | 1   | 45          | 400  | 0.424          | 169.6       | 3.39                                 | 1.25  | Foundation Failure |  |  |  |  |
| 68        | 45                      | 4     | 0         | 2     | 8     | 20                            | 50                         | 0            | 10000       | 0.35  | 0.2                   | C_45_4_0_8_50_0_2_D   | 2   | 45          | 400  | 0.4224         | 168.96      | 3.38                                 | 1.25  | Foundation Failure |  |  |  |  |
| 69        | 45                      | 8     | 0         | 2     | 8     | 20                            | 50                         | 0            | 10000       | 0.35  | 0.2                   | C_45_8_0_8_50_0_2_D   | 4   | 45          | 400  | 0.5324         | 212.96      | 4.26                                 | 1.25  | Base failure_EQ    |  |  |  |  |
| 70        | 45                      | 2     | 0         | 2     | 16    | 20                            | 50                         | 0            | 10000       | 0.35  | 0.2                   | C_45_2_0_16_50_0_2_D  | 1   | 45          | 400  | 0.4475         | 179         | 3.58                                 | 1.25  | Foundation Failure |  |  |  |  |
| 71        | 45                      | 4     | 0         | 2     | 16    | 20                            | 50                         | 0            | 10000       | 0.35  | 0.2                   | C_45_4_0_16_50_0_2_D  | 2   | 45          | 400  | 0.4424         | 176.96      | 3.54                                 | 1.25  | Foundation Failure |  |  |  |  |
| 72        | 45                      | 8     | 0         | 2     | 16    | 20                            | 50                         | 0            | 10000       | 0.35  | 0.2                   | C_45_8_0_16_50_0_2_D  | 4   | 45          | 400  | 0.5406         | 216.24      | 4.32                                 | 1.25  | Base failure_EQ    |  |  |  |  |
| 73        | 45                      | 2     | 0         | 2     | 2     | 20                            | 100                        | 0            | 20000       | 0.35  | 0.2                   | C_45_2_0_2_100_0_2_D  | 1   | 45          | 1000 | 0.4186         | 418.6       | 4.19                                 | 2.50  | Foundation Failure |  |  |  |  |
| 74        | 45                      | 4     | 0         | 2     | 2     | 20                            | 100                        | 0            | 20000       | 0.35  | 0.2                   | C_45_4_0_2_100_0_2_D  | 2   | 45          | 800  | 0.5087         | 406.96      | 4.07                                 | 2.50  | Foundation Failure |  |  |  |  |
| 75        | 45                      | 8     | 0         | 2     | 2     | 20                            | 100                        | 0            | 20000       | 0.35  | 0.2                   | C_45_8_0_2_100_0_2_D  | 4   | 45          | 1000 | 0.4175         | 417.5       | 4.18                                 | 2.50  | Foundation Failure |  |  |  |  |
| 76        | 45                      | 2     | 0         | 2     | 4     | 20                            | 100                        | 0            | 20000       | 0.35  | 0.2                   | C_45_2_0_4_100_0_2_D  | 1   | 45          | 800  | 0.4827         | 386.16      | 3.86                                 | 2.50  | Foundation Failure |  |  |  |  |
| 77        | 45                      | 4     | 0         | 2     | 4     | 20                            | 100                        | 0            | 20000       | 0.35  | 0.2                   | C_45_4_0_4_100_0_2_D  | 2   | 45          | 800  | 0.5695         | 455.6       | 4.56                                 | 2.50  | Foundation Failure |  |  |  |  |
| 78        | 45                      | 8     | 0         | 2     | 4     | 20                            | 100                        | 0            | 20000       | 0.35  | 0.2                   | C_45_8_0_4_100_0_2_D  | 4   | 45          | 800  | 0.5219         | 417.52      | 4.18                                 | 2.50  | Foundation Failure |  |  |  |  |
| 79        | 45                      | 2     | 0         | 2     | 8     | 20                            | 100                        | 0            | 20000       | 0.35  | 0.2                   | C_45_2_0_8_100_0_2_D  | 1   | 45          | 800  | 0.4449         | 355.92      | 3.56                                 | 2.50  | Foundation Failure |  |  |  |  |
| 80        | 45                      | 4     | 0         | 2     | 8     | 20                            | 100                        | 0            | 20000       | 0.35  | 0.2                   | C_45_4_0_8_100_0_2_D  | 2   | 45          | 800  | 0.4451         | 356.08      | 3.56                                 | 2.50  | Foundation Failure |  |  |  |  |
| 81        | 45                      | 8     | 0         | 2     | 8     | 20                            | 100                        | 0            | 20000       | 0.35  | 0.2                   | C_45_8_0_8_100_0_2_D  | 4   | 45          | 800  | 0.4803         | 384.24      | 3.84                                 | 2.50  | Foundation Failure |  |  |  |  |
| 82        | 45                      | 2     | 0         | 2     | 16    | 20                            | 100                        | 0            | 20000       | 0.35  | 0.2                   | C_45_2_0_16_100_0_2_D | 1   | 45          | 800  | 0.5913         | 473.04      | 4.73                                 | 2.50  | Foundation Failure |  |  |  |  |
| 83        | 45                      | 4     | 0         | 2     | 16    | 20                            | 100                        | 0            | 20000       | 0.35  | 0.2                   | C_45_4_0_16_100_0_2_D | 2   | 45          | 800  | 0.5655         | 452.4       | 4.52                                 | 2.50  | Foundation Failure |  |  |  |  |
| 84        | 45                      | 8     | 0         | 2     | 16    | 20                            | 100                        | 0            | 20000       | 0.35  | 0.2                   | C_45_8_0_16_100_0_2_D | 4   | 45          | 800  | 0.5696         | 455.68      | 4.56                                 | 2.50  | Foundation Failure |  |  |  |  |
| 85        | 45                      | 2     | 0         | 2     | 2     | 20                            | 200                        | 0            | 40000       | 0.35  | 0.2                   | C_45_2_0_2_200_0_2_D  | 1   | 45          | 1600 | 0.7747         | 1239.52     | 6.20                                 | 5.00  | Foundation Failure |  |  |  |  |
| 86        | 45                      | 4     | 0         | 2     | 2     | 20                            | 200                        | 0            | 40000       | 0.35  | 0.2                   | C_45_4_0_2_200_0_2_D  | 2   | 45          | 1600 | 0.5299         | 847.84      | 4.24                                 | 5.00  | Foundation Failure |  |  |  |  |
| 87        | 45                      | 8     | 0         | 2     | 2     | 20                            | 200                        | 0            | 40000       | 0.35  | 0.2                   | C_45_8_0_2_200_0_2_D  | 4   | 45          | 1600 | 0.6085         | 973.6       | 4.87                                 | 5.00  | Foundation Failure |  |  |  |  |
| 88        | 45                      | 2     | 0         | 2     | 4     | 20                            | 200                        | 0            | 40000       | 0.35  | 0.2                   | C_45_2_0_4_200_0_2_D  | 1   | 45          | 1600 | 0.5712         | 913.92      | 4.57                                 | 5.00  | Foundation Failure |  |  |  |  |
| 89        | 45                      | 4     | 0         | 2     | 4     | 20                            | 200                        | 0            | 40000       | 0.35  | 0.2                   | C_45_4_0_4_200_0_2_D  | 2   | 45          | 1600 | 0.5693         | 910.88      | 4.55                                 | 5.00  | Foundation Failure |  |  |  |  |
| 90        | 45                      | 8     | 0         | 2     | 4     | 20                            | 200                        | 0            | 40000       | 0.35  | 0.2                   | C_45_8_0_4_200_0_2_D  | 4   | 45          | 1600 | 0.6073         | 971.68      | 4.86                                 | 5.00  | Foundation Failure |  |  |  |  |
| 91        | 45                      | 2     | 0         | 2     | 8     | 20                            | 200                        | 0            | 40000       | 0.35  | 0.2                   | C_45_2_0_8_200_0_2_D  | 1   | 45          | 1600 | 0.5226         | 836.16      | 4.18                                 | 5.00  | Foundation Failure |  |  |  |  |
| 92        | 45                      | 4     | 0         | 2     | 8     | 20                            | 200                        | 0            | 40000       | 0.35  | 0.2                   | C_45_4_0_8_200_0_2_D  | 2   | 45          | 1600 | 0.5115         | 818.4       | 4.09                                 | 5.00  | Foundation Failure |  |  |  |  |
| 93        | 45                      | 8     | 0         | 2     | 8     | 20                            | 200                        | 0            | 40000       | 0.35  | 0.2                   | C_45_8_0_8_200_0_2_D  | 4   | 45          | 1600 | 0.6051         | 968.16      | 4.84                                 | 5.00  | Foundation Failure |  |  |  |  |
| 94        | 45                      | 2     | 0         | 2     | 16    | 20                            | 200                        | 0            | 40000       | 0.35  | 0.2                   | C_45_2_0_16_200_0_2_D | 1   | 45          | 1600 | 0.5958         | 953.28      | 4.77                                 | 5.00  | Foundation Failure |  |  |  |  |
| 95        | 45                      | 4     | 0         | 2     | 16    | 20                            | 200                        | 0            | 40000       | 0.35  | 0.2                   | C_45_4_0_16_200_0_2_D | 2   | 45          | 1600 | 0.5748         | 919.68      | 4.60                                 | 5.00  | Foundation Failure |  |  |  |  |
| 96        | 45                      | 8     | 0         | 2     | 16    | 20                            | 200                        | 0            | 40000       | 0.35  | 0.2                   | C_45_8_0_16_200_0_2_D | 4   | 45          | 1600 | 0.5791         | 926.56      | 4.63                                 | 5.00  | Foundation Failure |  |  |  |  |

N.F.:Not found.  
 Base failure EQ:Failed due to earthquake.  
 Base failure GR:Failed due to gravity.

Table B.3. List of results of finite elements models created for seismic condition ( $\beta= 45^\circ$ )

(Cont.).

| Model No. | GEOTECHNICAL PROPERTIES |       |           |       |       |                               | SLOPE SOIL PROPERTIES      |              |             |       |       |  | SEISMIC EFFECT |             | ANALYSIS RESULTS FOR SEISMIC LOADING |         |             |          |       |                    |
|-----------|-------------------------|-------|-----------|-------|-------|-------------------------------|----------------------------|--------------|-------------|-------|-------|--|----------------|-------------|--------------------------------------|---------|-------------|----------|-------|--------------------|
|           | $\beta$ (°)             | H (m) | $\lambda$ | B (m) | L (m) | $\gamma$ (kN/m <sup>3</sup> ) | $c_u$ (kN/m <sup>2</sup> ) | $\phi_u$ (°) | $E_u$ (kPa) | $v_u$ | $k_h$ |  | H/B            | $\beta$ (°) | Load                                 | Mstage  | $q_r$ (kPa) | $N_{e1}$ | cu/yB | Failure Mode       |
| 97        | 45                      | 2     | 0         | 2     | 2     | 20                            | 25                         | 0            | 5000        | 0.35  | 0.3   |  | 1              | 45          | 200                                  | 0.3472  | 69.44       | 2.78     | 0.63  | Base failure_EQ    |
| 98        | 45                      | 4     | 0         | 2     | 2     | 20                            | 25                         | 0            | 5000        | 0.35  | 0.3   |  | 2              | 45          | 200                                  | 0.1919  | 38.38       | 1.54     | 0.63  | Base failure_EQ    |
| 99        | 45                      | 8     | 0         | 2     | 2     | 20                            | 25                         | 0            | 5000        | 0.35  | 0.3   |  | 4              | 45          | 200                                  | N.F.    | N.F.        | N.F.     | 0.63  | Base failure_GR    |
| 100       | 45                      | 2     | 0         | 2     | 4     | 20                            | 25                         | 0            | 5000        | 0.35  | 0.3   |  | 1              | 45          | 200                                  | 0.3466  | 69.32       | 2.77     | 0.63  | Base failure_EQ    |
| 101       | 45                      | 4     | 0         | 2     | 4     | 20                            | 25                         | 0            | 5000        | 0.35  | 0.3   |  | 2              | 45          | 200                                  | 0.1919  | 38.38       | 1.54     | 0.63  | Base failure_EQ    |
| 102       | 45                      | 8     | 0         | 2     | 4     | 20                            | 25                         | 0            | 5000        | 0.35  | 0.3   |  | 4              | 45          | 200                                  | N.F.    | N.F.        | N.F.     | 0.63  | Base failure_GR    |
| 103       | 45                      | 2     | 0         | 2     | 8     | 20                            | 25                         | 0            | 5000        | 0.35  | 0.3   |  | 1              | 45          | 200                                  | 0.3457  | 69.14       | 2.77     | 0.63  | Base failure_EQ    |
| 104       | 45                      | 4     | 0         | 2     | 8     | 20                            | 25                         | 0            | 5000        | 0.35  | 0.3   |  | 2              | 45          | 200                                  | 0.1919  | 38.38       | 1.54     | 0.63  | Base failure_EQ    |
| 105       | 45                      | 8     | 0         | 2     | 8     | 20                            | 25                         | 0            | 5000        | 0.35  | 0.3   |  | 4              | 45          | 200                                  | N.F.    | N.F.        | N.F.     | 0.63  | Base failure_GR    |
| 106       | 45                      | 2     | 0         | 2     | 16    | 20                            | 25                         | 0            | 5000        | 0.35  | 0.3   |  | 1              | 45          | 200                                  | 0.345   | 69          | 2.76     | 0.63  | Base failure_EQ    |
| 107       | 45                      | 4     | 0         | 2     | 16    | 20                            | 25                         | 0            | 5000        | 0.35  | 0.3   |  | 2              | 45          | 200                                  | 0.1954  | 39.08       | 1.56     | 0.63  | Base failure_EQ    |
| 108       | 45                      | 8     | 0         | 2     | 16    | 20                            | 25                         | 0            | 5000        | 0.35  | 0.3   |  | 4              | 45          | 200                                  | N.F.    | N.F.        | N.F.     | 0.63  | Base failure_GR    |
| 109       | 45                      | 2     | 0         | 2     | 2     | 20                            | 50                         | 0            | 10000       | 0.35  | 0.3   |  | 1              | 45          | 600                                  | 0.3169  | 190.14      | 3.80     | 1.25  | Foundation Failure |
| 110       | 45                      | 4     | 0         | 2     | 2     | 20                            | 50                         | 0            | 10000       | 0.35  | 0.3   |  | 2              | 45          | 400                                  | 0.4255  | 170.2       | 3.40     | 1.25  | Foundation Failure |
| 111       | 45                      | 8     | 0         | 2     | 2     | 20                            | 50                         | 0            | 10000       | 0.35  | 0.3   |  | 4              | 45          | 400                                  | 0.3561  | 142.44      | 2.85     | 1.25  | Base failure_EQ    |
| 112       | 45                      | 2     | 0         | 2     | 4     | 20                            | 50                         | 0            | 10000       | 0.35  | 0.3   |  | 1              | 45          | 600                                  | 0.2869  | 172.14      | 3.44     | 1.25  | Foundation Failure |
| 113       | 45                      | 4     | 0         | 2     | 4     | 20                            | 50                         | 0            | 10000       | 0.35  | 0.3   |  | 2              | 45          | 400                                  | 0.3919  | 156.76      | 3.14     | 1.25  | Foundation Failure |
| 114       | 45                      | 8     | 0         | 2     | 4     | 20                            | 50                         | 0            | 10000       | 0.35  | 0.3   |  | 4              | 45          | 400                                  | 0.3561  | 142.44      | 2.85     | 1.25  | Base failure_EQ    |
| 115       | 45                      | 2     | 0         | 2     | 8     | 20                            | 50                         | 0            | 10000       | 0.35  | 0.3   |  | 1              | 45          | 400                                  | 0.3791  | 151.64      | 3.03     | 1.25  | Foundation Failure |
| 116       | 45                      | 4     | 0         | 2     | 8     | 20                            | 50                         | 0            | 10000       | 0.35  | 0.3   |  | 2              | 45          | 400                                  | 0.3825  | 153         | 3.06     | 1.25  | Foundation Failure |
| 117       | 45                      | 8     | 0         | 2     | 8     | 20                            | 50                         | 0            | 10000       | 0.35  | 0.3   |  | 4              | 45          | 400                                  | 0.3546  | 141.84      | 2.84     | 1.25  | Base failure_EQ    |
| 118       | 45                      | 2     | 0         | 2     | 16    | 20                            | 50                         | 0            | 10000       | 0.35  | 0.3   |  | 1              | 45          | 400                                  | 0.3714  | 148.56      | 2.97     | 1.25  | Foundation Failure |
| 119       | 45                      | 4     | 0         | 2     | 16    | 20                            | 50                         | 0            | 10000       | 0.35  | 0.3   |  | 2              | 45          | 400                                  | 0.3728  | 149.12      | 2.98     | 1.25  | Foundation Failure |
| 120       | 45                      | 8     | 0         | 2     | 16    | 20                            | 50                         | 0            | 10000       | 0.35  | 0.3   |  | 4              | 45          | 400                                  | 0.3596  | 143.84      | 2.88     | 1.25  | Base failure_EQ    |
| 121       | 45                      | 2     | 0         | 2     | 2     | 20                            | 100                        | 0            | 20000       | 0.35  | 0.3   |  | 1              | 45          | 800                                  | 0.4472  | 357.76      | 3.58     | 2.50  | Foundation Failure |
| 122       | 45                      | 4     | 0         | 2     | 2     | 20                            | 100                        | 0            | 20000       | 0.35  | 0.3   |  | 2              | 45          | 800                                  | 0.4472  | 357.76      | 3.58     | 2.50  | Foundation Failure |
| 123       | 45                      | 8     | 0         | 2     | 2     | 20                            | 100                        | 0            | 20000       | 0.35  | 0.3   |  | 4              | 45          | 800                                  | 0.4208  | 336.64      | 3.37     | 2.50  | Foundation Failure |
| 124       | 45                      | 2     | 0         | 2     | 4     | 20                            | 100                        | 0            | 20000       | 0.35  | 0.3   |  | 1              | 45          | 800                                  | 0.39625 | 317         | 3.17     | 2.50  | Foundation Failure |
| 125       | 45                      | 4     | 0         | 2     | 4     | 20                            | 100                        | 0            | 20000       | 0.35  | 0.3   |  | 2              | 45          | 800                                  | 0.4344  | 347.52      | 3.48     | 2.50  | Foundation Failure |
| 126       | 45                      | 8     | 0         | 2     | 4     | 20                            | 100                        | 0            | 20000       | 0.35  | 0.3   |  | 4              | 45          | 800                                  | 0.3991  | 319.28      | 3.19     | 2.50  | Foundation Failure |
| 127       | 45                      | 2     | 0         | 2     | 8     | 20                            | 100                        | 0            | 20000       | 0.35  | 0.3   |  | 1              | 45          | 800                                  | 0.3726  | 298.08      | 2.98     | 2.50  | Foundation Failure |
| 128       | 45                      | 4     | 0         | 2     | 8     | 20                            | 100                        | 0            | 20000       | 0.35  | 0.3   |  | 2              | 45          | 800                                  | 0.4308  | 344.64      | 3.45     | 2.50  | Foundation Failure |
| 129       | 45                      | 8     | 0         | 2     | 8     | 20                            | 100                        | 0            | 20000       | 0.35  | 0.3   |  | 4              | 45          | 800                                  | 0.3744  | 299.52      | 3.00     | 2.50  | Foundation Failure |
| 130       | 45                      | 2     | 0         | 2     | 16    | 20                            | 100                        | 0            | 20000       | 0.35  | 0.3   |  | 1              | 45          | 800                                  | 0.3894  | 311.52      | 3.12     | 2.50  | Foundation Failure |
| 131       | 45                      | 4     | 0         | 2     | 16    | 20                            | 100                        | 0            | 20000       | 0.35  | 0.3   |  | 2              | 45          | 800                                  | 0.3841  | 307.28      | 3.07     | 2.50  | Foundation Failure |
| 132       | 45                      | 8     | 0         | 2     | 16    | 20                            | 100                        | 0            | 20000       | 0.35  | 0.3   |  | 4              | 45          | 800                                  | 0.3785  | 302.8       | 3.03     | 2.50  | Foundation Failure |
| 133       | 45                      | 2     | 0         | 2     | 2     | 20                            | 200                        | 0            | 40000       | 0.35  | 0.3   |  | 1              | 45          | 1600                                 | 0.3773  | 679.14      | 3.40     | 5.00  | Foundation Failure |
| 134       | 45                      | 4     | 0         | 2     | 2     | 20                            | 200                        | 0            | 40000       | 0.35  | 0.3   |  | 2              | 45          | 1600                                 | 0.4287  | 685.92      | 3.43     | 5.00  | Foundation Failure |
| 135       | 45                      | 8     | 0         | 2     | 2     | 20                            | 200                        | 0            | 40000       | 0.35  | 0.3   |  | 4              | 45          | 1600                                 | 0.4222  | 675.92      | 3.38     | 5.00  | Foundation Failure |
| 136       | 45                      | 2     | 0         | 2     | 4     | 20                            | 200                        | 0            | 40000       | 0.35  | 0.3   |  | 1              | 45          | 1600                                 | 0.4112  | 657.92      | 3.29     | 5.00  | Base failure_EQ    |
| 137       | 45                      | 4     | 0         | 2     | 4     | 20                            | 200                        | 0            | 40000       | 0.35  | 0.3   |  | 2              | 45          | 1600                                 | 0.4119  | 659.04      | 3.30     | 5.00  | Base failure_EQ    |
| 138       | 45                      | 8     | 0         | 2     | 4     | 20                            | 200                        | 0            | 40000       | 0.35  | 0.3   |  | 4              | 45          | 1600                                 | 0.4049  | 647.84      | 3.24     | 5.00  | Foundation Failure |
| 139       | 45                      | 2     | 0         | 2     | 8     | 20                            | 200                        | 0            | 40000       | 0.35  | 0.3   |  | 1              | 45          | 1600                                 | 0.4065  | 650.4       | 3.25     | 5.00  | Foundation Failure |
| 140       | 45                      | 4     | 0         | 2     | 8     | 20                            | 200                        | 0            | 40000       | 0.35  | 0.3   |  | 2              | 45          | 1600                                 | 0.4092  | 654.72      | 3.27     | 5.00  | Foundation Failure |
| 141       | 45                      | 8     | 0         | 2     | 8     | 20                            | 200                        | 0            | 40000       | 0.35  | 0.3   |  | 4              | 45          | 1600                                 | 0.3671  | 587.36      | 2.94     | 5.00  | Base failure_EQ    |
| 142       | 45                      | 2     | 0         | 2     | 16    | 20                            | 200                        | 0            | 40000       | 0.35  | 0.3   |  | 1              | 45          | 1600                                 | 0.3479  | 556.64      | 2.78     | 5.00  | Base failure_EQ    |
| 143       | 45                      | 4     | 0         | 2     | 16    | 20                            | 200                        | 0            | 40000       | 0.35  | 0.3   |  | 2              | 45          | 1600                                 | 0.339   | 542.4       | 2.71     | 5.00  | Foundation Failure |
| 144       | 45                      | 8     | 0         | 2     | 16    | 20                            | 200                        | 0            | 40000       | 0.35  | 0.3   |  | 4              | 45          | 1600                                 | 0.415   | 664         | 3.32     | 5.00  | Foundation Failure |

N.F.:Not found.  
 Base failure\_EQ:Failed due to earthquake.  
 Base failure\_GR:Failed due to gravity.